

**Phytochemical and cytotoxicity studies on *Arbutus pavarii*,
Asphodelus aestivus, *Juniperus phoenicea* and *Ruta
chalepensis* growing in Libya**

Afaf Mohamed Al Groshi

A thesis submitted in fulfilment of the requirements of Liverpool John
Moores University for the degree of Doctor of Philosophy

February 2019

ABSTRACT

The work incorporates systematic bioassay-guided phytochemical and cytotoxicity/anticancer studies on four selected medicinal plants from the Libyan flora. Based on information on their traditional medicinal uses and the literature survey, *Juniperus phoenicea* L. (Fam: Cupressaceae), *Asphodelus aestivus* Brot. (Fam: Asphodelaceae), *Ruta chalepensis*. L (Fam: Rutaceae) and *Arbutus pavarii* Pampan. (Fam: Ericaceae) have been selected for investigation in the current endeavour. The four plants are well-known Libyan medicinal plants, which have been used in Libyan traditional medicine for the treatment of various human ailments, including both tumours and cancers. The cytotoxic activity of the *n*-hexane, dichloromethane (DCM) and methanol (MeOH) extracts of these plants were assessed against five human tumour cell lines: urinary bladder cancer [EJ-138], liver hepatocellular carcinoma [HEPG2], lung cancer [A549], breast cancer [MCF7] and prostate cancer [PC3] cell lines. The cytotoxicity at different concentrations of these extracts (0, 0.8, 4, 20, 100 and 500 µg/mL) was evaluated by the MTT assay. The four plants showed notable cytotoxicity against the five aforementioned human tumour cell lines with different selectivity indexes on prostate cancer cells. Accordingly, the cytotoxic effect of various chromatographic fractions from the different extracts of these plants at different concentrations (0, 0.4, 2, 10, 50 and 250 µg/mL) revealed different cytotoxic properties.

Twenty-nine compounds were isolated from different fractions of these plants: three bioflavonoids, amentoflavone (**25**), cupressoflavone (**24**) and sumaflavone (**76**); four diterpenes. 13-*epi*-cupressic acid (**42**), imbricatholic acid (**41**), 3-hydroxy sandaracopimaric acid (**44**) and dehydroabietic acid (**46**), one alkanol (heptacosanol)

and two lignans, deoxypodophyllotoxin (**29**) and β -peltatin methyl ether (**28**)] from *J. phoenicea* leaves; one flavonoid, luteolin (**22**), four anthraquinones [aleo-emodin (**13**), chrysophanol anthrone (**79**), 10, 10`chrysophanol bianthrone (**80**) and C- α -rhamnopyranosyl bianthracene-9, 9', 10 (10'H)-trione glycoside (**81**) and *p*-hydroxyphenethyl *trans*-ferulate (**82**) from *A. aestivus* leaves and tubers; three alkaloids, kokusaginine (**61**), graveoline (**60**), and 4-hydroxy-2-nonyl-quinoline (**85**), three coumarins, bergapten (**63**), chalepin (**64**) and chalepinsin (**65**), one alkane, tetradecane, two flavonoid glycosides, rutin (**52**) and methoxy rutin (**83**) and 3`, 6`-disinapoylsucrose (**84**) from *R. chalepensis* aerial parts; one hydroquinone- β -D-glucopyranoside, arbutin (**53**) and two pentacyclic triterpenes, methyl betulinate (**89**) and ursolic acid (**88**) from *A. pavarii* leaves.

Twenty-three isolated compounds were tested for their cytotoxicity against the most sensitive cancer cell lines. Eight compounds revealed good cytotoxic activity: cupressoflavone (**24**), sumaflavone (**76**), epicupressic acid (**42**), luteolin (**22**), chalepin (**64**) and 4-hydroxy-2-nonyl-quinoline (**85**) were cytotoxic against the A549 with IC₅₀ values of 65, 77, 159, 76.9, 92 and 97.6 μ M, respectively, whilst, compound **64** showed toxicity also against EJ138 with an IC₅₀ value of 117 μ M. C- α -rhamnopyranosyl bianthracene-9, 9', 10 (10'H)-trione (**81**) and ursolic acid (**88**) were toxic against the prostate cancer cell line with IC₅₀ values of 62 μ M and 8.22 μ M, respectively. The study findings also indicated that compounds **24**, **64** and **88**-induced cell death might involve the plasma membrane damage resulting in the release of LDH enzyme from the necrotic cells.

DEDICATION

I would like to dedicate my thesis to my beloved late mother Fatma Elamin El Gadamsi. Although she is no longer here with us to celebrate this achievement, she waited patiently for this day to come. She taught me great resilience when she fought against cancer multiple times, I learnt not to give up and work hard until I achieve what I desired for and although her loss was a heart breaker, I am glad that I made her proud.

ACKNOWLEDGEMENTS

Firstly, I would like to thank my God, the most gracious and merciful for supporting me and giving me the strength to carry on this study.

I gratefully acknowledged the Libyan Government for the PhD scholarship.

My deep gratitude to my supervisor Prof Satya Sarker for his continuous support, patience, motivation, immense knowledge and guidance in all the stages of my research and in the writing of my thesis.

My profound gratitude is expressed to my supervisors: Dr Andrew Evans and Dr Fyaz Ismail whose help and support were the main reason of my development and who provided me with assistance, and perceptive comments in all the stages of this research.

I would like to express my deep and sincere gratitude to my advisor Dr Lutfun Nahar for her suggestions, guidance, encouragement and support throughout this study.

I would also like to acknowledge the EPSRC National Mass Spectrometry Service, Swansea, UK for MS analyses of my samples.

Many thanks go to Dr Nicola Dempster and Mr. Robert Allen for their always help to run my NMR and MS samples. Special thanks go to Mr Daniel Graham for his assistance all the times.

Thanks also extend to all my colleagues who helped me during this work and shared with them the best memories, namely; Mrs Laila Kafu, Miss Georgiana Alexander, Mrs Shaymaa Al Majmaie, Miss Hiba El Jasim, Miss Ruba Bunyan, Dr. Stephanie Tamdem, Dr. Sammar El Taib and Dr Sushmitta Nuth.

I would also like to thank all the staff members of the department of school of pharmacy and bimolecular sciences to everyone who supported me in my research in the Liverpool John Moores University.

To my dear husband Mr. Khalifa Garoushi, for his assistance, encouragement, and support all the times. He made my dream real. I am so grateful to him.

My sisters and brothers I cannot imagine my life without you. Always find you when I need any help. Thanks for always being there for me.

It is my pleasure to convey thanks to my son in law Mr. Soufian Al Bougdadi for his help and support.

Last, but certainly not least, they are the beginning of everything beautiful in my life, my lovely, daughters Amel, Amna and Hager and my sweetheart son Anas.

Contents

<u>Contents</u>	<u>Page No.</u>
Abstract	I
Dedication	III
Acknowledgments	IV
List of figures	XI
List of tables	XXII
List of abbreviations	XXVII
Chapter 1: Introduction	
1.1 Cancer	1
1.1.1 History of cancer	1
1.1.2 Incidence of cancer	2
1.1.3 Anticancer natural products	4
1.1.4 Mechanism of action of anticancer natural products	9
1.1.4.1 Mechanisms of cell death	9
1.1.4.2 Classification of anticancer agents according to their chemical structure and mechanism of action	9
1.2 The family Asphodelaceae	13
1.2.1 Classification of the family Asphodelaceae	13
1.2.2 Chemical characteristics of the family Asphodelaceae	14
1.2.3 Traditional uses of the family Asphodelaceae	14
1.2.4 The genus <i>Asphodelus</i> L.	14
1.2.4.1 Active constituents of the genus <i>Asphodelus</i>	15
1.2.4.2 Traditional uses of the genus <i>Asphodelus</i>	15
1.2.5 <i>Asphodelus aestivus</i> Brot.	15
1.2.5.1 Traditional uses of <i>A. aestivus</i>	16
1.2.5.2 Previous phytochemical work of <i>A. aestivus</i>	16
1.2.5.3 Previous biological work of <i>A. aestivus</i>	19
1.3 The family Cupressaceae	21
1.3.1 Classification of the Cupressaceae	21
1.3.2 Chemical characteristics of the Cupressaceae family	22
1.3.3 Traditional uses of the Cupressaceae	22

1.3.4	The genus <i>Juniperus</i> L.	23
1.3.4.1	Species of the genus <i>Juniperus</i>	23
1.3.4.2	Active constituents in the genus <i>Juniperus</i>	23
1.3.4.3	Traditional uses of the genus <i>Juniperus</i>	24
1.3.5	<i>Juniperus phoenicea</i> L.	24
1.3.5.1	Traditional uses of <i>J. phoenicea</i>	25
1.3.5.2	Previous phytochemical work of <i>J. phoenicea</i>	26
1.3.5.3	Previous biological work of <i>J. phoenicea</i>	31
1.4	The family Ericaceae	35
1.4.1	Traditional uses of the family Ericaceae	35
1.4.2	The genus <i>Arbutus</i> L.	36
1.4.2.1	Active constituents in the genus <i>Arbutus</i>	36
1.4.2.2	Traditional uses of the genus <i>Arbutus</i>	36
1.4.3	<i>Arbutus pavarii</i> Pamp.	36
1.4.3.1	Traditional uses of <i>A. pavarii</i>	37
1.4.3.2	Previous phytochemical work of <i>A. pavarii</i>	37
1.4.3.3	Previous biological work of <i>A. pavarii</i>	39
1.5	The family Rutaceae	42
1.5.1	Classification of the family Rutaceae	42
1.5.2	Chemical characteristics of the family Rutaceae	43
1.5.3	Traditional uses of the family Rutaceae	43
1.5.4	The genus <i>Ruta</i>	43
1.5.4.1	Active constituents in the <i>Ruta</i> genus	44
1.5.4.2	Traditional uses of the genus <i>Ruta</i>	44
1.5.5	<i>Ruta chalepensis</i> L.	45
1.5.5.1	Traditional uses of <i>R. chalepensis</i>	45
1.5.5.2	Previous phytochemical work of <i>R. chalepensis</i>	46
1.5.5.3	Previous biological work of <i>R. chalepensis</i>	49
1.6	Objectives of this study	55
Chapter 2: Materials and Methods		
2.1	Phytochemical work	58
2.1.1	General materials	58

2.1.2	Plant materials	58
2.1.3	Extraction of plant materials	59
2.1.4	Fractionation techniques	59
2.1.4.1	Solid phase extraction (SPE)	59
2.1.4.2	Vacuum liquid chromatography (VLC)	60
2.1.5	Chromatographic techniques	61
2.1.5.1	Thin layer chromatography (TLC)	61
2.1.5.2	Column liquid chromatography (CLC)	62
2.1.6	Spectroscopic techniques	64
2.1.6.1	Ultraviolet-visible spectroscopy (UV-Vis)	64
2.1.6.2	Mass spectrometry (MS)	64
2.1.6.3	Nuclear magnetic resonance (NMR)	66
2.1.6.3.1	One-dimensional techniques	66
2.1.6.3.2	Two-dimensional techniques	67
2.1.7	Isolation of compounds	69
2.2	Bioassay for potential cytotoxic/anticancer effects of extracts, fractions and compounds	72
2.2.1	Cancer cell lines selected	73
2.2.2	Routine cell culture	74
2.2.3	Cryopreservation of cells	75
2.2.4	The MTT cytotoxicity assay	76
2.2.5	Determination of IC ₅₀ values	78
2.2.6	Determination of selectivity index (SI)	79
2.2.7	Statistical analysis	79
2.2.8	LDH assay of cell membrane integrity (LDH release assay)	80
Chapter 3: Results and Discussions		
3.1	<i>Juniperus phoenicea</i>	83
3.3.1	Extraction	83
3.1.2	Preliminary analytical TLC screening	83
3.1.3	Analytical HPLC screening for the MeOH extract of <i>J.</i> <i>phoenicea</i> leaves	85

3.1.4	Screening of <i>J. phoenicea</i> extracts for cytotoxic activity	86
3.1.5	Chromatographic fractionation of the extracts	87
3.1.5.1	Vacuum liquid chromatography fractionation (VLC)	87
3.1.5.2	Solid phase extraction (SPE)	89
3.1.6	Screening of <i>J. phoenicea</i> fractions for cytotoxic activity	91
3.1.7	Isolation of compounds from <i>J. phoenicea</i>	92
3.1.7.1	The MeOH extract (JPM)	92
3.1.7.2	The <i>n</i> -hexane extract (JPH)	93
3.1.7.3	HPLC-MS screening of the <i>n</i> -hexane extract (JPH)	94
3.1.7.4	The DCM extract (JPD)	96
3.1.8	Characterization of isolated compounds from <i>J. phoenicea</i>	99
3.1.8.1	Characterization of biflavonoids	99
3.1.8.2	Characterization of diterpenes	106
3.1.8.3	Characterization of lignans	115
3.1.9	Cytotoxic effect of the isolated compounds from <i>J. phoenicea</i> leaves	119
3.1.9.1	The LDH results	125
3.2	<i>Aesphodelus aestivus</i>	130
3.2.1	Extraction	130
3.2.2	Preliminary analytical TLC screening of <i>A. aestivus</i> leaves extracts	130
3.2.3	Preliminary analytical TLC screening of <i>A. aestivus</i> tuber extracts	132
3.2.4	Analytical HPLC screening of the <i>A. aestivus</i> leaves MeOH extract	133
3.2.5	Analytical HPLC screening of the <i>A. aestivus</i> tubers MeOH extract	134
3.2.6	Screening of <i>A. aestivus</i> extracts for cytotoxic activity	135
3.2.7	Chromatographic fractionation of the extracts	136
3.2.7.1	Vacuum liquid chromatography fractionation (VLC)	136
3.2.7.2	Solid phase extraction (SPE)	139
3.2.8	Screening of <i>A. aestivus</i> fractions for cytotoxic activity	141
3.2.9	Isolation of compounds from <i>A. aestivus</i>	142

3.2.9.1	The MeOH extract (AEM)	142
3.2.9.2	The DCM extract (AED)	149
3.2.10	Characterization of isolated compounds from <i>A. aestivus</i>	151
3.2.10.1	Characterization of flavonoids	151
3.2.10.2	Characterization of anthraquinones	155
3.2.10.3	Characterization of ferulate derivative	168
3.2.11	Cytotoxic effect of the isolated compounds from <i>A. aestivus</i>	171
3.3	<i>Ruta chalepensis</i>	178
3.3.1	Extraction	178
3.3.2	Preliminary analytical TLC screening	178
3.3.3	Analytical HPLC screening of the MeOH extract of <i>R. chalepensis</i> aerial parts	179
3.3.4	Screening of <i>R. chalepensis</i> extracts for cytotoxic activity	181
3.3.5	Chromatographic fractionation of the extracts	182
3.3.5.1	Vacuum liquid chromatography (VLC)	183
3.3.5.2	Solid phase extraction (SPE)	184
3.3.6	Screening of <i>R. chalepensis</i> DCM fractions for cytotoxic activity	186
3.3.7	Isolation of compounds from <i>R. chalepensis</i>	187
3.3.7.1	The MeOH extract (RCM)	187
3.3.7.2	The DCM extract (RCD)	190
3.3.7.3	The <i>n</i> -hexane extract (RCH)	193
3.3.8	Characterization of isolated compounds from <i>R. chalepensis</i> aerial parts	199
3.3.8.1	Characterization of flavonoids	199
3.3.8.2	Characterization of disinapoylsucrose	205
3.3.8.3	Characterization of coumarins	208
3.3.8.4	Characterization of alkaloids	214
3.3.8.5	Characterization of alkane	220
3.3.8.6	Characterization of dehydromoskashan derivative	221
3.3.9	Cytotoxic effect of the isolated compounds from <i>R. chalepensis</i> aerial parts	225
3.3.10	The LDH results	228

3.4	<i>Arbutus pavarii</i>	235
3.4.1	Extraction	235
3.4.2	Preliminary analytical TLC screening	235
3.4.3	Analytical HPLC screening for MeOH extract of <i>A. pavarii</i> leaves	236
3.4.4	Screening of <i>A. pavarii</i> extracts for cytotoxic activity	238
3.4.5	Chromatographic fractionation of the extracts	239
3.4.5.1	Vacuum liquid chromatography (VLC)	239
3.4.5.2	Solid phase extraction (SPE)	240
3.4.6	Screening of <i>A. pavarii</i> leaves DCM fractions for cytotoxic activity	241
3.4.7	Isolation of compounds from <i>A. pavarii</i> leaves	241
3.4.7.1	The MeOH extract (APM)	241
3.4.7.2	The DCM extract (APD)	242
3.4.8	Characterization of isolated compounds from <i>A. pavarii</i> leaves	243
3.8.4.1	Characterization of hydroquinone glycoside	243
3.4.8.2	Characterization of pentacyclic triterpenes	245
3.4.9	Cytotoxic effect of ursolic acid (2) from <i>A. pavarii</i> leaves	251
3.4.10	The LDH results	252
	Conclusion	256
	References	258
	Meetings, Conferences and Publications	
	290	
	Appendix	294

List of figures

<u>Figure</u>		<u>Page</u>
Figure 1.1	Anticancer natural products	8
Figure 1.2	<i>Asphodelus aestivus</i>	15
Figure 1.3	Isolated compounds from <i>A. aestivus</i>	18
Figure 1.4	<i>Juniperus phoenicea</i>	25
Figure 1.5	Isolated compounds from <i>J. phoenicea</i>	31
Figure 1.6	<i>Arbutus pavarii</i>	37
Figure 1.7	Isolated compounds from <i>A. pavarii</i>	39
Figure.1.8	<i>Ruta chalepensis</i>	45
Figure 1.9	Isolated compounds from <i>R. chalepensis</i>	49
Figure 2.1	The reduction of MTT into formazan	76
Figure 3.1.1	TLC for the three extracts of <i>J. phoenicea</i> leaves	84
Figure 3.1.2	Analytical HPLC chromatogram of the MeOH extract of <i>J. phoenicea</i> leaves (observed at 320 nm, the green chromatogram)	85
Figure 3.1.3	TLC analysis (mobile phase: 20% EtOAc in <i>n</i> -hexane) of the VLC fractions of the <i>n</i> -hexane extract of the leaves of <i>J. phoenicea</i>	88
Figure 3.1.4	TLC analysis (mobile phase: 5% MeOH in DCM) of the VLC fractions of the <i>n</i> -hexane extract of the leaves of <i>J. phoenicea</i>	88
Figure 3.1.5	Analytical HPLC chromatograms of SPE fraction 1 of JPM (observed at 310 nm)	90
Figure 3.1.6	Analytical HPLC chromatograms of SPE fraction 2 of JPM (observed at 310 nm)	90
Figure 3.1.7	Analytical HPLC chromatograms of SPE fraction 3 of JPM (observed at 310 nm)	90
Figure. 3.1.8	Analytical HPLC chromatograms of SPE fraction 4 of JPM (observed at 310 nm)	91

Figure 3.1.19	Analytical HPLC chromatogram of isolated compounds from SPE fraction 3 JPM (observed at 310 nm)	93
Figure 3.1.20	Analytical HPLC chromatogram of isolated compounds from SPE fraction 4 JPM (observed at 310 nm)	93
Figure 3.1.22	Isolation of the compounds JPH3 and JPD567 from <i>J. phoenicea</i> . <i>n</i> -hexane F3 and F5	94
Figure 3.1.23	LC-MS screening for the <i>n</i> -hexane extract of <i>J.phoenicea</i> leaves	96
Figure 3.1.24	HPLC chromatogram of the active VLC fraction 4 of the DCM extract (JPD) (observed at 250 nm)	97
Figure 3.1.25	Fractionation of JPD extract every 5 min (observed at 250 nm)	98
Figure 3.1.26	HPLC chromatogram of JPD fraction F4 (observed at 250 nm)	98
Figure 3.1.27	HPLC chromatogram of JPD fraction F5 (observed at 250 nm)	99
Figure 3.1.28	HPLC chromatogram of JPD fraction F6 (observed at 250 nm)	99
Figure 3.1.29	Structure of biflavonoids 25 and 76 from JPM	100
Figure 3.1.30	U.V. spectrum of cupressoflavone (24) in MeOH	101
Figure 3.1.31	¹ H NMR spectrum (600 MHz, DMSO-d ₆) of cupressoflavone (24)	101
Figure 3.1.32	¹³ C NMR spectrum (150 MHz, DMSO-d ₆) of cupressoflavone (24)	102
Figure 3.1.33	HMBC spectrum of cupressoflavone (24)	102
Figure 3.1.34	¹ H NMR spectrum (600 MHz, CD ₃ OD) of amentoflavone (25)	103
Figure 3.1.35	¹ H NMR spectrum (300 MHz, DMSO-d ₆) of amentoflavone (25)	104
Figure 3.1.36	¹ H NMR spectrum (300 MHz, DMSO-d ₆) of sumafavone (76)	105

Figure 3.1.37	¹ H NMR spectrum (600 MHz, CDCl ₃) of 13- <i>epi</i> -cupressic acid (42)	108
Figure 3.1.38	¹³ C NMR spectrum (150 MHz, CDCl ₃) of 13- <i>epi</i> -cupressic acid (42)	109
Figure 3.1.39	HMBC correlations of 13- <i>epi</i> -cupressic acid (42)	109
Figure 3.1.40	¹ H NMR spectrum (600 MHz, CDCl ₃) of imbricatolic acid (41)	110
Figure 3.1.41	¹³ C NMR spectrum (150 MHz, CDCl ₃) of imbricatolic acid (41)	111
Figure 3.1.42	¹ H NMR spectrum (600 MHz, CDCl ₃) of 3-hydroxy sandaracopimaric (44)	112
Figure 3.1.43	¹³ C NMR spectrum (150 MHz, CDCl ₃) of 3-hydroxy sandaracopimaric (44)	112
Figure 3.1.44	¹ H NMR spectrum (600 MHz, CDCl ₃) of dehydroabietic acid (46)	115
Figure 3.1.45	¹³ C NMR spectrum (150 MHz, CDCl ₃) of dehydroabietic acid (46)	115
Figure 3.1.46	¹ H NMR spectrum (600 MHz, CDCl ₃) of β-methylpeltatin A methyl ether (28)	118
Figure 3.1.47	¹³ C NMR spectrum (150 MHz, CDCl ₃) of β-methylpeltatin A methyl ether (28)	118
Figure 3.1.48	Structure of heptacosane-14-ol (77)	119
Figure 3.1.49:	¹ H NMR spectrum (400 MHz, CDCl ₃) of heptacosane-14-ol (77)	119
Figure 3.1.50	¹³ C NMR spectrum (75 MHz, CDCl ₃) of heptacosane-14-ol (77)	120
Figure 3.1.51	The structure of etoposide standard (78)	121
Figure 3.1.52	The cytotoxic activity of cupressoflavone (24) against lung cancer cell line (A549)	122
Figure 3.1.53:	The cytotoxic activity of sumaflavone (76) against lung cancer cell line (A549)	122
Figure 3.1.54	The cytotoxic activity of 13- <i>epi</i> -cupressic acid (42) against lung cancer cell line	123

Figure 3.1.55	The cytotoxic activity of imbricatolic acid (41) against lung cancer cell line	123
Figure 3.1.56	The cytotoxic activity of imbricatolic acid (41) against prostate cancer cell line	124
Figure 3.1.57	The cytotoxic activity of 3-hydroxy sandaracopimaric acid (44) against lung cancer cell line	124
Figure 3.1.58	The cytotoxic activity of deoxydophyllotoxin (29) mixture against lung cancer cell line	125
Figure 3.1.59	The cytotoxic activity of etoposide (78) against lung cancer cell line	125
Figure 3.1.60	LDH Release result for cupressoflavone (24) against the lung cancer cell lines (A549)	126
Figure 3.2.1	TLC for the three extracts of <i>A. aestivus</i> leaves	132
Figure 3.2.2	TLC for the three extracts of <i>A. aestivus</i> tubers.	133
Figure 3.2.3	Analytical HPLC chromatogram of the MeOH extract of <i>A. aestivus</i> leaves (observed at 220 nm)	134
Figure 3.2.4	Analytical HPLC chromatogram of the <i>A. aestivus</i> tubers MeOH (Observed at 220 nm)	135
Figure 3.2.5	TLC analysis (mobile phase: 5% MeOH in DCM) of the VLC (1) fractions of the AETD	138
Figure 3.2.6	TLC analysis (mobile phase: 5% MeOH in DCM) of the VLC (2) fractions of AETD	139
Figure 3.2.7	Analytical HPLC chromatogram of SPE fraction 1 of AELM (observed at 220 nm)	140
Figure 3.2.8	Analytical HPLC chromatogram of SPE fraction 2 of AELM (observed at 220 nm)	141
Figure 3.2.9	Analytical HPLC chromatogram of SPE fraction 3 of AELM (observed at 220 nm)	141
Figure 3.2.10	Analytical HPLC chromatogram of SPE fraction 4 of AELM (observed at 220 nm)	141
Figure 3.2.11	HPLC chromatograms of isolated compounds from SPE fraction 2 AELM (observed at 220 and 254 nm)	143

Figure 3.2.12	HPLC chromatogram of isolated compounds from SPE fraction 3 AELM (observed at 254 nm)	144
Figure 3.2.13	HPLC chromatogram of isolated compounds from SPE fraction 4 AELM (observed at 254 nm)	144
Figure 3.2.14	Fractionation of AETM extract every 5 min (observed at 290, 254, 310 nm)	145
Figure 3.2.15	Analytical HPLC chromatogram of AETM Fraction 4 (observed at 366 nm)	146
Figure 3.2.16	LC-MS screening for the AETM Fraction 4	146
Figure 3.2.17	HPLC chromatograms of isolated compounds from the DCM extract (observed at 254, 290 and 366 nm)	150
Figure 3.2.18	Crystals from the DCM extract of <i>A. aestivus</i> tubers VLC (1) (AETD4)	151
Figure 3.2.19	Crystals from the DCM extract of <i>A. aestivus</i> tubers VLC (2) (AETD3)	151
Figure 3.2.20	HPLC chromatogram of isolated compounds from the active AETD fraction 4 (VLC 2) (observed at 366 nm)	152
Figure 3.2.21	U.V. spectrum of Luteolin (22) in MeOH	153
Figure 3.2.22	MS spectrum of Luteolin (22)	154
Figure 3.2.23	¹ H NMR spectrum (600 MHz, CD ₃ OD) of luteolin (22)	154
Figure 3.4.24	¹³ C NMR spectrum (75 MHz, CD ₃ OD) of luteolin (22)	155
Figure 3.2.25	Structure of anthraquinones isolated from <i>A. aestivus</i>	156
Figure 3.2.26	¹ H NMR spectrum (600 MHz, CD ₃ OD) of aloe-emodin anthrone (13)	157
Figure 3.2.27	¹ H NMR spectrum (600 MHz, CDCl ₃) of aloe-emodin anthrone (13)	158
Figure 3.2.28	HMBC correlations (600 MHz, CD ₃ OD) of aloe-emodin anthrone (13)	158
Figure 3.2.29	Reduction of aloe-emodin anthrone (13)	158
Figure 3.2.30	MS of the reduced aloe-emodin anthrone (13)	159
Figure 3.2.31	Structure of chrysophanol (79) isolated from <i>A. aestivus</i> tubers	160

Figure 3.2.32	¹ H NMR spectrum (600 MHz, CDCl ₃) of chrysophanol anthrone (79)	160
Figure 3.2.33	Structure of chrysophanol-10,10'-bianthrone (80)	163
Figure 3.2.34	¹ H NMR spectrum (600 MHz, CDCl ₃) of chrysophanol 10, 10'-bianthrone (80)	163
Figure 3.2.35	Structure of C- α -rhamnopyranosyl bianthracene-9, 9', 10 (10'H)-trione glycoside (81)	165
Figure 3.2.36	The UV absorbance (MeOH) of C- α -rhamnopyranosyl bianthracene-9, 9', 10 (10'H)-trione glycoside (81)	166
Figure 3.2.37	¹ H NMR spectrum (600 MHz, CD ₃ OD) of C- α -rhamnopyranosyl bianthracene-9,9',10 (10'H)-trione glycoside (81)	166
Figure 3.2.38	HSQC correlations (600, 150 MHz, CD ₃ OD) of C- α -rhamnopyranosyl bianthracene-9,9',10 (10'H)-trione glycoside (81)	168
Figure 3.2.39	HMBC correlations (600, 150 MHz, CD ₃ OD) of C- α -rhamnopyranosyl bianthracene-9,9',10 (10'H)-trione glycoside (81)	168
Figure 3.2.40	Structure of <i>p</i> -hydroxy-phenethyl <i>trans</i> -ferulate (82)	169
Figure 3.2.41	¹ H NMR spectrum (600 MHz, CD ₃ OD) of <i>p</i> -hydroxy-phenethyl <i>trans</i> -ferulate (82)	170
Figure 3.2.42	MS spectrum (atmospheric solid analysis probe, +ve mode) of <i>p</i> -hydroxy-phenethyl <i>trans</i> -ferulate (82)	171
Figure 3.2.43	The cytotoxic activity of luteolin (22) against the prostate cancer cell line	173
Figure 3.2.44	The cytotoxic activity of C- α -rhamnopyranosyl bianthracene-9,9',10 (10'H)-trione glycoside (81) against the prostate cancer cell line	173
Figure 3.3.1	TLC for the three extracts of <i>R. chalepensis</i> aerial parts	179
Figure 3.3.2	Analytical HPLC chromatogram of the MeOH extract of <i>R. chalepensis</i> aerial parts (observed at 220 nm)	180

Figure 3.3.3	TLC analysis (mobile phase: Toluene: EtOAc /Acetic acid = 25:24:1) of the VLC fractions of the <i>n</i> -hexane extract of <i>R. chalepensis</i> aerial parts	183
Figure 3.3.4	TLC analysis (mobile phase: 20% EtOAc in <i>n</i> -hexane) of the VLC fractions of the DCM extract of <i>R. chalepensis</i> aerial parts	183
Figure 3.3.5	Analytical HPLC chromatograms of SPE fraction 1 of RCM (observed at 250 nm)	185
Figure 3.3.6	Analytical HPLC chromatograms of SPE fraction 2 of RCM (observed at 250 nm)	185
Figure 3.3.7	Analytical HPLC chromatograms of SPE fraction 3 of RCM (observed at 250 nm)	186
Figure 3.3.8	Analytical HPLC chromatograms of SPE fraction 4 of RCM (observed at 250 nm)	186
Figure 3.3.9	HPLC chromatogram of isolated compounds from SPE fraction 2 RCM (observed at 310 nm)	188
Figure 3.3.10	Purification of the compound RCMF2-2 (observed at 310 nm)	188
Figure 3.3.11	Purification of the compound RCMF2-4 (observed at 310 nm)	188
Figure 3.3.12	Analytical HPLC chromatogram of RCMF2-3 (observed at 250 nm)	189
Figure 3.3.13	Analytical HPLC chromatogram of RCMF2-4-1 (observed at 250 nm)	189
Figure 3.3.14	HPLC chromatogram of isolated compounds from RCM SPE fraction 3 (observed at 310 nm)	190
Figure 3.3.15	Purification of the compound RCMF3-2 (observed at 310 nm)	190
Figure 3.3.16	HPLC chromatogram of isolated compounds from the RCD fraction 5 (observed at 366 nm)	191
Figure 3.3.17	HPLC chromatograms of isolated compounds from the RCD F6 [observed at 220 nm (green), 254 nm (blue), and 366 nm (red)]	191

Figure 3.3.18	Purification of peak 2 isolated from RCD F6 (observed at 310 nm)	192
Figure 3.3.19	HPLC chromatogram for the RCD F7 (observed at 310 nm)	192
Figure 3.3.20	Purification of the compound RCDF7-9 (observed at 310 nm)	193
Figure 3.3.21	Crystals of the compound RCHF2 from <i>R. chalepensis</i>	193
Figure 3.3.22	PTLC separation (mobile phase: 20% EtOAc in <i>n</i> -hexane) of the RCH VLC F4	194
Figure 3.3.23	Purified compounds from RCHF4-3 mixture	194
Figure 3.3.24	Isolation of the compounds RCHF7-2 and RCHF7-7 from RCH F7	195
Figure 3.3.25	Fraction 5+6+7 from <i>R. chalepensis n</i> -hexane	195
Figure 3.3.26	Isolation of compounds from RCH fraction 40%	197
Figure 3.3.27	HPLC chromatogram of isolated compounds from the RCH fraction 50% (wavelength = 310 nm)	197
Figure 3.3.28	Isolation of compounds from RCH fraction 50%	198
Figure 3.3.29	HPLC chromatogram of isolated compounds from the RCH fraction 60% (wavelength = 310 nm)	198
Figure 3.3.30	HPLC chromatogram of isolated compounds from RCH fraction 80% (wavelength = 310 nm)	199
Figure 3.3.31	Structure of flavonoids isolated from <i>R. chalepensis</i> aerial parts	200
Figure 3.3.32	¹ H NMR spectrum (600 MHz, CD ₃ OD) of rutin (52)	201
Figure 3.3.33	¹ H NMR spectrum (600 MHz, CD ₃ OD) of methoxy rutin (83)	202
Figure 3.3.34	¹ H NMR spectrum (600 MHz, CD ₃ OD) of methoxy rutin (83) compared with rutin (52)	204
Figure 3.3.35	NOESY spectrum (600 MHz, CD ₃ OD) of methoxy rutin (83)	204
Figure 3.3.36	HMBC correlation of methoxy rutin (83)	205
Figure 3.3.37	Structure of 3'', 6''-disinapoylsucrose (84)	206

Figure 3.3.38	¹ H NMR spectrum (600 MHz, CD ₃ OD) of 3'', 6''-disinapoilsucrose (84)	206
Figure 3.3.39	¹³ C NMR spectrum (150 MHz, CD ₃ OD) of 3'', 6''-disinapoilsucrose (84)	207
Figure 3.3.40	HMBC correlation of 3'', 6''-disinapoilsucrose (84)	207
Figure 3.3.41	¹ H NMR spectrum (600 MHz, CDCl ₃) of bergapten (63)	209
Figure 3.3.42	¹ H NMR spectrum (600 MHz, CDCl ₃) of chalepin (64)	210
Figure 3.3.43	¹ H NMR spectrum (600 MHz, CD ₃ OD) of chalepentin (65)	211
Figure 3.3.44	NOESY spectrum (600 MHz, CD ₃ OD) of chalepentin (65)	212
Figure 3.3.45	¹ H NMR spectrum (600 MHz, CDCl ₃) of kokusaginine (61)	215
Figure 3.3.46	¹³ C NMR spectrum (150 MHz, CDCl ₃) of kokusaginine (61)	215
Figure 3.3.47	¹ H NMR spectrum ¹ H NMR (600 MHz, CD ₃ COCD ₃) of graveoline (60)	216
Figure 3.3.48	¹³ C NMR spectrum (150 MHz, CD ₃ COCD ₃) of graveoline (60)	217
Figure 3.3.49	Structure of 4-hydroxy-2-nonyl-quinoline (85)	217
Figure 3.3.50	¹ H NMR spectrum of 4-hydroxy-2-nonyl-quinoline (85)	218
Figure 3.3.51	¹³ C NMR spectrum of 4-hydroxy-2-nonyl-quinoline (85)	218
Figure 3.3.52	Structure of tetradecane crystals (86)	220
Figure 3.3.53	¹ H NMR spectrum (400 MHz, CDCl ₃) of RCHF ₂ crystals (86)	221
Figure 3.3.54	Structure of dehydromoskashan derivative (87)	222
Figure 3.3.55a:	MS spectrum (atmospheric solid analysis probe) of dehydromoskashan derivative (87)	222

Figure 3.3.55b	MS spectrum (atmospheric solid analysis probe) of dehydromoskashan moiety	223
Figure 3.3.56	¹ H NMR spectrum (600 MHz, CDCl ₃) of dehydromoskashan derivative. (87)	223
Figure 3.3.57	¹³ C NMR spectrum (150 MHz, CDCl ₃) of dehydromoskashan derivative (87)	224
Figure 3.3.58	HSQC spectrum of dehydromoskashan derivatives (87)	224
Figure 3.3.59	HMBC spectrum of dehydromoskashan derivative (87)	225
Figure 3.3.60	Cytotoxicity of chalepin (64) in EJ138 cells according to the MTT assay	227
Figure 3.3.61	Cytotoxicity of chalepin (64) in A549 cells according to the MTT assay	227
Figure 3.3.62	Toxicity of 4-hydroxy-2-nonyl quinolinol (85) in A549 cells according to the MTT assay	228
Figure 3.3.63	LDH Release result for chalepin (64) against the lung cancer cell lines (A549)	229
Figure 3.3.64	Structure activity relationship of the three furanocoumarines isolated from <i>R. chalepensis</i>	231
Figure 3.4.1	TLC for the three extracts of <i>A. pavarii</i> leaves	236
Figure 3.4.2	Analytical HPLC chromatogram the MeOH extract of <i>A. pavarii</i> leaves (observed at 320 nm)	237
Figure 3.4.3	TLC analysis (mobile phase: 20% EtOAc in <i>n</i> -hexane) of the VLC fractions of the DCM extract of <i>A. pavarii</i> leaves	240
Figure 3.4.4	HPLC chromatograms of separated compounds from the APM extract (observed at 254, 280 and 366 nm)	242
Figure 3.4.5	HPLC chromatogram of separated compounds from SPE fraction 4 of APM (observed at 215 nm)	242
Figure 3.4.6	HPLC chromatogram of separated compounds from the active VLC F4 of APD (observed at 215 nm)	243
Figure 3.4.7	¹ H NMR spectrum of (600 MHz, CD ₃ COCD ₃) of arbutin (53)	244
Figure 3.4.9	The ¹ H- ¹³ C HSQC experiment (CD ₃ COCD ₃) of arbutin (53)	244

Figure 3.4.10	Structure of ursolic acid (88)	246
Figure 3.4.11	U.V.spectrum of ursolic acid (88) in MeOH	246
Figure 3.4. 12	MS spectrum of ursolic acid (88)	246
Figure 3.4.13	¹ H NMR spectrum (600 MHz, CD ₃ OD) of ursolic acid (88)	247
Figure 3.4.14	¹³ C NMR spectrum (150 MHz, CD ₃ OD) of ursolic acid (88)	247
Figure 3.3.15	COSY experiment of ursolic acid (88)	248
Figure 3.3.16	The ¹ H- ¹³ C HSQC experiment of ursolic acid (88)	248
Figure 3.4.17	Structure of betulinic acid methyl ester (89)	250
Figure 3.4.18	UV spectrum of betulinic acid methyl ester (89) in MeOH	250
Figure 3.4.19	¹ H NMR spectrum (600 MHz, CDCl ₃) of betulinic acid methyl ester (89)	251
Figure 3.4.20	Cytotoxicity of ursolic acid (88) in PC3 cells according to the MTT assay	251
Figure 3.4.21	LDH Release result for ursolic acid (88) against the prostate cancer cell lines (PC3)	252

List of tables

<u>Table</u>		<u>Page</u>
Table 2.1	Chemicals, solvents and materials	58
Table 2.2	The Libyan medicinal plants used in this study	58
Table 2.3	The weights of different dried and ground parts of the four Libyan medicinal plants	59
Table 2.4	Isolation of compounds from the four Libyan medicinal plants under study	69
Table 2.5	The cancer cell lines used in this study (ECACC)	73
Table 3.1.1	Percentage yield of the three extracts obtained from <i>J. phoenicea</i> leaves	83
Table 3.1.2	R _f values of different extracts of <i>J. phoenicea</i>	84
Table 3.1.3	UV-Vis data for all major peaks obtained from diode array detector	85
Table 3.1.4a	The IC ₅₀ (μg/mL) of <i>n</i> -hexane, DCM and MeOH extracts of <i>J. phoenicea</i> leaves on the selection of five human cancer cell lines	86
Table 3.1.4b	The IC ₅₀ (μg/mL) values for JPD and JPH extracts on PC3 and PNT2 cells and the selectivity index (SI) using the normal human prostate cells (PNT2)	87
Table 3.1.5	Weights of the VLC fractions of the extracts JPH and JPD	89
Table 3.1.6	Weights of the SPE fractions of the MeOH extract of <i>J. phoenicea</i> leaves	89
Table 3.1.7	The IC ₅₀ (μg/mL) of the VLC and SPE fractions of the three extracts of <i>J. phoenicea</i> leaves against A549 (human lung carcinoma) cells	91
Table 3.1.8	¹ H NMR for the bioflavonoids: cupressoflavone (24), amentoflavone (25), and sumaflavone (76)	106
Table 3.1.9	¹³ C NMR data of bioflavonoids: cupressoflavone (24), and amentoflavone (25)	107

Table 3.1.10	¹ H NMR (600 MHz, CDCl ₃) for diterpenes: 13- <i>epi</i> -cupressic acid (42), imbricatolic acid (41) and 3-hydroxy sandaracopimaric acid (44).	113
Table 3.1.11	¹³ C NMR (150 MHz, CDCl ₃) for diterpenes: 13- <i>epi</i> -cupressic acid (42), imbricatolic acid (41) and 3-hydroxy sandaracopimaric acid (44)	114
Table 3.1.12	The IC ₅₀ (μM) of different isolated compounds from <i>J. phoenicea</i> leaves on A549 lung cancer cells.	121
Table 3.1.13	The IC ₅₀ (μM) of imbricatolic acid on PC3 lung cancer cells	121
Table 3.2.1	Percentage yield of the three extracts obtained from both <i>A. aestivus</i> leaves (AEL) and tubers (AET	131
Table 3.2.2	R _f values of different extracts of <i>A. aestivus</i> leaves	132
Table 3.2.3	R _f values of different extracts of <i>A. aestivus</i> tubers	133
Table 3.2.4	UV-Vis data for all major peaks obtained from diode array detector	134
Table 3.2.5a	The IC ₅₀ (μg/mL) of <i>n</i> -hexane, DCM and MeOH extracts of both <i>A. aestivus</i> leaves and tubers on the selection of five human cancer cell lines	136
Table 3.2.5b	The IC ₅₀ (μg/mL) values for AET DCM extract on PC3 and PNT2 cells and the selectivity index (SI) using the normal human prostate cells (PNT2)	137
Table 3.2.6	Weights of the VLC (1) fractions of the extract AETD	138
Table 3.2.7	Weights of the VLC (2) fractions of the extract AETD	139
Table 3.2.8	Weights of the SPE fractions of the MeOH extract of <i>A. eastivus</i> leaves	140
Table 3.2.9	The IC ₅₀ (μg/mL) of DCM fractions from VLC (1) AET on PC3 (human prostate cancer cell line)	142
Table 3.2.10	The IC ₅₀ (μg/mL) of DCM fractions from VLC (2) AET on PC3 (human prostate cancer cell line)	142
Table 3.2.11	¹ H NMR (600 MHz, CD ₃ OD) and ¹³ C NMR (150 MHz, CD ₃ OD) of luteolin (22)	155

Table 3.2.12	¹ H NMR (600 MHz) for the anthrone anthraquinones: aloe-emodin (13) and chrysophanol (79)	161
Table 3.2.13	¹³ C NMR (150 MHz) of aloe-emodin (13) and DEPT NMR (75 MHz) of chrysophanol (79)	161
Table 3.2.14	¹ H NMR (600 MHz, CDCl ₃) and DEPT NMR (150 MHz, CDCl ₃) of chrysophanol-10, 10'-bianthrone (80)	164
Table 3.2.15	¹ H NMR (600 MHz, CD ₃ OD) and ¹³ C NMR (150 MHz, CD ₃ OD) of C- α -rhamnopyranosyl bianthracene-9, 9', 10 (10'H)-trione glycoside (81)	167
Table 3.2.16	¹ H NMR (600 MHz, CD ₃ OD).and ¹³ C NMR (150 MHz, CD ₃ OD) of <i>p</i> -hydroxy-phenethyl <i>trans</i> -ferulate (82)	170
Table 3.2.17	The IC ₅₀ (μ M) of different isolated compounds from <i>A. eastivus</i> tubers on PC3 lung cancer cells	172
Table 3.3.1	Percentage yield of the three extracts obtained from <i>R. chalepensis</i> aerial parts	178
Table 3.3.2	R _f values of different extracts of <i>R. chalepensis</i> aerial parts	179
Table 3.3.3	UV-Vis data for all major peaks obtained from diode array detector	180
Table 3.3.4a	The IC ₅₀ (μ g/mL) of <i>n</i> -hexane, DCM and MeOH extracts of <i>R. chalepensis</i> aerial parts on the selection of five human cancer cell lines	181
Table 3.3.4b	The IC ₅₀ (μ g/mL) values for RC DCM extract on PC3 and PNT2 cells and the selectivity index (SI) using the normal human prostate cells (PNT2)	182
Table 3.3.5	Weights of the VLC fractions of the extracts RCH and RCD	184
Table 3.3.6	Weights of the SPE fractions of the MeOH extract of <i>R. chalepensis</i> aerial parts	184
Table 3.3.7	The IC ₅₀ (μ g/mL) of the VLC DCM fractions of <i>R. chalepensis</i> aerial parts fractions against EJ138 (human bladder carcinoma cells)	187

Table 3.3.8	Different weights of Fraction 5+6+7 from <i>n</i> -hexane layer of <i>R. chalepensis</i>	196
Table 3.3.9	¹ H NMR (600 MHz, CD ₃ OD) for flavonoid glycosides: Rutin (51) and methoxy rutin (83)	203
Table 3.3.10	¹³ C NMR (150 MHz, CD ₃ OD) for the flavonoid glycosides rutin (52) and methoxy-rutin (83)	203
Table 3.3.11	¹ H NMR (600 MHz) of the coumarins: bergapten (63), chalepin (64) and chalepentin (65)	212
Table 3.3.12	¹³ C NMR (150 MHz) of the coumarins: bergapten (63), chalepin (64) and chalepentin (65)	213
Table 3.3.13	¹ H NMR spectrum (600 MHz, CDCl ₃) for alkaloids: kokusaginine (61), Graveoline (60), 4-hydroxy-2-nonyl-quinoline (85)	219
Table 3.3.14	¹³ C NMR (chemical shift) for alkaloids: kokusaginine (61), graveoline (60), 4-hydroxy-2-nonyl-quinoline (85) (CD ₃ OD)	220
Table 3.3.15	The IC ₅₀ (μM) of different isolated compounds from <i>R. chalepensis</i> aerial parts on A549 lung cancer cells.	226
Table 3.4.1	Percentage yield of the three extracts obtained from <i>A. pavarii</i> (APL) leaves	235
Table 3.4.2	R _f values of different extracts of <i>A. pavarii</i> leaves	236
Table 3.4.3	UV-Vis data for all major peaks obtained from diode array detector	237
Table 3.4.4a	The IC ₅₀ (μg/mL) of <i>n</i> -hexane, DCM and MeOH extracts of <i>A. pavarii</i> leaves on the selection of five human cancer cell lines	238
Table 3.4.4b	The IC ₅₀ (μg/mL) values for AP DCM extract on PC3 and PNT2 cells and the selectivity index (SI) using the normal human prostate cells (PNT2)	239
Table 3.4.5	Weights of the VLC fractions of the extract APD	240
Table 3.4.6	Weights of the SPE fractions of the MeOH extract of <i>R. chalepensis</i> aerial parts	241

Table 3.4.7	The IC ₅₀ (μg/mL) of DCM fractions of <i>A. pavarii</i> leaves fractions on PC3 (human prostate cancer cell line)	241
Table 3.4.8	¹ H NMR (600 MHz, CD ₃ COCD ₃) and ¹³ C NMR (150 MHz, CD ₃ COCD ₃) of arbutin (53)	245
Table 3.4.9	¹ H NMR (600 MHz, CD ₃ OD) and ¹³ C NMR (150 MHz, CD ₃ OD) of ursolic acid (88)	249

LIST OF ABBREVIATIONS

ACN	Acetonitrile
A549	Lung Carcinoma Cell Line
ANOVA	Analysis of Variance
ASAP	Atmospheric Solids Analysis Probe
^{13}C NMR	Carbon Nuclear Magnetic Resonance
CD_3COCD_3	Deuterated Acetone
CD_3OD	Deuterated Methanol
CDCl_3	Deuterated Chloroform
CLC	Column Chromatography
COSY	Correlation Spectroscopy
DAD	Diode Array Detector
DCM	Dichloromethane
DMSO	Dimethyl Sulfoxide
DNA	Deoxyribonucleic Acid
DEPT	Distortionless enhancement by polarisation transfer
DPPH	2,2-Diphenyl-1-Picrylhydrazyl
ECACC	European Collection of Authenticated Cell Cultures
EDTA	Ethylene Diamine Tetraacetic Acid
ESIMS	Electrospray Ionization Mass Spectrometry
EtOAc	Ethyl Acetate
ECACC	European Collection of Authenticated Cell Cultures
EJ138	Urinary Bladder Carcinoma Cell Line
FBS	Foetal Bovine Serum
GC-FID	Gas Chromatography with Flame Ionization Detector
^1H NMR	Proton Nuclear Magnetic Resonance
HEPG2	Liver Hepatocellular Carcinoma Cell Line
<i>n</i> -Hexane	Normal Hexane
HMBC	Heteronuclear Multiple Bond Correlation
HPLC	High-Pressure or High-Performance Liquid Chromatography
HRMS	High Resolution Mass Spectrometry
HSQC	Heteronuclear Single Quantum Correlation
LDH	Lactate Dehydrogenase

<i>m/z</i>	Mass to Charge
MCF7	Breast Adenocarcinoma Cell Line
MeOH	Methanol
MS	Mass Spectrometry
MTT	3-(4,5-Dimethyl Thiazolyl-2)-25-Diphenyltetrazolium Bromide
NAD	Nicotinamide Adenine Dinucleotide
NCI	National Cancer Institute
NOESY	Nuclear Over Hauser Effect Spectroscopy
PBS	Phosphate Buffered Saline
PC3	Prostate Adenocarcinoma Cell Line
PNT2	Normal Human Prostate Cell Line
RNA	Ribonucleic Acid
RPMI media	Roswell Park Memorial Institute media
SAR	Structure Activity Relationships
SPE	Solid Phase Extraction
TLC	Thin Layer Chromatography
UV/vis	Ultraviolet/Visible Spectrometry
VLC	Vacuum Liquid Chromatography

CHAPTER 1
INTRODUCTION

1.0 Introduction

1.1 Cancer

Cancer is a hyperproliferative disorder starts to occur, when normal cells in a specific part of the body begin to grow out of control. It can be defined as a disease in which there is an alteration in the control mechanisms that govern cell proliferation and differentiation that generally is due to DNA damage. Cancer cells tend to rapidly proliferate or increase in number, which can result in morbidity and mortality. Cancer or malignant neoplasms can metastasize to new and distant tissues through the lymph system and blood vessels. Tumours also often have an irregular shape, invade local tissue, and often ulcerate through the skin (Cooper, 2000).

1.1.1 History of cancer

The earliest evidence of human bone cancer was discovered in mummies in ancient Egypt, which were dated about 1600 BC in some ancient manuscripts. A recorded case of breast cancer from ancient Egypt in 1500 BC showed that there was no treatment for cancer but only palliative treatment. According to inscriptions, surface tumours were removed by surgery in a similar manner as they are removed today (Sudhakar, 2009).

The origin of the word cancer came from Greek physician Hippocrates (460–377 BC), who used the word *karkinos*, meaning carcinoma. The Hippocratic Corpus (diseases that produced masses) were described as *onkos* and the ulcerative and non-healing masses that included lesions ranging from benign processes to malignant tumors were described as *karkinos*. Hippocrates advised his patients on their diet, rest, and exercise

in cases of mild illnesses, but for more serious diseases, especially *karkinomas* he advocated for the purgatives, heavy metals, and surgery (Faguet, 2015).

In the last couple of hundred years, the innovations and advancement of research tools have helped researchers to explore different hypotheses on the nature of cancer, leading to an incremental increase in our understanding, and in the prevention and in the treatment of cancer. For instance, in 1775, Percivall Pott confirmed a relationship between exposure to chimney soot and the incidence of squamous cell carcinoma of the scrotum among chimney sweeps (Kipling & Waldron, 1975). Likewise, Rudolph Virchow in 1863 was the first person to identify the term "leukaemia" and the excess number of white blood cells in the blood of patients with leukaemia. He was also the first to describe the connection between inflammation and cancer (Androutsos, 2004). In 1882, the first radical mastectomy to treat breast cancer was performed by William Halsted, who believed that the more extensive the surgery, the less likely cancer would return (Young, 2013). The inheritance of a cancer risk was first reported by the Brazilian ophthalmologist Hilário de Gouvêa in 1886, who provided the first documented evidence that cancer can be inherited. Likewise, the virus-cancer link was confirmed by Peyton Rous. He was awarded the Nobel Prize in physiology or medicine in 1966 for his discovery of tumour-inducing viruses known as Rous sarcoma virus. He also reported the carcinogenicity of certain environmental and industrial agents as well as that of ultraviolet radiation (Faguet, 2015).

1.1.2 Incidence of cancer

Cancer is still one of the major causes of human morbidity and mortality throughout the world, despite notable advances in treatments. In the United States, cancer is the second leading cause of death after cardiovascular disease. Approximately one in four

deaths are caused by cancer (Manju *et al.*, 2012). According to GLOBOCAN (a project of the International Agency for Research on Cancer), an estimated 14.1 million new cancer cases and 8.2 million deaths were reported in 2012 worldwide. These figures are expected to increase by at least 70% by 2030 (Torre *et al.*, 2015). Records reveal that lung cancer is the leading cause of cancer death among males, whereas breast cancer is the leading cause of cancer death among females. On the other hand, colorectal cancer deaths are higher in the more developed countries in both females and males. However, in less developed countries, liver and stomach cancers are the leading causes of males' cancer death while cervical cancer is the most leading cause of females' cancer deaths. Although the incidence rates for all cancers are twice as high in more developed countries than less developed countries, but mortality rates are only 8-15% higher in more developed countries (Torre *et al.*, 2015; Antoni *et al.*, 2016).

In Libya, like all countries, cancer is also a major health problem, but epidemiological data in Libya are sparse (El Mistiri *et al.*, 2015). However, 'The Benghazi Cancer Registry' has managed to collect data on all new cases diagnosed in Eastern Libya and also data from medical and mortality records from multiple other sources. The leading cancers in males were found to be lung, colorectal and bladder, whereas in females, the leading malignancy was breast, followed by colorectal and uterine cancers. Lung and breast cancers were the most common causes of cancer deaths in adults. In the paediatric age group, the most frequently occurring cancer was identified as lymphoid leukaemia. Despite some progress in cancer prevention, Libya still lacks effective control programmes for cancer, which is also the case within many countries of the Eastern Mediterranean Region (El Mistiri *et al.*, 2015).

1.1.3 Anticancer natural products

Several types of chemical compounds have been isolated from natural sources of either plant, marine or microbial origin and have played an important role in the drug discovery and treatment of different diseases. Their study includes the investigation of their structure, biosynthesis, potential uses, and purpose of their presence in the organism. The isolated products are usually secondary metabolites and their derivatives, which should be well-characterized molecules with a high degree of purity. This helps to provide the source of inspiration for FDA-approved compounds, drug discovery, and development (Nautiyal *et al.*, 2013).

Natural products have made a significant impact on the discovery of compounds that kill cancer cells, and over 60% of all cancer drugs that are currently in clinical use are either natural products or owe their origin to a natural source (Sarker & Nahar, 2012). There is increasing evidence suggesting that there are new anticancer drugs leads to be discovered from the marine environment. Many marine-derived agents have proven potential to inhibit the growth of human cancer cells both *in vivo* and *in vitro* models. Some of these agents have been approved for use in humans, for example, cytarabine, yondelis (ET743), eribulin, dolastatin 10 and monomethylauristatin E (MMAE or vedotin) (Newman & Cragg, 2014). Several steroid dimers reported from various marine organisms such as cephalostatins and ritterazines showed potent cytotoxicity against the lymphocytic leukaemia cell line (P388) (Nahar & Sarker, 2012). Cephalostatin 1 (Figure 1.1) (**1**) proved its activity as anticancer agent tested by the US National Cancer Institute (NCI) (Moser, 2008; Nahar & Sarker, 2012).

Numerous plants are well-known sources of clinically useful anticancer drugs. For example, *Catharanthus rosea* (vinblastine, vincristine, and vinorelbine), *Podophyllum*

hexandrum (etoposide and teniposide), *Taxus brevifolia* (paclitaxel and docetaxel) and *Camptotheca acuminata* (topotecan and irinotecan) (Heinrich *et al.*, 2012).

Vinca alkaloids (vinblastine, vincristine, and vinorelbine) (Figure 1.1) (2, 3 and 4), respectively, are naturally occurring, or semi-synthetic nitrogenous bases obtained from the Madagascar periwinkle plant *Catharanthus roseus* (Apocynaceae). They are asymmetrical dimeric compounds formed by condensation of the vindoline and catharanthine subunits (Brunton *et al.*, 2011). Vinca alkaloids were used for the treatment of diabetes due to their hypoglycemic effect. It was noted that the extracts of *C. roseus* decreased the white blood cell counts and caused bone marrow depression in experimental rats and subsequently revealed activity against leukemic experimental mice (Cragg & Newman, 2005). They are primarily used in combination with other anticancer drugs for the treatment of different types of cancers, including breast, lung, haematological (leukaemias and lymphomas) and testicular cancers (Cragg & Newman, 2005; Brunton *et al.*, 2011).

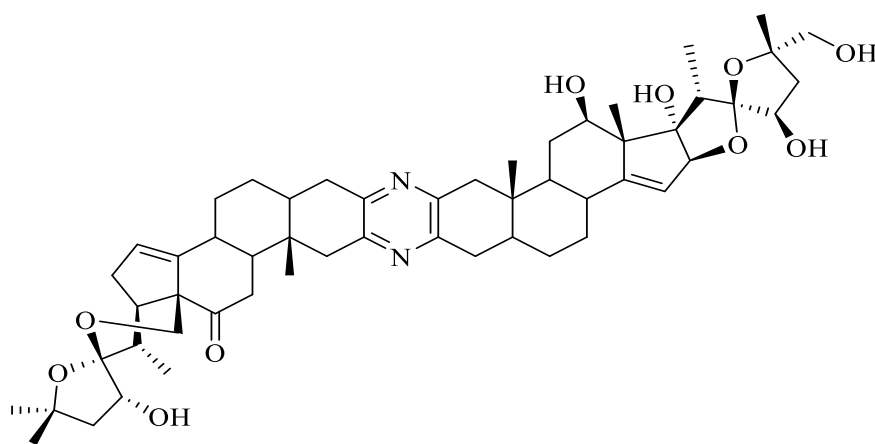
The discovery of paclitaxel (Taxol) (Figure 1.1) (5), a diterpene ester from the inner bark of the Pacific Yew, *Taxus brevifolia* (Taxaceae), is another example of a natural product success in drug discovery. Recently, it has been revealed that Taxol was produced by a fungal endophyte, which can grow on semisynthetic media. The fungus was isolated from the phloem tissue of the Pacific Yew Tree (Priyadarshini & Aparajitha, 2012). Paclitaxel is an effective anticancer agent against ovarian and advanced breast cancer, lung, liver, leukaemia, head and neck cancers. Clinical use of paclitaxel was limited because of the extremely small amount of drug obtained from the crude bark extract, and its poor water solubility. Therefore, many studies were carried out in an effort to develop this product by synthetic methods. The modification of the side chain linked to the taxane ring at C₁₃ has led to the identification of the

more potent anticancer analog, docetaxel (Brunton *et al.*, 2011; Priyadarshini & Aparajitha, 2012).

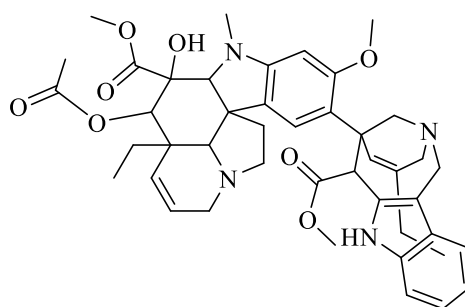
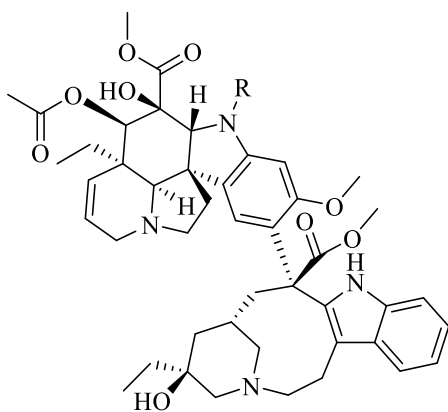
Podophyllotoxin (Figure 1.1) (6) is a lignan isolated from the rhizomes of American mayapple (*Podophyllum peltatum*) Fam. Berberidaceae. It was used traditionally by the American Indians as an emetic, cathartic and anthelmintic agents (Brunton *et al.*, 2011). Podophyllotoxin has been also found in other genera such as *Anthriscus*, *Cassia*, *Catharanthus*, *Commiphora*, *Diphylleia*, *Dysosma*, *Haplophyllum*, *Hernandia*, *Hyptis*, *Juniperus*, *Nepeta*, *Polygala*, *Linum*, *Teucrium* and *Thuja* (Gordaliza *et al.*, 2004). Podophyllotoxin was found to be unsuitable for clinical use as an anticancer agent due to its toxic side effects. The semisynthetic derivatives of podophyllotoxin, etoposide, and teniposide have proved to be excellent antitumour drugs (Arroo *et al.*, 2002). They are extensively used in the treatment of lung cancer, testicular cancer, ovarian, leukaemia, and lymphoma. Teniposide has higher plasma protein binding and higher potency than etoposide (Canel *et al.*, 2000; Cragg & Newman, 2005; Lee & Xiao, 2005). β -peltatin-A-methyl ether was found in *Anthriscus sylvestris*, *Bursera permollis*, *B. fagaroides*, *B. simaruba*, *Juniperus phoenicea*, *Libocedrus plumose* and some *Linum* species (Cairnes *et al.*, 1980). β -Peltatin-A-methyl ether has been reported to have cytotoxic activity against number of cancer cell lines (Wickramaratne *et al.*, 1995; Rojas-Sepúlveda *et al.*, 2012). Notably, the biological activity of the semisynthetic compounds was shown to be affected by the presence of a transfused lactone ring (Arroo *et al.*, 2002).

Camptothecin (Figure 1.1) (7) is a quinoline alkaloid first derived from the Chinese ornamental tree *Camptotheca acuminata* Fam. Nyssaceae in 1966. Camptothecin possesses high cytotoxic activity in a variety of cell lines with the major drawback being its high toxicity in urinary bladder (Rauter *et al.*, 2013). Topotecan and

irinotecan (Figure 1.1) (**8**, **9**), respectively, are semisynthetic derivatives of camptothecin and are used for the treatment of ovarian, lung and colorectal cancers (Creemers *et al.*, 1996; Bertino, 1997; Rahier *et al.*, 2005). All camptothecins are characterized by the presence of a labile lactone ring (Figure 1.1) (**7**, **8** and **9**). The hydroxyl group and S-conformation of the chiral center at C₂₀ in the lactone ring are essential for the biological activity of the compound. However, substitutions on the A and B rings of the quinoline alkaloid's moiety improve water solubility and enhance the potency of camptothecins (Brunton *et al.*, 2011).

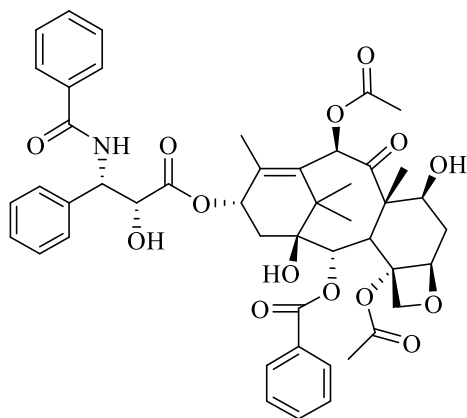


1

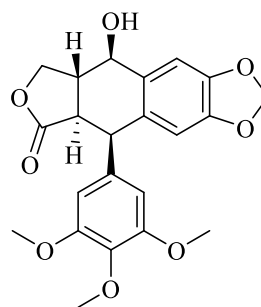


4

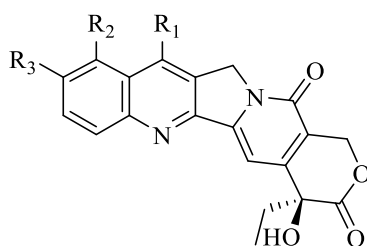
Compound No.	R
2	CH ₃
3	CHO



5



6



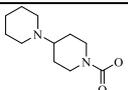
Compound No.	R ₁	R ₂	R ₃
7	H	H	H
8	H	(CH ₂)N(CH ₃) ₂ H	OH
9	H	H	

Figure 1.1: Anticancer natural products

1.1.4 Mechanism of action of anticancer natural products

Anticancer natural products act on multiple pathways to inhibit carcinogenesis by interfering with invasion, growth, survival, and metastasis. The wide activity spectrum of these products can result in suppression of tumour growth by induction of apoptosis, down-regulation of genes, anti-metastatic activity, and inhibition of microtubule function or alteration of the structure of DNA. A wide variety of mechanisms exist for anticancer activity. Different compounds have different mechanisms see 1.1.4.2

1.1.4.1 Mechanisms of cell death

There are two main types of cell death: apoptosis and necrosis. Necrotic cell death is caused by gross cell injury and results in the death of groups of cells within a tissue. It is characterized by cell swelling, cytoplasmic vacuoles formation, and swollen endoplasmic reticulum. Apoptosis is an alternative way of cell death to necrosis, it is a normal process of programmed cell death (happens during development) and is characterized by specific DNA changes and without any inflammatory response. It triggers if mistakes are identified in DNA replication. Loss of this protective mechanism would allow mutant cells to continue to divide and grow, thereby conserving mutations in subsequent cell divisions. Many anticancer agents and radiotherapy induce mutations in cancer cells, which are not sufficient to cause cell death, but which can be recognized by the cell, triggering apoptosis (Elmore, 2007; Payne & Miles, 2008; Matsuura *et al.*, 2016).

1.1.4.2 Classification of anticancer agents according to their chemical structure and mechanism of action

In general, anticancer drugs were categorized as chemotherapy, hormonal therapy, and immunotherapy. The chemotherapeutic agents can be classified according to their chemical structure and mechanism of action into the following classes: alkylating

agents, antibiotics, antimetabolites, mitosis inhibitors, platinum compounds and topoisomerase I and II inhibitors (Espinosa *et al.*, 2003; Payne & Miles, 2008).

Alkylating agents

Alkylating agents are compounds that specifically link with their alkyl group to a chemical moiety in nucleic acids or proteins by a covalent bond. Mostly, they are bipolar compounds, which help them to form bridges between DNA strands and to interfere with the enzymes action involved in DNA replication leading to cell death. The most serious damage happens during the S-phase because the cell has less time to get rid of the damaged fragments. Examples of these Alkylating agents are tetrazines, nitrogen mustards, nitrosureas, and procarbazine (Payne & Miles, 2008).

Antibiotics

Mostly, anticancer antibiotics have been produced from bacterial and fungal sources (*Streptomyces* species) by affecting the synthesis and function of nucleic acids in different pathways. For instance, anthracyclines antibiotics such as daunorubicin, doxorubicin, and epirubicin. These antibiotics intercalate with DNA and the enzyme topoisomerase II. The anthracyclines stabilize the DNA topoisomerase II complex and thus prevent reconnection of the strands (Payne & Miles, 2008).

Antimetabolites

Antimetabolites are compounds that compete with naturally occurring substances (due to the similarity in structure) such as amino acids, nucleosides, and vitamins for the active site of an essential enzyme or receptor. These antimetabolites may be phase-specific, i.e. act during the S-phase of the cell cycle or may be directly incorporated into DNA or RNA. These antimetabolites are folic acid antagonists, purine analogues and pyrimidine analogues (Payne & Miles, 2008).

Mitotic inhibitors

Vinca alkaloids are cell cycle specific agents that specifically target β tubulin (the building block of the microtubules) and block its polymerization with α tubulin, causing further inhibition of the microtubule mitotic spindle assembly, leading to metaphase arrest and subsequent inhibition of mitosis (Himes, 1991; Payne, 2008; Brunton *et al.*, 2011; Moudi *et al.*, 2013).

Paclitaxel and other taxanes bind to the protein tubulin, stabilizing and protecting microtubule against disassembly, leading to cell cycle arrest in mitosis. They differ from the vinca alkaloids in that they bind to a different β -tubulin site (Brunton *et al.*, 2011). Direct activation of apoptotic pathways has also been suggested to be critical to the cytotoxicity of these anticancer drugs. Paclitaxel may also have a role in treating some kinds of cancer by enhancing or mutating certain signaling factors (Cragg & Newman, 2004; Kingston, 2005; Payne 2008; Priyadarshini & Aparajitha, 2012).

Heavy metals

Platinum agents such as carboplatin, cisplatin, and oxaliplatin are organic heavy metal complexes, which diffuse into a cell, lose their ions and cross-link with the DNA strands (intra- and inter strand), resulting in inhibition of DNA, RNA and protein synthesis (Payne & Miles, 2008).

Topoisomerase inhibitors

The DNA topoisomerases are nuclear enzymes that are responsible for altering the 3D structure of DNA by reducing the twisting stress in supercoiled DNA, allowing selected regions of DNA to become sufficiently relaxed to ease replication, repair, and transcription. Topoisomerase I and II inhibitors mediate DNA strand breakage and resealing and have become the target of cancer therapy (Brunton *et al.*, 2011).

Camptothecin analogues irinotecan and topotecan act as topoisomerase I inhibitors (Rahier *et al.*, 2005). They bind to the topoisomerase I–DNA covalent complex preventing DNA replication. This binding yields an intermediate complex in, which the tyrosine of the enzyme is bound to the phosphate end of the DNA strand preventing DNA re-ligation during synthesis and causes the complex to collide with the replication fork, leading to DNA double-strand breaks and cell death (Brunton *et al.*, 2011). Podophyllotoxin derivatives etoposide and teniposide inhibit topoisomerase II enzyme preventing DNA synthesis and replication (Liu, 1989) These drugs form a stable ternary complex with topoisomerase II and DNA leading to their breakage and the accumulation of DNA strand breaks leads to cell-cycle arrest (Arroo *et al.*, 2002; Brunton *et al.*, 2011).

Despite the advancements in the treatment of cancer over the last decades, cancer is still one of the major causes of death. Currently, many anticancer drugs exhibit limited efficacy, severe side effects, and are expensive. For this reason, the discovery of novel anticancer agents that lack some of these disadvantages is still required. The Libyan Mediterranean Coast is characterized by its rich biodiversity. Its natural resources constitute a source of income for many poor rural people. In Libyan folk medicine, a number of medicinal plants have been used as remedies for cancers and tumours, but potential anticancer properties of these plants have not yet been fully and systematically investigated to provide the scientific rationale for their folklore uses (Elmezogi. *et al.*, 2013).

The current study has been designed to evaluate four selected medicinal plants (*Arbutus pavarii*, *Asphodelus aestivus*, *Juniperus phoenicea* and *Ruta chalepensis*) from the Libyan flora as putative sources of anticancer agents and incorporates a

rational, systematic bioassay-guided phytochemical and cytotoxic/anticancer approach aimed at discovering any bioactive molecules that may be responsible for their reported cytotoxic/anticancer activity.

1.2 The family Asphodelaceae

The Asphodelaceae is a relatively small but widespread plant family. It is widely distributed in the arid areas throughout South Africa, but some species occur naturally in the Mediterranean region e.g. *Asphodelus* species (Dagne & Yenesew, 1994; Heinrich *et al.*, 2012; Myanmar Medicinal Plant Database, 2006).

1.2.1 Classification of the family Asphodelaceae

The Asphodelaceae family is represented by 12 genera and 600 species. The Asphodelaceae is often included in the Liliaceae family, which comprises more than 250 genera and 3700 species. It has recently been reclassified into smaller families namely, the Asphodelaceae, Alliaceae, Asparagaceae, Dracaenaceae, Eriospemiaceae, and Hyacinthaceae. The Asphodelaceae family consists of the sub-families Asphodeloideae and Alooideae (Dagne & Yenesew, 1994). The widely recognized genera in the sub-family Asphodeloideae are *Asphodeline*, *Asphodelus*, *Bidbine*, *Eremriis*, *Emiphlacirs*, *Jodrellia*, *Paradisea*, *Sirnethis*, and *Trachandra*. However, a few genera are identified in the succulent sub-family Alooideae, namely *Aloe*, *Astroloba*, *Chortolirion*, *Gasteria*, *Haworthia*, and *Kniphofia*. Most species classified under this family, are perennial herbs with rhizomes and bulbs (Dagne & Yenesew, 1994; Treutlein *et al.*, 2003).

1.2.2 Chemical characteristics of the family Asphodelaceae

The phytochemical information on the Asphodelaceae family is still quite sparse. Therefore, it is so difficult to provide a general chemotaxonomic data. However, most species of this family are rich in anthraquinones and anthraquinone glycosides, which are responsible for the laxative effect of these species. The most commonly known anthraquinones are aloe-emodin, anthrone-C-glycosides, and chrysophanol. Polysaccharides also accumulate in the gel of the *Aloe vera* leaves. Many of the health benefits associated with *Aloe vera* have been attributed to the polysaccharides (Dagne & Yenesew, 1994; Heinrich *et al.*, 2012; Myanmar Medicinal Plant Database, 2006).

1.2.3 Traditional uses of the family Asphodelaceae

Most species of the Asphodelaceae family have been used traditionally as laxatives and purgatives. They have also been used in the treatment of arthritis, hypertension, stress, eczema, skin irritations and burns. *Aloe* leaves are extensively used in the cosmetics preparations and for the treatment of many diseases (Edhun & Qian, 2010; Radha & Laxmipriya, 2015).

1.2.4 The genus *Asphodelus* L.

The genus *Asphodelus* consists of approximately 17 species, namely, *Asphodelus acaulis*, *A. aestivus*, *A. ayadii*, *A. bakeri*, *A. bentorainhae*, *A. cerasiferus*, *A. fistulosus*, *A. gracilis*, *A. lusitanicus*, *A. macrocarpus*, *A. ramosus*, *A. refractus*, *A. roseus*, *A. serotinus*, *A. tenuifolius* and *A. viscidulus*. The species are rich in anthranoids, anthraquinones glycosides, flavonoids, steroids, triterpenes (El-Fattah *et al.*, 1997; Calis *et al.*, 2006).

1.2.4.1 Active constituents of the genus *Asphodelus*

The genus *Asphodelus* has also been extensively studied, again because it contains a variety of valuable active ingredients. Its species are rich in anthranoids, anthraquinones glycosides, flavonoids, steroids and triterpenes (El-Fattah *et al.*, 1997; Calis *et al.*, 2006).

1.2.4.2 Traditional uses of the genus *Asphodelus*

Several species of the genus *Asphodelus* have been used in folk medicine in the treatment of skin disorders such as psoriasis, parasites and microbial infection and as skin lightening agents in freckles (Petrillo *et al.*, 2016).

1.2.5 *Asphodelus aestivus* Brot.

Asphodelus aestivus (Figure 1.3), commonly known as White Asphodel or Gamon is a common spring-flowering geophyte distributed along the Southern Alps to the western Balkans, in meadows and heathland of central Spain. It is also found in the continent Africa, mainly in Libyan territory.

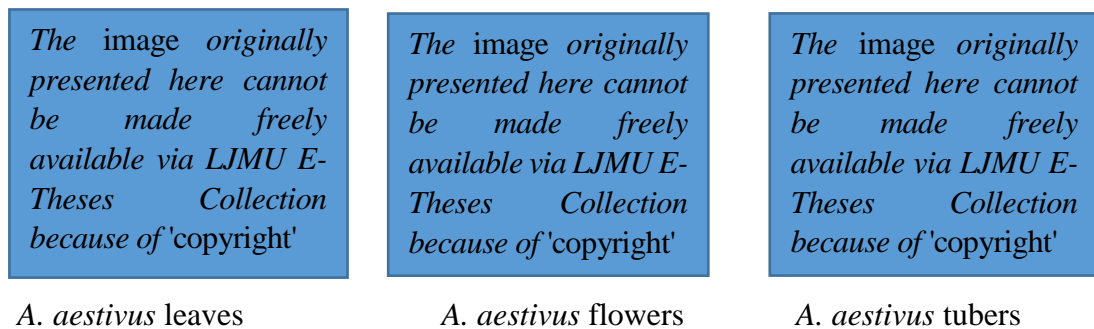


Figure 1.2: *Asphodelus aestivus*

1.2.5.1 Traditional uses of *A. aestivus*

A. aestivus has been utilized traditionally for culinary and medicinal purposes. Traditionally, the tuber and roots of this plant are used to treat hemorrhoids, nephritis, burns, wounds and some skin diseases (Aslantürk & Çelik, 2013). It has been also used in the eastern Mediterranean region of Libya for the treatment of arthritis, rheumatic diseases, ovulation and skin diseases (El-Mokasabi, 2014).

1.2.5.2 Previous phytochemical work of *A. aestivus*

All the previous phytochemical investigations performed on the tubers of *Asphodelus* species resulted in the isolation of anthranoides, flavonoids and triterpenes. However, a study applied by Calıs *et al.* in 2006 on the fresh leaves of *A. aestivus* revealed also the presence of flavone C-glycosides, anthranoides (1, 8-dihydroxy-anthraquinones), adenosine nucleoside, two amino acids, phenylalanine (**10**) and tryptophan (**11**), and chlorogenic acid (**12**) (Calıs *et al.*, 2006; Birincioglu *et al.*, 2015).

Anthranoids

Three anthranoides were isolated from the MeOH extract of *A. aestivus* leaves by using chromatographic techniques (CC) using Sephadex LH-20. These anthranoides are aloe-emodin (**13**), aloe-emodin acetate (**14**) and chrysophanol 1-*O*-gentiobioside (**15**) (Calıs *et al.*, 2006).

Flavonoids

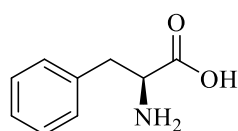
Five flavone C-glycosides were isolated from the water-soluble part of the MeOH extract of *A. aestivus* fresh leaves. These flavonoids are isoorientin (**16**), isovitexin (**17**), isoorientin 4'-*O*- β -glucopyranoside (**18**), 6''-*O*-(malonyl)-isoorientin (**19**) and

6''-O-[(S)-3-hydroxy-3-methylglutaroyl]-isoorientin (**20**). The main components of the extract are apigenin (**21**), luteolin (**22**) and their β -D-glucopyranosides. (Calis *et al.*, 2006).

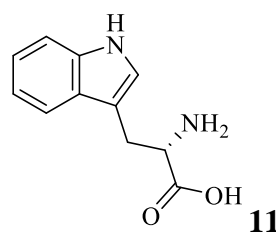
Micellaneous

The isolated oil from *A. aestivus* seeds was analyzed by gas chromatography (GC) to reveal two components, butyric acid (76.26%) and nervonic acid (3.65%), which were identified by GC-FID and GC/MS analysis (Fafal *et al.*, 2016).

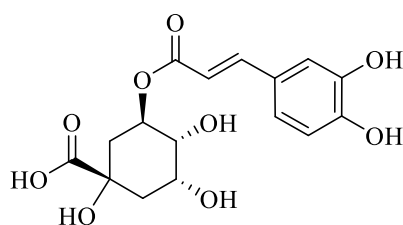
High amounts of *n*-alkanes, saturated fatty acids and minor amounts of acyclic diterpenes were isolated from the flowers essential oil of *A. aestivus* from Cyprus. Seventeen compounds were identified in the essential oil comprising 96.2% of the oil. The major components of the essential oil were hexadecanoic acid 35.6%, pentacosane 17.4%, tricosane 13.4% and heptacosane 8.4% (Polatoğlu *et al.*, 2016).



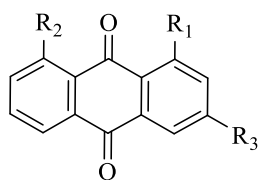
10



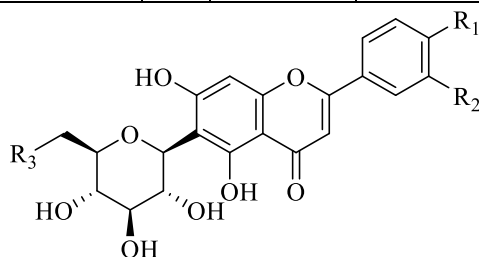
11



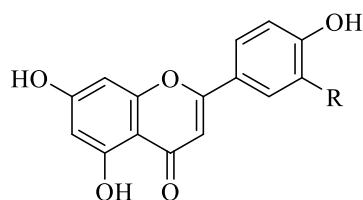
12



Compound No.	R ₁	R ₂	R ₃
13	OH	OH	-CH ₂ OH
14	OH	OH	-CH ₂ -OCOCH ₃
15	OH	O-Glu-Glu	-CH ₃



Compound No.	R ₁	R ₂	R ₃
16	OH	OH	OH
17	OH	H	OH
18	-O-Glu	OH	OH
19	OH	OH	-O-CO-CH ₂ -COOH
20	OH	OH	-O-CO-CH ₂ -C(CH ₃)(OH)-CH ₂ -COOH



Compound No.	R
21	H
22	OH

Figure 1.3: Isolated compounds from *A. aestivus*

1.2.5.3 Previous biological work of *A. aestivus*

Toxicity

A severe neurologic syndrome with intense neuronal pigmentation was reported in the sheep after ingestion of *A. aestivus* leaves and seeds in the meadow in Aydin region (Turkey.) Neurological signs were observed, such as ataxia, paresis, and convulsion. Toxicity was reported for anthranoids (from the green leaves of *Asphodelus* spp.) and bianthrone C-glycosides in tubers of *Asphodelus* spp. (Birincioglu *et al.*, 2015).

The antioxidant activity

A study was undertaken in Turkey on *A. aestivus* leaves to investigate the antioxidant activity of the plant. The study analyzed the total flavonoid, the contents of chlorophyll and carotenoid, the metal chelating ability, the carotene bleaching effect and the antioxidant activity, 2,2-diphenyl-1-picryl-hydrazyl (DPPH), 2,2'-azino-bis (3-ethylbenzothiazoline-6sulfonic acid) diammonium salt (ABTS), *N, N*-dimethyl-*p*-phenylenediamine dihydrochloride (DMPD), superoxide, hydroxyl and nitric oxide (NO) scavenging assays. The results revealed that they all had strong antioxidant activity. The radical scavenging and the metal chelating activities of the aqueous extract were higher than that of the ethanolic extract whereas the ethanolic extract revealed higher levels of carotene bleaching activity (Peksel *et al.*, 2012; Peksel *et al.*, 2013). However, another antioxidant study was applied on the tubers of *A. aestivus*, which also showed significant scavenging antioxidant activity using the (DPPH) assay (Aslantürk, 2013).

The antimicrobial activity

The antifungal activity of both the ethanol and water extracts of *A. aestivus* leaves was tested against *Aspergillus niger*. The results showed higher activity in the ethanol

extract than water extract at the concentrations of 0.25 and 0.50 mg/mL. However, both the ethanol and water extracts exhibited similar activities at the concentration of 1 mg/mL. Standard antifungal drug fluconazole exhibited higher activity than the extracts tested (Peksel *et al.*, 2012).

The antimicrobial activity of the oil from *A. aestivus* seeds was assessed against both Gram+ve and Gram-ve bacteria and three strains of yeast using the disc diffusion and broth micro-dilution methods. The oil showed moderate antibacterial activity against *Escherichia coli*, *Klebsiella pneumonia*, *Pseudomonas aeruginosa*, *Staphylococcus aureus*, *Staphylococcus epidermidis*, and as well as antifungal activity against *Candida albicans* and *Candida krusei* (Fafal *et al.*, 2016).

The antimicrobial activity of *A. aestivus* tuber extracts (*n*-hexane, MeOH, and aqueous extracts) was assessed against seven species of bacteria and two strains of fungus. The results showed higher antibacterial activity against Gram+ve bacteria than the Gram-ve bacteria with the highest activity in the *n*-hexane layer (Bozyel *et al.*, 2016).

The cytotoxic activity

The cytotoxic and apoptotic activities of *A. aestivus* extracts on MCF-7 breast cancer cells were evaluated by trypan blue exclusion assay, comet assay and Hoechst propidium iodide double staining (Aslantürk & Celik, 2013). The results demonstrate that cytotoxic and apoptotic properties of *A. aestivus* extract show differentiation to extract type. Several studies have demonstrated that the main anthraquinones of rhubarb: emodin, aloe-emodin, and rhein, inhibit the growth and proliferation of various cancer cells (Huang *et al.*, 2007).

The pesticidal activity

The roots of *A. aestivus* Brot. were investigated against *Tetranychus cinnabarinus* Boisd (the carmine spider mite) as a biopesticide. The root extract revealed ovicidal activity and reduced hatched number compared with the standard dicofol. The results showed the strong acaricide activity of the root extract, which could be helpful in reducing environmental pollution associated with synthetic pesticides used in the management of pest programmes (Gencsoylu, 2009).

1.3 The family Cupressaceae

The Cupressaceae consists of ornamental plants. It is characterized by monoecious, subdioecious or (rarely) dioecious shrubs and trees, the leaves are scale to linear, opposite or whorled and usually paired or in threes, the ovules of female cones: 1-20/cone scale; the cone scales are fused to bracts. The microsporangia of male cones: 2-10/ microsporophyll; the pollen is usually without any appendages. Members of this family are found worldwide, but particularly in North Africa, Mediterranean region, and South America. This family includes all the gymnosperm family, which are considered as the most important conifer family in recent horticulture. Members of this family are important for their woody plants, fruit, and resinous matter and as ornamentals (Bell & Hemsley, 2001; Encyclopedia Britannica 2012; Taghreed *et al.*, 2017).

1.3.1 Classification of the family Cupressaceae

The family Cupressaceae is considered as the largest conifer family in terms of genera, and the third-largest one in terms of species, it includes 27 genera and 142 species and is usually placed in the order Pinales. The following is the botanical taxon of the family:

Kingdom: Plantae

Subkingdom: Tracheobionta (Vascular plants)

Superdivision: Spermatophyta (seed plants)

Division (Phylum): Coniferophytes (Conifers plants)

Class: Pinopsida

Order: Pinales

Family: Cupressaceae

The following are the genera included in the Cupressaceae family: *Chamaecyparis*, *Cryptomeria*, *Cunninghamia*, *Cupressus*, *Diselma*, *Fitzroya*, *Glyptostrobus*, *Juniperus*, *Libocedrus*, *Metasequoia*, *Microbiota*, *Neocallitropsis*, *Papuacedrus*, *Platycladus*, *Sequoia*, *Sequoiadendron*, *Taiwania*, *Taxodium*, *Tetraclinis*, *Thuja*, *Thujopsis* and *Widdringtonia* (Rich. ex Bartling. 1830. Cupressaceae. The Gymnosperm Database, assessed on 12-2017).

1.3.2 Chemical characteristics of the Cupressaceae family

Numerous publications have reported the presence of many biologically active compounds from the Cupressaceae such as bioflavonoids, diterpenes, essential oils and sterols (List & Horhammer, 1979; Morte & Honrubia, 1996).

1.2.3 Traditional uses of the Cupressaceae

Many species of the Cupressaceae family have been used traditionally as antiseptic, antispasmodic, antipyretic, astringent, decongestant, respiratory antiseptic (Ibrahim *et al.*, 2017).

1.2.4 The genus *Juniperus* L.

The *Juniperus* is the largest genus in the family Cupressaceae. It consists of approximately 60 species. These are distributed in the northern hemisphere from the Arctic Circle to the African Tropics Mountains. The genus *Juniperus* has been categorized into three sections: Caryocedrus, oxycedrus, and sabina. Caryocedrus is mainly distributed in the eastern Mediterranean region whereas, the other two sections are distributed throughout the Northern Hemisphere (Zanoni & Adams, 1975; Seca & Silva, 2005).

1.3.4.1 Species of the genus *Juniperus*

The following are some juniper species included in the genus *Juniperus*

Juniperus angosturana, *J. arizonica*, *J. ashei*, *J. barbadensis*, *J. bermudiana*, *J. blancoi*, *J. brevifolia*, *J. californica*, *J. cedrus*, *J. chinensis*, *J. coahuilensis*, *J. comitana*, *J. communis*, *J. convallium*, *J. deppeana*, *J. drupacea*, *J. durangensis*, *J. excelsa*, *J. flaccida*, *J. foetidissima*, *J. formosana*, *J. gracilior*, *J. horizontalis*, *J. indica*, *J. jaliscana*, *J. komarovii*, *J. maritima*, *J. martinezii*, *J. monosperma*, *J. monticola*, *J. occidentalis*, *J. osteosperma*, *J. oxycedrus*, ***J. phoenicea***, *J. pinchotii*, *J. pingii*, *J. poblana*, *J. procera*, *J. procumbens*, *J. przewalskii*, *J. pseudosabina*, *J. recurva*, *J. rigida*, *J. sabina*, *J. saltillensis*, *J. saltuaria*, *J. saxicola*, *J. scopulorum*, *J. semiglobosa*, *J. squamata*, *J. standleyi*, *J. taxifolia*, *J. thurifera*, *J. tibetica*, *J. virginiana*, (Linnaeus, 1753; Kangshan *et al.*, 2010).

1.3.4.2 Active constituents in the genus *Juniperus*

The genus *Juniperus* is considered as the main source of cedarwood oil, which has high industrial importance. The genus revealed the presence of terpenoids

(sesquiterpenoids, bicyclic diterpenoids, and tricyclic diterpenoids), coumarins, flavonoids, lignans and with significant biological activity (Seca & Silva, 2005).

1.3.4.3 Traditional uses of the genus *Juniperus*

Juniperus species have been used traditionally as antiseptic, antitussive, diuretic, carminative, hypoglycaemic, haemostatic activities, antifertility agents, stomachic and carminative and as cold remedies. They have also been used in the treatment of rheumatic arthritis and urinary infections (Prakash, 1986; Swanston-Flatt *et al.*, 1990; Wichtl, 1994; But *et al.*, 1997; Wang *et al.*, 2002). In Saudi Arabia, *Juniperus* species have been used as a remedy for jaundice and tuberculosis, whereas in Bhutan, they are used as an insect repellent and for treatment of fever. On the whole, these traditional uses have supporting positive scientific evidence showing various bioactivities of *Juniperus* species (Seca & Silva, 2005).

1.2.5 *Juniperus phoenicea* L.

Juniperus phoenicea (Phoenician Juniper or Arâr) (Figure 1.5) is an evergreen plant usually growing as either a bush or tree. It is distributed throughout the Mediterranean region, ranging from Morocco and Portugal east to Turkey and Egypt. It is also found in Madeira, the Canary Islands and on the mountains of Western Saudi Arabia near the Red Sea. It mostly prefers to grow at low altitudes close to the coast but can be found at an altitude of 2,400 m in the south of its range within the Atlas Mountains (El Sawi & Motawe, 2008). *J. phoenicea* is a well-known Libyan medicinal plant, which has been used in the Libyan traditional medicine for the treatment of various human ailments. Although 70 *Juniperus* spp. grow throughout the world, only *J. phoenicea* and *J. oxyderus* are found in Libya.

The image originally presented here cannot be made freely available via LJMU E-Theses Collection because of 'copyright'

The image originally presented here cannot be made freely available via LJMU E-Theses Collection because of 'copyright'

Figure 1.4: *Juniperus phoenicea*.

1.3.5.1 Traditional uses of *J. phoenicea*

J. phoenicea has been used in Libyan traditional medicine for the treatment of various human ailments including tumours and cancers. This plant is used in folk medicine to treat rheumatism, gout, oedema, diarrhoea, poor appetite and urinary tract diseases. It is also reported to eliminate gastrointestinal bacteria and parasites (Qnais *et al.*, 2005; Aljaiyash *et al.*, 2014). Some tribes use it as a female contraceptive (Aljaiyash *et al.*, 2014). The juniper berry has been studied as a possible treatment for diet-controlled diabetes mellitus (Sánchez de Medina *et al.*, 1994).

1.3.5.2 Previous phytochemical work of *J. phoenicea*

Several compounds have previously been isolated from the leaves and berries of *J. phoenicea* grown in various countries i.e., carbohydrates, fatty acids, furanone glycosides, phenolics (e.g., flavonoids and biflavones, phenylpropanoids and lignans), terpenoids and sterols (El-Sawi *et al.*, 2007; El-Sawi & Motawe, 2008; Ennajar, *et al.*, 2010; Derwich, *et al.*, 2011; El-Sawi *et al.*, 2013; Alzand *et al.*, 2014) (Figure 1.5).

Coumarins

Eight species from the genus *Juniperus* revealed the presence of six coumarins but only the coumarin skimmin compound (**23**) was detected in *J. phoenicea* (Figure 1.5) (Comte *et al.*, 1996; Seca & Silva, 2007).

Flavonoids

More than sixty flavonoid compounds were identified in different *Juniperus* species mainly biflavonol and flavone derivatives. The following flavonoids were isolated from *J. phoenicea* compounds (**24-27**): cupressuflavone (**24**), amentoflavone (**25**), hinokiflavone (**26**) and robustaflavone (**27**) (Fatma *et al.*, 1979; Seca & Silva, 2007).

Lignans

Sixty-two lignans were isolated from different *Juniperus* species. The lignan Podophyllotoxin found in small amounts in these species. A study published in 1998 by Muranaka *et al.* about the production of podophyllotoxin by callus culture of *J. chinensis*, to increase its production (Muranaka *et al.*, 1998; Seca & Silva, 2007). The following lignans were reported from *J. phoenicea*, compounds (**28-30**) (Seca & Silva, 2007): β -methylpeltatin A (**28**), deoxypodophyllotoxin (**29**) (Cairnes *et al.*, 1980; Dawidar *et al.*, 1991; San Feliciano *et al.*, 1992) and shonanin (**30**) (San Feliciano *et al.*, 1993; Hussein *et al.*, 2003).

Sterols

Four types of sterols were revealed in different species of the *Juniperus* (Seca & Silva, 2007). Sitosterol is the most abundant one in these species and only β -sitosterol (**31**) was isolated by Tabacik and Laporthe from *J. phoenicea* in 1971 (Seca & Silva, 2007).

Terpenoids

Terpenoids (sesqui-, di- and triterpenoids) have been used as special chemosystematic markers in conifers (Otto and Wilde, 2001), being both cuparanes and widdranes were restricted to species of the family Cupressaceae. Triterpenes were not identified yet in *Juniperus* species and monoterpenes were mainly detected in juniper essential oil.

Monoterpenes:

Monoterpenes (Figure 1.6) predominantly α -pinene (**32**), β -carene (**33**), limonene (**34**), myrcene (**35**), phellandrene (**36**), sabinene (**37**), and terpinyl acetate (**38**) were identified in berries and leaves of *J. phoenicea* ssp. from different regions with chemical variability in their composition (Angioni *et al.*, 2003; Cosentino, *et al.*, 2003; Barrero *et al.*, 2006; El-Sawi *et al.*, 2007; Achak *et al.*, 2008; Ennajar, *et al.*, 2009; Ennajar, *et al.*, 2010; Mazari *et al.*, 2010; Ait-Ouazzou *et al.*, 2012; Bekhechi *et al.*, 2012).

Sesquiterpenoids:

A large number of sesquiterpenoid classes are identified in the *Juniperus* genus (Seca & Silva, 2007). The following sesquiterpenoids were isolated from *J. phoenicea*: α -cadinol methyl ether, β -caryophyllen, caryophyllene oxide, elemol (Dawidar *et al.*, 1991), γ -cadinene (**39**), β -selinene, germacrene and α -humulene (**40**) (Dawidar *et al.*, 1991; San Feliciano *et al.*, 1992; Seca & Silva, 2007).

Bicyclic diterpenoids:

Bicyclic diterpenes, mainly the diterpene labdane type are found in the *Juniperus* genus (Seca & Silva, 2007). The following diterpenoids were isolated from *J. phoenicea*: eperu-13(14)-ene-8 β ,15-diol, labd-8(17)-ene-12-hydroxy-19-oic acid (Tabacik and Laporthe, 1971), 8,15-dihydroxy-labda-13*E*-en-19-oic acid (San Feliciano *et al.*, 1992), sclareolic acid (San Feliciano *et al.*, 1993), imbricatolic acid, imbricatalic acid (**41**), 15-methyl-imbricatalic acid, (+)-enantio-oliveric acid, *cis*-communic acid and *trans*-communic acid (Tabacik and Laporthe, 1971; Pascual-Teresa *et al.*, 1978; Dawidar *et al.*, 1991; Barrero *et al.*, 2004).

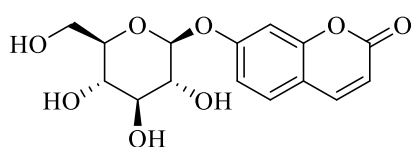
Tricyclic diterpenoids:

A large number of the tricyclic diterpenes, exclusively abietane, labdane, and pimarane type, were isolated from the *Juniperus* species (Seca & Silva, 2007). The following diterpenes were isolated from the leaves and the fruits of *J. phoenicea*: sandaracopimaric acid (**42**), 3 β -hydroxy-sandaracopimaric acid (**43**), pimaric acid (**44**), 3 α -acetoxy-labda-8,13(16)-14-triene-19-oic acid (juniperexcelsic acid), 3 α -hydroxy-labda-8(17), 13(16)-14-triene-19-oic acid, 4-epi-abietic acid, 4-epi-abietol, dehydroabietic acid (**45**) and dihydroxyabieta-8,11,13-triene-1-one (San Feliciano *et al.*, 1992; Comte *et al.*, 1995; El Sawi & Motawe, 2008; González *et al.*, 2010).

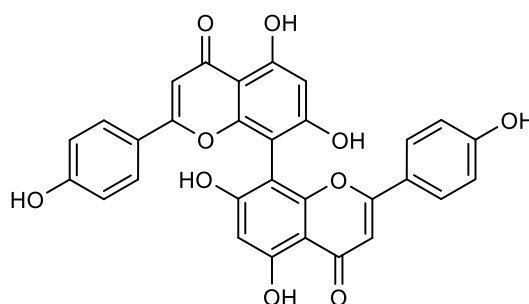
Phenylpropane glycosides:

Juniperoside was isolated from the acetone extract of the aerial parts of *J. phoenicea*. Two phenylpropanoids, junipetriolside A (3-methoxy-4-hydroxy-phenylpropane-7,8-(2',1'-*O*- β -D-glucopyranosyl-7,8,9-triol) and junipetriolside B (3-methoxy-4-*O*- β -D-glucopyranosyl-phenylpropane-7,8,9-triol) were isolated from the MeOH extract of *J. phoenicea* aerial parts along with the rare compound, guaiacylglycerol (3-

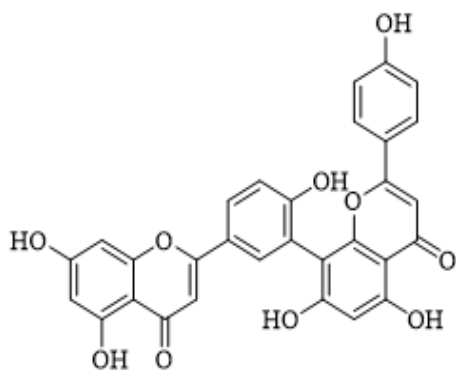
methoxy-4-hydroxy-phenylpropane-7,8,9,-triol) (Comte *et al.*, 1997). Two norterpenoids were isolated from the aerial parts of *J. phoenicea*, which are 3-oxo- α -ionol glucosides named junipeionoloside and 6-hydroxy-junipeionoloside & along with a known norterpenoid glucoside: roseoside, dearabinosyl pneumonanthoside and a sesquiterpenoid glucoside, dihydrophaseic acid 4'-O- β -D-glucopyranoside (Champavier *et al.*, 1999).



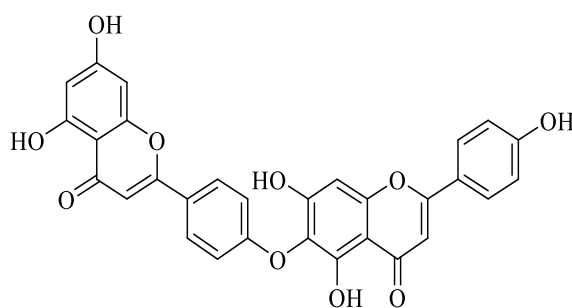
23



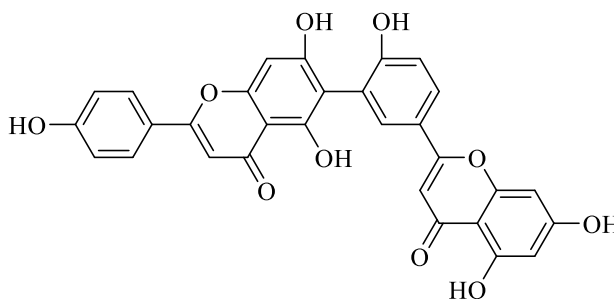
24



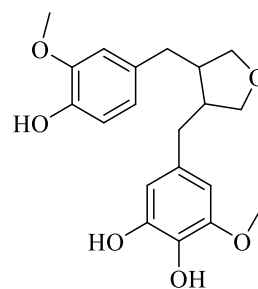
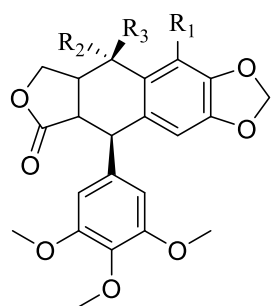
25



26

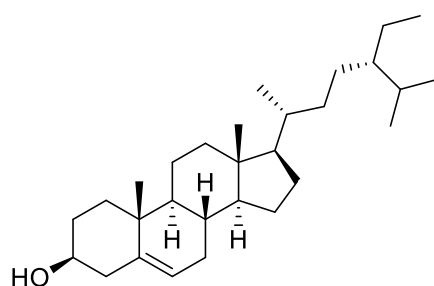


27

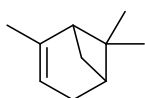


30

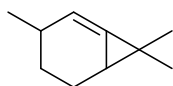
Compound No.	R ₁	R ₂	R ₃
28	OCH ₃	H	H
29	H	H	H



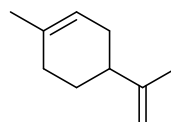
31



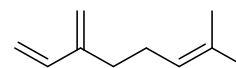
32



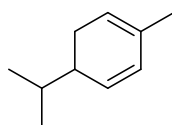
33



34



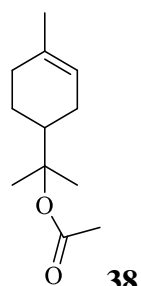
35



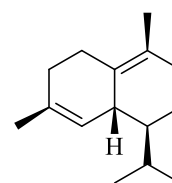
36



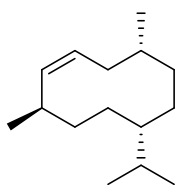
37



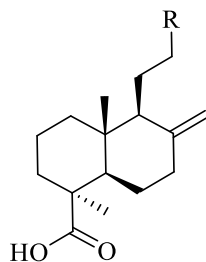
38



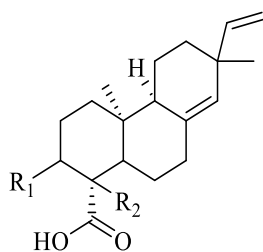
39



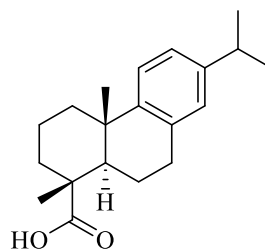
40



Compound No.	R
41	-CH(CH ₃)(OH)-CH=CH ₂
42	-CH(CH ₃)-CH ₂ -CH ₂ -OH



Compound No.	R ₁	R ₂
43	H	H
44	OH	H
45	H	CH ₃



46

Figure 1.5: Isolated compounds from *J. phoenicea*

1.3.5.3 Previous biological work of *J. phoenicea*

Various biological activities for *J. phoenicea* have been reported to date.

Toxicity study

The median lethal doses (LD₅₀) of the total and successive extracts of *J. phoenicea* L. growing in Egypt revealed the safety of the plant. The leaf extract was less toxic than the fruit extract where their LD₅₀ recorded 7.9 g. kg⁻¹ b.wt and 7.5 g. kg⁻¹ b.wt, respectively (El-Sawi *et al.*, 2013).

The antioxidant activity

Antioxidant activity of this plant was determined using the ABTS radical-scavenging assay with the strongest antioxidant effect being found with the MeOH extract (Ennajar *et al.*, 2009; Ennajar *et al.*, 2010). Evaluation of fruit extracts of Turkish *Juniperus* species for their antioxidant, anticholinesterase, and antimicrobial activities revealed the effective inhibition of linoleic acid oxidation by the MeOH extract of *J. phoenicea* (Ozturk *et al.*, 2011).

The antimicrobial activity

J. phoenicea essential oils from different countries exhibited moderate antibacterial and antifungal activities (Stassi *et al.*, 1996; Angioni, *et al.*, 2003; El-Sawi, *et al.*, 2008; Derwich *et al.*, 2010; Ennajar, *et al.*, 2010; Mazari *et al.*, 2010; Ait-Ouazzou, *et al.*, 2012; Alzand *et al.*, 2014). Elmhdwi *et al.* (2015) demonstrated that the extracts from *J. phoenicea* had antibacterial activity against both Gram +ve and Gram -ve bacteria including multiple-drug-resistant (MDR) strains. This activity was attributed to the abundance of α -pinene and the overall chemical constituents of these extracts.

Accordingly, the Sardinian *Juniperus* essential oils and the isolated compound δ -3-carene showed antimicrobial activity against fungi, particularly *Aspergillus flavus*, when tested on some foodborne pathogens and spoilage microorganisms (Cosentino, *et al.*, 2003). Two studies were applied on the Algerian *J. phoenicea* essential oils, the first study was applied against five bacterial strains (three Gram +ve and two Gram -ve), and 3 fungi and showed a moderate antibacterial and antifungal activities (Khadidja & Nassima, 2010). The second study was applied against nine bacterial strains, *e.g.*, *Enterobacter cloacae*, *E. coli*, *Pseudomonas syringae*, *Salmonella sp.*, *Serratia liquefaciens*, *S. marcescens*, *Shigella sp.*, *S. aureus*, *S. aureus* (MRSA). The

results showed that the Gram-ve bacteria were more resistant than the Gram+ve bacterial strains (Ramdani1 *et al.*, 2013). The antiviral activities of fifty extracts prepared from fifteen species of Tunisian traditional medicinal plants (including the extract of *J. phoenicea* aerial parts) were tested against *herpes simplex* virus type 1 (HSV-1). Only eight extracts showed some degree of antiviral activity where *J. phoenicea* did not exhibit any antiherpetic activity. (Sassi, *et al.*, 2008). Notably, the essential oils of *J. phoenicea* leaves and berries are grown in Egypt showed high activity against *A. flavus*, *Bacillus subtilis*, *Candida pseudotropicalis*, *E. coli*, and *S. aureus* (El-Sawi *et al.*, 2007). Another study was applied by Ennajar *et al.*, 2010, showed that essential oils strongly inhibited the growth of Gram+ve microorganisms and *Mucor ramannianus*, but was inactive against Gram-ve strains (Ennajar *et al.*, 2010). Lastly, the antimicrobial activity of *Mentha pulegium*, *J. phoenicea* and *Cyperus longus* essential oils from Morocco has been evaluated against seven bacterial strains of significant importance for food hygiene (four Gram +ve, *S. aureus*, *Enterococcus faecium*, *Listeria monocytogenes* and *L. monocytogenes* and three Gram -ve bacteria: *Salmonella Enteritidis*, *E. coli* and *Pseudomonas aeruginosa*). According to the results, *M. pulegium* showed the best bacteriostatic and bactericidal effect, followed by *J. phoenicea* and *C. longos* (Ait-Ouazzou *et al.*, 2012).

The antidiarrhoeal activity

The aqueous extract of *J. phoenicea* showed an antidiarrhoeal effect *in vivo* on experimental rat models of diarrhoea by reducing intestinal fluid accumulation and inhibiting intestinal motility (Qnais *et al.*, 2005).

The cytotoxic activity

The cytotoxicity of the abietane diterpenoids isolated from Moroccan *J. phoenicea* and *J. thurifera* was tested against five tumour cell lines (A-549, HCT-116, PSN1, SKBR3 and T98G cell lines) and one normal BAE-1 cell line. Three of the abietane derivatives showed cytotoxic activity at 2.5 µg/mL (Barrero *et al.*, 2004). *J. phoenicea* extracts obtained using different pressures (200 and 300 bar) showed cytotoxic activity against different cell lines and were also active against a single-stranded RNA⁺virus (Marongiu *et al.*, 2004). The essential oils of *J. phoenicea* leaves and berries grown in Egypt showed high cytotoxic activities against brain and cervix human cell lines, while berry oil was slightly more active than leaf oil against lung, liver, and breast human cell lines (El-Sawi *et al.*, 2007).

The cytotoxic activity of the extracts of *J. phoenicea* fruits grown in Egypt against *Erlich ascitis* carcinoma was confined to petroleum ether extract, which was also highly active against three human tumour cell lines, namely, liver, lung, and breast carcinoma cell lines. Seven diterpenes were isolated from the petroleum ether fruit extracts together with β-sitosterol and tested against a human liver carcinoma cell line. Four diterpenes (sandaracopimaric acid, juniperexcelsic acid, 4-*epi*-abietic acid, 4-*epi*-abietol) showed higher activity than cisplatin (El Sawi & Motawe, 2008).

Cairnes & Ekundayo (1980) showed that the ethanolic extract of *J. phoenicea* twigs and leaves and two isolated compounds, desoxi-podophyllotoxin and *p*-peltatin-methyl ether, were cytotoxic in the KB cell cultures (human cervix carcinoma). A MeOH extract of *J. phoenicea* from Saudi Arabia and Indonesia displayed high cytotoxicity in Vero (normal monkey kidney) and HEP-2 (human laryngeal carcinoma) cell lines (Latif *et al.*, 2014). In addition, this plant was also displayed

significant cytotoxicity against both MCF7 (human breast adenocarcinoma) and HCT-116 (human colon carcinoma) cell lines (Aljaiyash *et al.*, 2014).

1.4 The family Ericaceae

The Ericaceae is represented by 124 genera and approximately 4250 species and it is considered the 14th species-rich family in the flowering plants (Stevens, 2001; Christenhusz & Byng, 2016).

The botanical taxon of the family is classified as follows:

Kingdom: Plantae

Subkingdom: Tracheobionta (Vascular plants)

Superdivision: Spermatophyta (seed plants)

Division: Magnoliophyta (flowering plants)

Class: Magnoliopsida- Dicotyledons

Subclass: Dilleniidae

Order: Ericales

Family: Ericaceae –Health family

The following are some genera from the Ericaceae family: *Agarista*, *Andromeda*, *Arbutus*, *Arctostaphylos*, *Bejaria*, *Calluna*, *Cassiope*, *Chamaedaphne*, *Elliotia*, *Erica*, *Galtheria*, *Oxydendrum*, *Symphyia*, and *Zenobia* (Kartesz *et al.*, 2018).

1.2.1 Traditional uses of the family Ericaceae

Some members of Ericaceae family produce fleshy berries which are edible and commonly eaten fresh or dried. Traditionally some genera are used as antiseptic,

diuretics and laxatives and in the treatment of a headache, arterial hypertension, arthritis and urinary infections (Migue *et al.*, 2014; Pavlović *et al.*, 2014).

1.4.2 The genus *Arbutus* L.

The genus *Arbutus* L. belongs to the subfamily *Arbutioideae* or *Vaccinioideae* and the family Ericaceae or Arbuteae. It includes approximately twelve species; three are distributed in the Mediterranean region and Europe (*A. andrachne*, ***A. pavarii***, and *A. unedo*), eight in America, mainly in Mexico (*A. arizonica*, *A. glandulosa*, *A. Gray*, *A. madrensis*, *A. mollis*, *A. occidentalis*, *A. tessellate* and *A. xalapensis*) and one in the Canary Islands (*A. canariensis*). *Arbutus pavarii* Pampanini is a species endemic to Al-Jabal El-Akhdar on the Northeastern coast of Libya (González–Elizondo. *et al.*, 2012; Alsabri *et al.*, 2013; Miguel *et al.*, 2014).

1.4.2.1 Active constituents in the genus *Arbutus*

The phytochemical studies on the *Arbutus* Genus revealed the presence of many constituents such as flavonoids, irridoid glycosides, organic acids, phenolic compounds, tannins, sterols and triterpenes (Hasan *et al.*, 2011).

1.2.1.2 Traditional uses of the genus *Arbutus*

The *Arbutus* species are cultivated as ornamental and food plants. The leaves and barks are traditionally used for treatment of cold and tuberculosis (Hasan *et al.*, 2011).

1.4.3 *Arbutus pavarii* Pamp.

Arbutus pavarii (Figure 1.9) (Strawberry tree) is commonly known as “Shmeri”. It is an evergreen shrub or a small tree that is recorded among endemic medicinal species in Al-Jabal El-Akhdar, Libya (Hasan *et al.*, 2011; Alsabri *et al.*, 2013).

The image originally presented here cannot be made freely available via LJMU E-Theses Collection because of 'copyright'



Figure 1.6: *Arbutus pavarii*

1.4.3.1 Traditional uses of *A. pavarii*

A. pavarii has been used traditionally as a remedy for gastritis and kidney diseases (El-Darier & El-Mogaspi, 2009; Hasan *et al.*, 2011; Louhaichi *et al.*, 2011; Hegazy *et al.*, 2013). Berries are a good source of minerals, nutrients, carbohydrates, and antioxidants (due to high vitamin C contents). It is also used in honey production and as ornamental trees. The branches are used as a fuel, the leaves, fruits, and barks are used in tanning processes (Hasan *et al.*, 2011; Alsabri *et al.*, 2013).

1.4.3.2 Previous phytochemical work of *A. pavarii*

The phytochemical screening of *A. pavarii* revealed the presence of simple phenolics, polyphenolic such as flavonoids, tannins, glycosides, free reducing sugars, triterpenes, and sterols (Alsabri *et al.*, 2013; Asheg *et al.*, 2014) (Figure 1.7).

Flavonoids

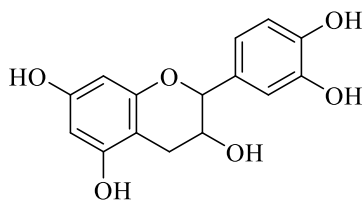
Apigenin (**47**) epicatechin (**48**), hesperidin (**49**), quercetin (**50**), naringin (**51**), and rutin (**52**), were isolated from the *A. pavarii* aerial parts (El Hawary *et al.*, 2016). The

MeOH extract of *A. pavarii* revealed total flavonoid contents 206.1- μ g rutin equivalent/g. HPLC analysis revealed that rutin (**52**) was the most abundant in *A. pavarii* MeOH extract (5096.13 ppm), whereas kaempferol was the least abundant flavonoid (2.20 ppm).

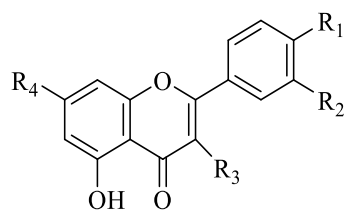
Simple phenolics

Arbutin (**53**), gallic acid (**54**), pyrogallol (**55**) are simple phenolic compounds, which were reported from the *A. pavarii* aerial parts (El Hawary *et al.*, 2016). Assessment of the total phenolic contents of *A. pavarii* aerial parts was performed by HPLC. The MeOH extract of *A. pavarii* revealed total phenolic 163.6 μ g gallic acid equivalent / g. HPLC analysis of the phenolic contents in the extract revealed that pyrogallol was the most abundant phenolic compound in *A. pavarii* MeOH extract (11041.9 ppm) while the least abundant phenolic was cinnamic acid (8.6 ppm) (El Hawary *et al.*, 2016).

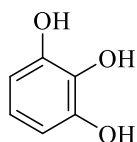
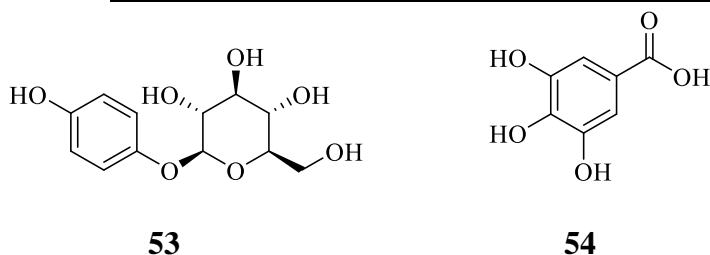
A study has been carried out recently on the aerial parts of *A. pavarii*. Work using high performance thin layer chromatography (HPTLC) showed a profile of constituents including arbutin, methyl gallate as the major phenolic components in the butanol fraction of *A. pavarii* (El Shibani, 2017)



48



Compound No.	R ₁	R ₂	R ₃	R ₄
47	OH	H	H	OH
49	OCH ₃	OH	H	-O-Glu-Rh
50	OH	OH	OH	OH
51	OH	H	H	-O-Glu-Rh
52	OH	OH	-O-Glu-Rh	OH



55

Figure 1.7: Isolated compounds from *A. pavarii*

1.4.3.3 Previous biological work of *A. pavarii*

Few scientific studies have confirmed the traditional uses of *A. pavarii*. There are only a couple of studies that have provided evidence for the antioxidant, antimicrobial and antiproliferative activities of *A. pavarii* (Hasan *et al.*, 2011; Alsabri *et al.*, 2013; El Hawary *et al.*, 2016).

The antioxidant activity Alsabri *et al.* (2013) carried out an antioxidant study on the aerial parts of *A. pavarii*. The antioxidant evaluation was performed using the 2,2-diphenyl-1-picrylhydrazyl (DPPH) assay. The results exhibited a potent antioxidant activity using both the MeOH and chloroform extracts with IC₅₀ of 4.55±1.90 µg/mL and 21.55±1.1 µg/mL, respectively, while the *n*-hexane extract showed negative

results (Alsabri *et al.*, 2013). In addition, the leaves of *A. pavarii* exhibited the highest antioxidant activity among three Libyan plants (*Pegnanum harmal*, *Pistachia atlantica*, and *Fagonia bruguieri*) with the highest content of flavonoids (1504.28±80.89 mg Rutin g⁻¹), a relatively high phenolics content (1217.14±50.52 mg GAE g⁻¹) and significant free-radical-scavenging activity (Alghazeer *et al.*, 2016).

The antimicrobial activity

The antimicrobial study was performed using the ethanolic extract of *A. pavarii*. The results revealed high activity against *Pseudomonas areugenosa* and some Gram +ve bacteria with low antifungal and antibacterial activity against most of the tested Gram -ve bacteria such as *Klebsiella pneumonia* and *E. coli* (Hasan *et al.*, 2011).

Moreover, an antimicrobial study was carried out by Alsabri *et al.* (2013) on the aerial parts of *A. pavarii* by using the agar well diffusion method. The MeOH extract showed an antimicrobial effect against *S. aureus*, *E. coli* and *C. albicans* with zones of inhibition of 20 mm, 18 mm and 21 mm and the (MICs) of 4.8 mg/mL, 9.30 mg/mL, and 4.76 mg/mL, respectively, using ciprofloxacin (MIC of 0.25 and 10 mg/mL, zones of inhibition of 24, 32 mm against *S. aureus*, *E. coli*) and amphotericin B (MIC of 0.5 mg/mL, zone of inhibition of 22 mm against *C. albicans*) as positive controls. Another study by Alghazeer *et al.* (2016) showed the high growth inhibition capacity towards five bacterial strains: *Staphylococcus aureus*, *Bacillus subtilis*, *Streptococcus faecalis*, *Escherichia coli*, and *Salmonella typhi*.

The cytotoxic activity

A. pavarii phytochemical screening revealed the presence of simple and polyphenolic active compounds that have been documented to reduce the risk of cancer. The

antiproliferative activity of the aerial parts of *A. pavarii* extracts (*n*-hexane, chloroform, and MeOH) on both lung carcinoma (A549) and breast adenocarcinoma (MCF7) cancer cells was evaluated by the MTT assay. The results were within the limits of the American National Cancer Institute for cytotoxic activity (less than 30 $\mu\text{g}/\text{mL}$) (Alsabri *et al.*, 2013). Another cytotoxic study was undertaken by El Hawary on the MeOH extract of the aerial part of *A. pavarii* against the HEPG2 and T47D cancer cell lines. *A. pavarii* extract resulted in potential cytotoxicity on both types of cells with IC_{50} of 19.7 ± 2.8 and 19 ± 0.65 ($\mu\text{g}/\text{mL}$), respectively (El Hawary *et al.*, 2016).

Miscellaneous

A study was carried out using *A. pavarii* to determine its effect on performance and cecal coliform count of 1260 one-day-old male Cobb broiler chickens. The dietary treatments included a basal diet with no additive (control) and other dietary treatments with (*A. pavarii*) at the rate of 0.5 g and 1 g/kg of basal diet. The results revealed that *A. pavarii* had a significant effect on body performance of broiler chickens compared to the control. Coliform counts in the cecum of birds receiving 1% *A. pavarii* were significantly lower than those of control group from early weeks of treatments. These results emphasize the potential biotic role of *A. pavarii* together with the immune modulating effects on treated birds (Asheg *et al.*, 2014).

1.5 The family Rutaceae

The Rutaceae family is commonly known as Rue or citrus family. It is a family of flowering plants, herbs, shrubs or trees. The leaves are simple or compound, alternate or opposite, gland-dotted, and exstipulate. Flowers are usually hermaphrodite and actinomorphic (Gunaydin & Savcib, 2005). The Rutaceae family is widely distributed throughout the tropical and temperate regions, especially in Australia, the Mediterranean region and South Africa (Roy & Rahman, 2016).

1.5.1 Classification of the family Rutaceae

The Rutaceae family is represented by 150 genera and approximately 1500 species and it is usually placed in the order Sapindales (Roy & Rahman, 2016). The following is the botanical taxon of the family:

Kingdom: Plantae

Subkingdom: Tracheobionta (Vascular plants)

Superdivision: Spermatophyta (seed plants)

Division (Phylum): Magnoliophyta (flowering plants)

Class: Magnoliopsida

Subclass: Rosidea

Order: Sapindales

Family: Rutaceae {USDA, NRCS, 2017}

The principal genera of this family are *Citrus*, *Fortunella*, *Ptelea*, *Ruta*, *Murraya*, and *Zanthoxylum* (Supabphol & Tangjitjareonkun, 2014).

1.5.2 Chemical characteristics of the family Rutaceae

Most members of the Rutaceae family are aromatic plants due to the presence of a mixture of volatile aroma compounds concentrated in the leaves, fruits, and seeds of the plants (Supabphol & Tangjitjareonkun, 2014). The aromatic smell of these plants is due to the presence of a pellucid gland.

Many publications reported the presence of different chemical constituents from the Rutaceae including alkaloids, coumarins, furanocoumarins, flavonoids and volatile oils (Lewis, 1983; Supabphol & Tangjitjareonkun, 2014). The most abundant alkaloids derived from this family are dictamnine (**58**), graveoline (**60**), kokusaginine (**61**) and skimmianine (**62**). Moreover, coumarins such as bergapten (**63**), psoralen (**71**), and xanthotoxin (**70**) are widely distributed in the plant kingdom and are present in notable amounts in the Rutaceae family (Kostova *et al.*, 1999; Emam *et al.*, 2010; Benazir *et al.*, 2011; Adamska-Szewczyk *et al.*, 2016).

1.5.3 Traditional uses of the family Rutaceae

The members of the Rutaceae family are potential sources of many medicinal substances and have been used traditionally in the treatment of insomnia, headaches, nervousness, bronchitis, stomatitis, menstrual problems, abortifacient, rheumatism, snake bites and also in perfume industry (Benazir *et al.*, 2011; Adamska-Szewczyk *et al.*, 2016).

1.5.4 The genus *Ruta*

The genus *Ruta* might include from eight to forty species. The most well-known species are *R. graveolens*, *R. montana*, ***R. chalepensis***, *subsp. latifolia* and *R. chalepensis subsp. angustifolia* (Zellagui *et al.*, 2012). The three most distributed

species *R. chalepensis* L., *R. graveolens* L. and *R. montana* (L.) L. are morphologically similar (Zeichen de Sa *et al.*, 2000). The genus is represented in Libya by two species: *R. chalpensis* L. and *R. graveolens* L.

1.5.4.1 Active constituents in the *Ruta* genus

The *Ruta* genus is rich in essential oils with variability in composition among species. 2-Undecanone, nonanone, decanone are the most abundant essential oils of *R. chalepensis* L. from Greece, where the main component was found to be 2-methyl octyl acetate (44.0%). Additionally, thirty-six compounds were reported in the aerial parts of *R. corsica*, with 2-nonyl acetate (42.9%) as the major component. Moreover, *R. montana* from Tunisia yielded 5.51% of essential oils (Mejrib *et al.*, 2010). The main factors, which influence the chemical composition of leaf essential oils, were the collection period, geographical origin and genetic structures (Zellagui *et al.*, 2012; Bennaoum *et al.*, 2017).

1.2.1.2 Traditional uses of the genus *Ruta*

The *Ruta* genus was used in the ancient Corpus Hippocraticum (the systematic record of the medical practice of the Mediterranean world), the collection of sixty-two documents written between the 5th century BCE and the 2nd century (Pollio *et al.*, 2008). The *Ruta* spp. was mainly administered by Hippocratic physicians as an abortifacient and emmenagogue and as a specific remedy against pulmonary diseases (Pollio *et al.*, 2008). The ethnobotanist Paolo Maria Guarrera (Italy) listed more than hundred uses for the following species: *R. angustifolia* Pers., *R. chalepensis* L., *R. corsica* DC., and *R. graveolens* L. (Zellagui *et al.*, 2012).

1.5.5 *Ruta chalepensis* L.

Ruta chalepensis (fringed rue) (Figure 1.11) is an ancient native Libyan medicinal herb of the Mediterranean region and is also found in many parts of the temperate and tropical countries in the world. The flowers are cymes with 4–5 sepals, 4–5 petals, 8–10 stamens and a superior ovary. The oil glands are present in leaves, which have a strong deterrent odour (Gunaydin & Savcib, 2005; Gonzalez-Trujano *et al.*, 2006).



Figure. 1.8: *Ruta chalepensis*

1.5.5.1 Traditional uses of *R. chalepensis*

The medicinal value of *R. chalepensis* for the treatment of nervous disorders was recorded by Dioscorides. In Saudi Arabia, a decoction of *R. chalepensis* aerial parts is used as antipyretic, analgesic and for the treatment of rheumatism. *R. chalepensis* is also used traditionally in India for the treatment of rheumatism, menstrual disorders, dropsy, and neuralgia. In China, the roots are used as an antivenom and the leaves are infused with vinegar and used in the treatment of convulsions and other nervous

disorders in children (Gunaydin & Savci, 2005). The Libyan *R. chalepensis* was used against rheumatic affections, ecchymosis and as a scorpion repellent and also for some dermatological diseases. It was also used in Libya as a contraceptive, an abortifacient, an emmenagogue for women, an anti-epileptic and as a tonic to new-born babies (De Natale and Pollio, 2008 & 2012).

1.5.5.2 Previous phytochemical work of *R. chalepensis*

Several phytochemical studies on *R. chalepensis* indicated that it is a valuable plant because of its composition (Gunaydin & Savci, 2005). This plant produces alkaloids, coumarins, essential oil, flavonoids and tannins (Emam *et al.*, 2010) (Figure 1.9).

Alkaloids

Phytochemical screening of *R. chalepensis* has shown the presence of many alkaloids such as arborinine (**56**), chaloridone (**57**), dictamnine (**58**), furoquinoline (**59**), graveoline (**60**), kokusaginine (**61**) and skimmianine (**62**) (Emam *et al.*, 2010; Schmelzer & Gurib-Fakim, 2013).

Coumarins

The roots of *R. chalepensis* var. *latqolia* revealed the isolation of coumarins: bergapten (**63**), chalepin (**64**), chalepentin (**65**), daphnoretin (**66**), isopimpinellin (**67**), rutacultin (**68**), 1-hydroxy-*N*-methylfuroacridone, marmasin (**69**) and xanthatoxin (**70**) (Ulubelen & Güner, 1988). Phytochemical screening of *R. chalepensis* aerial parts revealed the presence of coumarins **63-66**, **69**, **70** and psoralen (**71**): (Emam *et al.*, 2010; Schmelzer & Gurib-Fakim, 2013).

Essential oils

The characteristic odour of *R. chalepensis* and its essential oil is due to the compound methyl *n*-nonyl ketone (**72**). This compound was extracted (47.25% yield) from the volatile oil of *R. chalepensis* grown in Anatolia. The essential oil was obtained by steam distillation and investigated by using gas-liquid chromatography and further separation by column chromatography (Gunaydin & Savci, 2005).

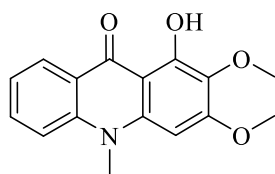
The volatile oils extracted from the flowers and leaves of *R. chalepensis* were found mostly to be dominated by ketone compounds, particularly 2-undecanone derivative (89.89 and 85.94 % of flowers and leaves oils, respectively) (Akkaria *et al.* 2015). Another study reported the domination of ketone constituents in the essential oil composition of *R. chalepensis*; 2-undecanon (48.28%) and 2-nonanon (27%) (Majdoub *et al.* 2014). However, the analysis of *R. chalepensis* essential oils that were collected from the north of Tunisia showed qualitative and quantitative differences in their composition, depending on the parts used, the drying process and the duration of extraction. Thirteen major compounds were isolated during this study using GC–MS. The main components were 2-undecanone (77.18%), 2-decanone (8.96%) and 2-dodecanone (2.37%). The ketone 2-Undecanone yielded 100% of *R. chalepensis* essential oil from the flowers. Camphor was identified exclusively in the essential oil of leaves (2.46%) while pulegone was identified only in the stem essential oil (32.11%) (Mejrib *et al.*, 2010).

Flavonoids

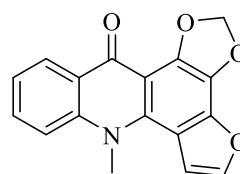
Phytochemical screening of *R. chalepensis* has shown the presence of flavonoids, rutin (**52**) and isorhamnetin (**73**) (Ulubelena & Terem, 1988; Martínez-Pérez *et al.*, 2017).

Shikimic acid derivatives

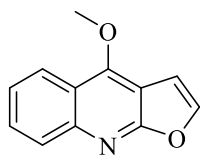
Two shikimic acid derivatives were also obtained from the chloroform extract of *R. chalepensis* aerial parts: moskachan D (**74**) and dehydromoskachan C (**75**). (Ulubelen & Güner, 1988).



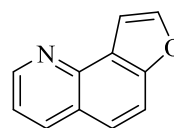
56



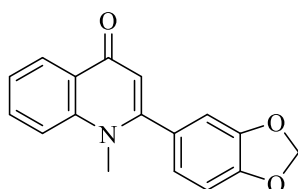
57



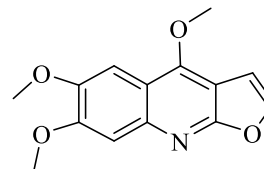
58



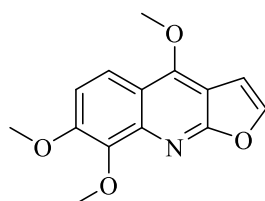
59



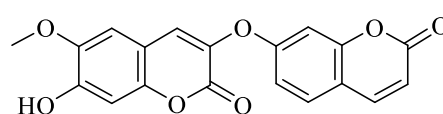
60



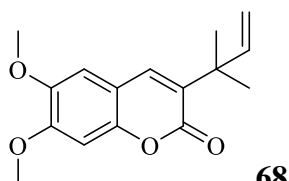
61



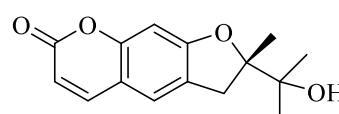
62



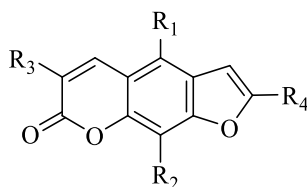
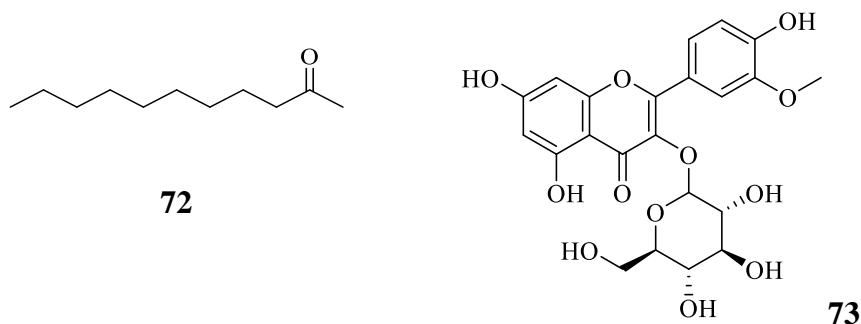
66



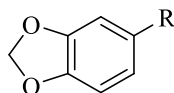
68



69



Compound No.	R ₁	R ₂	R ₃	R ₄
63	H	-OCH ₃	H	H
64	H	H	-C(CH ₃) ₂ -CH-CH ₂	-C(CH ₃) ₂ (OH)
65	H	H	-C(CH ₃) ₂ -CH-CH ₂	H
67	-OCH ₃	-OCH ₃	H	H
70	-OCH ₃	H	H	H
71	H	H	H	H



Compound No.	R
74	(CH ₂) ₄ CHOH-CH ₂
75	(CH ₂) CH=CH ₂

Figure 1.9: Isolated compounds from *R. chalepensis*

1.5.5.3 Previous biological work of *R. chalepensis*

Different biological activities have been associated with the Rutaceae family, for example, antimicrobial (Ali *et al.*, 2008; SSSA *et al.*, 2010), antidiarrhoeal (Mandal *et al.*, 2010), anticholinesterasic (Cardoso-Lopes, 2010), antileishmanial (Carlos

Andres *et al.*, 2011), antiprotozoal (Severino *et al.*, 2009), larvicidal (Rajkumar & Jebanesan, 2008; Emam *et al.*, 2009) and antioxidant activities (Wansi *et al.*, 2006).

The analgesic antipyretic, anti-inflammatory activity

R. chalepensis aerial parts were studied for their analgesic, antipyretic and anti-inflammatory activities. The ethanolic extract did not show any analgesic activity using the hot plate reaction-time test in mice. However, it produced a significant inhibition of cotton pellet granuloma and carrageenan-induced paw oedema in the mice and in rats. The reputed antipyretic activity was tested by the reduction of yeast-induced hyperthermia in mice (Al-Said *et al.*, 1990).

The central nervous system depressant activity (CNS)

R. chalepensis aerial parts were studied for their CNS depressant activity. The spontaneous motor activity in mice and conditioned avoidance responding (CAR) in rats revealed a dose-dependent depression of the central nervous system in treated animals (Al-Said *et al.*, 1990).

The antifertility activity

The antifertility activity of *R. chalepensis* and *R. chalepensis* var. *latifolia* was carried out on female rats (Zeichen *et al.*, 2000). Some species from the Rutaceae are reputed to possess such an activity, for instance, *R. graveolens*, which is a close congener of *R. chalepensis* (Ulubelen *et al.*, 1986) and has been used as an abortifacient and emmenagogue (Kong *et al.*, 1989). Alkaloids and coumarins were isolated from the *R. chalepensis* and *R. chalepensis* var. *latifolia* to find the source of activity. Coumarins such as chalepin (**64**), and xanthotoxin (**70**) exhibited antifertility effect, with the development of cystic and atretic follicles in the ovaries of female rats as well as glomerulocapsular adhesion in the kidneys. Alkaloids such as arborinine (**56**),

fagarine, graveoline (**60**), kokusaginine (**61**) and skimmianine (**62**) did not show any antifertility activity (Ulubelen *et al.* 1994). Infusions of *R. chalepensis* leaves were administered orally at doses of 0.16, 0.80-and 1.60 g/kg/ day during the organogenic period in pregnant mice. The results revealed perinatal and histological changes in placenta and foetuses, which confirmed the toxic effect of *R. chalepensis* on the embryo (Zeichen *et al.*, 2000).

The antioxidant activity

The ethanol and aqueous extracts of *R. chalepensis* collected from Bejaia region in Algeria were investigated *in vitro* for their antioxidant activity. The phenolic compounds composition of the extracts was separated by HPLC-UV. The antioxidant activity was assessed by the scavenging activity of DPPH (2,2-diphenyl-2-picrylhydrazyl). *R. chalepensis* ethanol extract was found to have a higher amount of total phenolics (72.08 ± 1.94 mg), flavonoids (31.90 ± 2.12) and flavonols (13.22 ± 0.86 mg) compared to the aqueous extract, which had total amounts of phenolics of 39.71 ± 0.22 mg, flavonoids of 1.96 ± 0.12 mg and flavonols of 3.00 ± 0.2586 mg. The ethanol extract also showed potent antioxidant activity ($IC_{50} = 51.18 \pm 1, 14$ μ g/mL) and a high reducing power ($IC_{50} = 660 \pm 8, 3$ μ g/mL). This study suggests that *R. chalepensis* could be used as a promising source of natural antioxidant agents and as an encouragement for the isolation of more bioactive and phenolic compounds (Terkmane *et al.*, 2017).

A study was undertaken in Tunisia on the MeOH and aqueous extracts of *R. chalepensis* aerial parts to investigate the antioxidant activity of the plant using DPPH and ABTS assays. Both extracts exhibited high antioxidant activity with IC_{50} values of 54.1 ± 1.5 and 73.6 ± 2.6 μ g/ml, respectively, for DPPH assay. Likewise, the results

showed high antioxidant against the ABTS^{•+} radical 92.4 % and 87.5% at the highest concentration of 3 mg/mL. *R. chalepensis* exhibited potent antioxidant activities, which could be well correlated with the phenolic and flavonoid contents of this plant (Ben Sghaier *et al.*, 2018).

The antimicrobial activity

Two quinoline alkaloids (2-{6'-(2H-benzo[d]1'',3''-dioxolen-5''-yl)hexyl}-hydroquinolin-4-one and 2-{6'-(2Hbenzo[d]1'',3''-dioxolen-5''-yl)hexyl}-4-methoxyquinoline and nine other alkaloids, dictamnine (**58**), pteleine, skimmianine (**62**), rutacridone, isogravacridonechlorine, maculosidine, graveoline (**60**), graveolinine, and 4-methoxy-1-methyl-2(1H)-quinolinone, and coumarins, chalepensis (**65**) and umbelliferone, were isolated from *R. chalepensis* roots collected from the Saudi desert. All the isolated compounds were tested for their antimicrobial activity against a wide range of microorganisms, using a modified microtiter-plate method. The furoquinoline alkaloid, pteleine showed moderate antimicrobial activity by inhibiting the growth of *Mycobacterium smegmatis*, *Bacillus subtilis*, *S. aureus* and *C. albicans*, with an MIC range of 50-100 µg/ mL, while moskachan C (**75**), dictamnine (**58**), skimmianine (**62**) and isogravacridone chlorine were less active (MIC 100 µg/ mL) against *M. smegmatis* and *B. subtilis* and inactive against the other microorganisms (El Sayed *et al.*, 2000).

Another antimicrobial study was carried out by Emam (2010), to investigate the antifungal activity of compounds from the chloroform layer of *R. chalepensis* leaves. This work yielded the new furanoalkaloid quinolone 5-(1', 1'-dimethylallyl)-8-hydroxyfuroquinoline as well as, biscoumarin daphnoretin. The antifungal activity of the isolated compounds was evaluated against the three fungi; *Rhizoctonia solani*,

Sclerotium rolfsii, and *Fusarium solani*, a phytopathogenic types of fungi, which affect some crops e.g., potato, sugar beet and tomato crops. The results showed a decrease in the germination percentage (G %) of *R. solani* and *S. rolfsii sclerotia*. This decrease in the germination was enhanced by the increase in the concentration of the two compounds. Biscoumarin daphnoretin exhibited stronger inhibition of *S. rolfsii sclerotia* (79.83%, 83.7%, and 88%) whereas lower inhibition in the range of 70.03%, 76.7%, and 70.7% was shown by the furanoalkaloid quinolone for *R. solani*, *S. rolfsii*, and *F. solani*, respectively, at a concentration of 20 µg/mL. However, *S. rolfsii* was found to be more sensitive to both compounds than the fungus *R. solani* (Emam *et al.*, 2010).

The antibacterial activities of the ethanol, acetone and aqueous extracts of *R. chalepensis* collected from Eritrea were investigated against *S. aureus* and *E. coli* using the disc diffusion method and minimum inhibitory concentration assays. The acetone extract of *R. chalepensis* exhibited the maximum growth inhibition (8.5 mm) against *E. coli* while the ethanol extract showed the maximum growth inhibition against *S. aureus* (8 mm) (Babu-Kasimala *et al.*, 2014).

The Cytotoxic activity

The cytotoxicity of MeOH extract of *R. chalepensis* aerial parts was evaluated against three cell lines (human bladder carcinoma RT112, human laryngeal carcinoma Hep2 and human myelogenous leukaemia K562). *R. chalepensis* extract showed dose dependant cytotoxic activity, when incubated with the three tumour cell lines (ranging from 2.53 ± 0.21 to 133.05 mg/L) and did not show any activity on the normal human cells PBMC (Khlifia *et al.*, 2013). Another cytotoxic study on T-leukaemic cells and lymphoblast cancer cells and normal blood cells was carried out on the ethanol extract

of *R. chalepensis* collected from Algeria using the MTT assay. The results revealed a high cytotoxic effect of the extract on the blood cancer cells but no effect on the normal blood cells (Terkmane *et al.*, 2017). These results of the last two studies suggest that *R. chalepensis* might be a potential source of a novel pharmaceutical agent for treatment of cancer and further investigations should be carried out to isolate bioactive compounds from this plant.

The pesticidal activity

A bioassay-guided insecticidal study was undertaken on *R. chalepensis* leaves. The aqueous ethanol extract has revealed larvicidal and antifeedant activities against the larvae *Spodoptera littoralis* (Boised). The study involved the isolation of some compounds from the ethanol extract that might be responsible for the larvicidal and antifeedant activities. This study resulted in the separation of two different alkaloidal compounds, which were characterized as rutamine and 3-(2",2"dimethyl butenyl) 3'-hydroxy di-hydrofuropsoralen that were responsible for larvicidal and antifeedant activities against *S. littoralis* larvae with LC₅₀ of 1.598, 1.215 mg/mL (Emam *et al.*, 2009). Accordingly, the volatile oils extracted from the flowers and leaves of *R. chalepensis* exhibited significant insecticidal and anthelmintic activity against third and fourth instars larvae of *Orgyia trigotephras* compared with the chemical standard insecticide delta-metrine and the reference anthelmintic drug albendazole. The flowers oil of *R. chalepensis* at a concentration of 0.5% showed higher activity than the leaves oil on the third instar larvae with a mean mortality time (MMT) of 1.40 min and 1.27 min, respectively. The MMT of the fourth instar larvae was found to be 42.53min for the oil from the flowers and 20.68 min for the oil from the leaves. The anthelmintic effects against *Haemonchus contortus* worm in sheep were measured by egg hatching and inhibition of worm motility, when compared with the reference drug albendazole.

Both essential oils exhibited ovicidal activity at all the tested concentrations (0.125, 0.25, 0.5 and 1 mg/mL). The leaves volatile oil had higher inhibitory effects on egg hatching than flowers volatile oil with $IC_{50} = 0.145$ mg/mL and $IC_{50} = 0.398$ mg/mL, respectively. The chemical composition study showed that the essential oils samples were mostly dominated by ketone compounds, particularly 2-undecanone derivative (89.89 and 85.94 % of flowers and leaves oils, respectively). It was found that 2-undecanone might be a potential constituent for the insecticidal and anthelmintic constituent of *R. chalepensis* volatile oil (Ntalli *et al.*, 2011; Akkaria *et al.*, 2015).

The essential oil of *R. chalepensis* showed insecticidal activity against both the adults and larvae *Tribolium castaneum* (a stored product pest). The results showed higher activity against adults ($LC_{50} = 176.075$ μ L/L air and $LC_{90} = 291.9$ μ L/L air) than larvae ($LC_{50} = 415.348$ μ L/L air and $LC_{90} = 685.907$ μ L/L air). These *R. chalepensis* results are promising and might have future potential use in the food storage industry (Majdoub *et al.* 2014). The efficacy of MeOH extract of *R. chalepensis* aerial parts was evaluated against *Culex pipiens* larvae. The larvicidal activity of *R. chalepensis* proved to be effective against *C. pipiens* larvae without any human or animal risk (Abdel-Sattar *et al.*, 2014).

1.6 Objectives of this study

- i. The main objectives of this study were to: obtain crude extracts from a selection of four Libyan medicinal plants: *Arbutus pavarii*, *Asphodelus aestivus*, *Juniperus phoenicea* and *Ruta chalepensis* by Soxhlet extraction using various solvents of different polarities;
- ii. carry out a systematic, bioassay-guided phytochemical and cytotoxic/anticancer study on the different crude extracts and assess

quantitative bioactivity and cytotoxicity of the purified compounds using the 3-(4,5-dimethyl thiazolyl-2)-25-diphenyltetrazolium bromide (MTT) assay;

- iii. isolate and identify bioactive molecules with potential anticancer and/or cytotoxic properties from these plants using different chromatographic and spectroscopic techniques.

CHAPTER 2
MATERIALS AND METHODS

2.0 Materials and Methods

2.1 Phytochemical work

2.1.1 General materials

The chemicals, solvents and materials used in the phytochemical work are illustrated in Table 2.1

Table 2.1: Chemicals, solvents and materials

Chemicals, solvents and materials	Manufacturer
<i>n</i> -Hexane	Fisher Scientific
Dichloromethane	Fisher Scientific
Methanol	Fisher Scientific
Ethyl acetate	Fisher Scientific
SPE cartridge	(Strata) [®] Phenomenex
Silica gel for column	Fluka [®]
Silica TLC plates	Merck [®]
Silica gel for VLC	Merck [®]

2.1.2 Plant materials

Four Libyan medicinal plants were collected from different sites from Libya between 2013-2016. Specimens from these plants were identified based on the Flora of Libya at the Faculty of Science Herbarium, Tripoli-Libya, and a voucher specimens numbers have been retained there (Table 2.2). All parts used were air-dried, powdered and kept in a tightly closed amber coloured container.

Table 2.2: The Libyan medicinal plants used in this study

Plant Name	Site	Collection Year	Voucher Number
<i>Juniperus phoenicea</i> L.	Al-Bydaa city	2013	D68122
<i>Asphodelus aestivus</i> Brot.	Tarhona city	2014	D6857302
<i>Arbutus pavarii</i> Pamp.	Al-Jabal Al Akhdar	2016	D6854201
<i>Ruta chalepensis</i> L.	Al-Jabal Al Akhdar	2016	D6850101

2.1.3 Extraction of plant materials

The different parts (dried and ground) of the four plants (Table 2.3) were separately extracted by Soxhlet, sequentially, with *n*-hexane, DCM, and MeOH (800 mL each). Ten cycles were allowed for each extraction at temperatures near the boiling point of the solvents. All extracts were filtered, evaporated to dryness in a rotary evaporator (Cole-Parmer)[®] and finally stored at 4°C.

Table 2.3: The weights of different dried and ground parts of the four Libyan medicinal plants

Plant Name	Part Used	Weight (g)
<i>A. pavarii</i>	Leaves	150
<i>A. aestivus</i>	Leaves	208.5
	Tubers	159.3
<i>J. phoenicea</i>	Leaves	86.5
<i>R. chalepensis</i>	Aerial parts	138.6

2.1.4 Fractionation techniques

The different crude extracts of the four plants were initially fractionated into various discrete fractions using solid-phase extraction (SPE) for any MeOH extracts and vacuum liquid chromatography (VLC) for any *n*-hexane or DCM extracts.

2.1.4.1 Solid phase extraction (SPE)

Portions of the polar MeOH extracts of the four plants were pre-HPLC fractionated using the SPE technique. An SPE cartridge (20 g), which was pre-packed with reversed-phase silica C₁₈ was used as described by Sarker *et al.* (2005). The SPE cartridge was connected to a vacuum flask with an appropriate adapter, pre-rinsed by

flushing with 50 mL of MeOH followed by 100 mL of water. Each MeOH extract was dissolved in 10% MeOH in water and was loaded onto the SPE cartridge. A Step gradient protocol was applied successively with 200 mL each of 20%, 50% and 80% MeOH in water, and finally 100% MeOH. Four fractions were collected from each plant, dried by rotary evaporator and freeze dryer techniques and kept to be used for separation by HPLC (Sarker *et al.*, 2005).

2.1.4.2 Vacuum liquid chromatography (VLC)

VLC was carried out as described by Sarker *et al.* (2005). Portions of the non-polar extracts (*n*-hexane and DCM extracts) of the four plants were further fractionated by VLC where vacuum was used to achieve a compact packing of the column and to increase the flow rate of the mobile phase. In this method, the column was a Büchner funnel with a medium-porosity fritted glass disk with a piece of filter paper fitted flat into the bottom. The stationary phase was then poured (TLC-grade silica gel, 60 H). The funnel was then placed on the top of a vacuum flask fitted with a rubber vacuum seal and a vacuum applied to immobilise the stationary phase (Sarker *et al.*, 2005).

The column was pre-equilibrated with the first solvent in the elution series. Enough volumes of solvent were added through the column to wet the column thoroughly. Vacuum was released each time before the column dried and the wash solvent was then poured off.

Step gradient elution was carried out using *n*-hexane- EtOAc mixtures (200 mL) of increasing polarity (100% *n*-hexane, 20% EtOAc/*n*-hexane; 40% EtOAc/*n*-hexane; 60% EtOAc/*n*-hexane; 80% EtOAc /*n*-hexane; 100% EtOAc; 50% MeOH/ EtOAc). Similarly, the DCM extracts were fractionated by VLC on silica gel, starting elution

with *n*-hexane-DCM mixtures, and then increasing polarity with MeOH to yield seven fractions, which were dried by rotary evaporator and stored for further evaluation on cultured cells using the MTT assay.

2.1.5 Chromatographic techniques

Different chromatographic techniques were further applied for screening and separation of pure compounds from the extracts and fractions. These techniques were:

2.1.5.1 Thin layer chromatography (TLC)

Silica TLC plates (200 mm x 200 mm x 0.25 mm) were used for preliminary screening and separation of compounds.

Analytical thin layer chromatography

The lipophilic portions were preliminarily screened for the identification and verification of the purity of isolated compounds using different proportions of different mobile phases, for instance: EtOAc: *n*-hexane, MeOH/DCM and toluene: EtOAc: acetic acid (TEA), to achieve the best separation of pure compounds.

Preparative thin layer chromatography (PTLC)

The lipophilic portions were further purified using the PTLC technique. Thin bands (10-20 mg /mL) of the extracts or fractions to be purified were applied to the silica gel plates using capillary tubes. The plates were developed in a suitable freshly prepared solvent system. Single or multiple developments were employed to achieve a satisfactory separation.

Detection (location of compounds on chromatograms)

The three extracts, as well as the isolated pure compounds, were shown under short UV (254 nm) and long UV (366 nm). The separated compounds were detected by observing the plates under UV light then spraying with different reagents.

Anisaldehyde spray reagent for detection of the different types of compounds was colour specific for various classes of compound. For instance, flavonoids (yellow colour), glycosides (violet colour), tannins (dark brown colour at the bottom of the plate), sesquiterpenes (phosphorous green colour) and diterpenes (violet colour). The plates were heated at 100°C for 5 min or until coloration appears (Houssen & Jaspars, 1998; Sarker *et al.*, 2005). Dragendorff's reagent was used for the detection of alkaloids and heterocyclic nitrogen-containing compounds (orange, dark brown colour) (Houssen & Jaspars, 1998; Sarker *et al.*, 2005). Qualitative DPPH assay was sometimes performed by spraying a developed TLC plate with a DPPH solution (80 µg/mL) and a colour change was observed, from purple to yellow, on certain spots. This colour change showed that the stable free-radical DPPH can be reduced by some extracted phytochemicals, which therefore may act as free-radical scavengers (Sarker & Nahar, 2012).

2.1.5.2 Column liquid chromatography (CLC)

Normal column chromatography

Column chromatography (CLC) (15 x 2.5, 35 x 2.5 cm) was used for separation of pure compounds from both *n*-hexane and DCM fractions obtained from VLC, using silica gel as an adsorbent (60 A, 70-230 mesh, 63-200 µm). Preparation of column was carried out by using the wet method; the adsorbent was mixed well with solvent (*n*-hexane) creating a slurry, this was immediately poured into a sintered-glass column and allowed to settle by gentle tapping and washing with the solvent. The lipophilic fractions were mixed separately with silica gel and EtOAc in an alternative way to get freely loose powders. The powder was applied on the surface of the adsorbent and elution was performed with a gradient system of EtOAc: *n*-hexane (0%, 2%, 4%, 6%

and so on) as a mobile phase (52 mL each). Four mL fractions were collected in 13 test tubes each time. The collection of a large number of small portions improved the probability that each fraction may contain a pure compound, which may require significant work in the analysis of each fraction (Sarker & Nahar, 2012).

High-performance liquid chromatography (HPLC)

Reversed-phase HPLC was used in this study for both screening and isolation of compounds. The stationary phase in reversed-phase HPLC is non-polar, and the eluent is polar. The mobile phase comprises mixtures of water and organic solvents (or modifiers). Other additives, such as buffers, acids, bases, and ion-pair reagents may be incorporated into the eluting solvent. In this study 0.1%, TFA was added to all solvents used to help in sharpening the separated peaks. The organic solvents most commonly used in reverse phase HPLC are acetonitrile, MeOH and tetrahydrofuran (THF). Solutes tend to elute in order of increasing hydrophobicity, and elution is speeded up by increasing the proportion of organic modifier in the eluent. The yields were based on peak areas of the HPLC chromatogram (Kaushal & Srivastava 2010).

Analytical HPLC

All the MeOH extracts and the SPE fractions (F1- F4) were analytically screened by analytical reversed-phase HPLC (Dionex Ultimate 3000 UPLC). The Dionex HPLC is coupled with an autosampler, degasser, a photodiode array detector, and a computer with control and data analysis software (Chromeleon 7). Thermo Scientific™ Hypersil GOLD™ C18 column (150 mm x 4.6 mm, 5 mm), which connected to a guard column. The volume of injection used for analytical screening was 10-20 µL with a flow rate of 1 mL/min. This screening provided significant information on the types of compounds present, based on their retention times and their UV spectra.

Semi-preparative and preparative HPLC

The SPE fractions (F1- F4) of the MeOH extracts were dissolved in MeOH to achieve a concentration of 10 mg/mL. The fractions were then separated by semi-preparative and preparative reversed-phase HPLC using modular HPLC Systems (Agilent Technologies, 1200 Series), with a binary gradient pump, photodiode array detector and computer with control and data analysis software. In the semi-preparative isolation of compounds, a Phenomenex LC-18 stainless steel column (150 mm x 10 mm) was used for separation of small amounts of fractions with a volume of injection of 120 -200 μ L using a flow rate of 2 mL/min. For the isolation of large amounts of fractions, a preparative Phenomenex LC-18 stainless steel column 150 mm x 21.2 mm connected to a guard column was used and a larger injection volume of 900 μ L and a higher flow rate of 10 mL/min were also used.

2.1.6 Spectroscopic techniques

The following spectroscopic techniques were used for the structure elucidation of our isolated pure compounds.

2.1.6.1 Ultraviolet-visible spectroscopy (UV-Vis)

Ultraviolet (UV) spectra of the isolated compounds were obtained in methanol using WinAspect Plus, Specord[®] 210 Plus UV-Vis spectrometer.

2.1.6.2 Mass spectrometry (MS)

Mass spectrometry has played an essential role in the structure elucidation of isolated compounds from natural products due to its high sensitivity (microgram amounts of compounds can be detected) and because nominal molecular weight can be used as a search query in nearly all databases (Houssen & Jaspars, 1998). It is used to determine the molecular weights of compounds where the molecular ions or fragments are

formed with sufficient excitation energy and the relative abundances of these fragments usually are unique to the structure of the molecular ion. The mass-to-charge ratio (m/z) of the resulting molecular ions, fragmentation reactions, the types of functional groups, as well as the manner in which they are joined to form a unique molecular structure, will help to deduce structure from the mass spectrum. Molecules that cannot be ionized will not be detected (Smith *et al.*, 1991).

HPLC-MS is a hyphenated technique, which combines chromatographic (LC) with spectral methods (MS) to exploit the advantages of both. Chromatography produces pure or nearly pure fractions of chemical components in a mixture. Spectroscopy delivers particular information for identification using standards or library spectra (Phonde & Magdum, 2015). In this study, all the isolated pure compounds were sent to the EPSRC National Mass Spectroscopy Service (NMSS), Swansea, for the MS experiments to be carried out. Mass spectroscopic analyses were performed on a Finnigan MAT 95 spectrometer, GCT Premier, GCT Premier GC/MS and LTQ Orbitrap XL1.

LC-MS, Alliance system 2695 (Waters) was applied on the *J. phoenicea* crude extracts and the MeOH F₄ of *A. aestivus* tubers to detect any tentative compounds using electrospray ionization (ESI). A Phenomenex HPLC column C₁₈ (150 x 4.6) was used with a flow rate of 1 mL/min and a gradient of (10-100 % ACN/ H₂O) for 30 min and hold for 10 min. Using LC-MS-MS, some molecular ions are separated and subjected to a second fragmentation. The fragmentation pattern produced can give a lot of daughter peaks, which may help to get information about the parent structure (Phonde & Magdum, 2015).

2.1.6.3 Nuclear magnetic resonance (NMR)

Nuclear Magnetic Resonance (NMR) spectroscopy is a technique which is based on the interaction of radio frequency (RF) of the electromagnetic radiation (EMR) with unpaired nuclear spins. It revealed information on the number and types of protons (hydrogen) and carbons in the molecule and their relationships and other nuclei such as: ^9F , ^{35}Cl , ^{31}P etc. (Pretsch, 1997; Tesso, 2005).

The NMR experiments used can be classified into two major categories:

2.1.6.3.1 One dimensional technique

In one-dimensional NMR (1D-NMR), the conventional NMR spectrum are plots of frequency vs intensity, the chemical shifts and couplings are displayed on the same frequency axis (e.g. ^1H NMR, ^{13}C NMR, ^{13}C DEPT) (Williams and Fleming., 1989; Balci, 2005).

^1H NMR (Proton NMR) technique

Proton NMR is a plot of peak intensity signals arising by the different protons in a compound which is measured in parts per million (0-10 ppm). The area under the peaks revealed information regarding the protons number in the molecule, the signals position (chemical shift) describes the chemical and electronic environment of the protons, and the spin-spin splitting pattern provided information about the neighboring number of protons (vicinal or geminal) (Williams and Fleming, 1989; Balci, 2005).

^{13}C NMR technique

The comparison of the natural abundance of ^{13}C and ^1H nuclei clearly indicates that the ^1H nucleus is approximately 100 times more sensitive than that of ^{13}C (Balci, 2005).

The ^{13}C chemical shift ranges (0-200 ppm) for organic compounds is a plot of signals arising from the different carbons (^{13}C) in the molecule and can be identified by their characteristic shift values in the ^{13}C NMR spectra. The ^{13}C NMR signals normally appeared as singlets in the experiments because of the decoupling of the attached protons (Breitmaier, 2002).

DEPT technique

The distortionless enhancement by polarization transfer (DEPT) is an important NMR technique for determining the number of hydrogens attached to a given carbon atom to differentiate between CH, CH₂ and CH₃ (Breitmaier, 2002).

2.1.6.3.2 Two-dimensional techniques

Two-dimensional NMR (2D-NMR) spectroscopy may be defined as a spectral method in which the data are collected in two different time domains (X-Y co-ordinate axes). 2D-NMR are used to determine the structure of more complicated molecules (Pretsch and Clerc, 1997). In the case of 2-D NMR, the X-Y co-ordinate axes can be two frequency domains, and the observed signals are in the third dimension eg. ^1H - ^1H COSY, ^1H - ^1H NOESY, ^1H - ^{13}C HMBC and ^1H - ^{13}C HMQC (Kessler *et al.*, 1988; Rahman and Choudhary, 1996).

a) The Homonuclear correlated spectroscopy

H-H COSY technique

^1H - ^1H Correlation spectroscopy is a homonuclear HH coupling in which the chemical shift range of the proton spectrum is plotted on both dimensions which has square symmetry (Breitmaier, 2002).

H-H NOESY technique

The Nuclear Over Hauser Enhancement Spectroscopy is a useful technique to traces out the groups that are close in space in larger molecules, so that the nucleus irradiation detect the other nuclei by its resonance frequency (Williams and Fleming, 1989; Breitmaier, 2002).

b) The Heteronuclear correlated spectroscopy

HSQC: Heteronuclear single quantum coherence is the ^1H - ^{13}C correlation via one-bond coupling (Breitmaier, 2002).

HMBC: Heteronuclear multiple bond correlation is the ^1H - ^{13}C correlation via long-range coupling between proton and carbon (two or three bonds away) with great sensitivity. HMBC is a very useful technique for assigning complex structures (Kessler et al., 1988; Breitmaier, 2002).

In this study, crude extracts and pure compounds were subjected to NMR analysis at 300 MHz or 600 MHz (Ultra shield Bruker AMX 300 & 600 NMR spectrometers). NMR sample tubes (Wilmad) [®], OD: 5 mm, length: 7 inches, glass A material) and NMR solvents (Cambridge Isotope Laboratories (CIL) Inc.) were used to apply the samples of pure compounds. Despite the complex composition of the crude extracts, NMR spectra help to show the occurrence of secondary metabolites. For instance, aromatics, fatty acid esters, peptides, phenolics, steroids, sugars and terpenoids, functional groups such as –CHO, –NH, –OH, or –OMe. This tentative elucidation indicates the presence of the most abundant compound (s) or class of compounds in the extract. This information will help in the decision of whether the chromatographic separation should be either over normal or reversed phase chromatography, or size-exclusion chromatography (Gray *et al.*, 2012).

2.1.7 Isolation of compounds

The techniques used for fractionation of extracts and separation of pure compounds from *A. pavarii* leaves, *A. aestivus* leaves and tubers, *J. phoenicea* leaves and *R. chalepensis* aerial parts are summarized in Table 2.4.

Table 2.4: Isolation of compounds from the four Libyan medicinal plants under study

Plant	Extract	Wt (g)	Fractionation Technique	Gradient Used	Isolation Technique	Gradient Used
<i>A. pavarii</i> leaves	MeOH	1.45	SPE	30, 50, 80 and 100% MeOH / H ₂ O	Prep-HPLC	F1 and F2 (30- 100 % MeOH/ H ₂ O) F3 and F4 (50-100% MeOH/ H ₂ O)
	DCM	2.4	VLC	0, 5, 10, 30, 50, 80 and 100% EtOAc/ <i>n</i> -hexane and 50% MeOH / EtOAc	Prep-HPLC	50-100% gradient of ACN/H ₂ O.
	<i>n</i> -Hexane		Not fractionated	Not fractionated	Not isolated	Not isolated
<i>A. aestivus</i> leaves	MeOH	1.8	SPE	30, 50, 80 and 100% MeOH / H ₂ O	Prep-HPLC	30- 100 % MeOH/ H ₂ O
	DCM	0.5	Not fractionated	Not fractionated	Prep-HPLC	Different gradients of ACN/ H ₂ O

	<i>n</i> -Hexane		Not fractionated	Not fractionated	Not isolated	Not isolated
<i>A. aestivus</i> . tubers	MeOH	1.33	Not fractionated	Not fractionated	Prep-HPLC	30- 100 % ACN/ H ₂ O every 5 min.
	DCM	1.86	VLC	0, 10, 30, 50, 80 and 100% EtOAc / <i>n</i> -hexane and 50% MeOH / EtOAc	Prep-HPLC	Different gradients of ACN/ H ₂ O
	<i>n</i> -Hexane		Not fractionated	Not isolated	Not isolated	Not fractionated
<i>J. phoenicea</i> leaves	MeOH	1.4	SPE	30, 50, 80 and 100% MeOH / H ₂ O	Prep-HPLC	F1 and F2 (30- 100 % MeOH/ H ₂ O) F3 and F4 50-100% MeOH/ H ₂ O
	DCM	1.29	VLC	0, 50, 100% DCM / <i>n</i> -hexane, 10, 20, 30 and 50% MeOH/ DCM.	Prep-HPLC	50-100% gradient of ACN/H ₂ O
	<i>n</i> - Hexane	2.6	VLC	0, 5, 10, 30, 50, 80 and 100% EtOAc / <i>n</i> -hexane and 50% MeOH / EtOAc	CLC PTLC	gradient system of EtOAc: <i>n</i> -hexane
<i>R. chalepensis</i> aerial parts	MeOH	3.0	SPE	20, 50, 80 and 100% MeOH / H ₂ O	Prep-HPLC	F1 and F2 30- 100 % MeOH/ H ₂ O

						F3 and F4 50-100% MeOH/ H ₂ O
	DCM	2.05	VLC	0%, 50% and 100% DCM/ <i>n</i> -hexane, then, 10- 50% MeOH/ DCM.	PTLC Prep-HPLC	Different gradients of the following mobile phases: 1. EtOAc: <i>n</i> -hexane 2. Toluene: EtOAc: acetic acid (TEA) Different gradients of ACN/ H ₂ O.
	<i>n</i> -Hexane	3.26	VLC	0- 100% EtOAc / <i>n</i> -hexane and 50% MeOH / EtOAc	PTLC	Different gradients of the following mobile phases: 1. EtOAc: <i>n</i> -hexane 2. MeOH/ DCM. 3. Toluene: EtOAc: acetic acid (TEA)

2.2 Bioassays for potential cytotoxic/anticancer effects of extracts, fractions and compounds

2.2.1 Cancer cell lines selected

The human tumour cell lines that were selected for used during this study were obtained from the European Collection of Authenticated Cell Cultures (ECACC). Five human cancer cell lines were selected, which derived from different tumour types. These cell lines were A549, EJ-138, HEPG2, MCF7 and PC3. In addition, one normal human prostate cell line PNT2 was also selected (Table 2.5). All of the cancer cell lines were adherent epithelial cells derived from human carcinoma or adenocarcinoma.

Table 2.5 The cancer cell lines used in this study (ECACC)*.

	A549	EJ-138	HEPG2	MCF7	PC3	PNT2
Catalogue No	86012804	85061108	85011430	86012803	90112714	95012613
Tissue	Lung	Bladder	Liver	Breast	Prostate	Prostate
Tumour type	Human Caucasian lung carcinoma	Human bladder carcinoma	Human Caucasian hepatocyte carcinoma	Human Caucasian breast adenocarcinoma	Human Caucasian prostate adenocarcinoma	Human prostate normal, immortalised with SV40
Cell line description	Derived from a 58-year-old Caucasian male.	It has been shown by isoenzyme analysis and HLA profiles that EJ138 is in fact T24 human bladder carcinoma.	The Hep G2 cell line has been isolated from a liver biopsy of a 15 years Caucasian male suffering from hepatocellular carcinoma. B virus surface antigens have not been detected.	Established from the pleural effusion from a 69 year female Caucasian suffering from a breast adenocarcinoma.	Derived from a 62-year-old male Caucasian with a grade 4 prostatic adenocarcinoma	PNT2 cells were established by immortalisation of normal adult prostatic epithelial cells by transfection with a plasmid containing SV40 genome with a defective replication origin. The primary culture was obtained from a prostate of a 33-year-old male at post-mortem.

*The European Collection of Authenticated Cell Cultures (ECACC), a Culture Collection of Public Health England.

2.2.2 Routine cell culture

The cells were cultured in RPMI 1640 medium with w/stable glutamine (Biosera), supplemented with 10% (v/v) foetal bovine serum (FBS; Biosera) and 1% (v/v) 100X antibiotic/antimycotic solution (Gibco®) (complete medium). All cells were routinely cultured in T75 flasks at 37°C, 95% humidity, and 5% CO₂ in a Binder® incubator. Cells were grown to approximately 80% confluent before sub-culturing (passaging). To passage the cells, the complete medium was aspirated from each T75 flask and 20mL of phosphate buffered saline (PBS) was added to wash the cells of any remaining medium. The PBS was then removed and 1mL of 0.05% trypsin-EDTA solution (Gibco®) added to each T75 flask of cells. The cells were returned to the incubator to allow the enzyme to detach the cells from the flask surface. Cellular detachment was confirmed using light microscopy. The action of the trypsin-EDTA solution was neutralised by the addition of 5ml/flask complete medium. The subsequent cell suspension was used to seed new T75 flasks for routine cell maintenance or to seed 24-well plates for experimental purposes. For routine cell maintenance, the cells in the cell suspension were counted using a haemocytometer. This was used with complete medium to achieve a seeding concentration of 1×10^4 cells/mL (12.5 mL/T75 flask). Flasks of cells were returned to the incubator and the complete medium replaced with fresh complete medium daily until they had grown to approximately 80% confluent, when the passaging process was repeated. The passage number (a count of the number of passages) was recorded on each occasion.

2.2.3 Cryopreservation of cells

The primary purpose of cryopreservation is to ensure the continuous supply of each cell line during this study. Cell lines can be cryopreserved in a living state of suspended cellular metabolism at -196°C in liquid nitrogen (Bakhach, 2009). To achieve this, T75 flasks of cells for cryopreservation were harvested, when approximately 50% confluent (log phase of growth) by trypsinisation (as described in Section 2.2.2 above). The cell suspension from each flask was centrifuged at 1200 g for 5 min at 4°C to pellet the cells. The supernatant was aspirated off and the pellet of cells from each flask was re-suspended in freeze mixture [45% FBS, 45% RPMI 1640 medium, 10% dimethylsulfoxide (DMSO)] to achieve a cell concentration of $2-4 \times 10^6$ cells/mL. This cell suspension/freeze mixture was transferred to labelled cryovials (1 mL/cryovial). Cryovials of cells were immediately transferred to a cryogenic freezing container (able to provide $-1^{\circ}\text{C}/\text{min}$ cooling) and cooled to -80°C in a freezer. After 24 h, the cryovials of cells were moved to a liquid nitrogen storage vessel for long-term storage.

Thawing frozen cells

Cryovial/s of cells were removed from liquid nitrogen storage vessel as required and thawed rapidly at 37°C in a water bath. The contents of each cryovial was transferred to a universal tube and 10 mL of complete medium added to dilute the DMSO in the freeze mix because DMSO is toxic to cells at temperatures above 4°C . The cells were then centrifuged at 1200 g for 5 min at 4°C to pellet the cells. The supernatant containing DMSO was removed and the pellet of cells was re-suspended in 12.5 mL of complete medium. This was transferred to a labelled T75 flask and incubated at 37°C , 95%

humidity, and 5% CO₂ to allow the cells to recover and continue growing until passage or for experimental purposes.

2.2.4 The MTT cytotoxicity assay

The MTT assay is a simple colorimetric assay developed by Mosmann (1983) for measuring the metabolic activity in cells. A soluble, yellow, MTT substrate is taken up into cells through the endocytosis process, and then reduced by both the mitochondrial enzymes and the endosomal/lysosomal compartments to form a solid, crystalline, purple, formazan product (figure 2.1) (Evans, 2003; Lu *et al.*, 2012; Stockert *et al.*, 2012; Kuete *et al.*, 2017). A solubilisation solution (dimethyl sulfoxide or isopropanol) is added to dissolve the water-insoluble formazan crystals into a purple solution. The absorbance (560 nm) of purple solution after treatment of cells is measured using a spectrophotometer and compared to that of the untreated control. MTT assay is one of the most widely used methods in academic laboratories to analyse cell proliferation and viability as evidenced by thousands of publications (Lu *et al.*, 2012, Riss *et al.*, 2016; Kuete *et al.*, 2017).

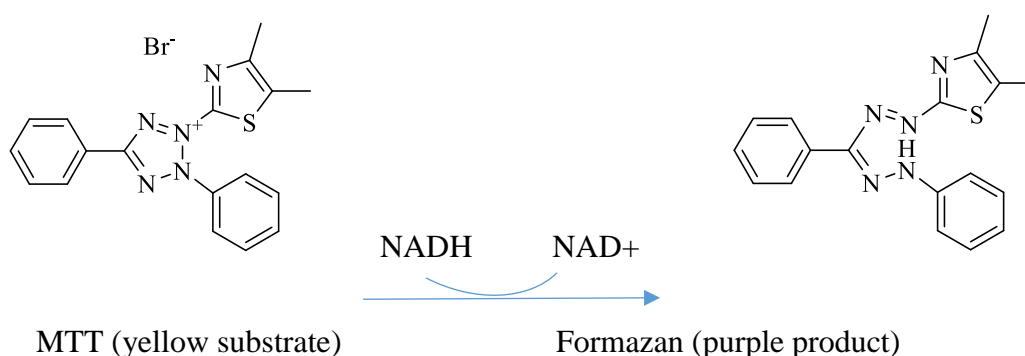


Figure 2.1 The reduction of MTT into formazan (Evans, 2003)

Method

In this study, the cytotoxic activity of the *n*-hexane, dichloromethane and MeOH extracts of *A. pavarii* leaves, *A. aestivus* leaves and tubers, *J. phoenicea* leaves and *R. chalepensis* aerial parts were assessed against the five human tumour cell lines using the MTT assay. The cancer cells used were breast adenocarcinoma cell line [MCF7], liver hepatocellular carcinoma cell line [HEPG2], lung carcinoma cell line [A549], prostate adenocarcinoma cell line [PC3] and urinary bladder carcinoma cell line [EJ-138]. The complete medium was aspirated from flasks of cells, and the cells then were then trypsinised to dislodge the cells (as described in Section 2.2.1). The trypsin was neutralised by the addition of a volume of complete medium to achieve a final cell concentration of 5×10^4 cells/ mL. This was then used to seed the wells of 24-well plates (1 mL/well). The 24-well plates of cells were incubated under 5% CO₂ at 37°C for 24 hr to allow the cells to adhere and start proliferating. The cells were then treated for 24 h with complete medium containing different concentrations of each extract (0, 0.005, 0.01, 0.05, 0.1 and 0.5 mg/mL), fractions (0, 0.00004, 0.002, 0.01, 0.05 and 0.25 mg/mL) or the isolated pure compounds (concentrations according to the amounts of the separated compound). The extracts, fractions and pure compounds had initially been solubilised in DMSO and so all treatments in complete medium were supplemented with varying amounts of DMSO to yield a final DMSO concentration of 0.01% (v/v) in every treatment (including the negative control). After the 24 h treatment, the medium in each well was replaced by 1 mL MTT working solution (500 µg/mL in complete medium) and incubated at 37°C for two hours. The MTT working solution was then removed, and the formazan crystals produced by viable cells were dissolved in isopropanol (0.5 mL/well) and gently shaken

on an orbital shaker until a homogeneous colour was obtained. 100µl (x4 from each well of the 24-well plate) was transferred into wells of 96-well plates. The absorbance of the reduced MTT was then determined by a Clario-star plate reader at 560 nm (Nemati *et al.*, 2013). The absorbance readings of the treated cells were expressed as a percentage of the mean absorbance reading for the negative control cells.

2.2.5 Determination of IC₅₀ values

Data interpretation

The absorbance values of treated cells that are found to be lower than the control cells indicate a reduction in the viability of the cells and is taken as a measure of cytotoxicity. The cytotoxicity results were evaluated by plotting the percentage of control absorbance against the correspondent concentrations. Linear regression analysis with 95 % confidence limit and R² were used to define dose-response curves and to compute the concentration of extracts, fractions, and compounds needed to reduce absorbance of the formazan by 50 % (IC₅₀) (Patel, *et al.*, 2009).

Determination of IC₅₀ value

IC₅₀ is the concentration of a drug that is required to reduce viability by 50 % of the cells. IC₅₀ values were determined from a plot of a dose-response curve between the log of concentration and percentage viability. IC₅₀ values were determined as a concentration of drug at 50 % position on the Y-axis. IC₅₀ values were calculated using the nonlinear regression program 'Origin' (Patel, *et al.*, 2009). The US National Cancer Institute (NCI) Plant Screening Program guidelines, set limits of the *in vitro* cytotoxic

activity at IC₅₀ values in carcinoma cells less than 20 µg/ml for crude extracts and 4 µg/ml for pure compounds (incubation time between 48 and 72 h) (Boik, 2001; Mahvorasirikul *et al.*, 2010). However, in this study, the incubation time was 24 h and values for crude extracts greater than 100 µg/mL were considered as non-cytotoxic (Sahranavard *et al.* 2012).

2.2.6 Determination of selectivity index (SI)

The degree of selectivity of the extracts or compounds can be expressed by its selectivity index (SI) value. The selectivity index (SI) = The IC₅₀ (µg/mL) of extracts against the normal cells divided by the IC₅₀ (µg/mL) of extracts against the cancer cells. Selectivity value higher than 2 gives a selective toxicity towards cancer cells (Badisa, *et al.*, 2009; Demirgan, *et al.*, 2015).

2.2.7 Statistical analysis

All experiments were carried out in triplicate on separate occasions. Data were expressed as means \pm standard error of the mean derived from $n \geq 12$ from three separate occasions. The graphs were plotted using nonlinear regression with the use of Microsoft Excel version 2013. Statistical analyses were performed with Graph Pad Prism version 7.04. One-way ANOVA of multiple comparisons was applied (between control and different concentrations) using Dunnett's multiple comparison tests. The differences between groups were considered statistically non-significant (ns) at a P value ≥ 0.05 , significant (*) at a P value < 0.05 (0.01-0.05), very significant (**) at a P value < 0.01 (0.001 to 0.01), highly significant (***) at a P value < 0.0001 (0.0001-0.001).

2.2.8 LDH assay of cell membrane integrity (LDH release assay)

The Lactate Dehydrogenase (LDH) assay is a useful method for detection of necrosis. LDH is a soluble cytoplasmic enzyme that is released into extracellular space, when the plasma membrane is damaged. The leakage level can be determined by the conversion of a substrate into a product that is then quantified spectrophotometrically (Evans, 2003; Chan *et al.*, 2013). In this assay, the leakage of LDH into cell culture medium is detected by the presence of a substrate, a tetrazolium salt. Firstly, the LDH enzymes catalyze the oxidation of lactate to pyruvate, which leads to the release of reduced nicotinamide adenine dinucleotide (NADH) and secondly, the formation of a colored formazan product, which can be quantified using a spectrophotometer (Chan *et al.*, 2013).

Reagents

Stop solution (1M acetic acid), 10X lysis buffer (9% v/v Triton X-100 in distilled H₂O), LDH cytotoxicity detection kit produced by Roche (REF 11644793001), five bottles Catalyst (lyophilized), five bottles Dye Solution (45 ml each). The reaction mixture was prepared by mixing the catalyst one mL with 11.25 mL of the dye solution, 96 –well tissue culture plates.

Method

The columns 1 to 9 of the 96-well plate were seeded with cells in complete medium at a density of 1×10^5 cells/ ml (100 μ L/ well) and columns 10 to 12 filled with complete medium only (100 μ L/ well). The plates of cells were incubated under 5% CO₂ at 37°C for 24 hr to allow the cells to adhere and start proliferating. The pure compound to be tested was made up in complete medium at the concentration estimated to be its IC₅₀

value. For treatment, wells of cells in columns 1 to 3 of the 96-well plate were treated with the pure compound in complete medium (100 μ L/well). Wells in columns 4 to 12 were given complete medium only. After the 24 h treatment, the LDH release assay was carried out. Firstly, 10X lysis buffer (5 μ L/well) was added to the complete medium in wells in columns 7 to 9 and returned to the incubator for 15 min for lysis of cells to occur (high LDH release controls). After this period, 100 μ L/well of reaction mixture was added into every well on the 96-well plate (columns 1 to 12) and incubated for a further 15 min. at 37°C. After 15 min. incubation, 50 μ L/ well stop solution was added to each well of the 96-well plate (columns 1 to 12). Columns 1 to 3 of the 96-well plate were the compound-treated cells (test), columns 4 to 6 were untreated viable cells (low LDH release controls), columns 7 to 9 were viable cells that had been lysed to release LDH (high LDH release controls) and columns 10 to 12 were complete medium only (background reading controls). The absorbance values of each well were measured and recorded at 490 and 690 nm and the 690 nm values were then subtracted from the 490nm values. The average background reading (from wells in columns 10 to 12) was then subtracted from all other values. The average readings from wells in columns 1 to 3 were taken as the treated cell value, columns 4 to 6 as the low LDH release control value and columns 7 to 9 as the high LDH release control value.

CHAPTER 3

RESULTS AND DISCUSSIONS

3.0 Results and Discussions

3.1 *Juniperus phoenicea*

3.1.1 Extraction

Sequential Soxhlet extraction of the dried and ground leaves of *Juniperus phoenicea* (JPL) (85 g) afforded three extracts: *n*-hexane (JPH), dichloromethane (JPD), and MeOH (JPM). The percentage yields of these extracts are summarized in Table 3.1

Table 3.1.1: Percentage yield of the three extracts obtained from *J. phoenicea* leaves

Extract	% Yield
<i>n</i> -Hexane (JPH)	5.14
DCM (JPD)	2.48
MeOH (JPM)	28.57

3.1.2 Preliminary analytical TLC screening

The developed TLC plates of three extracts obtained from *J. phoenicea* were viewed under short (254 nm) and long (366 nm) UV light and then sprayed with anisaldehyde reagent followed by heating at 100°C for 5 min to reveal many violet coloured spots with R_f values ranging from 0.16 to 0.94 (Table 3.1.2). The violet colour suggested the presence of diterpenes in both the *n*-hexane and the DCM extracts (Kristanti & Tunjung 2015). Another plate was developed and sprayed with DPPH reagent and exhibited yellow spots, which indicated the presence of compounds with antioxidant properties (Figure: 3.1.1) (Chima *et al.*, 2014).

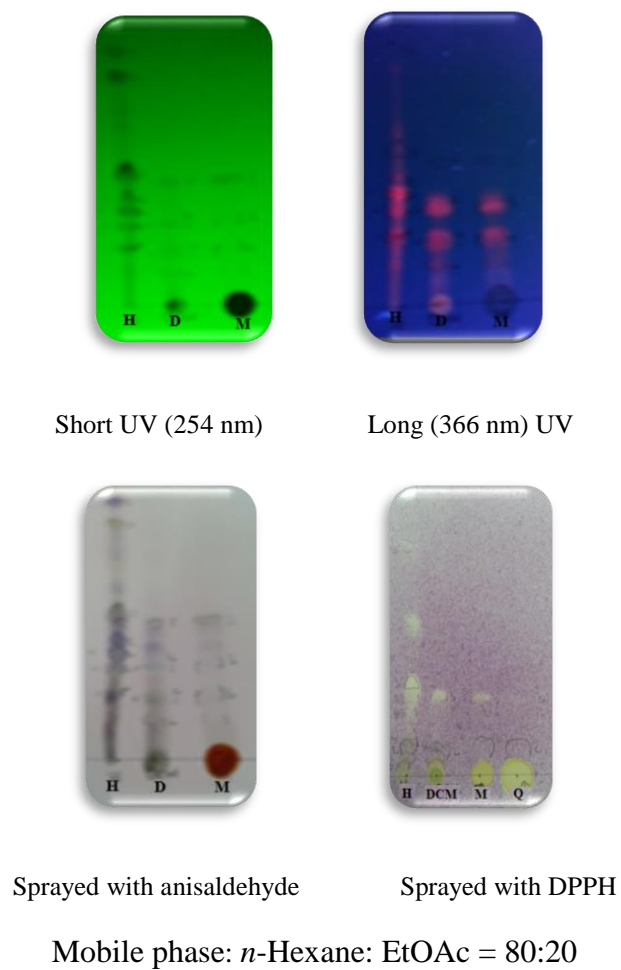


Figure 3.1.1: TLC for the three extracts of *J. phoenicea* leaves

Table 3.1.2: R_f values of different extracts of *J. phoenicea*

<i>n</i> -Hexane R_f values	DCM R_f values	MeOH R_f values
0.16, 0.25, 0.31, 0.36, 0.4, 0.5, 0.84 and 0.94	0.13, 0.2, 0.3, 0.3, 0.45	0.2, 0.3 and 0.47

3.1.3 Analytical HPLC screening for the MeOH extract of *J. phoenicea* leaves

The MeOH extract of *J. phoenicea* leaves (10 mg/mL) was analysed by Dionex Ultimate 3000 analytical HPLC coupled with a photodiode detector using a gradient mobile phase, 30-100% MeOH/H₂O for 30 min with a volume of injection of 20 µL and a flow rate of 1 mL/min. (Figure 3.1.2; Table 3.1.3).

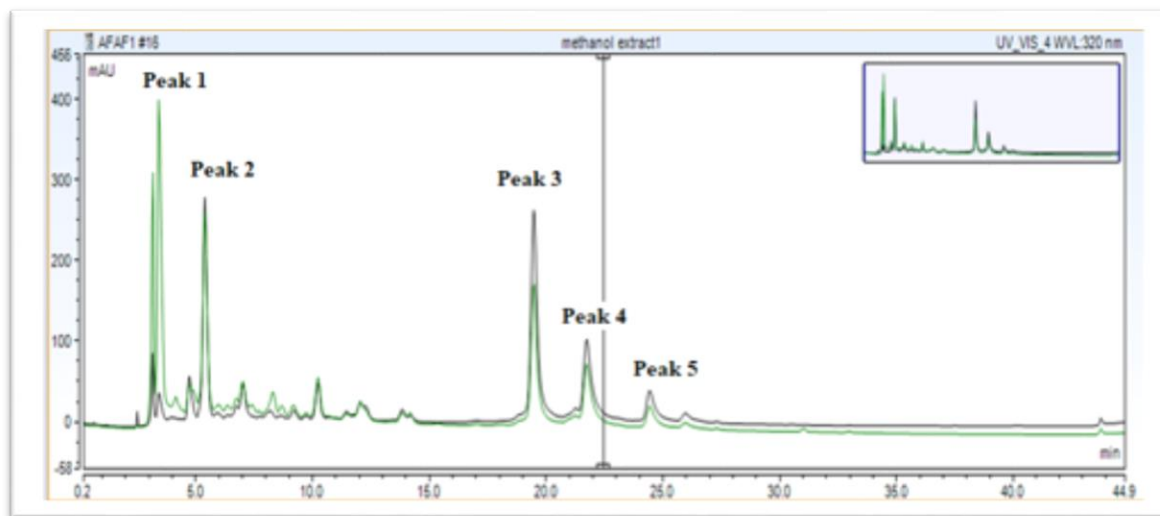


Figure 3.1.2: Analytical HPLC chromatogram of the MeOH extract of *J. phoenicea* leaves (observed at 320 nm, the green chromatogram)

Table 3.1.3: UV-Vis data for all major peaks obtained from diode array detector

Peak No.	Retention Time (min)	UV-Vis absorbances (λ_{max}) (nm)
1	3.2	224, 241 and 277
2	5.3	225 and 311
3	20	226, 273 and 330
4	21.9	225, 271 and 333
5	25	225, 276 and 326

3.1.4 Screening of *J. phoenicea* extracts for cytotoxic activity

The cytotoxic activity of JPH, JPD and JPM was assessed against five cancer cell lines; EJ138 (human bladder carcinoma), Hep G2 (human liver hepatocellular carcinoma), A549 (human lung carcinoma), MCF7 (human breast adenocarcinoma), and prostate cancer cell lines (PC3). The *n*-hexane (JPH) extract showed the highest level of activity against the different cancer cell lines with the only exception of the PC3 cancer cell line, against, which the JPD was most active (Figures: 3.1.3 and 3.1.4) and (Table 3.1.4). The selectivity index (SI) was also determined using the human normal prostate cell line (PNT2) for both active extracts JPH and JPD, which revealed a high degree of cytotoxic selectivity on prostate cancer cells (SI = 5). This indicated that the extracts were more cytotoxic to cancer cells than against normal cells (Musiliyu *et al.*, 2010). The IC₅₀ values of the extracts and the selectivity index are summarized in Table 3.1.4.b

Table 3.1.4a: The IC₅₀ (µg/mL) of *n*-hexane, DCM and MeOH extracts of *J. phoenicea* leaves on the selection of five human cancer cell lines

Cell type	IC ₅₀ values (µg/mL) (JPL)		
	JPH	JPD	JPM
EJ138	40 ± 0.75	50 ± 0.97	> 100
Hep G2	10 ± 1.48	42 ± 1.08	100 ± 0.90
A549	16 ± 1.56	13 ± 1.70	100 ± 1.47
MCF7	14 ± 1.30	16 ± 1.13	> 100
PC3	25 ± 0.93	4.9 ± 0.76	> 100

Values greater than 100 µg/mL were considered as non-cytotoxic (Sahranavard *et al.* 2012).

The results were mean values ± standard error of the mean derived from n ≥ 12 from three separate occasions.

Table 3.1.4b: The IC₅₀ (µg/mL) values for JPD and JPH extracts on PC3 and PNT2 cells and the selectivity index (SI) using the normal human prostate cells (PNT2).

Cell type	IC ₅₀ values (µg/mL)	
	JPH	JPD
PC3	25 ± 1.84	4.9 ± 0.76
PNT2	140 ± 1.84	20 ± 0.92
Selectivity index	5.6	4.08

Selectivity index (SI)= The IC₅₀ (µg/mL) of extracts against the normal cells divided by the IC₅₀ (µg/mL) of extracts against the cancer cells, where IC₅₀ is the concentration required to reduce viability by 50% of the cell population (Badisa, *et al.*, 2009).

3.1.5 Chromatographic fractionation of the extracts

The primary objective undertaken to fulfill this study was to carry out a systematic, bioassay-guided phytochemical and cytotoxic/anticancer survey on the different crude extracts. To approach this aim further fractionation of the *J. phoenicea* active extracts (JPH and JPD) was performed. Also, the inactive MeOH extract was fractionated aiming at isolation of major metabolites to have thorough understanding of the phytochemistry of *J. phoenicea*.

3.1.5.1 Vacuum liquid chromatography fractionation (VLC)

The active extracts JPH (2.6 g), and JPD (1.28 g) were further fractionated by VLC step gradient elution over silica gel to collect seven fractions from each extract (Figures 3.1.3 and 3.1.4), the weights of fractions are listed in Table 3.1.5

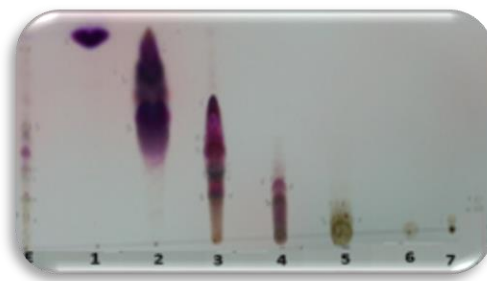


Figure 3.1.3: TLC analysis (mobile phase: 20% EtOAc in *n*-hexane) of the VLC fractions of the *n*-hexane extract of the leaves of *J. phoenicea*

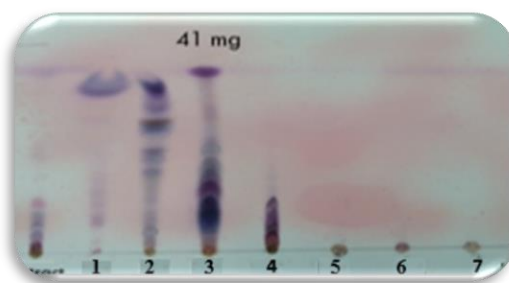


Figure 3.1.4: TLC analysis (mobile phase: 5% MeOH in DCM) of the VLC fractions of the *n*-hexane extract of the leaves of *J. phoenicea*

Table 3.1.5: Weights of the VLC fractions of the extracts JPH and JPD

Fraction	Mobile phase gradient	Weight of fraction (mg)	Fraction	Mobile phase gradient	Weight of fraction (mg)
JPHF1	100% <i>n</i> -hexane	82.5	JPDF1	100% <i>n</i> -hexane	15
JPHF2	10% EtOAc in <i>n</i> -hexane	555	JPDF2	50% DCM in <i>n</i> -hexane	20
JPHF3	30% EtOAc in <i>n</i> -hexane	998.7	JPDF3	100% DCM	41
JPHF4	50% EtOAc in <i>n</i> -hexane	655.5	JPDF4	10% MeOH in DCM	134
JPHF5	80% EtOAc in <i>n</i> -hexane	118.8	JPDF5	20% MeOH in DCM	128.5
JPHF6	100% EtOAc	22.1	JPDF6	30% MeOH in DCM	9.3
JPHF7	50% MeOH in EtOAc	103.7	JPDF7	40% MeOH in DCM	2.7

3.1.5.2 Solid phase extraction (SPE)

The MeOH extract of *J. phoenicea* leaves (JPM) was fractionated by SPE to collect four fractions (Figures 3.1.5-3.1.8; Table 3.1.6).

Table 3.1.6: Weights of the SPE fractions of the MeOH extract of *J. phoenicea* leaves

Fraction	Mobile phase gradient	Weight of fraction (mg)
JPMF1	20% MeOH in H ₂ O	895
JPMF2	50% MeOH in H ₂ O	135
JPMF3	80% MeOH in H ₂ O	54
JPMF4	100% MeOH in H ₂ O	25

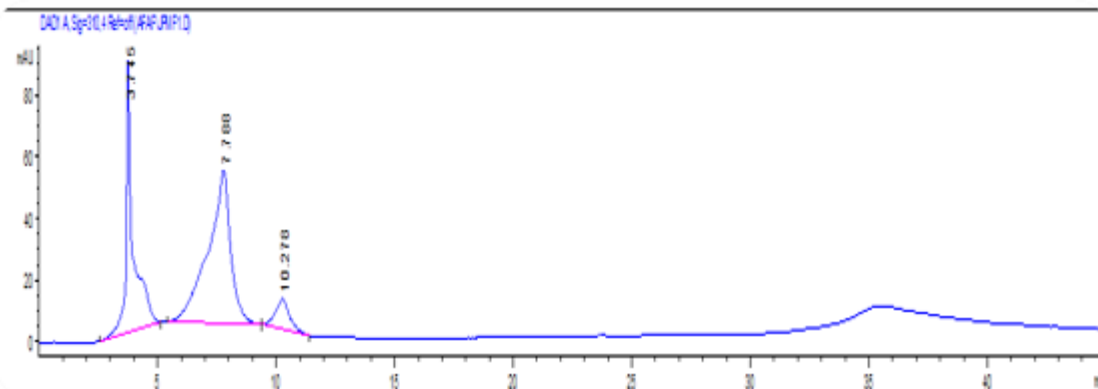


Figure 3.1.5: Analytical HPLC chromatograms of SPE fraction 1 of JPM (observed at 310 nm)

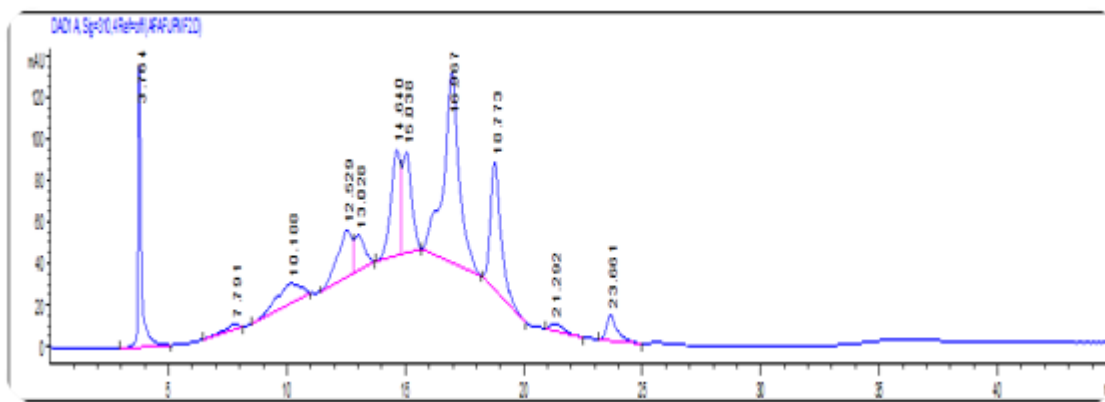


Figure 3.1.6: Analytical HPLC chromatograms of SPE fraction 2 of JPM (observed at 310 nm)

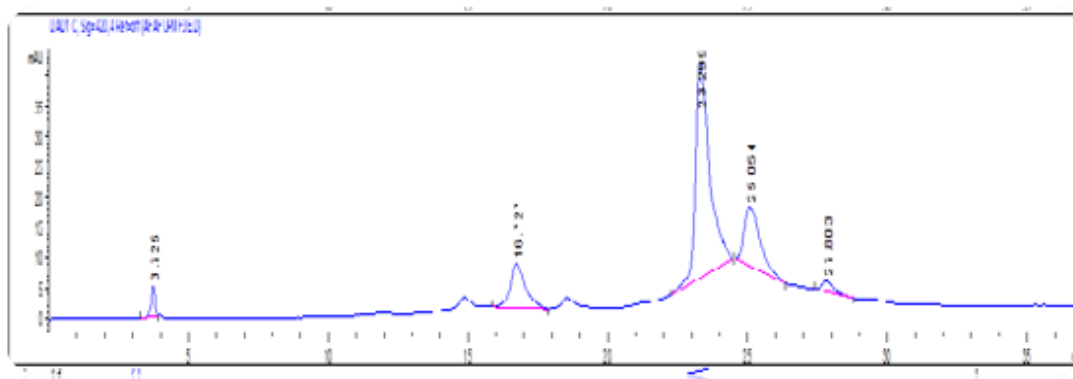


Figure 3.1.7: Analytical HPLC chromatograms of SPE fraction 3 of JPM (observed at 310 nm)

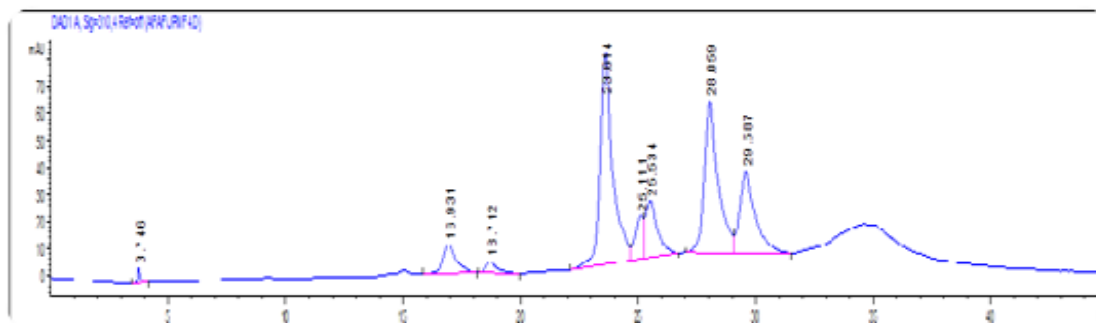


Fig. 3.1.8: Analytical HPLC chromatograms of SPE fraction 4 of JPM (observed at 310 nm)

3.1.6 Screening of *J. phoenicea* fractions for cytotoxic activity

The cytotoxic activity of the *n*-hexane, DCM, and MeOH fractions of *J. phoenicea* leaves was assessed against the most sensitive cancer cell line (human lung carcinoma cell line A549). The highest activity was revealed in the *n*-hexane F5, the DCM F4, and MeOH F3 and F4. The IC₅₀ values for the *n*-hexane, DCM and MeOH fractions of *J. phoenicea* leaves on A549 (human lung carcinoma) are summarised in Table 3.1.7.

Table 3.1.7: The IC₅₀ (µg/mL) of the VLC and SPE fractions of the three extracts of *J. phoenicea* leaves against A549 (human lung carcinoma) cells

Fraction	IC ₅₀ values (µg/mL)							
	F1	F2	F3	F4	F5	F6	F7	F8
<i>n</i> -Hexane	>100	62 ± 1.32	90 ± 1.33	30 ± 1.79	9.5 ± 0.87	NA	40 ± 1.14	NA
DCM	NA	60 ± 2.13	92 ± 1.44	19 ± 0.83	>1000	>1000	>1000	>1000
MeOH	>1000	>100	50 ± 1.46	85 ± 3.42	NA	NA	NA	NA

NA--- Non-applicable All experiments were carried out in triplicate on separate occasions. Data were expressed as means \pm standard error of the mean derived from $n \geq 12$ from three separate occasions.

3.1.7 Isolation of compounds from *J. phoenicea*

3.1.7.1 The MeOH extract (JPM)

Isolation of compounds from the SPE fractions 3 and 4 of JPM was done using semi-preparative HPLC technique (Agilent) employing a 30-100% gradient of MeOH in water for 30 min with a volume of injection of 200 μ L and a flow rate of 2 mL/min

The following compounds were isolated: JPMF3-1 (12 mg, $t_R = 20.0$ min), and JPMF3-2 (2.5 mg, $t_R = 21.9$ min) from SPE fraction 3, and JPMF4-1 (8 mg, $t_R = 19.9$ min), JPMF4-2 (2.0 mg, $t_R = 21.7$ min) and JPMF4-4 (0.7 mg, $t_R = 26.3$ min) from SPE fraction 4. JPMF3-1 had the same retention time of JPMF4-1, and similarly, JPMF3-2 and JPMF4-2 had the same retention time (Figures 3.1.19 and 3.1.20).

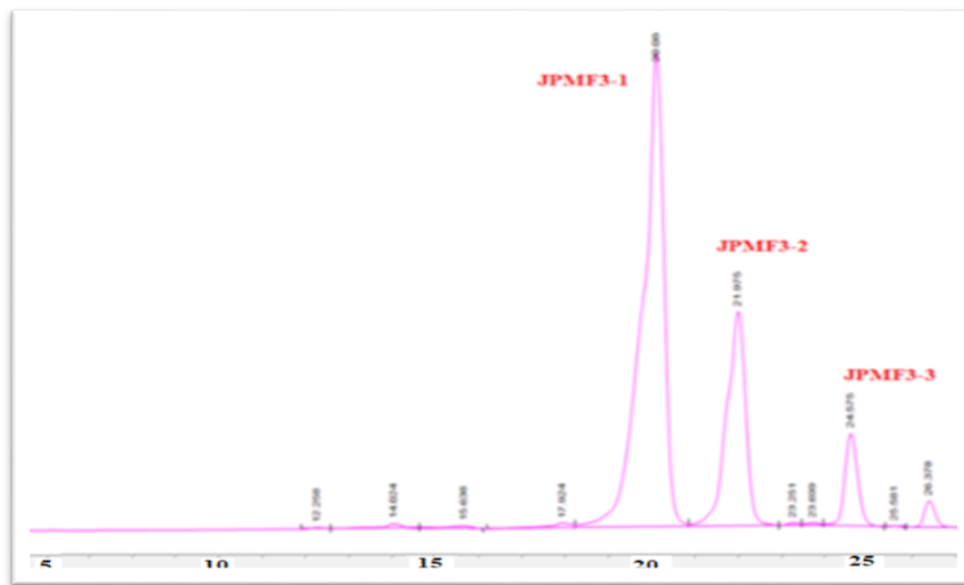


Figure 3.1.19: Analytical HPLC chromatogram of isolated compounds from SPE fraction 3 JPM (observed at 310 nm)

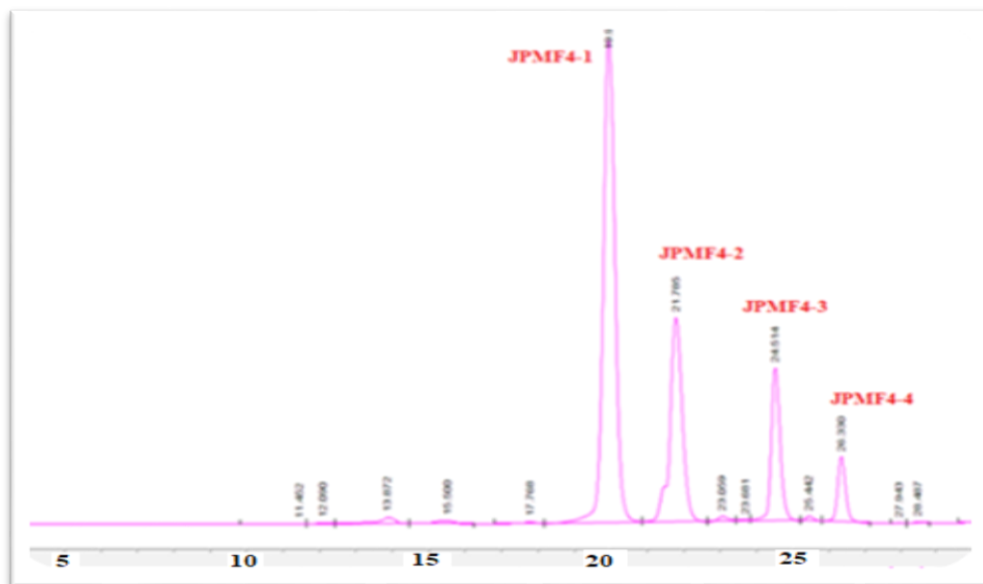


Figure 3.1.20: Analytical HPLC chromatogram of isolated compounds from SPE fraction 4 JPM (observed at 310 nm)

3.1.7.2 The *n*-hexane extract (JPH)

The active VLC fractions (F2, F3, and F5) of the *n*-hexane extract were subjected to normal column chromatography over silica gel, using a step gradient mobile phase comprising EtOAc (2%, 4%, 6% ----20%) in *n*-hexane (52 mL each) and collecting 4 mL each time leading to the isolation of JPH3 (8.2 mg, $R_f = 0.6$) and JPH567 (1.7 mg, $R_f = 0.86$), which was isolated with some impurity (Figure 3.1.22). JPHF2D was precipitated as a white powder in the tubes from the CLC applied on VLC fraction 2.

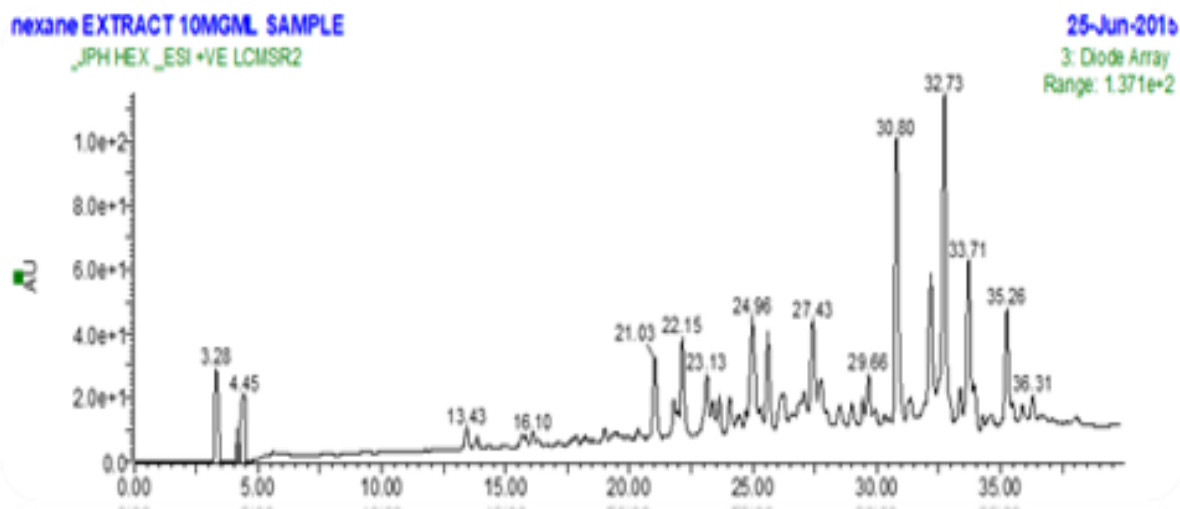


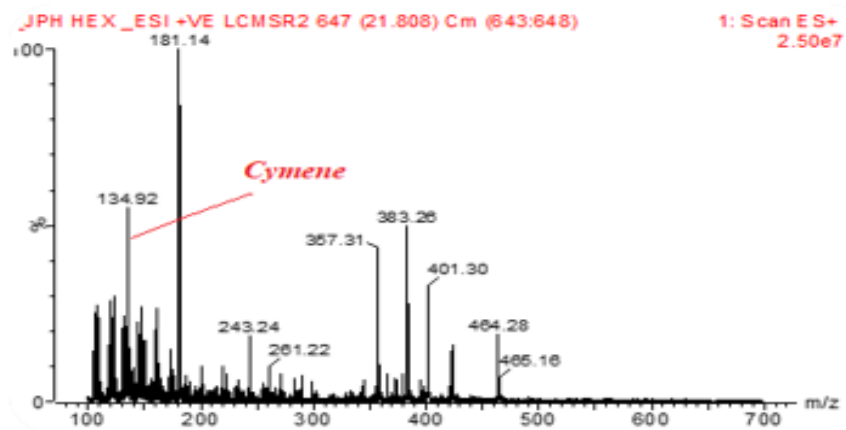
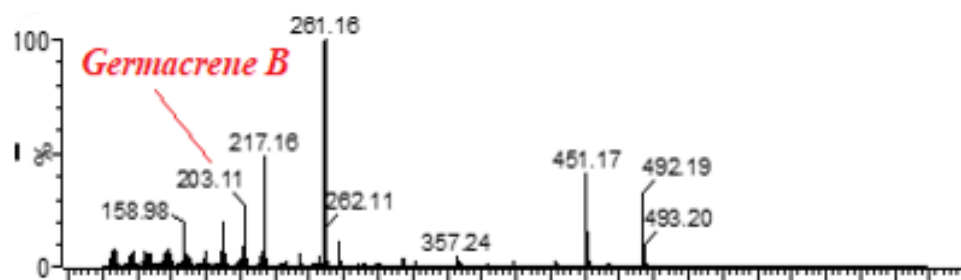
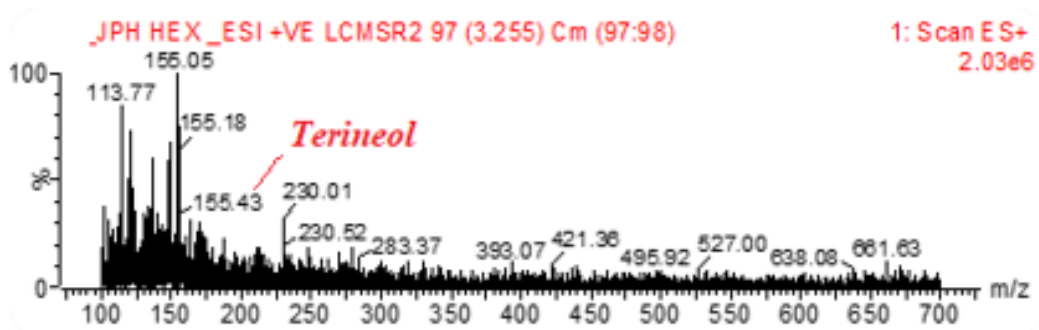
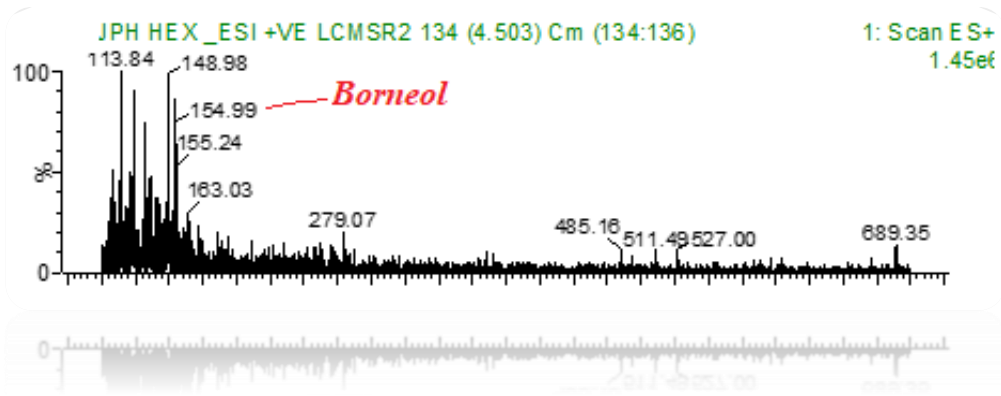
Mobile phase: Toluene: EtOAc: Acetic acid= 25:24:1

Figure 3.1.22: Isolation of the compounds JPH3 and JPD567 from *J. phoenicea.n*-hexane F3 and F5

3.1.7.3 HPLC-MS screening of the *n*-hexane extract (JPH)

The JPH was analysed by HPLC-MS to detect the molecular weights of the major metabolites, and thus to tentatively identify 3-hydroxy-sandaracopimaric acid (**44**), 13-*epi*-cupressic acid (**42**), and some essential oils components such as borneol, terpineol, δ -cymene, germacrene B (Figure 3.1.23).





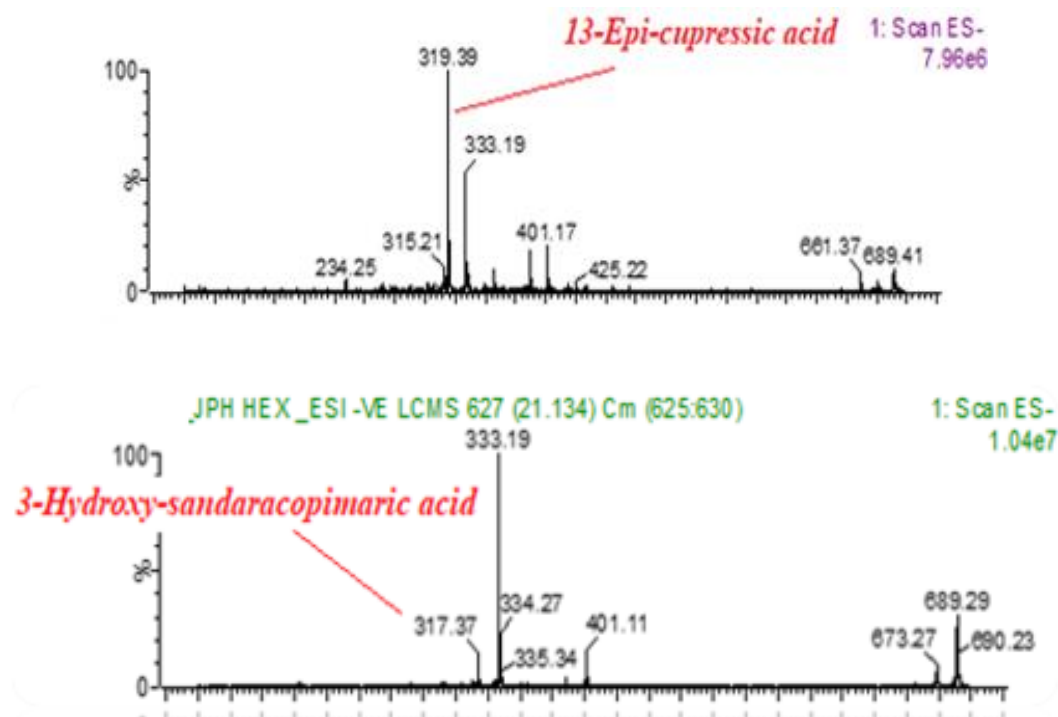


Figure 3.1.23: LC-MS screening for the *n*-hexane extract of *J. phoenicea* leaves

3.1.7.4 The DCM extract (JPD)

Separation of the active DCM VLC Fraction 4

The active DCM VLC Fraction 4 (130 mg) of *J. phoenicea* leaves was isolated by prep-HPLC using a gradient solvent system 50-100% ACN in water. This led to the isolation of the compounds: JPDF4-1 (1 mg, t_R = 9.82 min), JPDF4-2 (0.5 mg, t_R = 10.19 min), JPDF4-3 (2.4 mg, t_R = 11.14 min), JPDF4-5 (3.2 mg, t_R = 14.12 min), JPDF4-6 (10.3 mg, t_R = 15.56 min), JPDF4-8 (3 mg, t_R = 17.5 min), JPDF4-11 (4 mg, t_R = 24.60 min) and JPDF4-12 (2.2 mg, t_R = 29.90 min) (Figure 3.1.24).

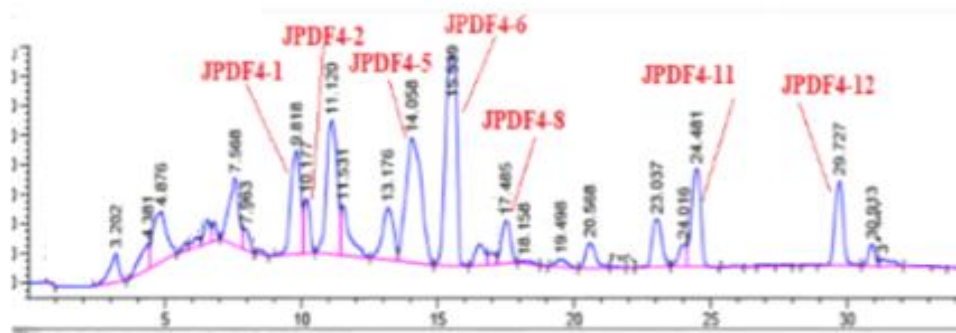


Figure 3.1.24: HPLC chromatogram of the active VLC fraction 4 of the DCM extract (JPD) (observed at 250 nm)

Separation of the DCM extract every 5 min

The total DCM extract (JPD) (1 g) was fractionated every 5 min by preparative reversed-phase HPLC using a gradient solvent system 50-100% ACN in water and a flow rate of 10 mL/min. Eight fractions [F1= 10.6 mg (0-5 min), F2= 12.2 mg (5-10 min), F3= 55 mg (10-15 min), F4= 35 mg (15-20 min), F5= 133 mg (20-25 min), F6= 40 mg (25-30 min), F7= 61 mg (30-35 min) and F8= 41 mg (35-40 min)] were obtained and allowed to dry (Figure 3.1.25).

JPD fraction 4 (35 mg) was further purified using the gradient of 50-100% MeOH /water over 30 min and flow rate of 10 mL/min. This led to the isolation of JPD4-2 (0.6 mg, t_R =18 min.) (Figure 3.1.26).

JPD fraction 5 (133 mg) was purified using the gradient of 60-80% MeOH /water over 30 min and flow rate of 10 mL/min to obtain two pure compounds JPD5-4 (11 mg, t_R = 34 min.) and JPD5-7 (3.4 mg, t_R =37.5 min) (Figure 3.1.27).

JPD fraction 5 (40 mg) was analysed by the linear gradient of 70-100% MeOH/water and flow rate of 10 mL/min to afford JPD6-2 (1.3 mg, t_R = 29.5) (Figure 3.1.28).

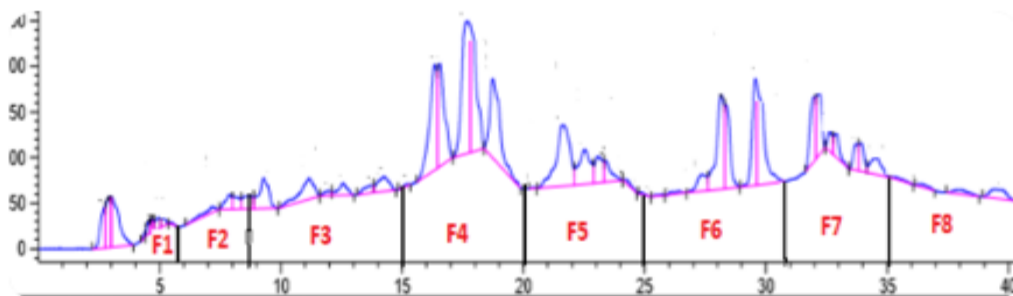


Figure 3.1.25: Fractionation of JPD extract every 5 min (observed at 250 nm)

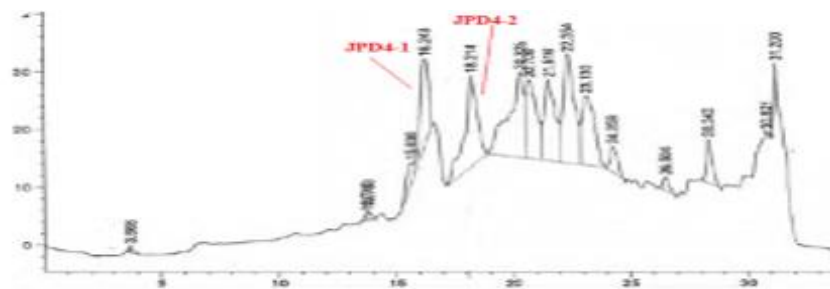


Figure 3.1.26: HPLC chromatogram of JPD fraction F4 (observed at 250 nm)

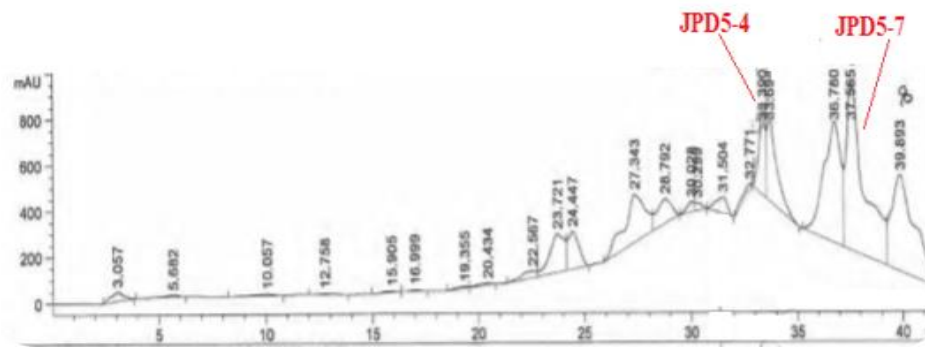


Figure 3.1.27: HPLC chromatogram of JPD fraction F5 (observed at 250 nm)

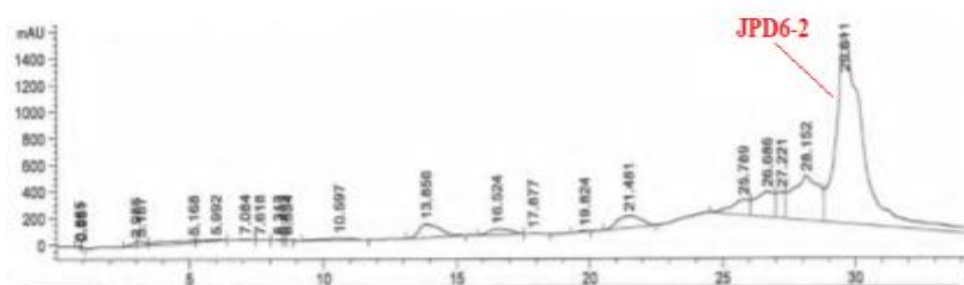
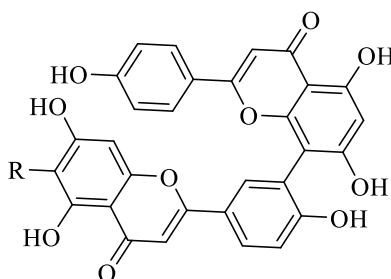


Figure 3.1.28: HPLC chromatogram of JPD fraction F6 (observed at 250 nm)

3.1.8 Characterization of isolated compounds from *J. phoenicea*

3.1.8.1 Characterization of biflavonoids

Three biflavonoids **24**, **25** and **76** were isolated from the SPE fractions F3 and F4 of JPM (Figures 1.5 and 3.1.29). All showed absorption bands at 270-275 nm and 330-332 nm, originating from the rings A and B of a flavonoid skeleton (Mabry *et al.*, 1970).



Compounds	R
Amentoflavone (25)	H
Sumaflavone (76)	OH

Figure 3.1.29: Structure of biflavonoids from JPM

Characterization of JPMF3-1 and JPMF4-1 as cupressoflavone (24)

Pale yellow powder; UV (MeOH) λ_{\max} : 204, 228, 274 and 330 nm (Figure 3.1.30); ^1H NMR (600 MHz, DMSO- d_6) Table (3.1.8) and Figure (3.1.31) indicated 5, 7, 4'-trihydroxy flavone dimers and showed two signals at δ_{H} 13.09 and 12.96 due to chelated phenolic hydroxyls. It also showed two single H-3 and H-3'' protons at δ_{H} 6.78 and 6.64 and two doublets ($J = 8.9$ Hz) at δ_{H} 6.74 and 7.49 assigned for H-3', 5'' and H-2', 6'', respectively. ^{13}C NMR (150 MHz, DMSO- d_6): Table 3.1.9 and Figure 3.1.32 exhibited 30 carbon atoms, two carbonyls at δ_{HC} 182.5. Analysis of the HMBC spectrum (Figure 3.1.33) showed correlations of the hydroxyl group with hydrogen bonded by cross peak at δ_{H} 13.22 (OH-5) (OH-5'') with C-5, C-5'' (δ 161.5), C-6, C-6'' (δ 99.3), and C-10, C-10'' (δ 104.0), which agree to those of cupressolavone (24) (Figure 1.5). ESIMS m/z 539 $[\text{M}+\text{H}]^+$, suggested the molecular formula $\text{C}_{30}\text{H}_{18}\text{O}_{10}$. All data were comparable to the published data (Alqasoumi *et al.*, 2013).

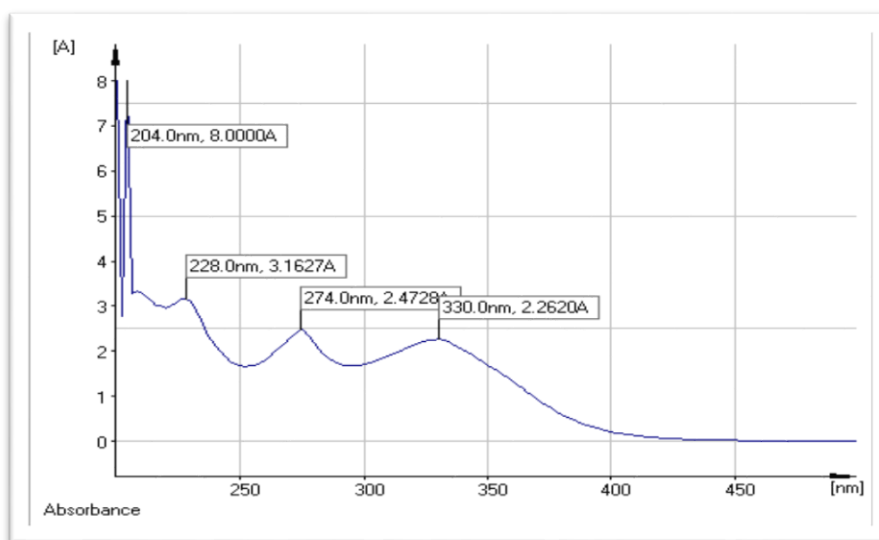


Figure 3.1.30: U.V. spectrum of cupressoflavone (24)
in MeOH

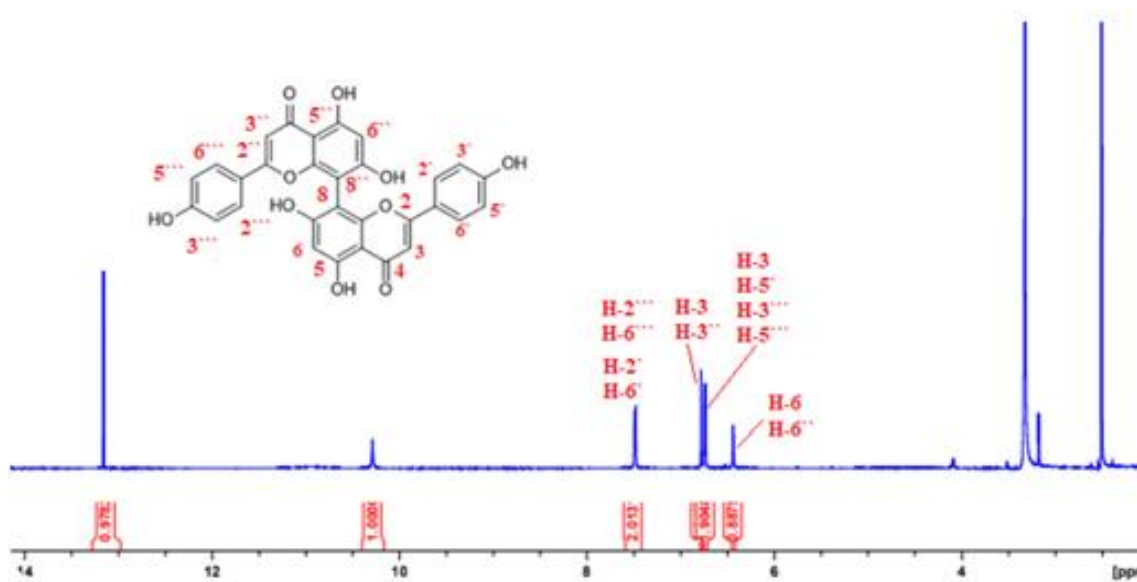


Figure 3.1.31: ^1H NMR spectrum (600 MHz, DMSO-d_6) of cupressoflavone (**24**)

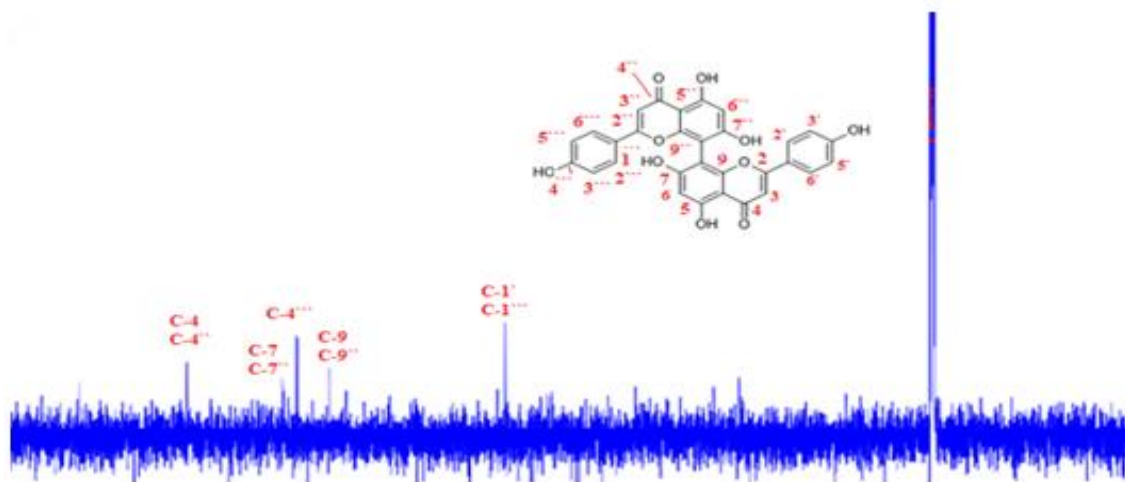


Figure 3.1.32 ^{13}C NMR spectrum (150 MHz, DMSO-d_6) of cupressoflavone (**24**)

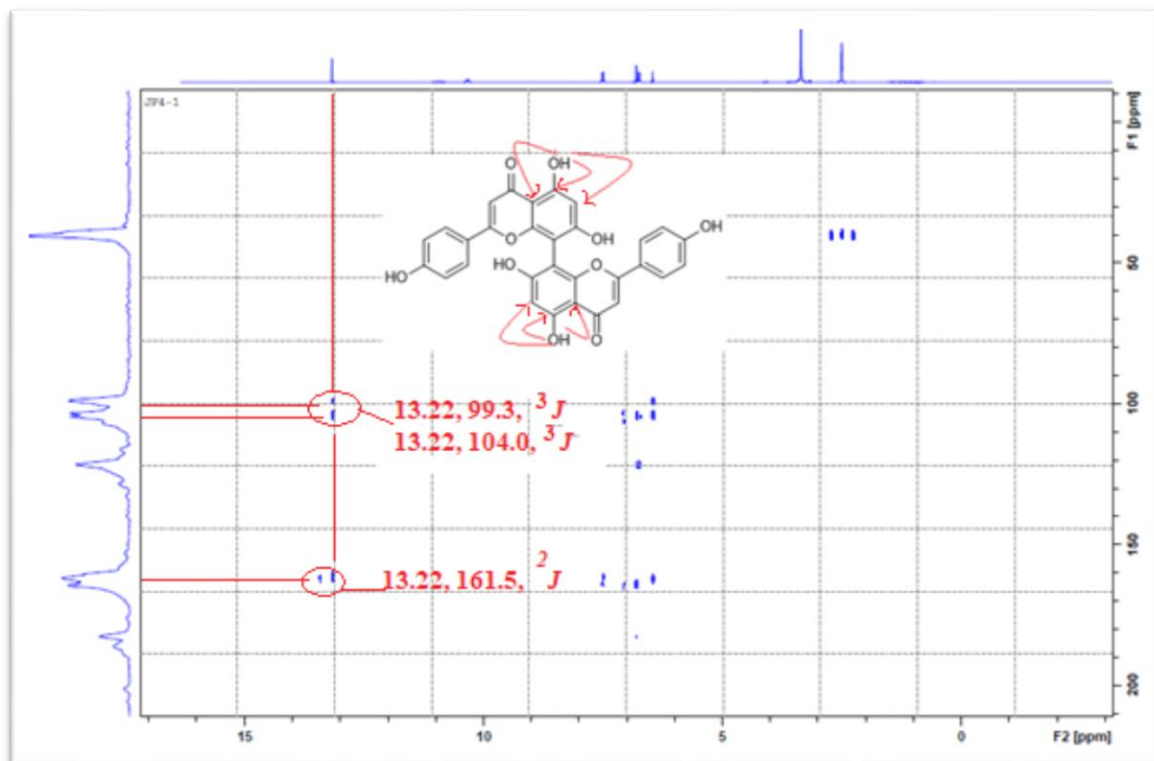


Figure 3.1.33: HMBC spectrum of cupressoflavone (**24**)

Characterization of JPMF3-2 and JPMF4-2 as amentoflavone (25)

Pale yellow amorphous powder; UV (MeOH) λ_{max} : 212, 270 and 332 nm; ^1H NMR (600 MHz, CD_3OD); Tables (3.1.8 and 3.1.9) and Figure (3.1.34). ESIMS m/z showed a peak at 539 $[\text{M}+\text{H}]^+$, indicating that the molecular formula could be $\text{C}_{30}\text{H}_{18}\text{O}_{10}$. ^1H NMR of compound **25** exhibited two doublets at δ_{H} 7.58 ($J = 8.8$ Hz, H-2''', H-6'''), and 6.74 ($J = 8.8$ Hz, H-3''', H-5''') assigned to an AA'BB' aromatic system. Signals of a trisubstituted aromatic ring containing one oxygenated carbon were observed at δ_{H} 8.00 (d, $J = 2.3$ Hz, H-2''), 7.14 (d, $J = 8.6$ Hz, H-6''), and 7.96 (dd, $J = 8.5; 2.2$ Hz H-5''), along with two broad singlets of a tetra substituted aromatic ring at δ_{H} 6.22 (br s, H-6) and 6.42 (br s, H-8) and one singlet at δ_{H} 6.40. ^1H NMR of compound **25** in $\text{DMSO}-d_6$ showed two

signals at δ_H 13.12 and 12.99 due to chelated phenolic hydroxyls (Figure 3.1.35). All data were comparable to the published data for amentoflavone (Markham *et al.*, 1987; Carbonezi *et al.*, 2007; Shaoguang *et al.*, 2014; Bais Abrol, 2016).

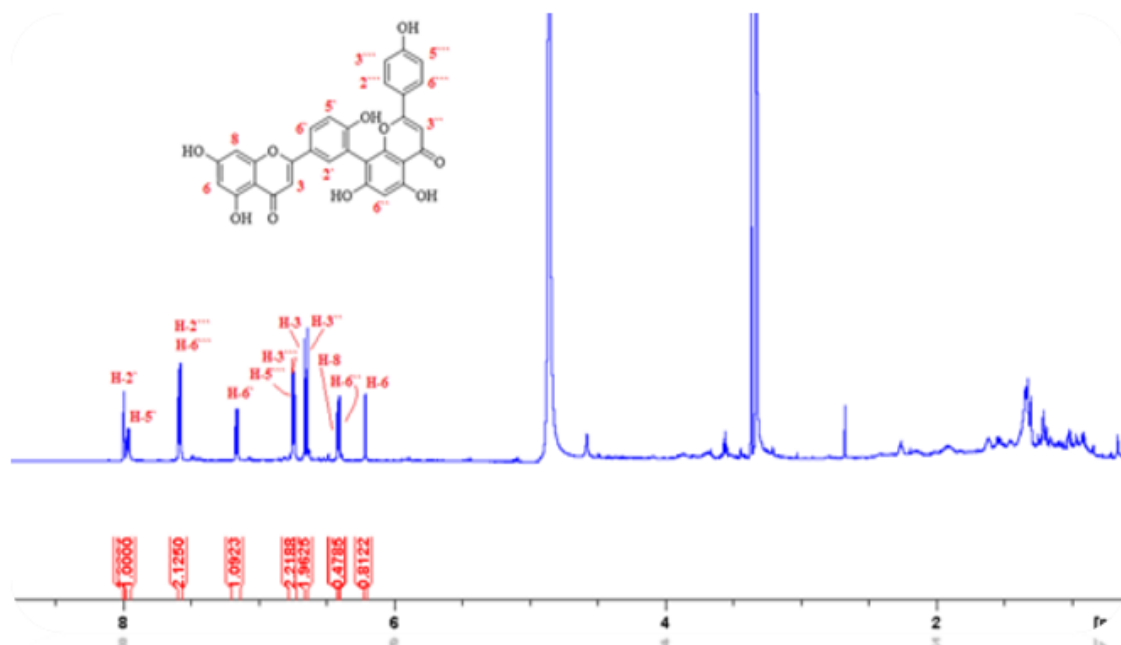


Figure 3.1.34: ^1H NMR spectrum (600 MHz, CD_3OD) of amentoflavone (**25**)

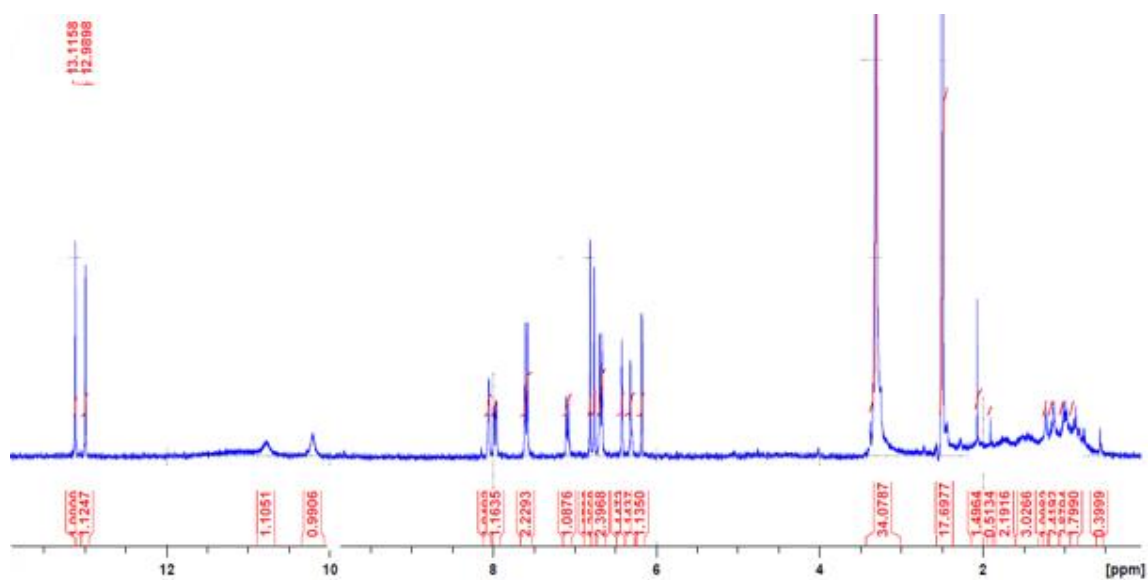


Figure 3.1.35: ^1H NMR spectrum (300 MHz, DMSO-d_6) of amentoflavone (**25**)

Characterization of JPMF4-4 as sumaflavone (76)

Amorphous yellow powder; UV (MeOH) λ_{max} : 224, 270 and 332 nm; ^1H NMR (300 MHz, DMSO- d_6); Table (3.1.8) and Figure (3.1.36) showed similar peaks to that of amentoflavone (25) with the absence of the singlet peak at δ_{H} 6.40 indicating the hydroxyl group at position C-6''. ESIMS m/z showed a peak at 554 $[\text{M}]^+$, indicating that the molecular formula could be $\text{C}_{30}\text{H}_{18}\text{O}_{11}$. All data were comparable to the published data of sumaflavone (76) (Markham *et al.*, 1987).

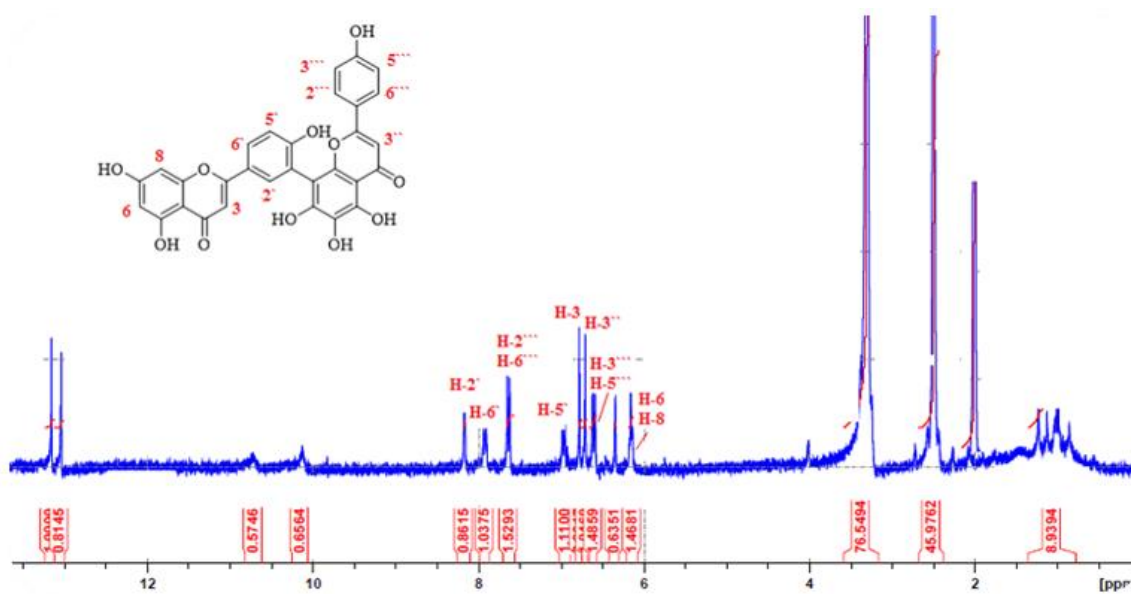
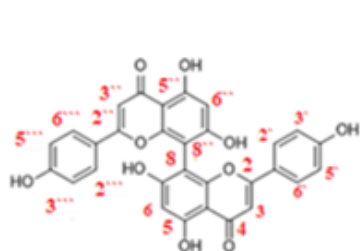
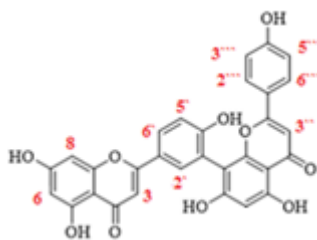


Figure 3.1.36: ^1H NMR spectrum (300 MHz, DMSO- d_6) of sumaflavone (76)

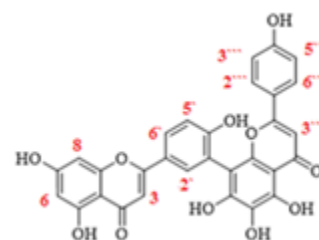
Table 3.1.8: ^1H NMR for the biflavonoids: Cupressoflavone (**24**), amentoflavone (**25**), and sumaflavone (**76**)



24



25



76

Position	Chemical Shift δ (ppm), multiplicity and J in Hz		
^1H	24* (300 MHz)	25** (600 MHz)	76** (300 MHz)
3	6.78 (s)	6.66 (s)	6.78 (s)
5	13.22 (s) (OH)	-	13.01 (s) (OH)
6	6.45 (s)	6.22 (br s)	6.16 (d, 2.0)
7	10.33 (s) (OH)	-	13.06 (s) (OH)
8		6.42 (br s)	
2 \wedge	7.49 (d, 8.9)	8.00 (d, 2.3)	8.17 (s)
3 \wedge	6.74 (d, 8.9)	-	
4 \wedge	10.33 (s) (OH)	-	
5 \wedge	6.74 (d, 8.9)	7.96 (dd, 8.5, 2.2)	7.0 (d, 8.6)
6 \wedge	7.49 (d, 8.9)	7.16 (d, 8.6)	7.92 (d, 8.8)
3 $\wedge\wedge$	6.78 (s)	6.64 (s)	6.71 (s)
6 $\wedge\wedge$	6.45 (s)	6.40 (s)	
2 $\wedge\wedge\wedge$	7.49 (d, 8.9)	7.58 (d, 8.8)	7.63 (d, 8.7)
3 $\wedge\wedge\wedge$	6.74 (d, 8.9)	6.74 (d, 8.8)	6.61 (d, 8.6)
5 $\wedge\wedge\wedge$	6.74 (d, 8.9)	6.74 (d, 8.8)	6.61 (d, 8.6)
6 $\wedge\wedge\wedge$	7.49 (d, 8.9)	7.58 (d, 8.8)	7.63 (d, 8.7)

*= (DMSO- d_6), **= (CD $_3$ OD)

Table 3.1.9: ^{13}C NMR data of biflavonoids: Cupressoflavone (**24**), and amentoflavone (**25**)

Position ^{13}C	Chemical Shift δ (ppm),		Position ^{13}C	Chemical Shift δ (ppm)	
	24* (75 MHz)	25** (150 MHz)		24* (75 MHz)	25** (150 MHz)
2	163.9	166.0	2 ^{''}	163.9	166.2
3	103.0	103.5	3 ^{''}	103.0	100.3
4	182.5	184.0	4 ^{''}	182.5	184.4
5	161.5	163.4	5 ^{''}	161.5	163.4
6	99.3	100.3	6 ^{''}	99.3	95.3
7	164.1	166.2	7 ^{''}	164.1	162.7
8	98.9	95.3	8 ^{''}	98.9	105.5
9	155.2	159.6	9 ^{''}	155.2	159.6
10	104.0	105.5	10 ^{''}	104.0	105.5
1 [`]	121.7	123.2	1 ^{'''}	121.7	123.4
2 [`]	128.4	133	2 ^{'''}	128.4	129.0
3 [`]	116.3	122.0	3 ^{'''}	116.3	117.0
4 [`]	161.3	161.5	4 ^{'''}	161.3	163.4
5 [`]	116.3	129	5 ^{'''}	116.3	117.0
6 [`]	128.4	117.0	6 ^{'''}	128.4	129.0

*= (DMSO- d_6), **= (CD₃OD)

3.1.8.2 Characterization of diterpenes

Five diterpenoids, one from the VLC fraction 3 of the *n*-hexane extract (JPH3), three from fraction 4 of the DCM extract (JPD4-5, JPD4-6, and JPD4-8) and one JPDF6-2 from fraction 6 of the DCM extract, were isolated. Two bicyclic diterpenes labdanes: 13- *epi*-cupressic acid (**42**) and imbricatolic acid (**41**), two tricyclic diterpenes; one pimarane, 3-hydroxy sandaracopimaric acid (**44**) and the other is an abietane, dehydroabietic acid (**46**) (Figure 1.5). The ^1H and ^{13}C NMR spectroscopic data (Tables 3.1.10 and 3.1.11) indicated

that they had 20 carbons, keto and hydroxyl groups, suggesting that they were diterpenes (Su *et al.*, 1994). ^1H - and ^{13}C -NMR of **42** and **41** showed two proton singlets at δ_{H} 4.49, 4.83 assigned for H-17. Both compounds showed an 18-CH₃ singlet (δ_{H} 1.24, δ_{C} 29.2) (δ_{H} 1.24, δ_{C} 30.6); 19-COOH (δ_{C} 183.2) (δ_{C} 183.4); 20-CH₃ singlet (δ_{H} 0.59, δ_{C} 12.9) (δ_{H} 0.60, δ_{C} 13.1) suggesting identical data for labdan-8(17)-ene skeleton (Su *et al.*, 1994).

Characterization of JPHF3, JPDF5-4, JPDF4-5 as 13- epi-cupressic acid (42)

Amorphous white powder; ^1H NMR (600 MHz, CDCl_3) and ^{13}C NMR (150 MHz, CDCl_3): Tables (3.1.10 and 3.1.11) and Figures (3.1.37 and 3.1.38) of **42** showed mono-substituted double bond (CH at δ_{H} 5.91, dd, $J = 10.2, 17.6$ Hz and δ_{C} 145.8; CH₂ at δ_{H} 5.06 dd, $J = 0.8, 10.6$ Hz, δ_{H} 5.21 dd, $J = 1.3, 17.2$ Hz and δ_{C} 145.8, 112.0 assigned for C-14 and C-15. The methyl singlet (δ_{H} 1.27, δ_{C} 28.3) was assigned to C-16 on an oxygenated fully substituted C-13 at δ_{C} 74.1 as indicated from HMBC experiment (Figure 3.1.39). ESIMS m/z showed a peak at 319 $[\text{M}-\text{H}]^-$, indicating that the molecular formula could be $\text{C}_{20}\text{H}_{32}\text{O}_3$. The data of **42** was identical with those reported for 13-*epi*-cupressic acid (Su *et al.*, 1994; Alqasoumi *et al.*, 2013).

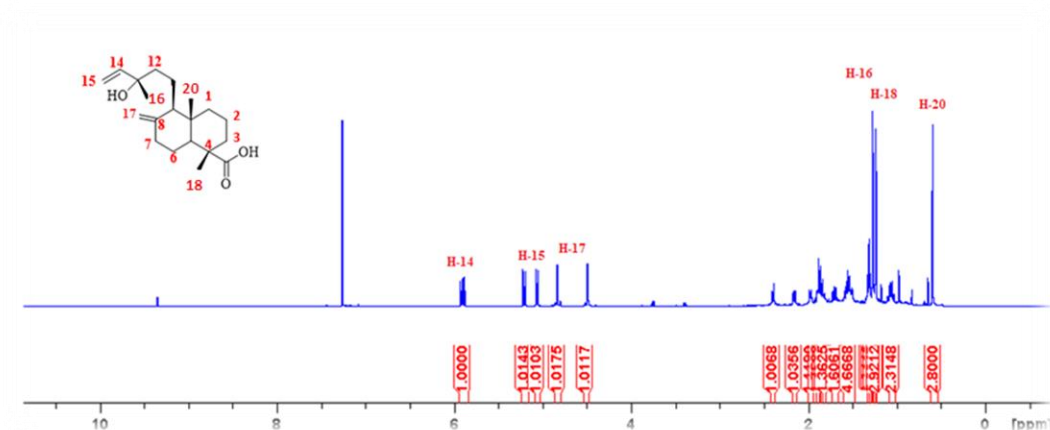


Figure 3.1.37: ^1H NMR spectrum (600 MHz, CDCl_3) of 13-*epi*-cupressic acid (**42**)

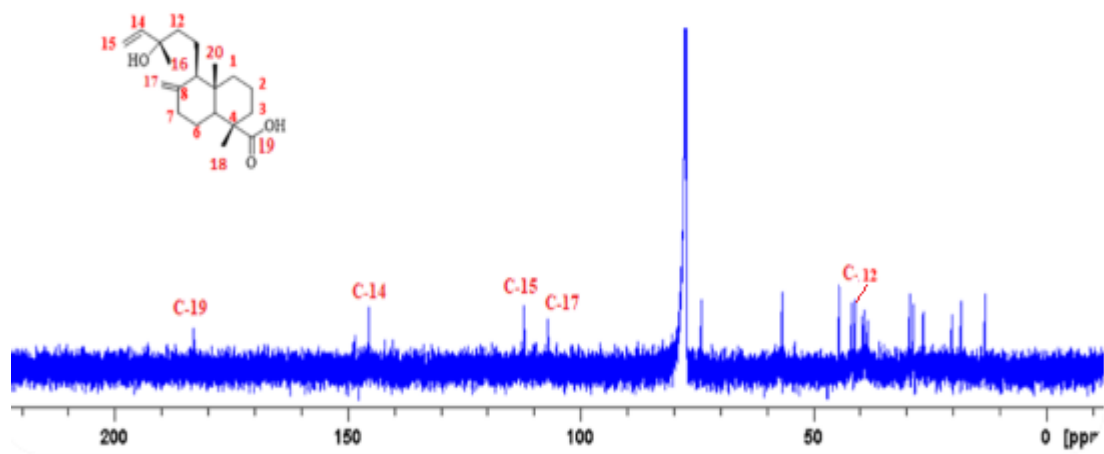


Figure 3.138: ^{13}C NMR spectrum (150 MHz, CDCl_3) of 13-*epi*-cupressic acid (42)

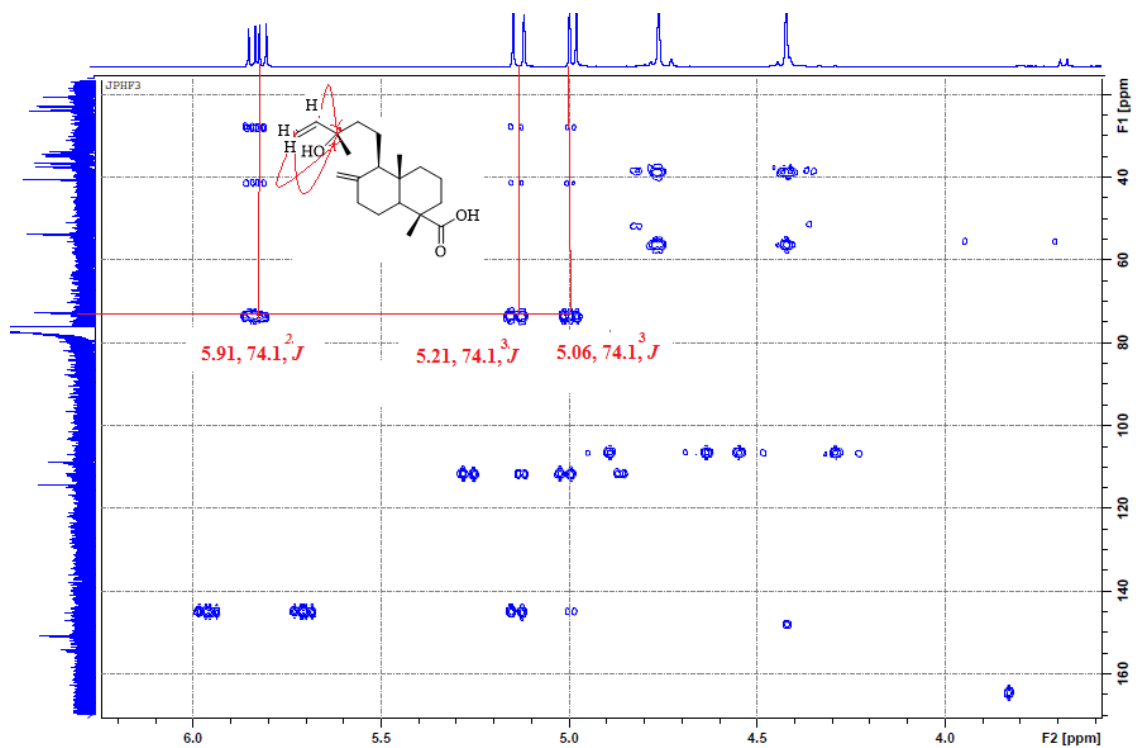


Figure 3.139: HMBC correlations of 13-*epi*-cupressic acid (42)

Characterization of JPDF4-6, JPDF5-4 as imbricatolic acid (41)

Amorphous white powder; data of both ^1H NMR (600 MHz, CDCl_3) and ^{13}C NMR (150 MHz, CDCl_3): Tables (3.1.10 and 3.1.11) and Figures (3.1.40 and 3.1.41) suggested the presence of carboxyl, hydroxyl (7.87, 7.90, 9.77 br s) and terminal methylene groups at δ_{H} 0.6 (s, $-\text{CH}_3$ at C-10); δ_{H} 0.90 (s, $-\text{CH}_3$ at C-13); 1.24 (s, $-\text{CH}_3$ at C-4); 3.67 (m, $-\text{CH}_2\text{OH}$), 4.83 and 4.49 (both s, =CH). The ESIMS m/z at 323 $[\text{M}-\text{H}]^-$ suggested the molecular formula $\text{C}_{20}\text{H}_{34}\text{O}_3$. All data were comparable to the published data (Wenkert & Buckwalter, 1972; Campelo & Fonseca 1975; Su *et al.*, 1994; Alqasoumi *et al.*, 2013). MS, ^1H and ^{13}C -NMR data Figures of **41** indicated the lack of the second double bond. The appearance of the C-16 methyl as doublet at δ_{H} 0.90 ($J = 6.5$ Hz) and the appearance of CH_2OH (δ_{H} 3.67 (m), δ_{C} 61.6) indicated a C-15 hydroxyl in **41**. The data of **41** was consistent with those reported for imbricatolic acid (Wenkert & Buckwalter, 1972).

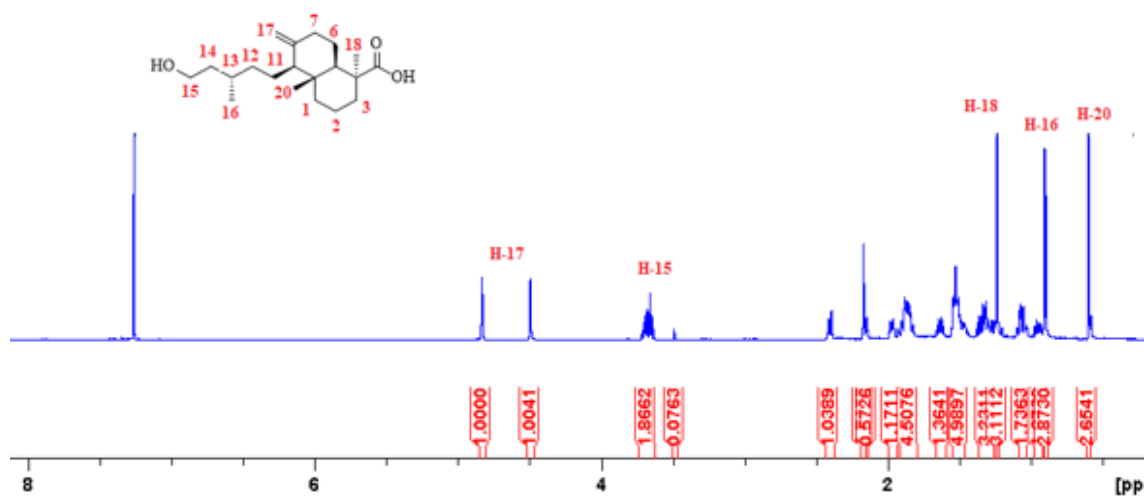


Figure 3.1.40: ^1H NMR spectrum (600 MHz, CDCl_3) of imbricatolic acid (**41**)

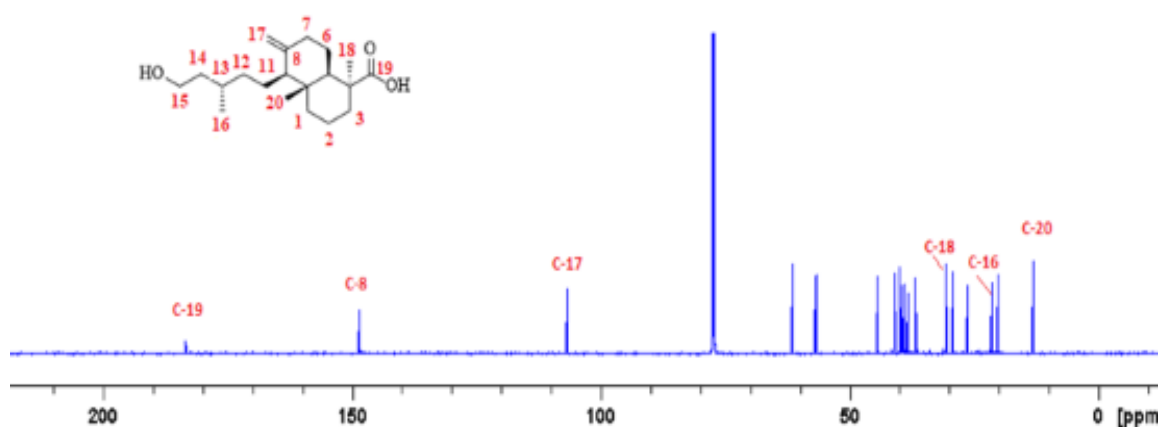


Figure 3.1.41: ^{13}C NMR spectrum (150 MHz, CDCl_3) of imbricatolic acid (**41**)

Characterization of JPDF5-7, JPDF4-8 as 3-hydroxy sandaracopimaric acid (44)

Amorphous white powder; UV (MeOH): λ_{max} : 210, 236 and 306 nm; ^1H NMR (600 MHz, CDCl_3) and ^{13}C NMR (150 MHz, CDCl_3): Tables (3.1.10 and 3.1.11) and Figures (3.1.42 and 3.1.43) showed pimarandiene skeleton with a C-8, C-14 double bond (δ_{C} 137.8 and δ_{C} 130.6) (Su *et al.*, 1994). There was also an oxygenated CH at δ_{H} 4.02 (dd, $J = 4.6, 11.8$ Hz) and δ_{C} 76.6, the location of the hydroxyl groups was assigned to C-3 based on the HMBC correlation. It also showed ESIMS m/z 317 $[\text{M}-\text{H}]^-$, consistent with the molecular formula $\text{C}_{20}\text{H}_{30}\text{O}_3$. Comparison of the data with data recorded in the literature identified **44** as 3 β -hydroxysandaracopimaric acid (Kozo & Takami, 1972; Wenkert and Buckwalter, 1972, Muhammad *et al.*, 1992; Su *et al.*, 1994; Alqasoumi *et al.*, 2013).

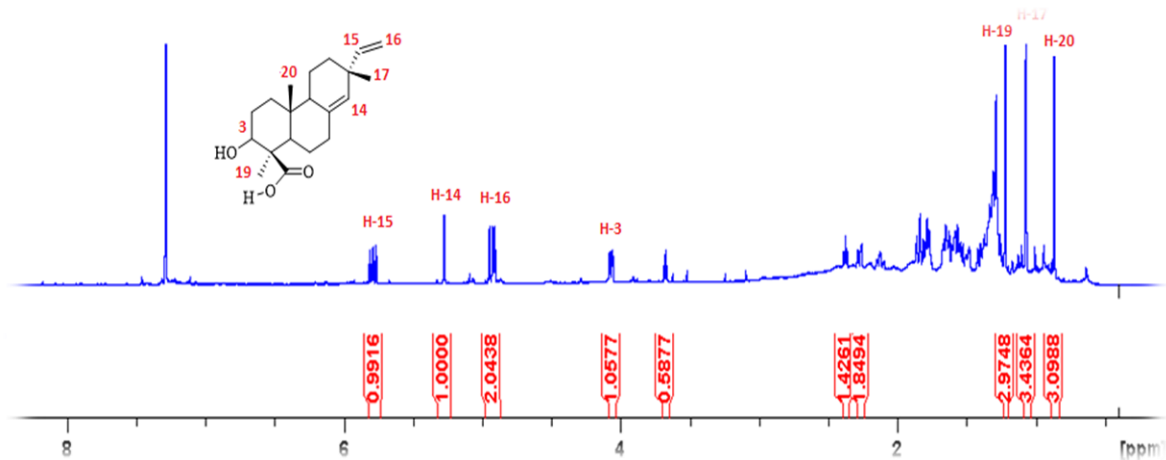


Figure 3.1.42: ^1H NMR spectrum (600 MHz, CDCl_3) of 3-hydroxy sandaracopimaric

(44)

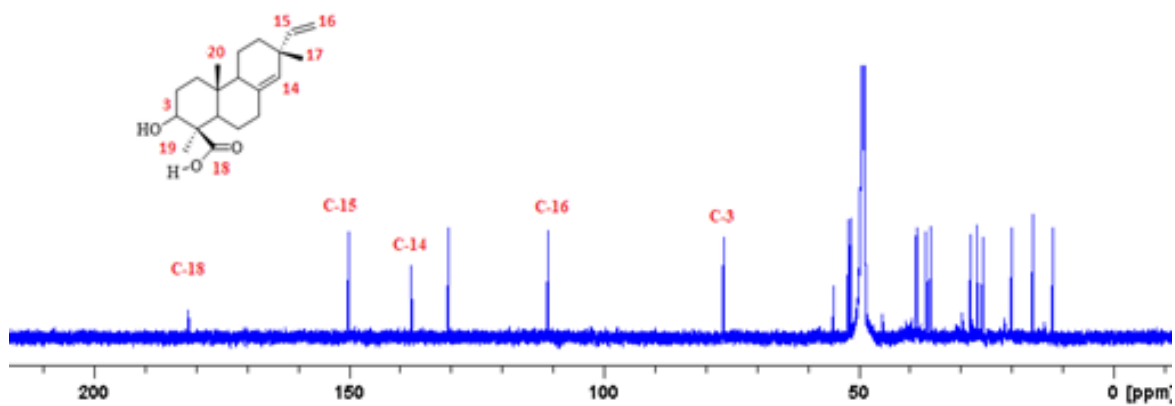
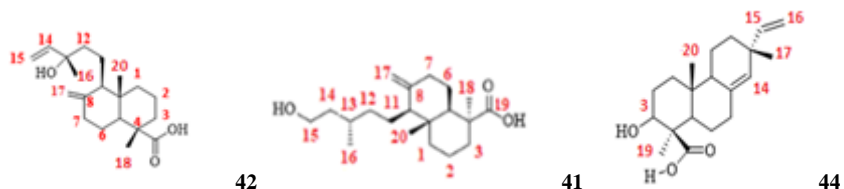


Figure 3.1.43: ^{13}C NMR spectrum (150 MHz, CDCl_3) of 3-hydroxy sandaracopimaric

(44)

Table 3.1.10: ^1H NMR (600 MHz, CDCl_3) for diterpenes: 13- *Epi*-cupressic acid (**42**), imbricatolic acid (**41**), 3-hydroxy sandaracopimaric acid (**44**) (CDCl_3).



Position	Chemical Shift δ (ppm), multiplicity and J in Hz		
^1H	42	41	44
1	1.05 (br s), 1.71(m)	0.95 (m); 1.86 (m)	1.07 (m), 1.21 (m)
2	1.50 (m), 1.71 (m)	1.45 (m); 1.86 (m)	1.38 (m), 1.45 (m)
3	1.04 (dd; 4.8; 13.9) 1.97, (br s)	1.06 (dd; 4.2; 13.3) 2.14 (br s)	4.02 (dd; 4.6, 11.8)
5	1.32 (m)	1.32 (m)	1.53 (m)
6	1.83 (m), 1.89 (m)	1.85 (m), 1.87 (m)	0.92 (m), 1.25 (m)
7	1.86,(m), 2.40 (br s)	1.88 (m), 1.99 (m)	1.86 (m), 2.23 (m)
9	1.50, m	1.91 (m) 2.40 (dd, 2.8, 8.8)	
11	1.32 (m), 1.45, (m)	1.36 (m)	1.38 (m), 1.50 (m)
12	1.32 (m), 1.57, (m)	1.29 (m)	1.2 (m), 1.24 (m)
13		1.34 (m)	-
14	5.91, dd, 10.2, 17.6	1.34 (m)	5.24 (s)
15	5.21, dd, 1.3. 17.2 5.06, dd, 10.7, 0.8	3.67 (m)	5.76 (dd; 10.4, 17.7)
16	1.27, s	0.90 (d, 6.5)	4.89 (d, 10.6), 4.90 (d, 17.5)
17	4.49 (s), 4.83 (s)	4.83 (s), 4.49(s)	1.04
18	1.24 (s)	1.24 (s)	-
19	-	-	1.18 (s)
20	0.59 (s)	0.60 (s)	0.83 (s)

Table 3.1.11: ^{13}C NMR (150 MHz, CDCl_3) for diterpenes: 13-*epi*-cupressic acid (**42**), imbricatolic acid (**41**), 3-hydroxy sandaracopimaric acid (**44**)

Position ^{13}C	Chemical Shift δ (ppm)			Position ^{13}C	Chemical Shift δ (ppm)		
	42	41	44		42	41	44
1	39.4	39.1	38.5	11	18.1	21.5	28.1
2	20.2	20.2	20	12	41.6	40.0	35.9
3	38.2	36.8	76.6	13	74.1	29.4	38.7
4	44.5	44.5	54.9	14	145.8	41.0	130.6
5	56.7	56.7	52.0	15	112.0	61.6	150.0
6	26.4	26.4	25.7	16	28.3	21.5	111.0
7	39.0	38.4	36.7	17	107.1	106.6	26.7
8	148.2	148.6	137.8	18	29.2	30.6	181.5
9	56.7	57.0	51.6	19	183.2	183.4	11.9
10	40.9	39.5	38.7	20	12.9	13.1	15.8

Characterization of JPDF6-2 as dehydroabietic acid (callistric acid) (46)

Amorphous white powder, The ESIMS m/z 301 $[\text{M}+\text{H}]^+$, confirmed the molecular formula $\text{C}_{20}\text{H}_{28}\text{O}_2$ as that of a diterpene. ^1H NMR data (600 MHz, CDCl_3) (Figure 3.1.44) showed aromatic protons including: two *ortho-meta* coupling at δ_{H} 7.00 (1H, dd, $J = 8.2$ Hz, 1.7) assigned to H-2' and δ_{H} 2.89 (1H, dd, $J = 5.6$ Hz, $J = 16.6$ Hz) assigned to H-7, two *ortho*-coupling at δ_{H} 7.18 (1H, d, $J = 8.2$, H-1') and δ_{H} 1.22 (6H, d, $J = 7.0$, H-7', H-8') and a broad singlet at δ_{H} 6.89 (1H, H-4'). All the aromatic signals indicated that this diterpene is abietane type. The signals at 2.82 (2H, m, H-6'), 1.60 (2H, m, H-6), 1.27 (3H, s, H-12), , 1.1 (3H, s, H-13) indicated that this compound might be dehydroabietic acid. The ^{13}C NMR (150 MHz, CDCl_3) (Figure 3.1.45) proved that where

it showed the 20 carbon signals of the tricyclic diterpenes including six aromatic carbons, carbonyl carbon at δ_C 181.6, four methyl signals at δ_C 21.7 (C-13), 20.9 (C-8') and 19.9 (C-12). All data were comparable to the published data of dehydroabietic acid (callistric acid) (**46**) (González *et al.*, 2010).

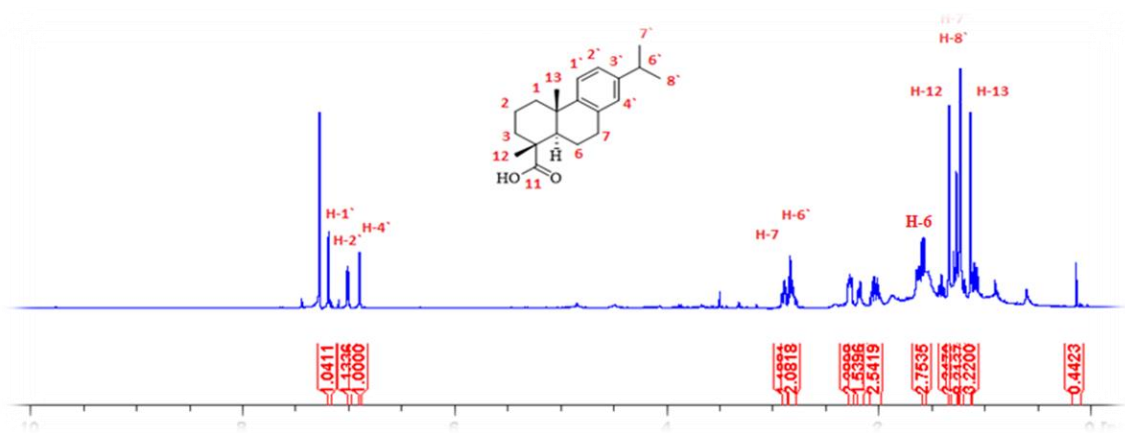


Figure 3.1.44: ¹H NMR spectrum (600 MHz, CDCl₃) of dehydroabietic acid (**46**)

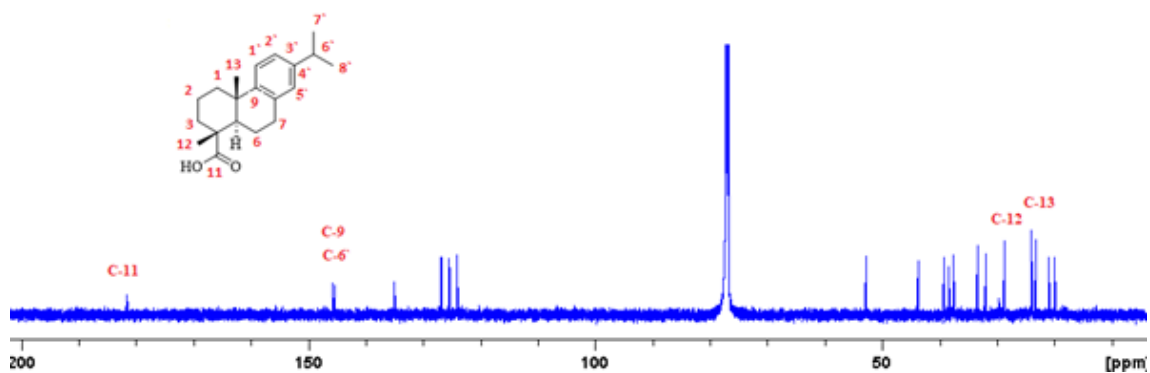


Figure 3.1.45: ¹³C NMR spectrum (150 MHz, CDCl₃) of dehydroabietic acid (**46**)

3.1.8.3 Characterization of lignans

Two lignans were isolated from the active F4 of *J. phoenicea* DCM extract [JPD4-1 (**29**) and JPD4-2 (**30**)] (Figure 1.5). The ^1H and ^{13}C NMR spectroscopic data (Figure 3.1.46, and Figure 3.1.47) and (Figure 1, Appendix) indicated that they belong to the furan subgroups. The presence of 3, 4, 5-trimethoxyphenyl, which are the most frequently occurring aromatic rings found in lignans (Tsopmoa *et al.*, 2013). The protonated aromatic carbons show signals at 106.2, 108.1 and 109.3 ppm. The singlet signal at 108.1 ppm was assigned to C-2' and C-6' (δ_{H} 6.53 and 6.36) for the two compounds **28** and **29**, respectively, while those at 106.2 and 109.3 ppm were attributed to C-3 and C-6, respectively for the compound **29**. By comparison with related data carbons suggesting that they are deoxydophyllotoxin **29** and β -peltatin methyl ether **28** (Figures 1.5) (Fonseca, *et al.*, 1980; Rojas-Sepúlveda *et al.*, 2012; Tsopmoa *et al.*, 2013).

Characterization of JPDF4-1 as a mixture of deoxydophyllotoxin and terpenoid (29)

Amorphous white powder; ^1H NMR (600 MHz, CDCl_3) δ 6.67 (1H, s, H-6), 6.53 (1H, s, H-3), 6.35 (2H, s, H-2', H-6'), 5.94 (2H, d, $J = 5.9$, O- CH_2 -O), 5.04 (1H, m, H-9 α , H-7'), 4.03 (1H, dd, $J = 11.5, 3.7$ Hz, H-9 β), 3.81 (3H, s, $\text{CH}_3\text{O}-4'$), 3.75 (6H, s, $\text{CH}_3\text{O}-3'$, $\text{CH}_3\text{O}-5'$), 2.92 (1H, dd, $J = 6.5, 17.4$ Hz, H-7), 2.80 (1H, m, H-8, H-8') and ^{13}C NMR (150 MHz, CDCl_3) δ 182.2 (C-9'), 151.8 (C-3', C-5'), 148.1 (C-4), 146.5 (C-6), 138.1 (C-1', C-4'), 136.6 (C-5), 134.0 (C-2), 132 (C-1), 111.9 (C-2', C-6'), 109.0 (C-6), 107.2 (C-3), 101.9 (O- CH_2 -O), 72.8 (C-9), 61.5 ($\text{CH}_3\text{O}-4'$), 56.5 ($\text{CH}_3\text{O}-3'$, $\text{CH}_3\text{O}-5'$), 47.7 (C-8'), 47.7 (C-7'), 32.7 (C-8), 39.5 (C-7). ESIMS m/z showed a peak at 399 $[\text{M}+\text{H}]^+$

indicating that the molecular formula could be C₂₂H₂₂O₇. All comparable data confirmed the structure of deoxydophyllotoxin (Rojas-Sepúlveda *et al.*, 2012).

Characterization of JPDF4-2 as β-peltatin methyl ether (28)

Amorphous white powder; ¹H NMR (600 MHz, CDCl₃) (Figure 3.1.46) δ 6.36 (2H, s, H-2', H-6'), 6.28 (1H, s, H-3), 5.88 (2H, d, *J* = 5.9, O-CH₂-O), 4.58 (1H, d, *J* = 4.3 Hz, H-7), 4.47 (1H, dd, *J* = 7.3, 1.3 Hz, H-9), 4.07 (3H, s, CH₃O -6), 3.94 (1H, t, *J* = 9.6 Hz), 3.80 (3H, s, CH₃O-4), 3.76 (6H, s, CH₃O-3, CH₃O-5), 3.17 (1H, dd, *J* = 5.1, 16.8 Hz, H-7), 2.66 (1H, d, *J* = 4.5, H-8'), 2.64 (1H, m, H-8), 2.45 (1H, dd, *J* = 10.6, 17.1 Hz, H-7) and ¹³C NMR (150 MHz, CDCl₃) (Figure 3.1.47) δ 175.5 (C-9'), 152.9 (C-3', C-5'), 148.6 (C-4), 145.1 (C-6), 138.1 (C-1', C-4'), 136.6 (C-5), 132.0 (C-2), 121.3 (C-1), 108.7 (C-2', C-6'), 104.8 (C-3), 101.3 (O-CH₂-O), 72.8 (C-9), 59.7 (CH₃O-6), 56.7 (CH₃O-3', CH₃O-5'), 55.7 (CH₃O-4') 47.7 (C-8'), 44.2 (C-7'), 32.7 (C-8), 27.9 (C-7). ESIMS *m/z* showed a peak at 429 [M+H]⁺, indicating that the molecular formula could be C₂₃H₂₄O₈. All data confirmed that compound **28** is β-peltatin methyl ether comparable to the published data (Rojas-Sepúlveda *et al.*, 2012).

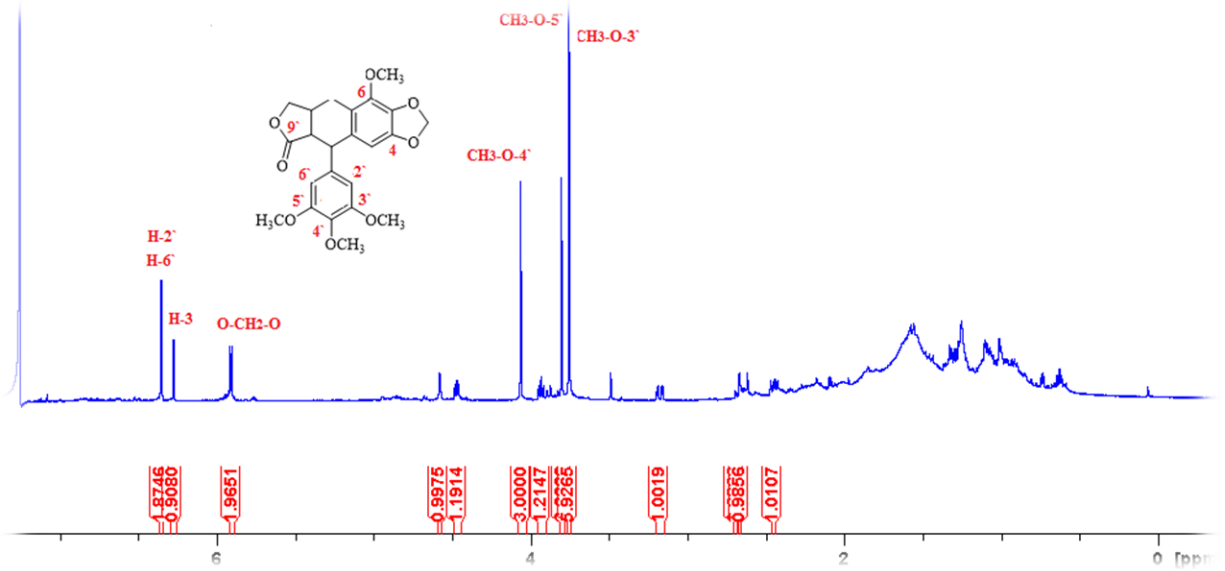


Figure 3.1.46: ¹H NMR spectrum (600 MHz, CDCl₃) of β -methylpeltatin A methyl ether (**28**)

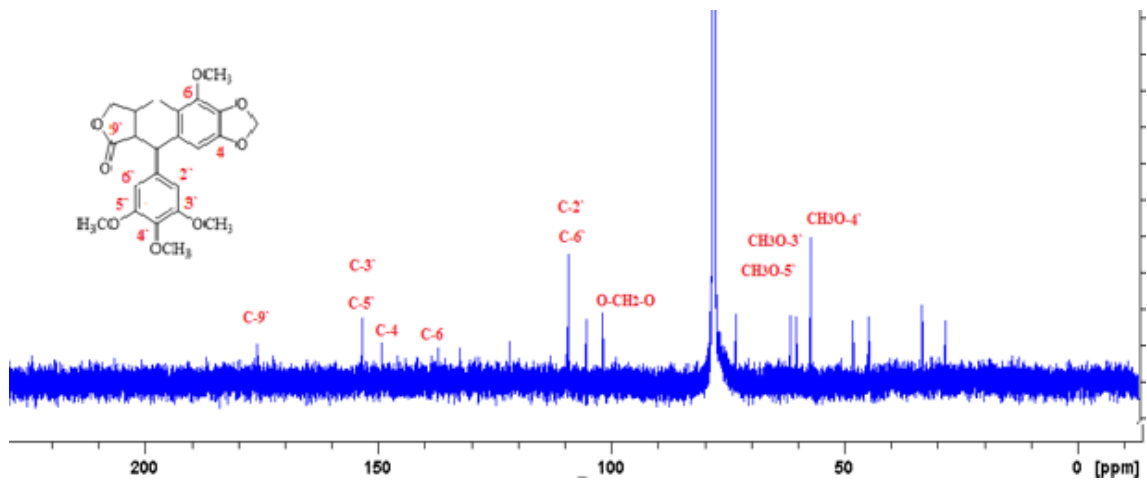


Figure 3.1.47: ¹³C NMR spectrum (150 MHz, CDCl₃) of β -methylpeltatin A methyl ether (**28**)

Characterization of JPHF2 D as aliphatic alcohol (heptacosane-14-ol) (77)

It appeared as a white amorphous powder. ESIMS showed the highest significant peak at m/z : 397 $[M+H]^+$. Consequently, the expected molecular weight was (396.73) attributed to $C_{27}H_{56}O$. 1H (400 MHz, $CDCl_3$) and ^{13}C NMR (75 MHz, $CDCl_3$), (Figures 3.1.49 and 3.1.50): δ 0.9 t (6H), 1.28 s, 1.4 m (4H), 3.61 (m), δ 14.094 (C-1-1'), 29.69 (C-2-13, C-2-13') and 125.00 (C-14). The NMR and MS spectra confirmed the structure of heptacosane-14-ol (Figure 3.1.48).

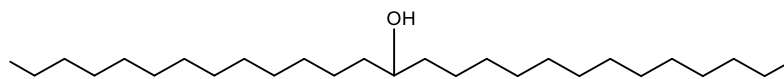


Figure 3.1.48: Structure of heptacosane-14-ol (77)

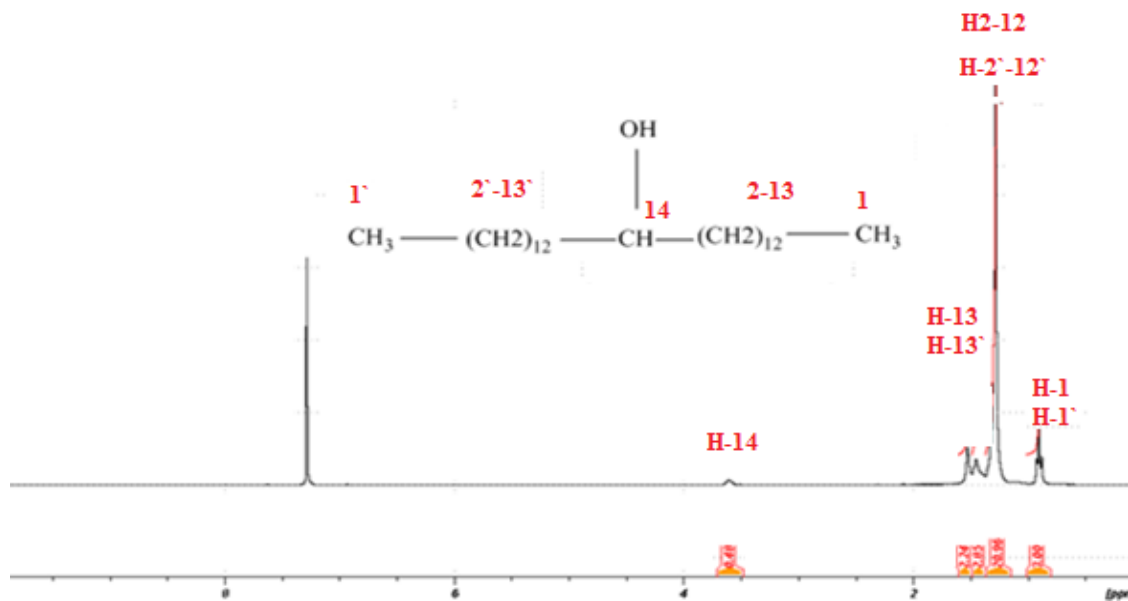


Figure 3.1.49: 1H NMR spectrum (400 MHz, $CDCl_3$) of heptacosane-14-ol (77)

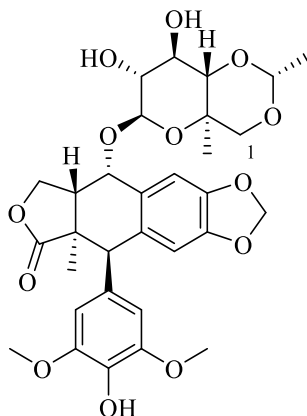


Figure 3.1.51: The structure of etoposide standard (**78**)

Table 3.1.12: The IC₅₀ (μM) of different isolated compounds from *J. phoenicea* leaves on A549 lung cancer cells.

Pure compound	IC ₅₀ μM
Cupressoflavone (24)	65 ± 1.55
Amentoflavone (25)	No activity
Sumaflavone (76)	77 ± 1.64
13- <i>Epi</i> -cupressic acid (42)	159 ± 1.16
Imbricatolic acid (41)	263 ± 2.45
3-Hydroxy sandaracopimaric acid (44)	223 ± 2.47
Deoxydophyllotoxin mixture (29)	2.79 ± 0.09
Etoposide (78)	61 ± 1.56

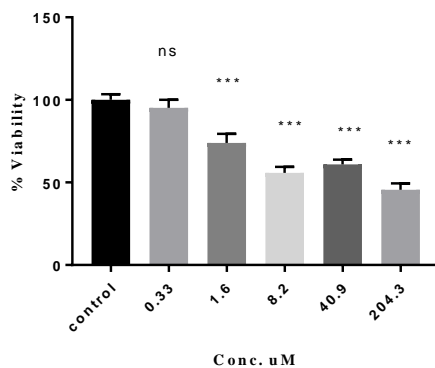
All experiments were carried out in triplicate on separate occasions.

Data are expressed as means a ± standard error of the mean.

Table 3.1. 13: The IC₅₀ (μM) of Imbricatolic acid **41** on PC3 lung cancer cells

Pure compound	IC ₅₀ μM
Imbricatolic acid (41)	204±1.82

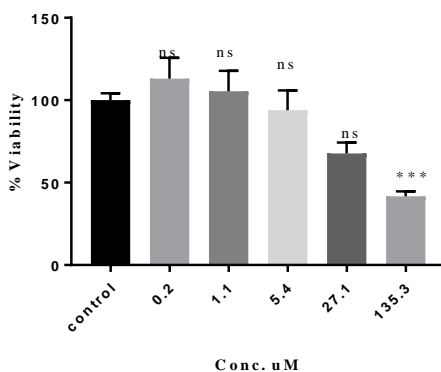
Cytotoxicity of cupressoflavone in A549 cells according to the MTT assay



All experiments were carried out in triplicate on separate occasions. Data were expressed as means \pm standard error of the mean derived from $n \geq 12$ from three separate occasions.

Figure 3.1.52: The cytotoxic activity of cupressoflavone (**24**) against lung cancer cell line (A549)

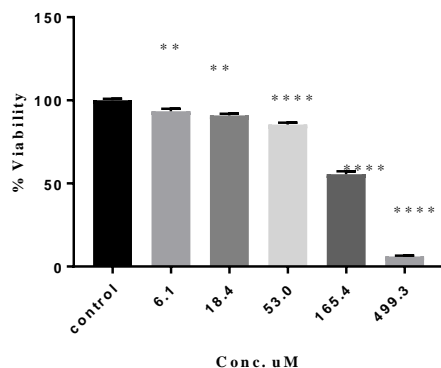
Cytotoxicity of sumaflavone in A549 cells according to the MTT assay



All experiments were carried out in triplicate on separate occasions. Data were expressed as means \pm standard error of the mean derived from $n \geq 12$ from three separate occasions.

Figure 3.1.53: The cytotoxic activity of sumaflavone (**76**) against lung cancer cell line (A549)

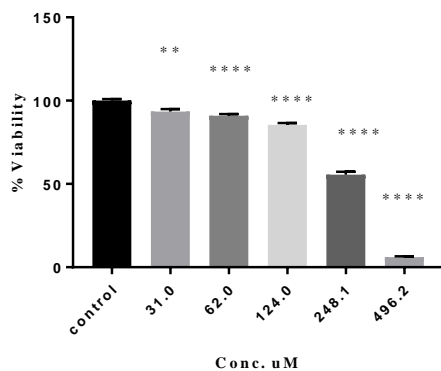
Cytotoxicity of 13-*epi*-cupressic acid in A549 cells according to the MTT assay



All experiments were carried out in triplicate on separate occasions. Data were expressed as means \pm standard error of the mean derived from $n \geq 12$ from three separate occasions.

Figure 3.1.54: The cytotoxic activity of 13-*epi*-cupressic acid (**42**) against lung cancer cell line

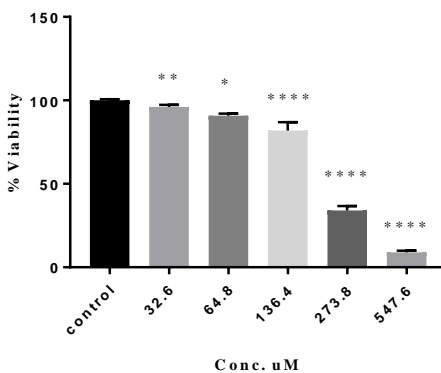
Cytotoxicity of imbricatolic acid in A549 cells according to the MTT assay



All experiments were carried out in triplicate on separate occasions. Data were expressed as means \pm standard error of the mean derived from $n \geq 12$ from three separate occasions.

Figure 3.1.55: The cytotoxic activity of imbricatolic acid (**41**) against lung cancer cell line

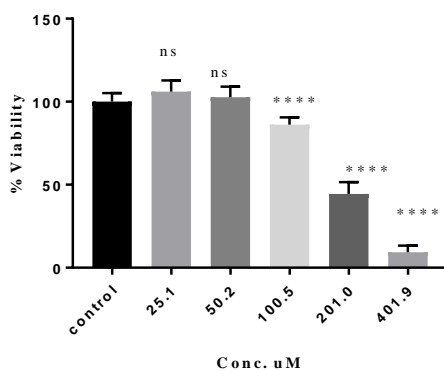
Cytotoxicity of imbricatolic acid in PC3 cells according to the MTT assay



All experiments were carried out in triplicate on separate occasions. Data were expressed as means \pm standard error of the mean derived from $n \geq 12$ from three separate occasions.

Figure 3.1.56: The cytotoxic activity of imbricatolic acid (**41**) against prostate cancer cell line

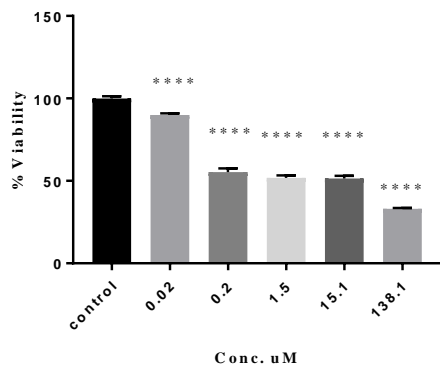
Cytotoxicity of 3-hydroxysandaracopimaric acid acid in A549 cells according to the MTT assay



All experiments were carried out in triplicate on separate occasions. Data were expressed as means \pm standard error of the mean derived from $n \geq 12$ from three separate occasions.

Figure 31.57: The cytotoxic activity of 3-hydroxy sandaracopimaric acid (**44**) against lung cancer cell line

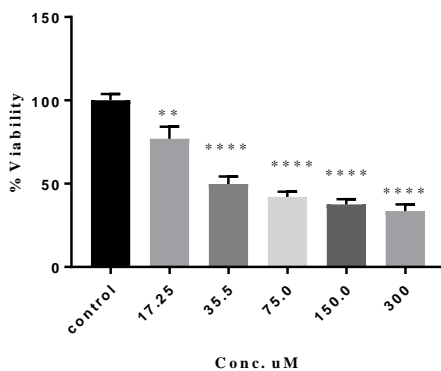
Cytotoxicity of deoxydophyllotoxin in A549 cells according to the MTT assay



All experiments were carried out in triplicate on separate occasions. Data were expressed as means \pm standard error of the mean derived from $n \geq 12$ from three separate occasions.

Figure 3.1.58: The cytotoxic activity of deoxydophyllotoxin (**29**) mixture against lung cancer cell line

Cytotoxicity of etoposide standard in A549 cells according to the MTT assay

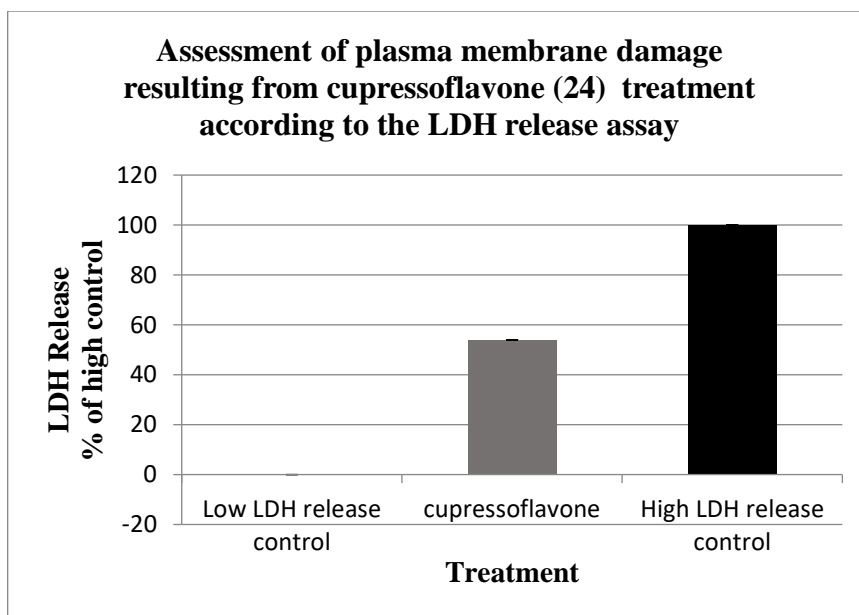


All experiments were carried out in triplicate on separate occasions. Data were expressed as means \pm standard error of the mean derived from $n \geq 12$ from three separate occasions.

Figure 3.1.59: The cytotoxic activity of etoposide (**78**) against lung cancer cell line

3.1.9.1 The LDH results

Results of the LDH assay presented in Figure 3.1.60 suggest that cupressoflavone (**24**) (isolated from JPM) causes cytotoxicity to the lung cancer cell lines (A549) at IC₅₀ value of 65 μ M, through damage to the cell membranes by measuring the LDH activity at two absorbances: 490 and 690 nm. The LDH activity was performed using a commercial cytotoxicity assay kit produced by Roche (REF 11644793001). The necrotic percentage was 54 %, which was expressed using the formula: (sample value/maximal release) \times 100% (Chan *et al.*, 2013).



Data were expressed as means \pm standard error of the mean derived from n =24.

Figure 3.1.60: LDH Release result for cupressoflavone (**24**) against the lung cancer cell lines (A549)

Discussion:

The Cupressaceae family is a conifer family with worldwide distribution. Many genera and species of this family have been reported for their cytotoxicity by inducing apoptosis in cancer cells (Kuetea *et al.*, 2013). In the present study, the cytotoxic effect of *J. phoenicea* leaves from the Cupressaceae family was tested against five human cancer cell lines, MCF7, HepG2, EJ138, A549, and PC3 using the MTT assay. *J. phoenicea* leaves extracts showed the highest level of cytotoxic activity against the human lung adenocarcinoma cell line A549 with the IC₅₀ values of 16, 13 and 100 µg/mL, respectively, for the *n*-hexane, DCM and MeOH extracts (Table 3.1.4). Whilst the DCM extract appeared to be the most cytotoxic extract against the PC3 cells, the *n*-hexane extract was the most cytotoxic across the board against HepG2 (human liver hepatocellular carcinoma), EJ138 (human bladder carcinoma) and MCF7 (human breast adenocarcinoma) having respective IC₅₀ values of 10, 40 and 14 µg/mL. Several phytochemicals, e.g., alkaloids, flavonoids, lignans, phenols, steroids and terpenes have been demonstrated to possess prominent cytotoxic properties against cancer cells (Fernando & Rupasinghe, 2013). Notably, all these groups of phytochemicals have previously been isolated from the leaves and berries of *J. phoenicea* (JP) and other *Juniperus* species (Cupressaceae) grown in different countries (Cairnes *et al.*, 1980; Comte *et al.*, 1997; Barrero *et al.*, 2004; Aboulela *et al.*, 2005). It was earlier reported that the genus *Juniperus* contains biflavones, which are mainly, amentoflavone (**25**), cupressuflavone (**24**) and hinokiflavone. Compounds **24** and **25** might act as useful taxonomic markers. However, in the present study applied on the species *J. phoenicea*, sumaflavone (**76**) was isolated for the first time from the leaves of this plant along with

the two biflavonoids cupressuflavone (**24**) and amentoflavone (**25**). In addition, cupressuflavone (**24**) and sumaflavone (**76**) showed for the first time cytotoxic activity against human lung cancer cells lines (A549) with IC_{50} of 65 and 77 μ M, respectively using the MTT assay. The LDH assay was also applied on cupressuflavone (**24**) against the lung cancer cell lines (A549), the results (Figure 3.1.60) suggest that cytotoxicity might be through damage to the cell membranes. The necrotic percentage was calculated as 56.3 % by using the formula (sample value/maximal release) \times 100% (Chan *et al.*, 2013). Amentoflavone (**25**) did not show any activity against these cancer cells. It has also been reported as weak cytotoxic agent against lung cancer cells A549 (Lee *et al.*, 2012). However, it exerted potent cytotoxic effects against both MCF-7 and HeLa cells, with IC_{50} s of 25 and 20 μ M, respectively (Lee *et al.*, 2012). The presence of the aromatic hydroxyl group at position 5 in the sumaflavone (**76**) structure may have played a role in the potentiation of the cytotoxic activity against the lung cancer cells A549 where is, the lack of this hydroxyl group in the amentoflavone (**25**) structure inhibited this activity. It has also been reported that the substitution of the aromatic hydroxyl group at position 5 in the A ring is essential for inhibiting the cell growth of human promyelocytic leukaemia cells (HL-60) (Li-Xia Chen *et al.*, 2014).

The chemical investigations of the genus *Juniperus* have revealed the presence of terpenes e.g. monoterpenes, diterpenoids, and sesquiterpenes (Seca & Silva 2007), which reported their cytotoxicity against many cancer cell lines (Zhao *et al.*, 2011). In this study, four diterpenoids (**42**, **41** and **44**) were isolated from *J. phoenicea* VLC *n*-hexane F3 and DCM (F4 and F6). Three terpenoids were tested for their cytotoxicity against the A549 cell lines. The 13-*epi*-cupressic acid **42** exhibited the highest cytotoxicity against the A549

cells with IC₅₀ value of 159 μM. Previously, cytotoxic activity against human lung cancer cells lines (A549) has been also reported with IC₅₀ > 30 μM, while the imbricatholic acid (**41**) showed the least cytotoxic effect with IC₅₀ value of 263 μM. It has been suggested that imbricatholic acid (**41**) induces cell cycle arrest in cellosaurus cell line cells (CaLu-6) (human, Caucasian, lung, adenocarcinoma) (De Marino *et al.*, 2011), and presented moderate cytotoxicity IC₅₀ values of 134 and 280 μM towards AGS cells and human lung fibroblasts, respectively (Hirschmann *et al.*, 2007). The diterpene 3-hydroxy sandaracopimaric acid (**44**) showed a moderate cytotoxicity with IC₅₀ value of 223 μM against human lung cancer cells lines (A549). However, there was no report on the the diterpene 3-hydroxy sandaracopimaric acid (**44**) against (A549). Lignans, which are also present in many species of the *Juniperus* genus at a low level (Seca & Silva, 2007; Renouard *et al.*, 2011) are well-known cytotoxic compounds against cancer cell lines. However, in our study, the VLC DCM F4 obtained from JP yielded two lignans. The ¹H and ¹³C NMR spectroscopic data indicated that they belong to the furan subgroups (Tsopmoa *et al.*, 2013), suggesting that they are deoxydiphyllotoxin (**29**) and β-peltatin methyl ether (**28**). Deoxydiphyllotoxin (**29**) was impure, as it is appeared to be mixed with diterpenoid compound, but its presence in the DCM F4 with the other lignan β-peltatin methyl ether (**28**) indicated the high potency of this fraction (IC₅₀ value = 19 μg/mL). The impure deoxydiphyllotoxin (**29**) was tested against the A549 lung cancer cells and exhibited high level of cytotoxicity with IC₅₀ value of 1.1 μg/mL.

Conclusion

The current findings support the traditional use of *J. phoenicea* for the treatment of tumours. It could be suggested that the cytotoxicity observed with the less-polar extracts

and fractions of *J. phoenicea* leaves was contributed by various cytotoxic terpenes **41**, **42** and **44** and lignans **28** and **29**. The cytotoxic activity revealed in the polar MeOH extract and fractions was due to the presence of cytotoxic bioflavonoids cupressuflavone (**24**) and sumaflavone (**76**).

3.2 *Aesphodelus aestivus*

3.2.1 Extraction

Sequential Soxhlet extraction of the dried and ground leaves of *Aesphodelus aestivus* (AEL) (150 g) and tubers (AET) (159.26 g) afforded three extracts for each part: *n*-hexane (AELH and AETH), dichloromethane (AELD and AETD), and MeOH (AELM and AETM). The percentage yields of these extracts are summarized in Table 3.2.1

Table 3.2.1: Percentage yield of the three extracts obtained from both *A. aestivus* leaves (AEL) and tubers (AET)

Extract	% Yield	Extract	% Yield
<i>n</i> -Hexane (AELH)	1.87	<i>n</i> -Hexane (AETH)	0.714
DCM (AELD)	1.06	DCM (AETD)	1.48
MeOH (AELM)	10.53	MeOH (AETM)	26.67

3.2.2 Preliminary analytical TLC screening of *A. aestivus* leaves extracts

The developed TLC plates of three extracts obtained from *A. aestivus* leaves were viewed under short (254 nm) and long (366 nm) UV light and then sprayed with anisaldehyde reagent followed by heating at 100°C for 5 min to reveal many violet and yellow coloured spots with R_f values ranging from 0.35 to 0.95 (Table: 3.2.2). The violet and the yellow colours suggested the presence of phenols, flavonoids, terpenes or sugars (Figure: 3.2.1) (Kristanti & Tunjung 2015).



Mobile phase: Toluene: EtOAc: Acetic acid = 25:24:1

Figure 3.2.1: TLC for the three extracts of *A. aestivus* leaves

Table 3.2.2: R_f values of different extracts of *A. aestivus* leaves

R_f values		
AELH	AELD	AELM
0.39, 0.59, 0.63, 0.74	0.39, 0.71	0.29, 0.59

3.2.3 Preliminary analytical TLC screening of *A. aestivus* tuber extracts

The developed TLC plates of three extracts obtained from *A. aestivus* tubers were viewed under short (254 nm) and long (366 nm) UV light and then sprayed with anisaldehyde reagent followed by heating at 100°C for 5 min to reveal many orange and phosphorus green coloured spots (Figure 3.2.2) with R_f values ranging from 0.16 to 0.94 (Table: 3.2.3).

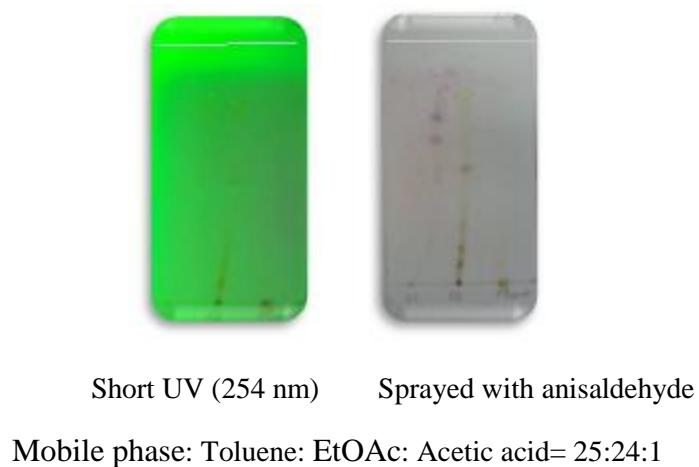


Figure 3.2.2: TLC for the three extracts of *A. aestivus* tubers.

Table 3.2.3: R_f values of different extracts of *A. aestivus* tubers

R_f values		
AETH	AETD	AETM
0.61, 0.69, 0.76	0.08, 0.17, 0.26, 0.47, 0.55, 0.8	0.0

3.2.4 Analytical HPLC screening of the *A. aestivus* leaves MeOH extract

The MeOH extract of *A. aestivus* leaves (10 mg/mL) was analysed by Dionex Ultimate 3000 analytical HPLC coupled with a photodiode array detector using a gradient mobile phase, 30-100% MeOH/H₂O for 30 min with a volume of injection of 20 μ L and a flow rate of 1 mL/min. (Figure 3.2.3 and Table 3.2.4).

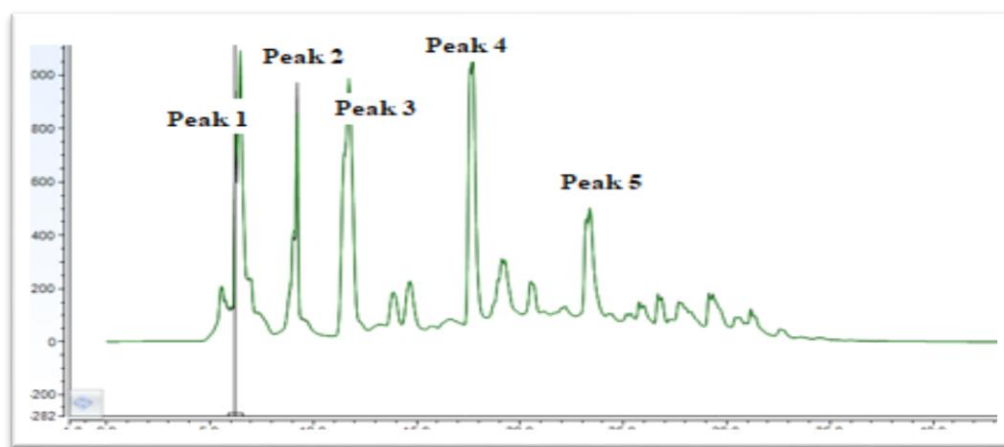


Figure 3.2.3: Analytical HPLC chromatogram of the MeOH extract of *A. aestivus* leaves (observed at 220 nm)

Table 3.2.4: UV-Vis data for all major peaks obtained from diode array detector

Peak No.	Retention time (min)	UV-Vis absorbances λ_{\max} (nm)
1	6.2	257
2	9.2	263
3	11.8	279
4	17.9	270, 350
5	23.2	254, 347

3.2.5 Analytical HPLC screening of the *A. aestivus* tubers MeOH extract

The MeOH extract of *A. aestivus* tubers (10 mg/mL) was analysed using the same HPLC set up and the mobile phase as shown above (Figure 3.2.4).

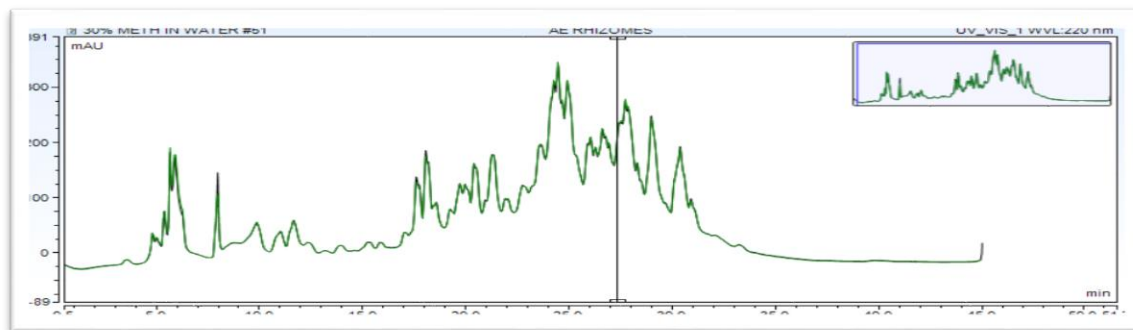


Figure 3.2.4: Analytical HPLC chromatogram of the *A. aestivus* tubers MeOH (Observed at 220 nm)

3.2.6 Screening of *A. aestivus* extracts for cytotoxic activity

The cytotoxic activity, according to the MTT assay, of both the AED and AEM extracts of leaves and tubers was assessed against five cancer cell lines; EJ138 (human bladder carcinoma), Hep G2 (human liver hepatocellular carcinoma), A549 (human lung carcinoma), MCF7 (human breast adenocarcinoma), and prostate cancer cell lines (PC3). The DCM *A. aestivus* tuber extract showed high cytotoxic activity against both the human lung carcinoma A549 and the prostate cancer PC3 cell lines with $IC_{50} = 16$ and $19 \mu\text{g/mL}$, respectively. However, the MeOH and *n*-hexane *A. aestivus* tuber extracts did not show any activity (Table: 3.2.5a). *A. aestivus* leaves (DCM extract) showed moderate cytotoxic activity against both the human liver hepatocellular carcinoma HepG2 cells and the human lung carcinoma A549 cells with IC_{50} values of 70 and $90 \mu\text{g/mL}$, respectively (Table: 3.2.5a).

The selectivity index (SI) of the active DCM extract of *A. aestivus* tubers was assessed by comparing the cytotoxicity results of the human normal prostate cell line (PNT2) with those of human prostate cancer cell line (PC3). The extract revealed high degree of cytotoxic selectivity towards the prostate cancer cells (SI = 26), which indicated the relative safety of the extract on the normal human cells. The IC₅₀ values of *A. aestivus* tuber extracts in both cell lines and the selectivity index are summarized in Table 3.2.5b.

Table 3.2.5a: The IC₅₀ (µg/mL) of *n*-hexane, DCM and MeOH extracts of both *A. aestivus* leaves and tubers on the selection of five human cancer cell lines

Cell type	IC ₅₀ values (µg/mL) (AEL)			IC ₅₀ values (µg/mL) (AET)		
	AELH	AELD	AELM	AETH	AETD	AETM
EJ138	> 100	> 100	> 100	> 100	> 100	> 100
Hep G2	> 100	70 ± 0.62	> 100	> 100	> 100	> 100
A549	> 100	90 ± 1.25	> 100	> 100	16 ± 0.76	> 100
MCF7	> 100	> 100	> 100	> 100	> 100	> 100
PC3	> 100	> 100	> 100	80 ± 0.94	19 ± 1.04	> 100

Values greater than 100 µg/mL were considered as non-cytotoxic (Sahranavard *et al.* 2012).

The results were mean values ± standard error of the mean derived from n ≥ 12 from three separate occasions.

Table 3.2.5b: The IC₅₀ (µg/mL) values for AET DCM extract on PC3 and PNT2 cells and the selectivity index (SI) using the normal human prostate cells (PNT2).

Cell type	IC ₅₀ values (µg/mL) (AETD)
PC3	19 ± 1.04
PNT2	500 ± 0.81
Selectivity index	26

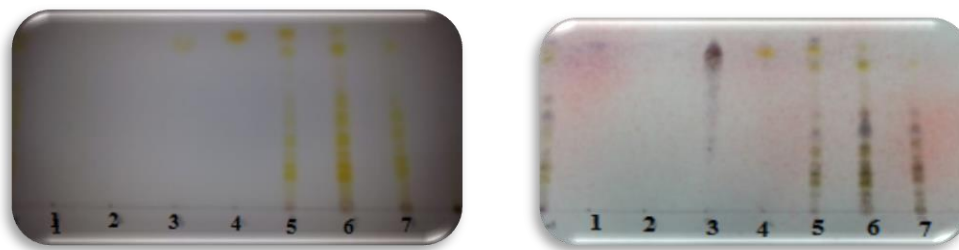
Selectivity index (SI)= The IC₅₀ (µg/mL) of extracts against the normal cells divided by the IC₅₀ (µg/mL) of extracts against the cancer cells, where IC₅₀ is the concentration required to reduce viability by 50% of the cell population (Badisa, *et al.*, 2009).

3.2.7 Chromatographic fractionation of the extracts

Following the systematic, bioassay-guided phytochemical and cytotoxic/anticancer study on *A. aestivus*, further fractionation of the active extract (AETD) was performed. However, the inactive MeOH extract of *A. aestivus* leaves was fractionated with the aim of isolating major metabolites to have thorough understanding of the phytochemistry of *A. aestivus*.

3.2.7.1 Vacuum liquid chromatography fractionation (VLC)

The active extract AETD was further fractionated two times by VLC over silica gel using two different solvent systems to collect seven fractions each time (Figure 3.2.5 and 3.2.6), the weights of fractions are listed in Tables 3.2.6 and 3.2.7



Observed under naked eye

Sprayed with anisaldehyde

Figure 3.2.5: TLC analysis (mobile phase: 5% MeOH in DCM) of the VLC (1) fractions of the AETD

Table 3.2.6: Weights of the VLC (1) fractions of the extract AETD (1.855 g)

Fraction	Mobile phase gradient	Weight of fraction (mg)
AETDF1	100% <i>n</i> -hexane	2.4
AETDF2	10% EtOAc in <i>n</i> -hexane	2.2
AETDF3	30% EtOAc in <i>n</i> -hexane	10.8
AETDF4	50% EtOAc in <i>n</i> -hexane	10.0
AETDF5	80% EtOAc in <i>n</i> -hexane	160.0
AETDF6	100% EtOAc	1272.3
AETDF7	50% MeOH in EtOAc	110.0

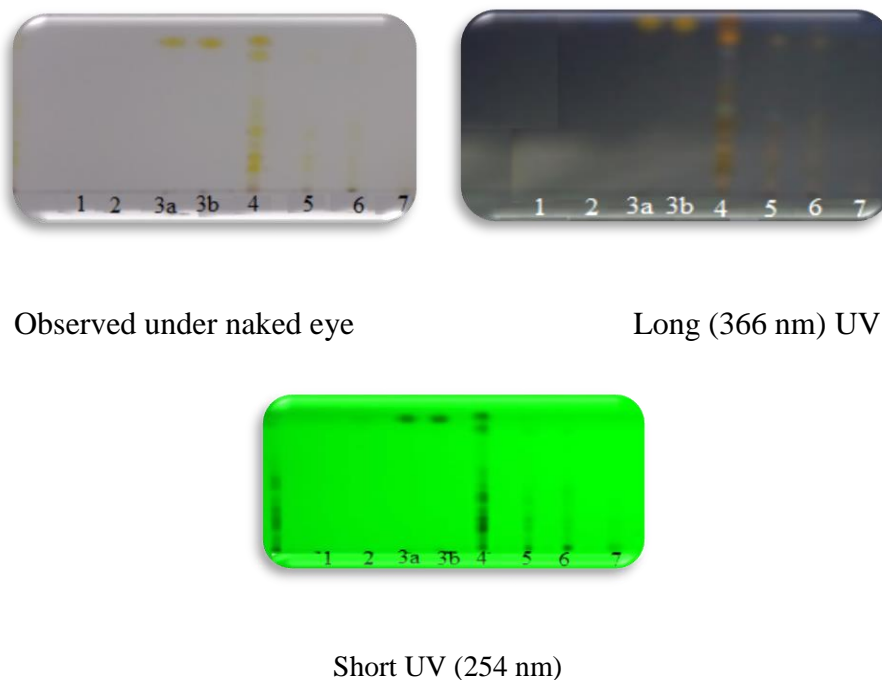


Figure 3.2.6: TLC analysis (mobile phase: 5% MeOH in DCM) of the VLC (2) fractions of AETD

Table 3.2.7: Weights of the VLC (2) fractions of the extract AETD (200 g)

Fraction	Mobile phase gradient	Weight of fraction (mg)
AETDF1	100% <i>n</i> -hexane	4.8
AETDF2	50% DCM/ <i>n</i> in hexane	2.7
AETDF3	100% DCM	3.0
AETDF4	10% MeOH in DCM	140
AETDF5	20% MeOH in DCM	11
AETDF6	30% MeOH in DCM	4.0
AETDF7	40% MeOH in DCM	9.8

3.2.7.2 Solid phase extraction (SPE)

The MeOH extract of *A. eastivus* leaves (AELM) (1.8 g) was fractionated by SPE to collect four fractions (Figures 3.2.7- 3.2.10; Table 3.2.8).

Table 3.2.8: Weights of the SPE fractions of the MeOH extract of *A. eastivus* leaves

Fraction	Mobile phase gradient	Weight of fraction (mg)
AELMF1	20% MeOH/H ₂ O	1043.3
AELMF2	50% MeOH/H ₂ O	51.2
AELMF3	80% MeOH/H ₂ O	35.3
AELMF4	100% MeOH/H ₂ O	44.3

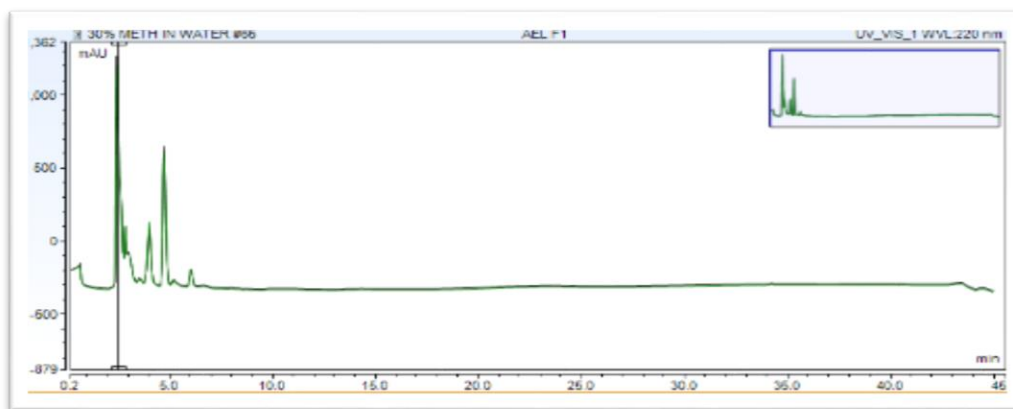


Figure 3.2.7: Analytical HPLC chromatogram of SPE fraction 1 of AELM (observed at 220 nm)

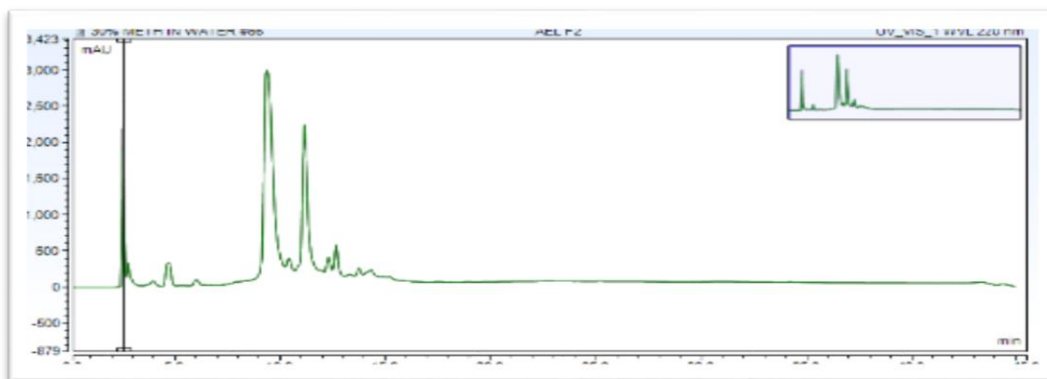


Figure 3.2.8: Analytical HPLC chromatogram of SPE fraction 2 of AELM (observed at 220 nm)

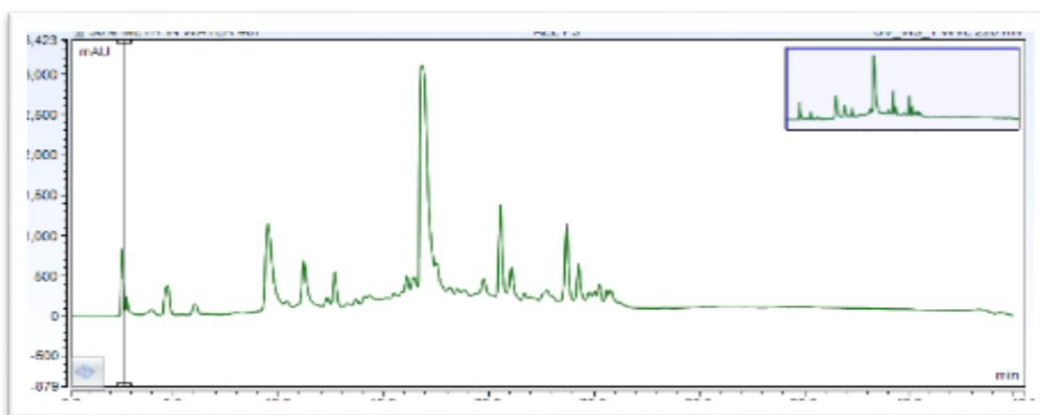


Figure 3.2.9: Analytical HPLC chromatogram of SPE fraction 3 of AELM (observed at 220 nm)

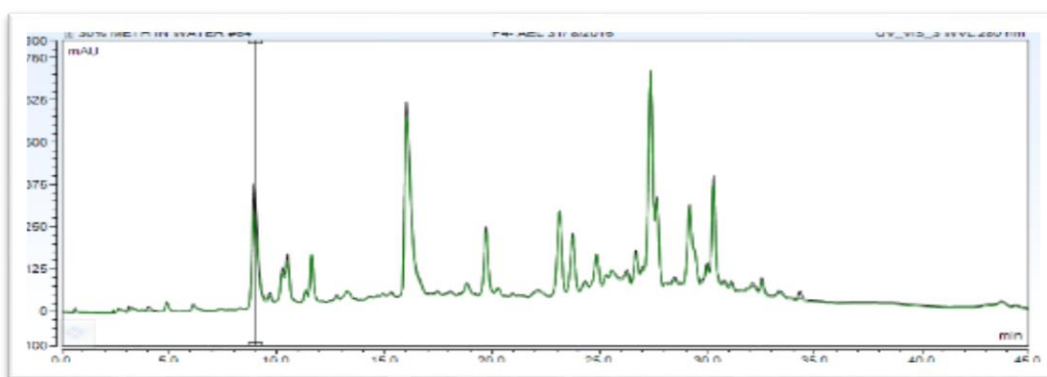


Fig. 3.2.10: Analytical HPLC chromatogram of SPE fraction 4 of AELM (observed at 220 nm)

3.2.8 Screening of *A. aestivus* fractions for cytotoxic activity

The cytotoxic activity of the DCM fractions obtained from both the two VLC chromatographic fractionation of *A. aestivus* tubers was assessed against the most sensitive cancer cell line (human prostate cancer cell line PC3). The highest activity was revealed in the DCM F4 obtained from the VLC (2) with IC₅₀ value of 21 µg/mL. The IC₅₀ values for the DCM fractions of *A. aestivus* tubers on PC3 are summarised in Tables 3.2.9 and 3.2.10.

Table 3.2.9: The IC₅₀ (µg/mL) of DCM fractions from VLC (1) AET on PC3 (human prostate cancer cell line).

Fraction	F1	F2	F3	F4	F5	F6	F7
IC ₅₀ µg/mL	>100	>100	>100	>100	73 ± 0.52		

All experiments were carried out in triplicate on separate occasions. Data were expressed as means a ± standard error of the mean derived from n ≥ 12 from three separate occasions.

Table 3.2.10: The IC₅₀ (µg/mL) of DCM fractions from VLC (2) AET on PC3 (human prostate cancer cell line)

Fraction	F1	F2	F3	F4	F5	F6	F7
IC ₅₀ µg/mL	>100	>100	>100	21 ± 1.56	98 ± 0.67	>100	>100

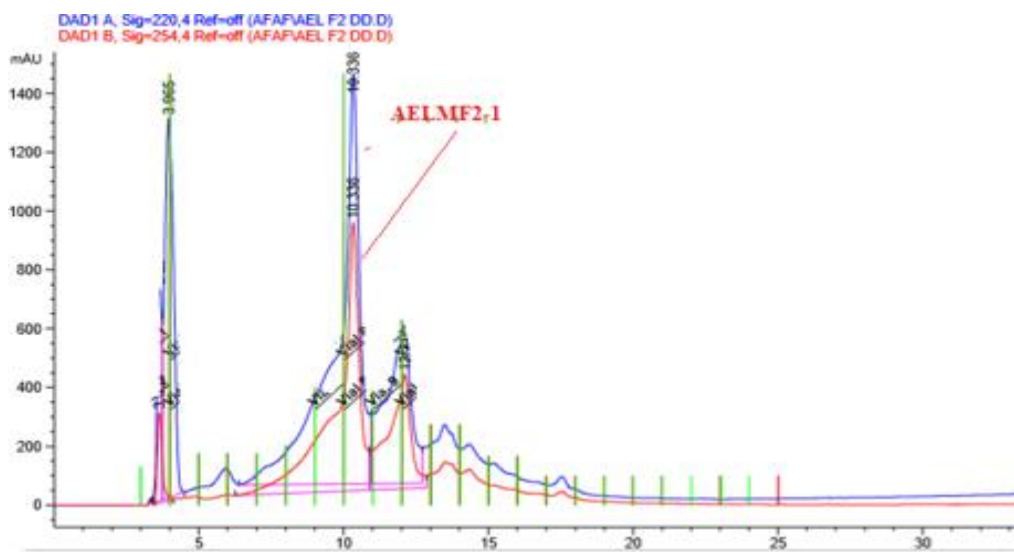
All experiments were carried out in triplicate on separate occasions. Data were expressed as means a ± standard error of the mean derived from n ≥ 12 from three separate occasions.

3.2.9 Isolation of compounds from *A. aestivus*

3.2.9.1 The MeOH extract (AEM)

The MeOH extract of AELM

Isolation of compounds from the SPE fractions 2, 3 and 4 of AELM was done using semi-preparative HPLC technique (Agilent) employing a 30-100% gradient of MeOH in water for 30 min with a volume of injection of 200 μ L and a flow rate of 2 mL/min. The following compounds were isolated: AELMF2-1 (2.9 mg, $t_R = 10.3$ min) (Figure 3.2.11) from SPE fraction 2, AELMF3-4 (5.7 mg, $t_R = 22$ min) (Figure 3.2.12) from SPE fraction 3, and AELMF4-2 (1.8 mg, $t_R = 19.5$) (Figure 3.2.13) from SPE fraction 4.



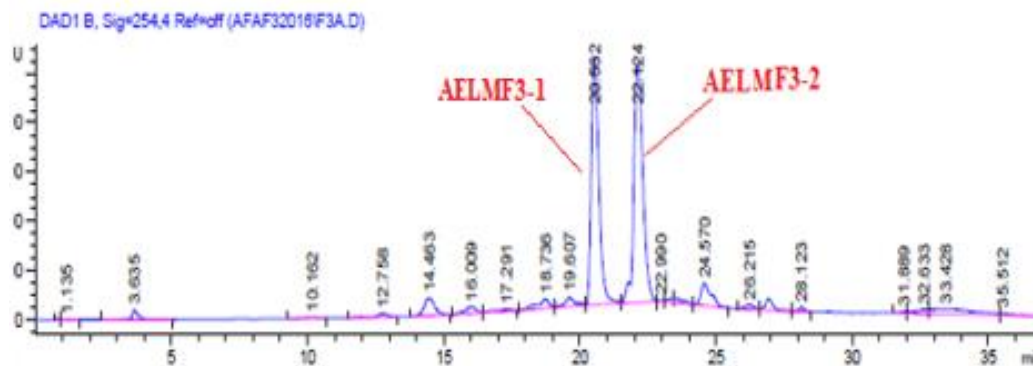


Figure 3.2.12: HPLC chromatogram of isolated compounds from SPE fraction 3 AELM (observed at 254 nm)

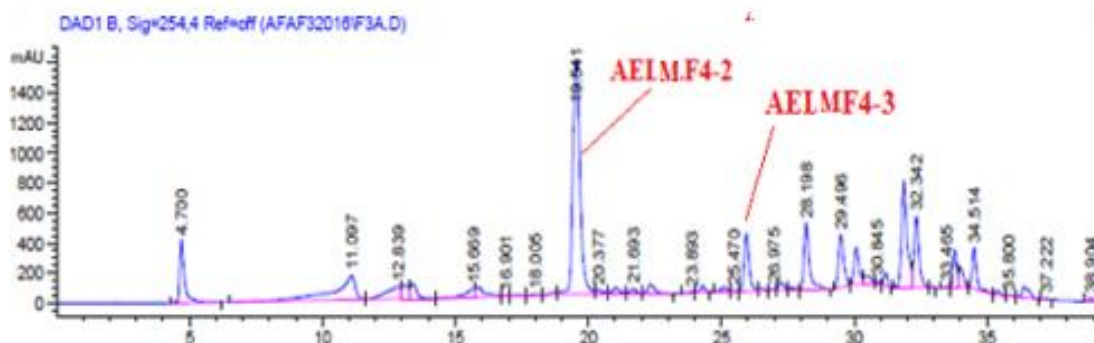


Figure 3.2.13: HPLC chromatogram of isolated compounds from SPE fraction 4 AELM (observed at 254 nm)

The MeOH extract of AETM

The total MeOH extract (AETM) (1.33 g) was fractionated every 5 min by preparative reversed-phase HPLC using a gradient solvent system 30-100% MeOH in water and a flow rate of 10 mL/min. Six fractions [F1= 14 mg (0-5 min), F2= 12.3 mg (5-10 min), F3 = 80.3 mg (10-15 min), F4 = 53.6 mg (15-20 min), F5 = 24.2 mg (20-25 min), F6 = 69 mg (25-31.8 min)] were obtained and allowed to dry (Figure 3.2.14).

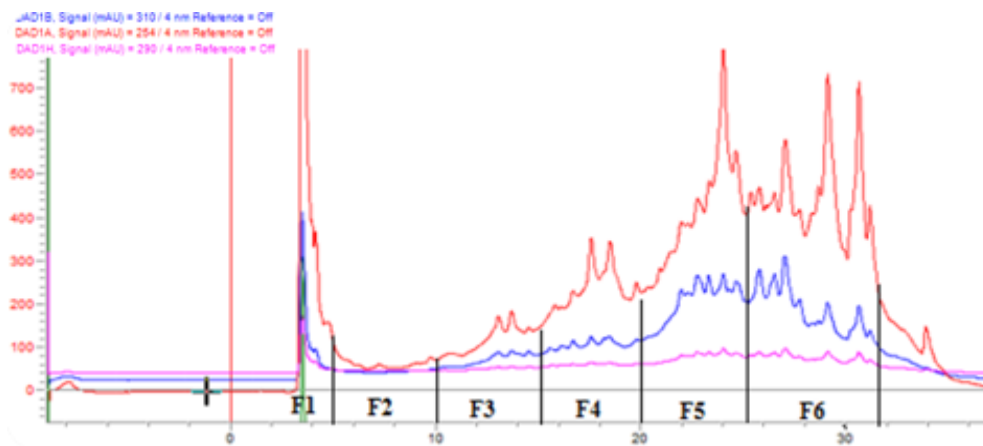


Figure 3.2.14: Fractionation of AETM extract every 5 min (observed at 290, 254, 310 nm)

HPLC-MS screening of AETM Fraction 4:

AETM Fraction 4 exhibited the most interesting ^1H NMR spectrum and HPLC (10-100% ACN/ H_2O gradient) chromatogram (Figure 3.2.15), so it was analysed by HPLC-MS to detect the molecular weights of the major metabolites, and thus to tentatively identify aleo-emodin 271 $[\text{M}+\text{H}]^+$ and aleo-emodin acetate 312 $[\text{M}+\text{H}]^+$, chrysophanol 255 $[\text{M}+\text{H}]^+$, chrysophanol-10,10'-bianthrone 479 $[\text{M}+\text{H}]^+$, and *p*-hydroxy transferulate 315 $[\text{M}+\text{H}]^+$ (Figure 3.2.16).

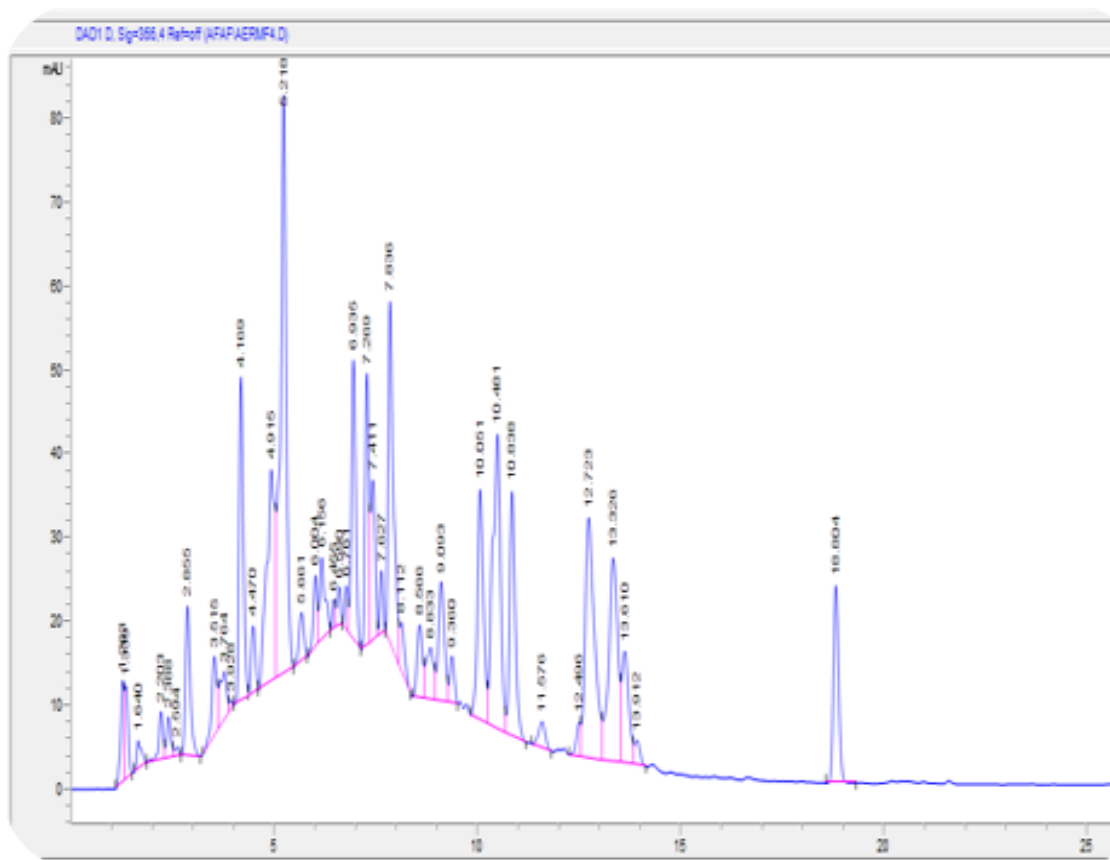


Figure 3.2.15: Analytical HPLC chromatogram of AETM Fraction 4 (observed at 366 nm)

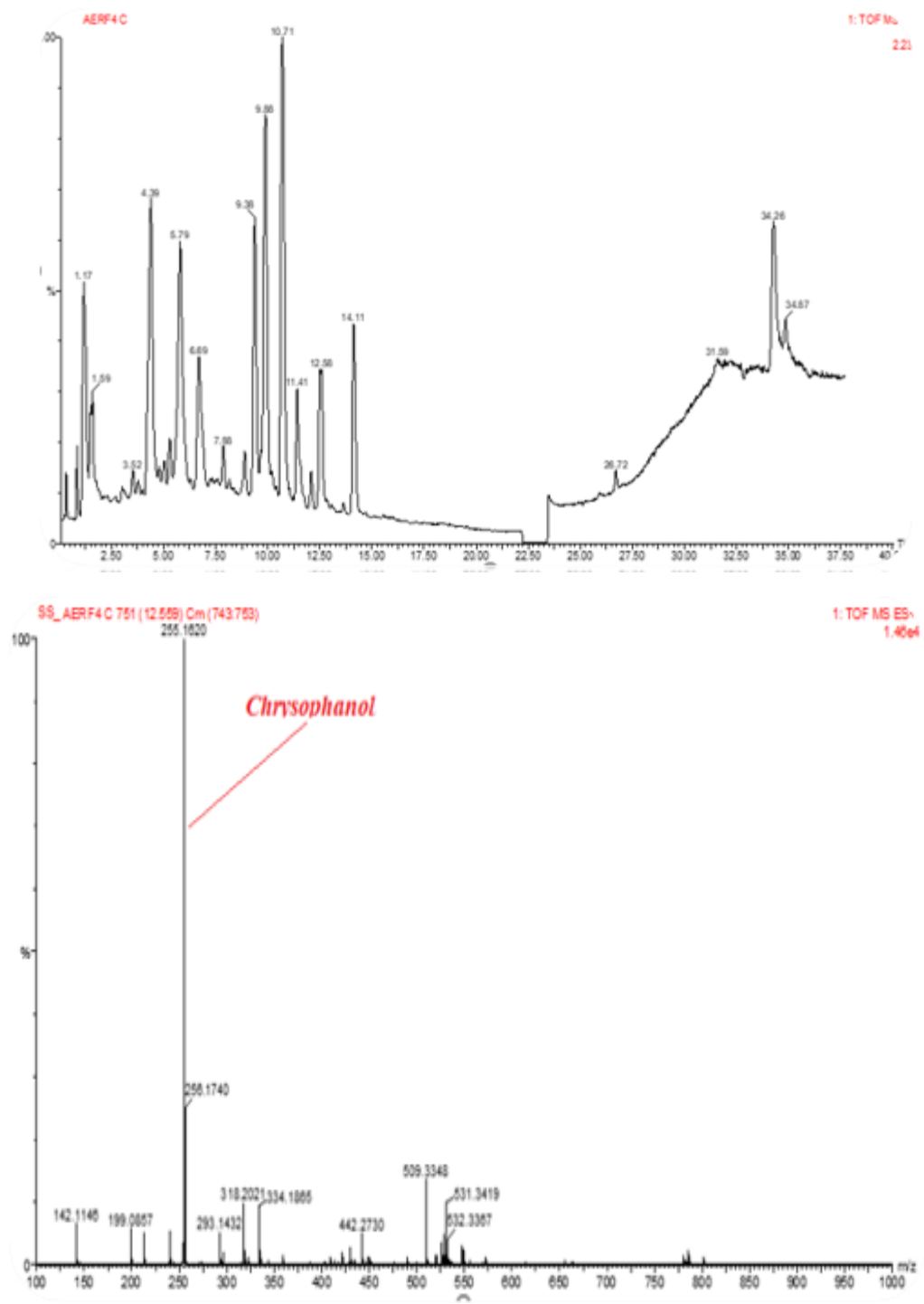
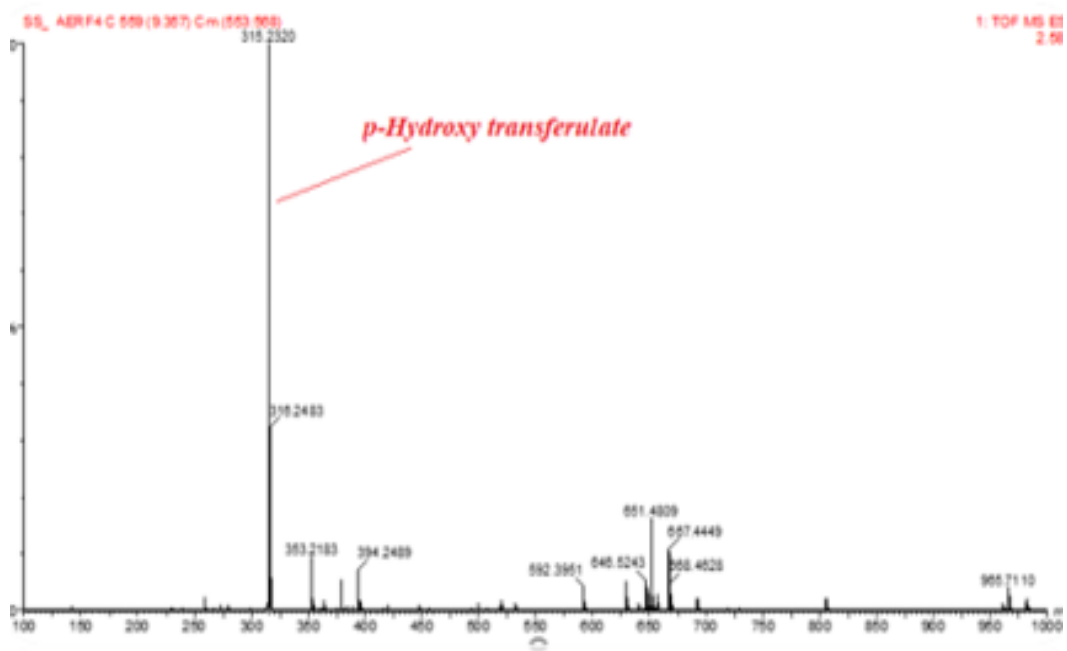
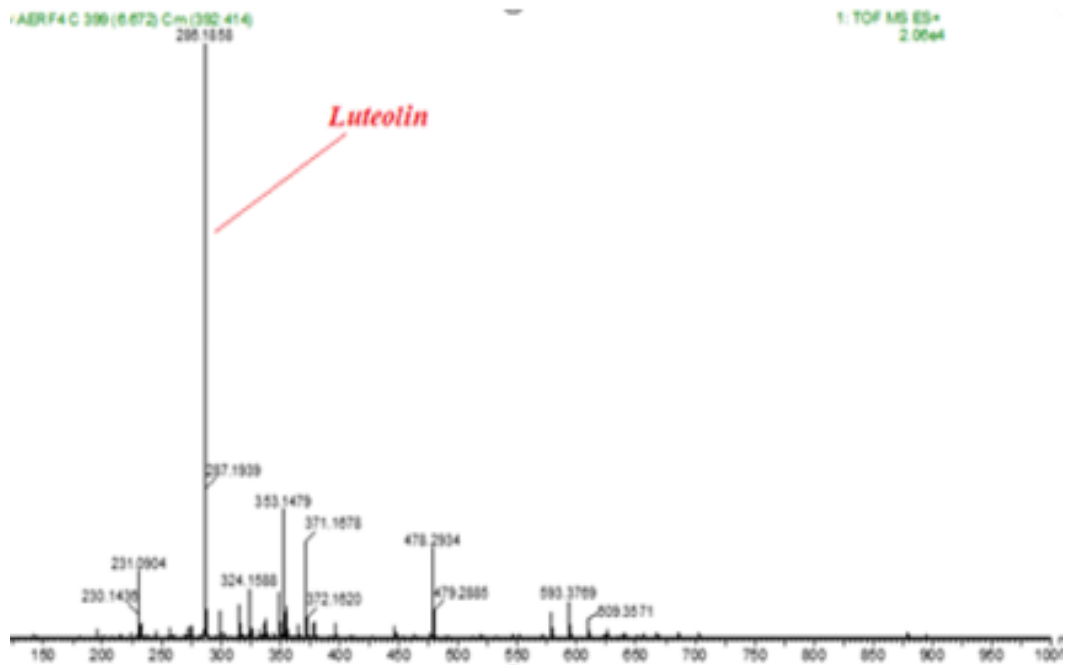
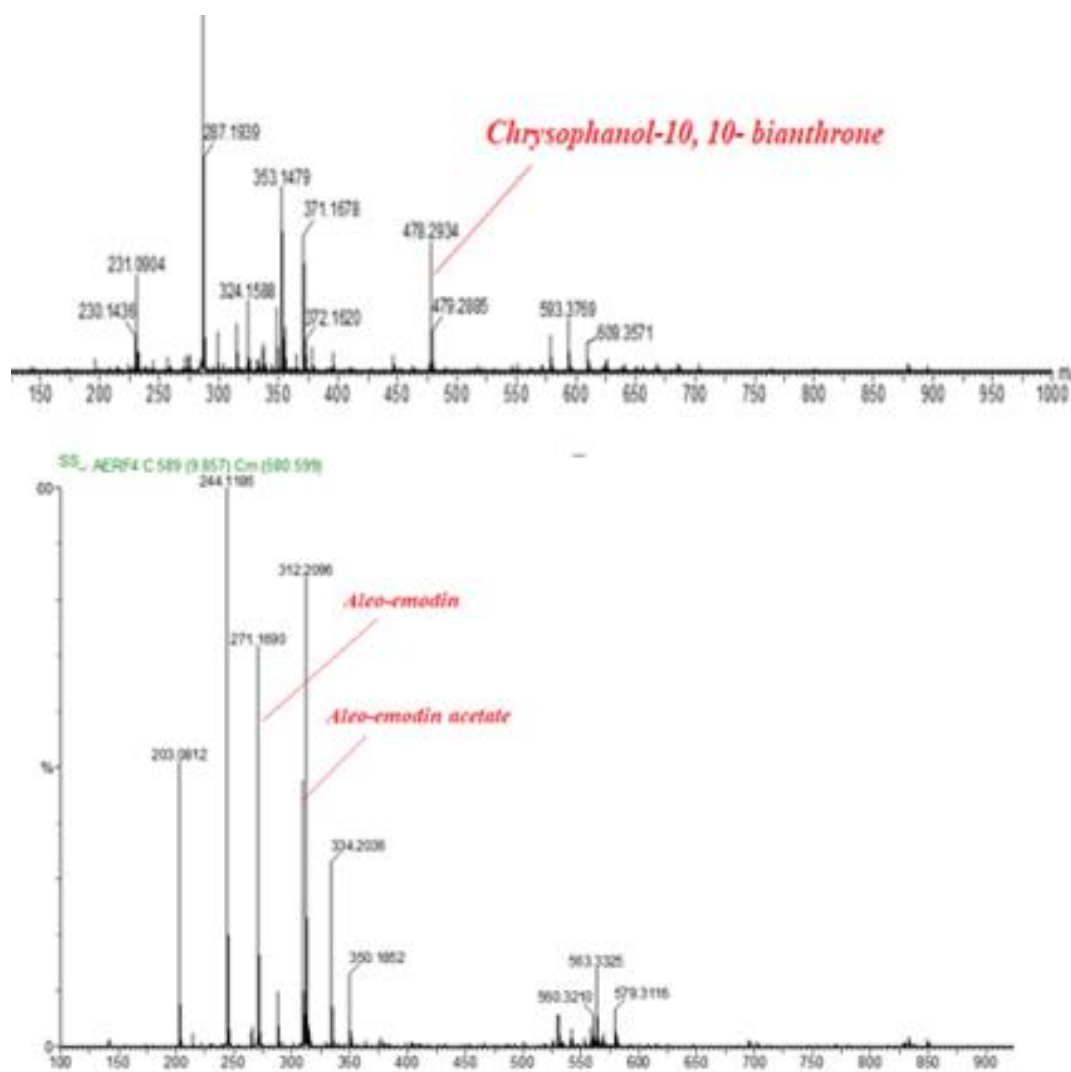


Figure 3.2.16: LC-MS screening for the AETM Fraction 4



Continued---- Figure 3.2.16: LC-MS screening for the AETM Fraction 4



Continued---- Figure 3.2.16: LC-MS screening for the AETM Fraction 4

3.2.9.2 The DCM extract (AED)

The DCM extract of AELM

The total DCM extract (AELDM) (500 mg) was separated by preparative reversed-phase HPLC using a gradient solvent system 30-100% ACN in water and a flow rate of 10 mL/min. This led to the isolation of AELD-3 (1 mg, t_R = 25.2 min) and AELD-5 (1.4 mg, t_R = 35.3 min) (Figure 3.2.17).

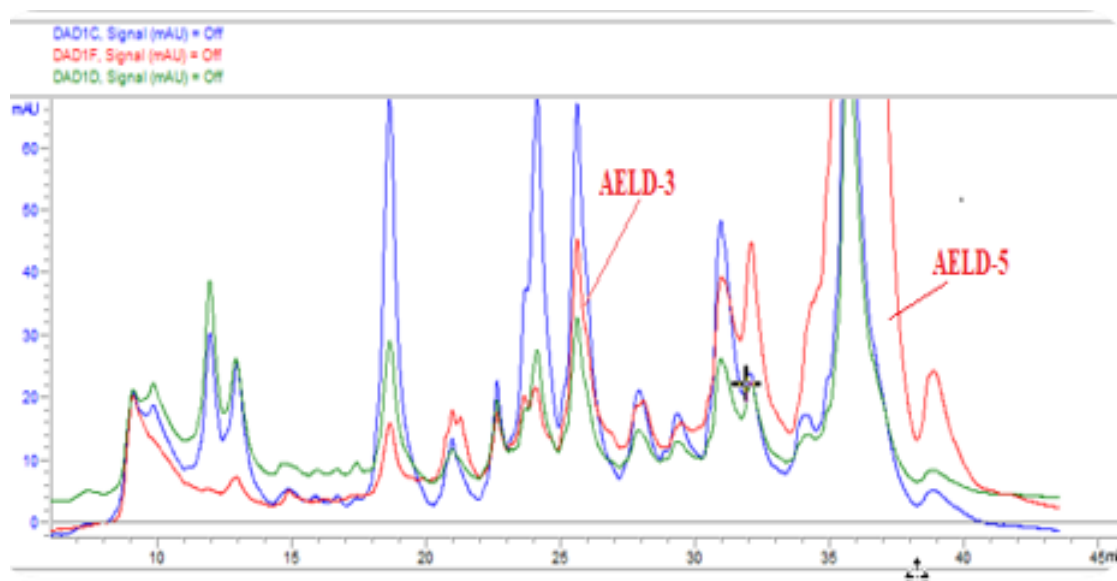


Figure 3.2.17: HPLC chromatograms of isolated compounds from the DCM extract (observed at 254, 290 and 366 nm)

The DCM extract of AET

Two pure compounds were completely crystallized from the VLC fractions 4 (VLC 1) and 3 (VLC 2) as following: AETD4 (10.8 mg, R_f = 9.5) (Figure 3.2.18) and AETD3 (3 mg, R_f = 9.0) (Figure 3.2.19)



Figure 3.2.18:
Crystals from the DCM extract of *A. aestivus* tubers VLC (1) (AETD4)

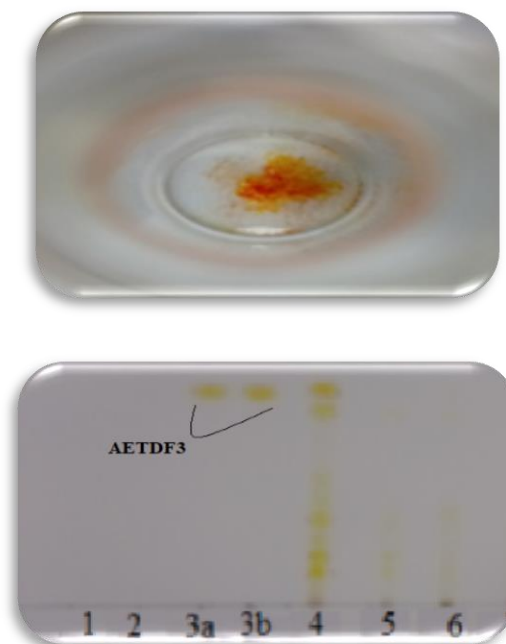


Figure 3.2.19:
Crystals from the DCM extract of *A. aestivus* tubers VLC (2) (AETD3)

Separation of the active DCM VLC (2) Fraction 4

The active DCM fraction 4 purified from VLC (2) (140 mg) of *A. aestivus* tubers was isolated by prep-HPLC using a gradient solvent system 50-100% ACN in water. This

afforded two major compounds: AETD4-6 (1.2 mg, t_R = 23.1 min), AETD4-11 (2 mg, t_R = 30.2 min), (Figure 3.2.20).

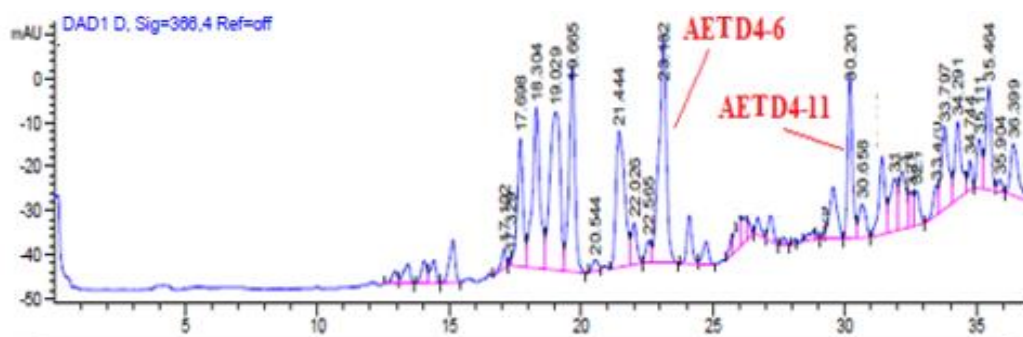


Figure 3.2.20: HPLC chromatogram of isolated compounds from the active AETD fraction 4 (VLC 2) (observed at 366 nm)

3.2.10 Characterization of isolated compounds from *A. aestivus*

3.2.10.1 Characterization of flavonoid

Characterization of AELF3-4 and AELF4-2 as the flavonoids luteolin (22)

One flavonoid **22** was isolated from the SPE fractions F4 of AELM (Figure 1.3). The UV-Vis spectrum of this compound exhibited two major absorption peaks (Figure 3.2.21) at λ_{max} : 256, 270 (sh) nm (Band –II) and 348 nm (Band –I) indicating this compound to be flavonoid (Mabry *et al.*, 1970). The ESIMS m/z showed a peak at: 287 $[M+H]^+$, indicated that the molecular formula could be $C_{15}H_{10}O_6$ (Figure 3.2.22). 1H NMR spectrum (600 MHz, CD_3OD) Table (3.2.11) and Figure (3.2.23) showed several common features for flavonoid skeleton, which include the presence of two *meta*-coupling aromatic protons assigning to H-6 at δ_H (6.46, d, J = 2.0 Hz, 1H) and H-8 at δ_H (6.23, d, J = 2.0 Hz, 1H) in ring A, *ortho*-coupled proton assigning to H-5' at δ_H (6.92, d, J = 8.4 Hz, 1H) and two

ortho- meta coupled aromatic protons assigning to H-2' at δ_H (7.42, d , $J = 2.4$ Hz) and H-6' at δ_H (7.41, dd, $J = 8.4$ Hz, $J= 2.4$. Hz) in ring B. A sharp singlet indicating the olefinic proton in the ring C at δ_H (6.56, H-3). This compound could be assigned to be luteolin (**22**). The COSY experiment showed proton-proton correlation from H-6' \leftrightarrow H 2' and H-6' \leftrightarrow H 5'. The further evidence of ^{13}C NMR (150 MHz, CD_3OD) Table (3.2.11) and Figure (3.2.24) showed the existence of 15 carbon signals were typical for flavone nucleus including 12 aromatic carbons attributed to two aromatic rings, two olefenic at δ_C 165.0 (C-2) and 102.5 (C-3), and the most deshielded carbon was assigned for carbonyl group of chromen nucleus δ_C 182.5 (C-4). All signals were comparable to the published data (Chaturvedula & Prakash 2013; Alwahsh *et al.*, 2015).

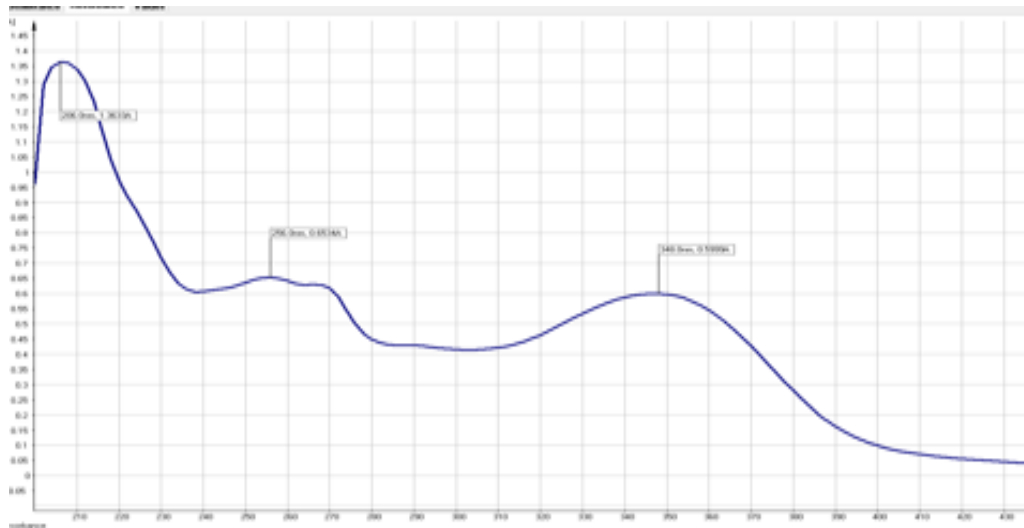


Figure 3.2.21: U.V. spectrum of Luteolin (**22**) in MeOH

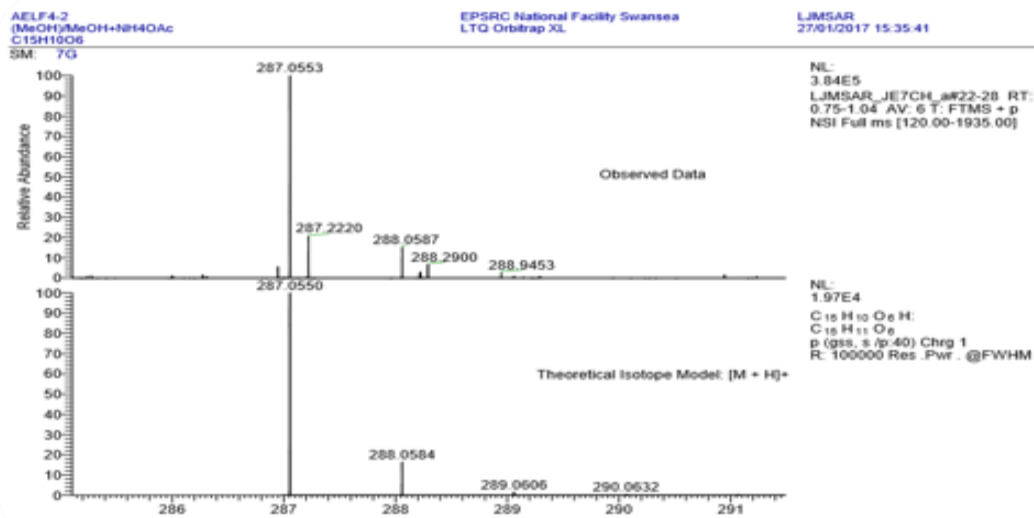


Figure 3.2.22: MS spectrum of Luteolin (22)

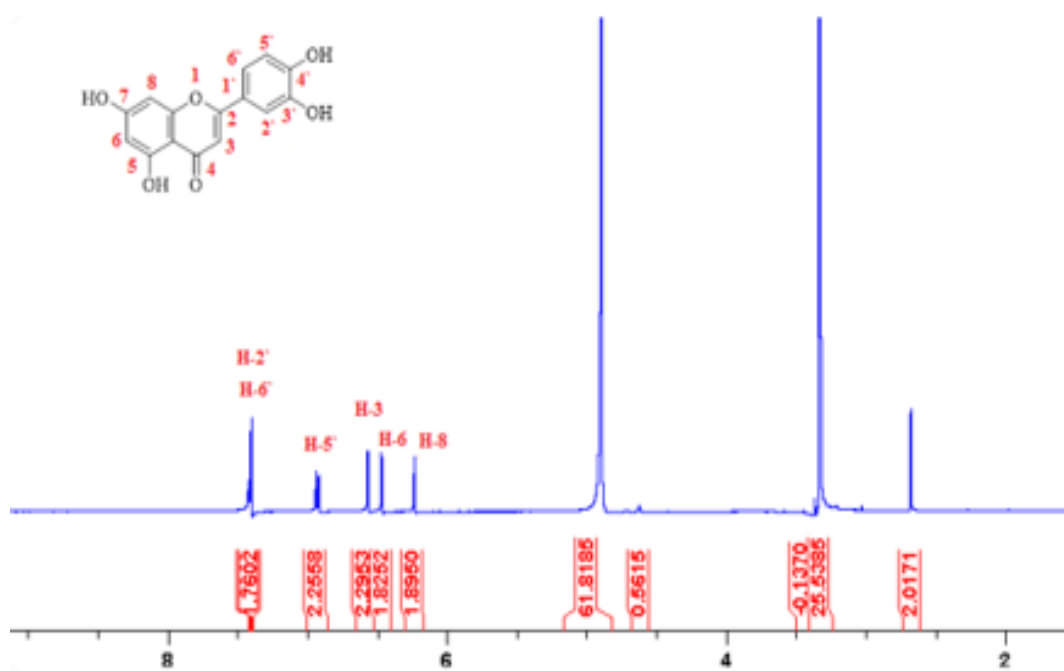


Figure 3.4.23: ¹H NMR spectrum (600 MHz, CD₃OD) of luteolin (22)

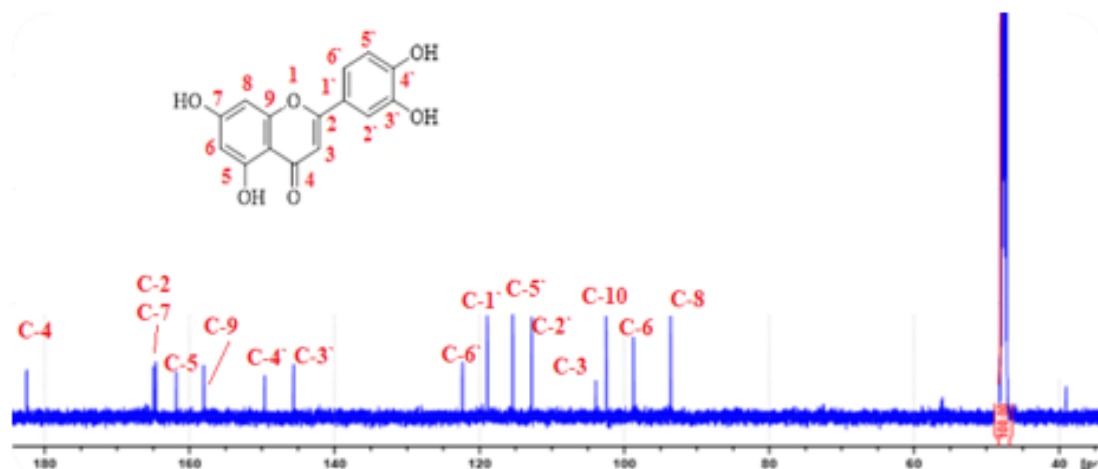


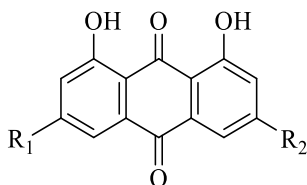
Figure 3.4.24: ^{13}C NMR spectrum (75 MHz, CD_3OD) of luteolin (**22**)

Table 3.2.11: ^1H NMR (600 MHz, CD_3OD) and ^{13}C NMR (150 MHz, CD_3OD) of luteolin (**22**)

Position	Chemical Shift δ (ppm) and J in Hz		Position	Chemical Shift δ (ppm) and J in Hz	
	^1H	^{13}C		^1H	^{13}C
2		165.0	10		103.9
3	6.56, s, 1H	102.5	1'		119.8
4		182.5	2'	7.42, d, 2.4	112.8
5		161.8	3'		145.7
6	6.46, d, 2.0, 1H	98.8	4'		149.6
7		164.7	5'	6.92, d, 8.4, 1H	115.4
8	6.23, d, 2.0, 1H	93.6	6'	7.41, dd; 8.4, 2.4	122.3
9		158.0			

3.2.10.2 Characterization of anthraquinones

Four anthraquinone compounds were isolated; one from the (AEL) DCM extract and the others from the VLC fractions 3 and 4 purified from the (AET) DCM extract. They were identified as two anthrones: aloe-emodin (**13**), and chrysophanol (**79**) (Figure 3.2.25) and two bianthrone: chrysophanol-10, 10'-bianthrone (**80**), and C- α -rhamnopyranosyl bianthracene-9,9',10 (10'H)-trione glycoside (**81**). ^1H NMR (600 MHz, CDCl_3) revealed the presence of four highly downfield proton signals as sharp singlets at δ_{H} (12.00 and 12.10 ppm) corresponding to hydroxyl groups involved in hydrogen bonding. ^{13}C NMR and DEPT (150 MHz, CD_3OD) and (150 MHz, CDCl_3) showed two carbonyl groups at δ_{C} (182.1, 193.5, 193.5) in the anthraquinones **13**, **79**, and **80**, respectively, a methyl group at (δ_{H} -2.47; δ_{C} -22.3) in compound **79** and two methyl groups in compound **80** at (δ_{H} -2.47; δ_{C} -22.3). All these data supported the suggestion of anthraquinone compounds Tables (3.2.12-3.2.14) and Figures (3.2.26, 3.2.33, and 3.2.35).



Compounds	R ₁	R ₂
Aloe-emodin (13)	CH ₂ OH	H
Chrysophanol (79)	H	CH ₃

Figure 3.2.25: Structure of anthraquinones isolated from *A. aestivus*

Characterization of AELD-5 and AELMF4-3 as aloe-emodin anthrone (13)

Orange powder, The ^1H NMR (600 MHz, CD_3OD) (Figure 3.2.26 and Table 3.2.12) spectrum of this compound showed signals characteristic to aloe-emodin structure. These

signals include two *meta*-coupled aromatic protons assigning to H-1 at δ_{H} (7.35, d, $J= 1.0$ Hz, 1H) and H-3 at δ_{H} (7.34, d, $J= 1.0$ Hz, 1H), a broad singlet assigned for H6 and H8 at δ_{H} 7.82 (1H, br s), and *ortho*-coupled protons assigned to H-7 at δ_{H} (1H, t, $J= 7.9$ Hz). The protons of both the oxygenated carbon, which appeared as a sharp singlet at δ_{H} 4.86 (2H, s) and the downfield proton singlets at δ_{H} (12.11 and 12.12 ppm) were clearly shown in the ^1H NMR (600 MHz, CDCl_3) spectrum (Figure 3.2.27). The ^{13}C NMR (150 MHz, CD_3OD) data (Table 3.2.13) showed that compound **13** has 15 carbon signals including two carbonyl carbons at δ_{C} 182.3 (C-9) and 187.5 (C-10), one hydroxyl aliphatic carbon at δ_{C} 62.7 (C-11), and 12 aromatic carbons including two hydroxyl aromatic carbons at δ_{C} 164.9 (C-4) and 166.4 (C-5). The important HMBC correlations (Figure 3.2.28) from H3 \rightarrow C-11 (3J), and H1 \rightarrow C-11 (3J) confirmed the position of the oxygenated carbon attached to position 2 indicating that this anthraquinone was aloe-emodin anthrone (**13**). All signals were comparable to the published data of aloe-emodin and suggested the molecular formula $\text{C}_{15}\text{H}_{10}\text{O}_5$ (Danielsen *et al.*, 1992). The ESIMS m/z : 273 $[\text{M}+\text{H}]^+$, which does not correspond to aloe-emodin, the reason might be that the compound was in solution for a time, so the carbonyl group was reduced to a hydroxyl group, when measured its MS (Figures 3.2.29 and 3.2.30).

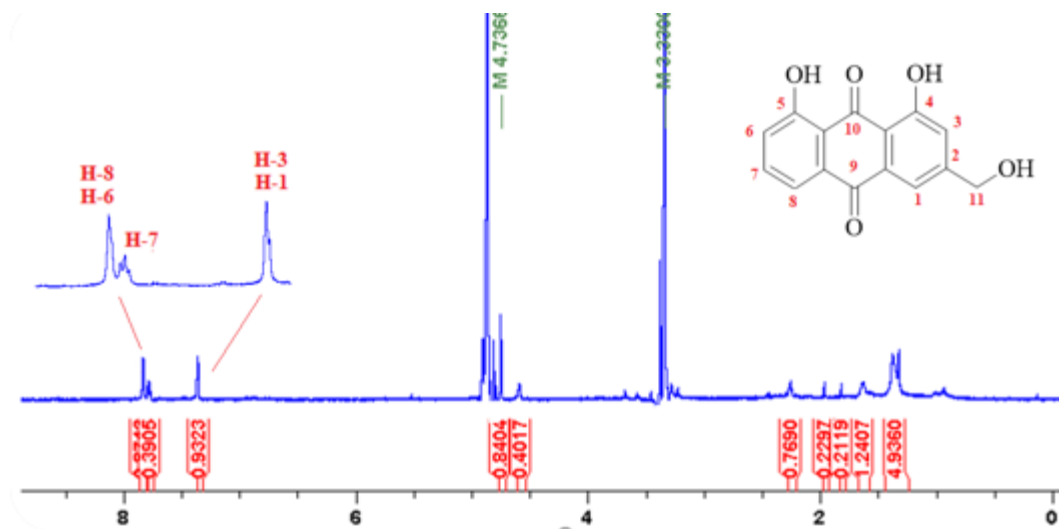


Figure 3.2.26: ^1H NMR spectrum (600 MHz, CD_3OD) of aloe-emodin anthrone

(13)

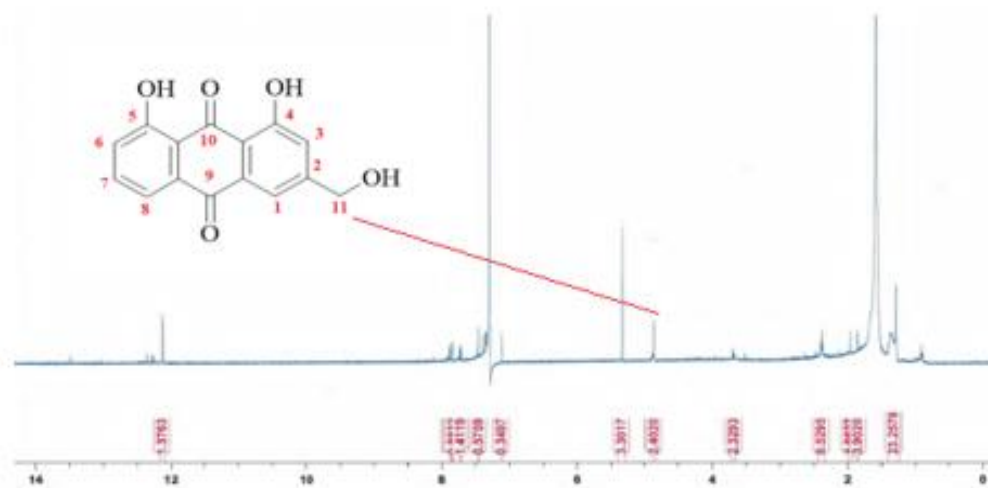


Figure 3.2.27: ^1H NMR spectrum (600 MHz, CDCl_3) of aloe-emodin anthrone

(13)

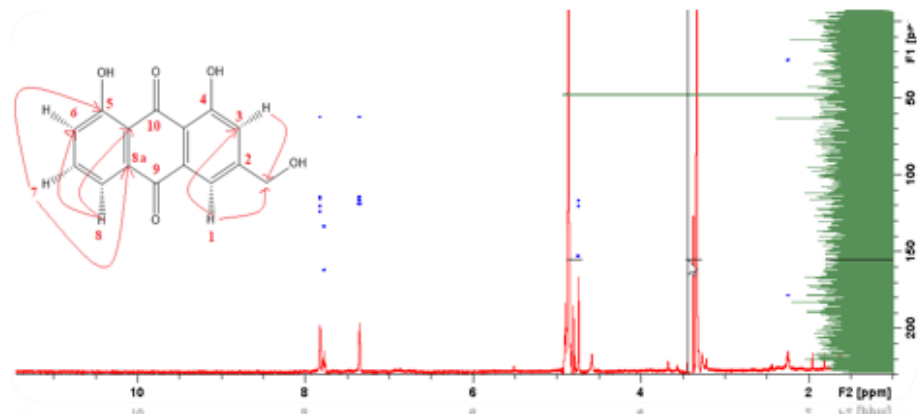


Figure 3.2.28: HMBC correlations (600 MHz, CD₃OD) of aleo-emodin anthrone (**13**)

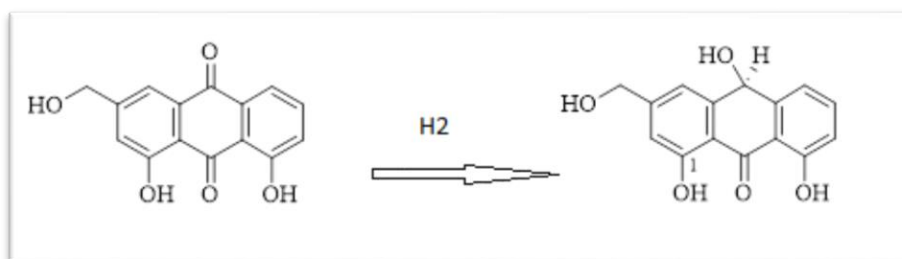


Figure 3.2.29: Reduction of aleo-emodin anthrone (**13**)

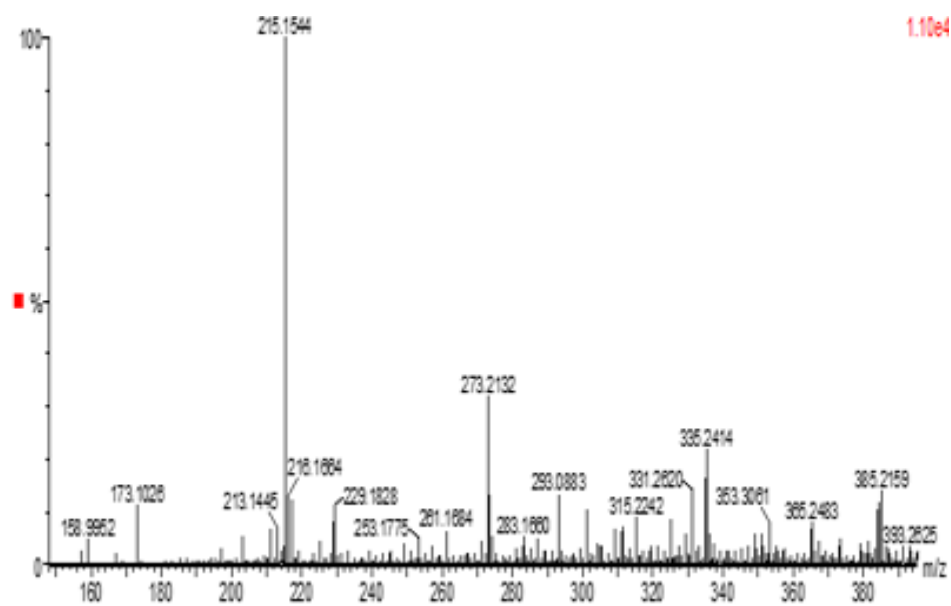


Figure 3.2.30: MS of the reduced aleo-emodin anthrone (**13**)

Characterization of AETDF3 as chrysophanol anthrone (79)

Orange red crystals, The ^1H NMR (600 MHz, CDCl_3) (Table 3.2.12 and Figure 3.2.32) showed *ortho-meta* coupled aromatic protons assigning to H-6 at δ_{H} (7.83, dd, $J = 1.2$ Hz, $J = 7.5$ Hz, 1H) and H-7 at δ_{H} (7.30, dd, $J = 1.1$ Hz, $J=8.3$ Hz, 1H), *ortho*-coupling at δ_{H} (7.67, d, $J = 7.4$ Hz, 1H) assigned to H-5, one singlet peak assigning to H-2 at δ_{H} (7.10, s, 1H) indicating the substitution at position 3 and the two highly downfield shifted proton signals at δ_{H} (12.00, 12.10). All these data indicated that this compound might be anthraquinone. The DEPT data (150 MHz, CDCl_3) (Table 3.2.13) confirmed that compound **79** is an anthraquinone anthrone where it exhibited 15 carbon atoms including 12 aromatic, two carbonyl groups at δ_{C} 193.5 (C-9), 179.5 (C-10), a methyl group at δ_{C} 22.3 (- CH_3). The ESIMS m/z : 255 $[\text{M}+\text{H}]^+$ confirmed the molecular formula $\text{C}_{15}\text{H}_{10}\text{O}_4$ as chrysophanol (**79**) (Figure 3.2.31). All data were comparable to the published data (Coopoosamy & Magwa, 2006).

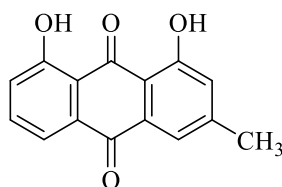


Figure 3.2.31: Structure of chrysophanol (**79**)

isolated from *A. aestivus tubers*

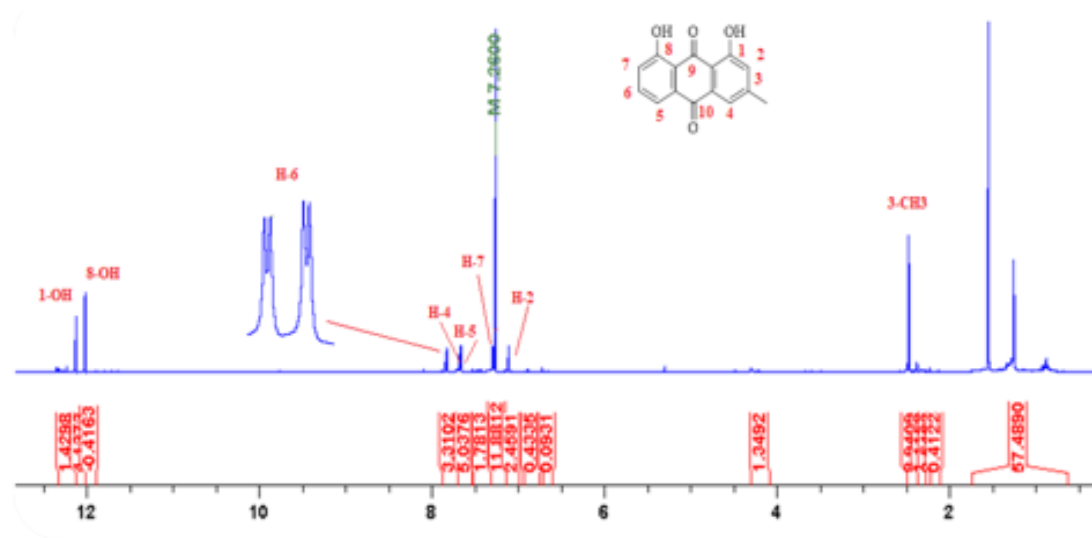
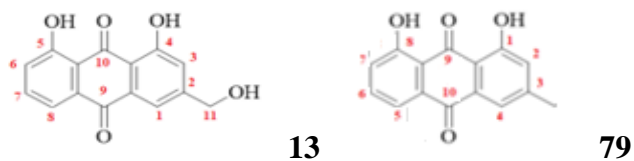


Figure 3.2.32: ^1H NMR spectrum (600 MHz, CDCl_3) of chrysophanol anthrone (79)

Table 3.2.12: ^1H NMR (600 MHz) for the anthrone anthraquinones: aloe-emodin (13) and chrysophanol (79)



Position	Chemical Shift δ (ppm), multiplicity and J in Hz	
	13**	79*
1	7.35, d, 1.02, 1H	
2		7.10, s, 1H
3	7.34, d, 1.02, 1H	
4		7.69, s, 1H
5		7.67, d, 7.4, 1H

6	7.82, br s, 1H	7.83, dd, 1.2, 7.5, 1H
7	7.77, t, 1H	7.30, dd; 1.14, 8.3, 1H
8	7.82, br s, 1H	
3-OCH3		2.47, s, 3H
8-OH		12.00, s
1-OH		12.10, s

**= (CD₃OD), *= (CDCl₃)

Table 3.2.13: ¹³CNMR (150 MHz) of aloe-emodin (**13**) and DEPT NMR (75 MHz) of chrysophanol (**79**)

Position	Chemical Shift δ (ppm)		Position	Chemical Shift δ (ppm)	
	¹³ C 13**	DEPT 79*		¹³ C 13**	DEPT 79*
1	121.0	162.8	9	182.3	193.5
2	155.0	121.4	10	187.5	179.5
3	124.0	149.3	10a	115.6	
4	164.9	120.0	3-CH3		22.3
5	166.4	119.9	8-OH		
6	124.0	137.0	1-OH		
7	136.9	124.6	COOH	168.6	
8	117.2	162.8			

**= (CD₃OD), *= (CDCl₃)

Characterization of AETDF4 and AETD4-11 as chrysophanol-10, 10'-bianthrone (80)

Brownish red crystals; The ESIMS m/z : 477 [M+H]⁺, confirmed the molecular formula C₃₀H₂₂O₆. ¹H NMR (600 MHz, CDCl₃) spectrum (Figure 3.2.34) showed data similar to chrysophanol as dimer. The *ortho-meta* coupled aromatic protons assigning to H-6 and H-6' at δ_H (7.83, dd, $J = 1.2$ Hz, $J = 7.5$ Hz, 1H) and H-7 and H-7' at δ_H (7.29, dd; $J = 1.1$ Hz, $J = 8.3$ Hz, 1H), *ortho-coupling* at δ_H (7.67, d, $J = 7.4$ Hz, 1H) assigned to H-5 and H-5', one singlet peak assigning to H-2 and H-2' at δ_H (7.10, s, 1H) indicating the substitution at position 3 and the four highly downfield shifted proton signals at δ_H (12.00

and 12.10 for 8-OH, 12.20 and 12.40 for 1-OH). DEPT NMR (150 MHz, CDCl₃) Table (3.2.14) and Figure (3.2.33) showed two carbonyl groups δ_c 193.6 (C-9, 9'), two methyl groups at (H-1.27; C-22.3) and the singlet peak at (H-4.41; C-56.4) assigned to the 10, 10' C-C linkage indicating that compound **80** is bianthrone anthraquinone. The bianthrone nucleus was confirmed by the 30 signals including 24 aromatic carbons. All data confirmed the compound **80** as chrysophanol-10,10'-bianthrone (Figure 3.2.33) and were comparable to the published data (Dos Santos & de Vasconcelos Silva 2008).

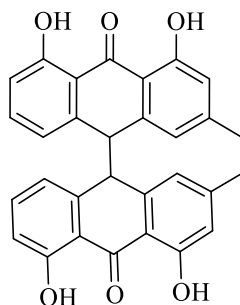


Figure 3.2.33: Structure of chrysophanol-10,10'-bianthrone (**80**)

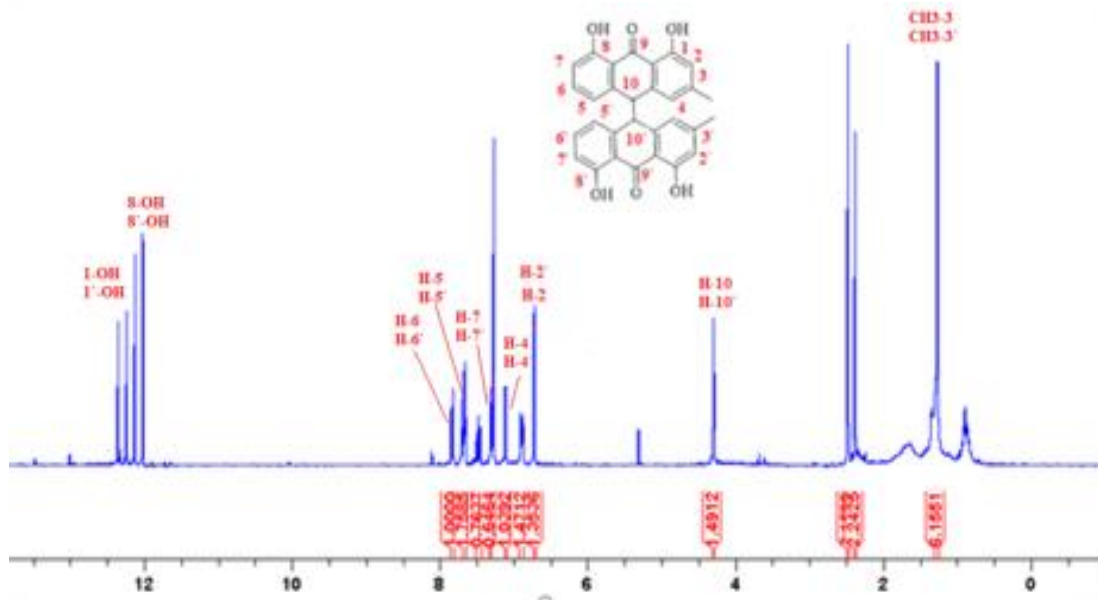


Figure 3.2.34: ¹H NMR spectrum (600 MHz, CDCl₃) of chrysophanol 10, 10'-bianthrone (**80**)

Table 3.2.14: ¹H NMR (600 MHz, CDCl₃) and DEPT NMR (150 MHz, CDCl₃) of chrysophanol-10, 10'-bianthrone (**80**)

	Chemical Shift δ (ppm), J in Hz			Chemical Shift δ (ppm), J in Hz	
Position	¹ H	DEPT	Position	¹ H	DEPT
1		162.4	1'		162.4
2	6.70, s, 1H	116.0	2'	6.70, s, 1H	116.0
3		148.0	3'		148.0
4	7.10, s, 1H	120.0	4'	7.10, s, 1H	120.0
5	7.67, d, 7.4, 1H	120.8	5'	7.67, d, 7.4, 1H	120.8
6	7.83, dd, 1.2, 7.5, 1H	137.0	6'	7.83, dd, 1.2, 7.5, 1H	137.0
7	7.29, dd; 1.14, 8.3, 1H	115.5	7'	7.29, dd; 1.14, 8.3, 1H	115.5
8	6.42, d, 15.6, 1H	162.7	8'	6.42, d, 15.6, 1H	162.7
9		193.6	9'		193.6
10	4.41, s, 1H	56.4	10'	4.41, s, 1H	56.4

3-CH3	1.27, s, 3H	22.3	3'-CH3	1.27, s, 3H	22.3
8-OH	12.00, s		8-OH	12.10, s	
1-OH	12.20, s		1-OH	12.40, s	

Characterization of AETDF4-6 as C- α -rhamnopyranosyl bianthracene-9, 9', 10 (10'H)-trione glycoside (**81**)

Brownish yellow powder, the UV-Vis spectrum (Figure 3.2.36) of this compound exhibited four major absorption peaks at λ_{\max} : 224 nm, 256, 368 and 440 nm indicating this compound to be anthraquinone (Anouar *et al.*, 2014). The ESIMS m/z showed a peak at: 637 [M-H]⁻, indicating the molecular formula C₃₆H₃₀O₁₁ (Figure 3.2.35). ¹H NMR (600 MHz, CD₃OD) (Figure 3.2.37 and Table 3.2.15) showed four *ortho*-coupling aromatic protons; the first one at δ_{H} (7.27, dd, $J = 7.0, 10.0$,) assigned for H-5 and H-5', the second at δ_{H} 7.67 (t, $J = 8.0$) assigned for H-6, the third and fourth *ortho*-coupling were at δ_{H} 7.58 (d, $J = 8.0$) pointed for H-7 and at δ_{H} 7.26 (d, $J = 9.0$) assigned for H-6', respectively. Compound **80** showed also three aromatic singlet protons, two are separated by a methyl group at δ_{H} (6.75, H-2') and (6.94, H-4') and a singlet proton at δ_{H} (7.34, H-2). A sharp singlet at δ_{H} 4.58 assigned for H-10', indicated the proton attached to the C-glycosidic linkage. This compound could be assigned as bianthracene. The ¹³C NMR (150 MHz, CD₃OD) Table (3.2.15) showed three carbonyl groups at δ_{C} 196.2 (C -9), 184.3 (C-10), and 194.9 (C-9') indicating that compound **81** (Figure 3.2.35) is bianthracene-trione. From the HSQC and HMBC correlations (Figures 3.2.38 and 3.2.39). The H-10' → C-2'' HMBC correlation confirmed the C-glycoside linkage of compound **80** (the lack of anomeric acetal-proton signals). The correlation between H-6' → C-4 indicated the exact

linkage of the two anthrone moieties in the bianthrone, All data were comparable to the published data (Adinolfi *et al.*, 1991).

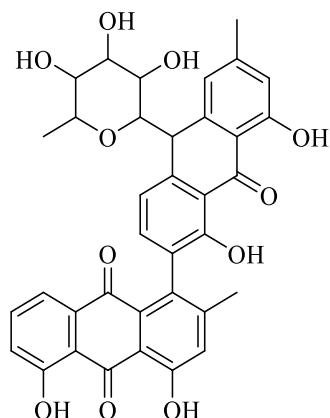


Figure 3.2.35: Structure of C- α -rhamnopyranosyl bianthracene-9, 9', 10 (10'H)-trione glycoside (**81**)

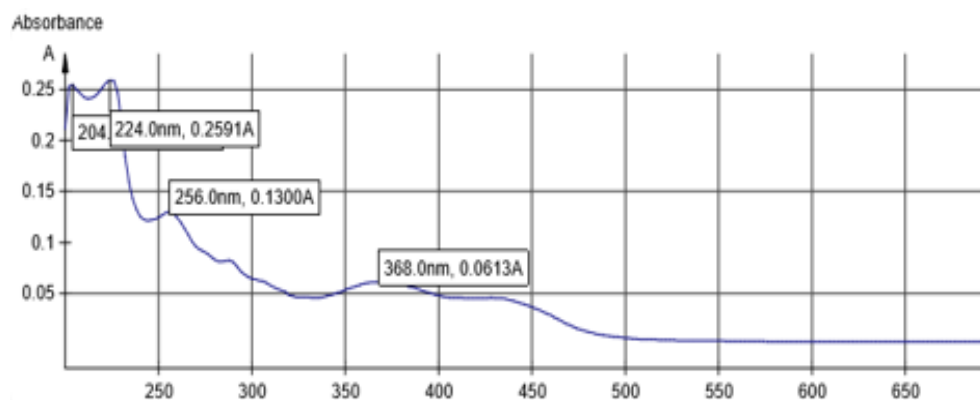


Figure 3.2.36: The UV absorbance (MeOH) of C- α -rhamnopyranosyl bianthracene-9, 9', 10 (10'H)-trione glycoside (**81**)

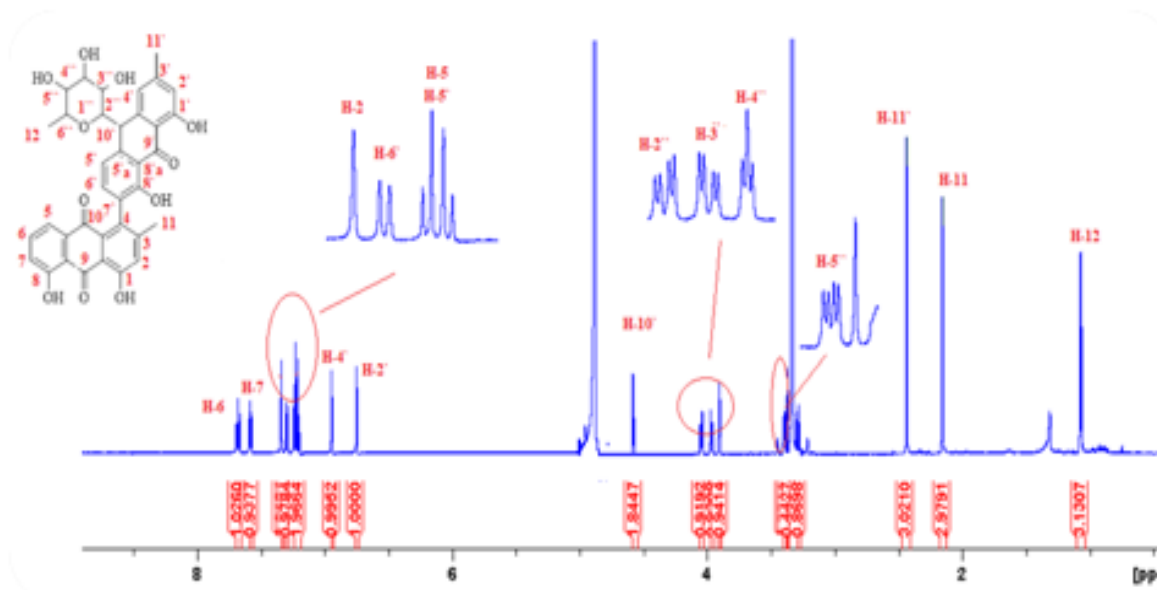


Figure 3.2.37: ^1H NMR spectrum (600 MHz, CD_3OD) of C- α -rhamnopyranosyl bianthracene-9,9',10 (10'H)-trione glycoside (**81**)

Table 3.2.15: ^1H NMR (600 MHz, CD_3OD) and ^{13}C NMR (150 MHz, CD_3OD) of C- α -rhamnopyranosyl bianthracene-9, 9', 10 (10'H)-trione glycoside (**81**)

Position	Chemical Shift δ (ppm), J in Hz		Position	Chemical Shift δ (ppm), J in Hz	
	^1H	^{13}C		^1H	^{13}C
2	7.34, s	125.6	4'	6.94, s	120.5
3		151.5	5'	7.27, dd: 7.0, 10.0	115.5
4		129.3	6'	7.26, d, 9.0	134.5
5	7.27, dd: 7.0, 10.0	124.5	7'		134.3
6	7.67, t, 8.0	136.8	8'		160.7
7	7.58, d, 8.0	121.6	9'		194.9
8		163.0	10'	4.58	45.2
9		196.2	11'	2.15, s	20.0
10		184.3	2''	3.96, dd; 3.1, 8.8	80.1

11	2.44, s	20.8	3 ^{''}	4.04, dd, 3.4, 8.5	
1 [`]		162.4	4 ^{''}	3.91, t, 2.9	
2 [`]	6.75, s	115.5	5 ^{''}	3.39, dd: 2.4, 6.2	47.5
3 [`]		149.3	6 ^{''} -12	1.07, d, 6.5	

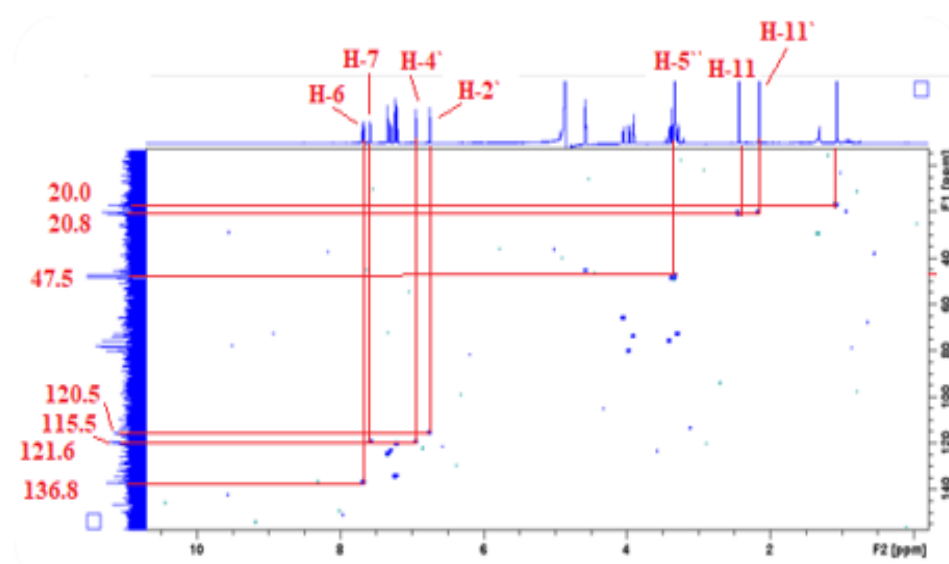


Figure 3.2.38: HSQC correlations (600, 150 MHz, CD₃OD) of C- α -rhamnopyranosyl bianthracene-9,9',10 (10'H)-trione glycoside (**81**)

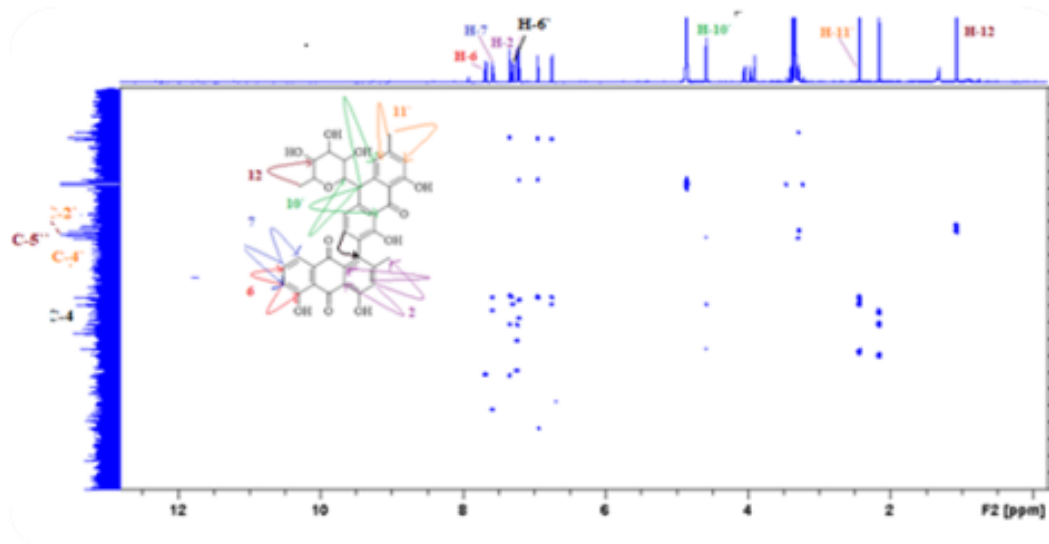


Figure 3.2.39: HMBC correlations (600, 150 MHz, CD₃OD) of C- α -rhamnopyranosyl bianthracene-9,9',10 (10'H)-trione glycoside (**81**)

3.2.10.3 Characterization of ferulate derivative

Characterization of ferulate derivative AELD-3 as p-hydroxy-phenethyl trans-ferulate (82)

Colourless powder; The UV-Vis spectrum of this compound exhibited only one major absorption peaks at λ_{\max} : 318 nm. The ESIMS m/z showed a peak at: 315 [M+H]⁺, significant peaks at m/z 193 [M+H]⁺ *p*-hydroxy phenethyl moiety and 120 [M+H]⁺ feruloyl moiety indicating that the molecular formula could be C₁₈H₁₈O₅ (Figure 3.2.41).

¹H NMR (600 MHz, CD₃OD) Table (3.2.16) and Figure (3.2.42) showed three aromatic signals; one *ortho-meta* coupling assigned to H-6 at δ_H 7.04 (dd, $J = 8.2$ Hz, $J = 1.7$ Hz, 1H), one *meta*-coupling at δ_H 7.14 (d, $J = 1.7$ Hz, 1H) assigned to H-2. It also showed aromatic *ortho* coupling at δ_H s; 6.80 (d, $J = 8.2$ Hz, 1H, H-5), 7.07 (d, $J = 8.0$ Hz, 2H, H-2'), 6.74 (d, $J = 8.5$ Hz, 2H, H-3'), 6.74 (d, $J = 8.5$ Hz, 2H, H-5'), 7.07 (d, $J = 8.0$ Hz, 2H, H-6'), 3.48 (t, $J = 7.3$ Hz, 2H, H-1'') and 2.77 (t, $J = 7.6$ Hz, 2H, H-2''). The two

doublets assigning to H-7 and H-8 appeared at δ_{H} 7.45 (d, $J = 15.7$ Hz, 1H) and δ_{H} 6.42 (d, $J = 15.6$ Hz, 1H) indicated that compound **82** was a *trans* isomer. A singlet peak at position 3.91(3H) indicated the presence of methoxy group in compound **82**. ^{13}C NMR (600 MHz, CD_3OD) revealed the presence of 18 carbon signals including 12 aromatic protons and one carbonyl at δ_{C} 169.5 All the mentioned data confirmed that the structure is *p*-hydroxy-phenethyl *trans*-ferulate (Figure 3.2.40). comparable to the published data (Darwish & Reinecke, 2003).

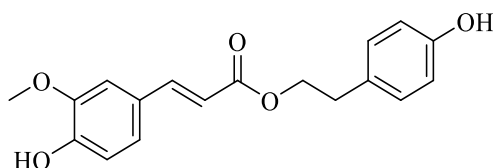


Figure 3.2.40: Structure of *p*-hydroxy-phenethyl *trans*-ferulate (**82**)

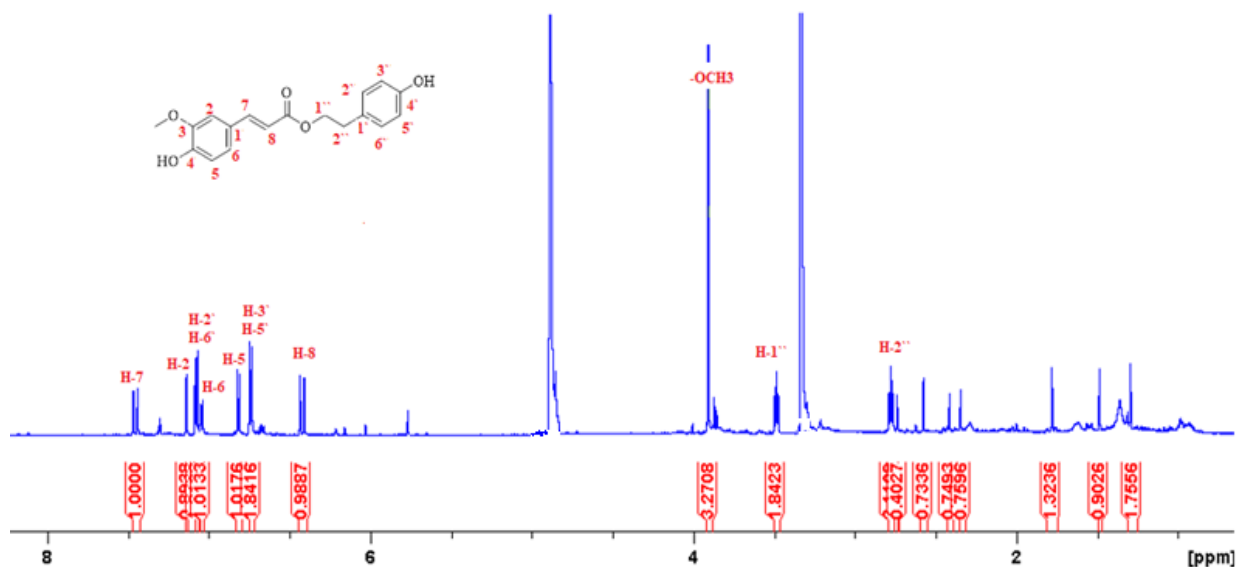


Figure 3.2.41: ^1H NMR spectrum (600 MHz, CD_3OD) of *p*-hydroxy-phenethyl *trans*-ferulate (**82**)

Table 3.2.16: ^1H NMR (600 MHz, CD_3OD).and ^{13}C NMR (150 MHz, CD_3OD) of *p*-hydroxy-phenethyl trans-ferulate (**82**)

Chemical Shift δ (ppm), <i>J</i> in Hz			Chemical Shift δ (ppm), <i>J</i> in Hz		
Position	^1H	^{13}C	Position	^1H	^{13}C
1			1`		131.5
2	7.14, d, 1.7, 1H	111.7	2`	7.07, d, 8.0, 2H	130.9
3		149.4	3`	6.74, d, 8.5, 2H	
4		150.1	4`		157.4
5	6.80, d, 8.2, 1H	116.4	5`	6.74, d, 8.5, 2H	
6	7.04, dd; 8.2, 1.7, 1H	123.4	6`	7.07, d, 8.0, 2H	
7	7.45, d, 15.7, 1H	142.1	1``	3.48, t, 7.3, 2H	42.7
8	6.42, d, 15.6, 1H	118.9	2``	2.77, t, 7.6, 2H	36.0
9		169.5	-OCH3	3.91, s, 3H	56.6

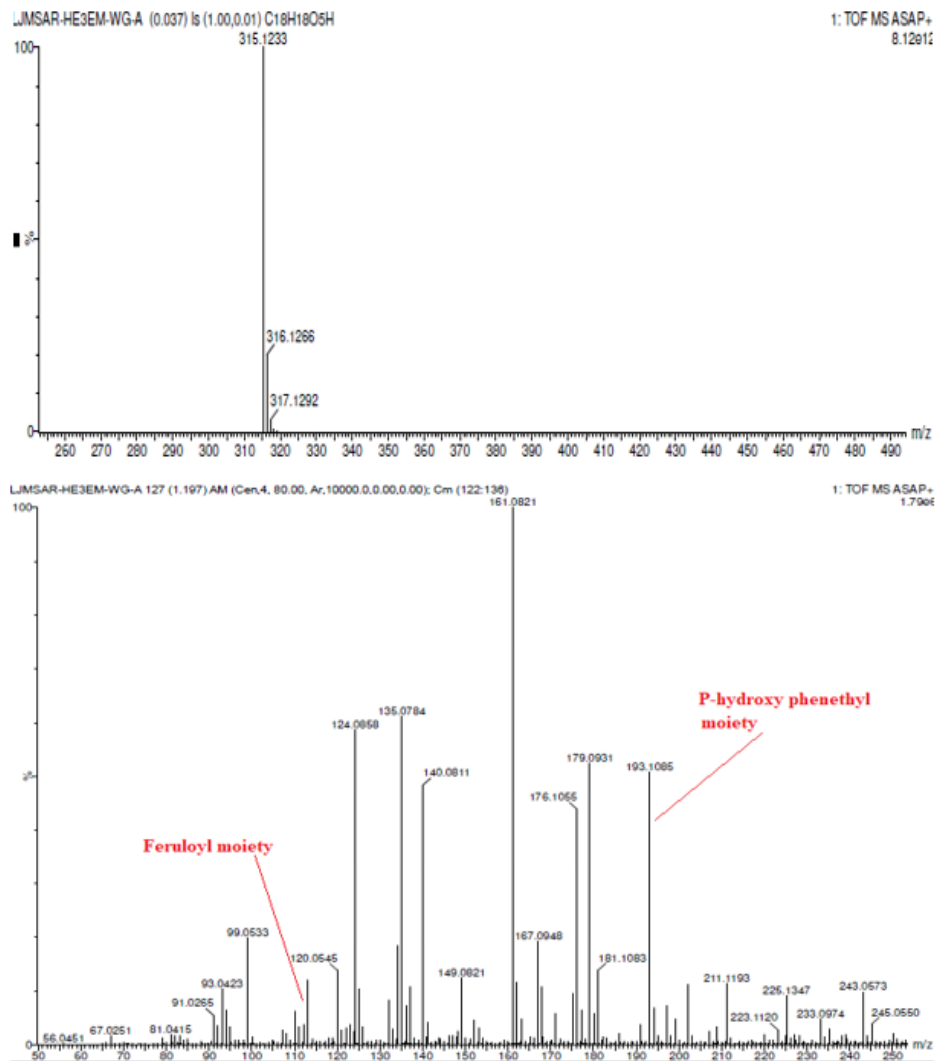


Figure 3.2.41: MS spectrum (atmospheric solid analysis probe, +ve mode) of *p*-hydroxy-phenethyl trans-ferulate (**82**)

3.2.11 Cytotoxic effect of the isolated compounds from *A. aestivus*

Results presented in Table 3.2.17 and Figures 3.2.43 and 3.2.44 show the IC_{50} values of the isolated compounds from the leaves and tubers of *A. aestivus* compared with the positive control etoposide. The cytotoxicity applied against both the human prostate and lung carcinoma cell lines for compounds **22**, **79**, **80** while compound **80** tested only

against prostate cancer cells. The most prominent cytotoxicity was observed with C- α -rhamnopyranosyl bianthracene-trione glycoside (**81**), which was separated from the active fraction DCM VLC F4 of AET. It revealed highly significant results at the concentrations 1.9, 16.9, and 153.3 μM , while the lower doses (0.02 and 0.2 μM) showed non-significant results. The IC_{50} value of compound **81** was 62 μM .

Compound **82** was tested against the hepatocellular carcinoma cells (HEPG2) but did not show any cytotoxic activity Table 3.2.17.

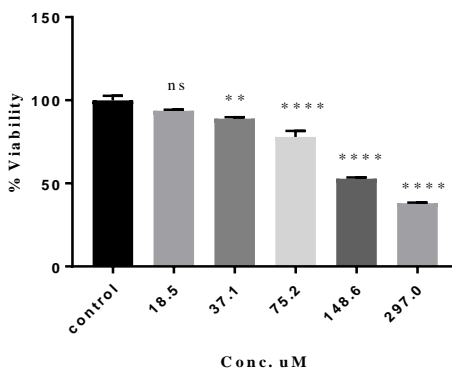
Table 3.2.17: The IC_{50} (μM) of different isolated compounds from *A. eastivus* tubers on PC3 lung cancer cells.

Pure compound	IC_{50} (μM) PC3	IC_{50} (μM) HEPG2	IC_{50} (μM) A549
Luteolin (22)	201 \pm 1.10	NA	76.9 \pm 1.11 after 48 h
C- α -rhamnopyranosyl bianthracene-trione glycoside (81)	62 \pm 1.61	NA	NA
Chrysophanol anthrone (79)	No activity*	NA	No activity*
Chrysophanol bianthrone (80)	No activity*	NA	No activity*
<i>p</i> -hydroxy-phenethyl trans-ferulate (82)	NA	No activity*	NA
Etoposide (78)	NA	NA	61 \pm 1.56

*No activity at the highest concentration of 500 μM NA--- Non-applicable

All experiments were carried out in triplicate on separate occasions. Data were expressed as means \pm standard error of the mean derived from $n \geq 12$ from three separate occasions.

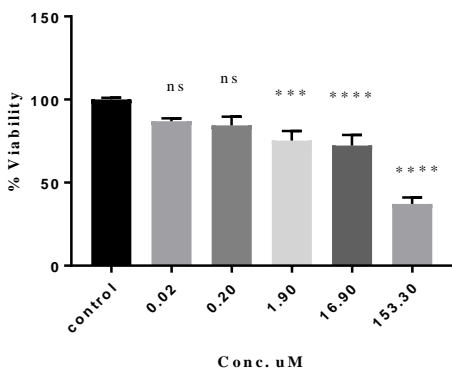
Cytotoxicity of luteolin in PC3 cells according to the MTT assay



All experiments were carried out in triplicate on separate occasions. Data were expressed as means \pm standard error of the mean derived from $n \geq 12$ from three separate occasions.

Figure 3.2.43: The cytotoxic activity of luteolin (**22**) against the prostate cancer cell line

Cytotoxicity of bianthracene trione in PC3 cancer cells according to the MTT assay



All experiments were carried out in triplicate on separate occasions. Data were expressed as means \pm standard error of the mean derived from $n \geq 12$ from three separate occasions.

Figure 3.2.44: The cytotoxic activity of C- α -rhamnopyranosyl bianthracene-9,9',10 (10'H)-trione glycoside (**81**) against the prostate cancer cell line

Discussion

Asphodelus L. (Asphodelaceae) is a genus distributed along the Mediterranean basin and has been reported for its biological activities such as anti-bacterial, anti-fungal, anti-parasitic, cytotoxic and anti-inflammatory activity. Previous phytochemical studies identified the main classes of compounds as 1, 8-dihydroxyanthracene derivatives, flavonoids, phenolic acid, and triterpenoids from the different species such as; *A. acaulis*, *A. aestivus*, *A. cerasiferus*, *A. fistulosus*, *A. albus*, *A. microcarpus*, *A. ramosus*, and *A. tenuifolius*. The aerial parts of these plants mostly revealed the presence of flavonoids such as luteolin, isovitexin and isoorientin, phenolic acids, and few anthraquinones while the roots have been reported to have mainly anthraquinone derivatives such as aloemodin, chrysophanol and triterpenoids derivatives (Malmir *et al.*, 2018).

In the present study, the cytotoxic activity of *A. aestivus* leaves and tubers from the Asphodelaceae family was tested using the MTT assay. This is the first time, to our knowledge, that the plant's cytotoxic activity has been assessed in the four human cancer cell lines, HepG2, EJ138, A549 and PC3. Only one other report is available on *A. aestivus* concerning its cytotoxic activity against the breast cancer cell line MCF7 (Aslantürk & Çelik, 2013). *A. aestivus* tuber extracts showed higher level of cytotoxic activity than the leaves. The DCM tuber extract showed high cytotoxic activity against both the human lung carcinoma A549 and the prostate cancer PC3 cell lines with IC₅₀ values 16 and 19 µg/mL, respectively (Figure: 3.2.4) and (Table 3.2.5), while the MeOH and *n*-hexane extracts did not show any cytotoxic activity in the cell lines used. *A. aestivus* leaves showed weak cytotoxicity against both the human liver hepatocellular carcinoma Hep G2 and the human lung carcinoma A549 with IC₅₀ value of 70 and 90 µg/ mL, respectively (Table 3.2.5). It is also of interest that the prostate cancer cells (PC3) were more sensitive

to *A. aestivus* tubers than normal prostate cells (PNT2) with high selective index (SI = 26). This selectivity might be attributed to the presence of anthraquinones as reported by Huang *et al.*, in 2007.

Anthraquinones are bioactive compounds derived from Aloe, Asphodelus, Purslane, Rhubarb, and Senna. Many biological studies revealed their antibacterial, antifungal, gastrointestinal and renal protective effects. In recent years, their reported anticancer activities have attracted more attention among several types of anthraquinones such as emodin, aloe-emodin, and rhein (Huang *et al.*, 2007).

In this study, four anthraquinones were isolated from *A. aestivus*; three from the tubers (VLC fractions (3 and 4): chrysophanol anthrone (**79**), chrysophanol-10,10'-bianthrone (**80**), and C- α -rhamnopyranosyl bianthracene-9, 9', 10 (10'H)-trione glycoside (**81**) and one anthraquinone from the leaves (DCM extract): aloe-emodin (**13**). Compounds **79**, **80**, and **81** were isolated for the first time from this species (Malmir *et al.*, 2018). However, compound **81** had been isolated from *A. ramosus* tubers in 1991 and chrysophanol 1-O-gentiobioside was only reported in *A. aestivus* while chrysophanol anthrone (**79**) isolated only in this study.

The three compounds **79-81** isolated from the VLC tuber fractions were tested for their cytotoxicity against the PC3 cell line. The bianthracene-trione (**81**) obtained from the active VLCF4, showed good cytotoxicity with IC₅₀ value of 62 μ M, which is reported for the first time, and might be responsible for the high potency of this fraction (IC₅₀ value = 21 μ g/mL). Compounds **79** and **80** did not show any activity. It has also been previously reported that chrysophanol (**79**) has weak cytotoxic activity (Huang *et al.*, 2007), and it shares a very similar chemical structure with cytotoxic emodin and aloe-emodin

anthraquinones. In addition, chrysophanol has been reported as an antitumor agent acting against the growth and proliferation of a mouse lymphocytic leukemic cell line (L1210), however, this result was not replicated in a human leukemia cell line (HL-60) (Lee *et al.*, 2011). Furthermore, anthraquinones including chrysophanol showed antiproliferative effects in human colon cancer cells (SW620) and human breast cancer cells (MCF7 and MDA-MB-231) (Lee *et al.*, 2011).

Additionally, in this study, *p*-hydroxy-phenethyl *trans*-ferulate (**82**) was isolated for the first time from *A. aestivus* leaves. It was previously isolated from *Heracleum lanatum* (Nakata *et al.*, 1982), *Oenanthe javanica* (Fujita *et al.*, 1995) and *Coriandrum sativum* (Taniguchi *et al.*, 1996) and has been reported to have antioxidant properties. Compound **82** was isolated from the DCM extract of *A. aestivus* leaves (AELD). This extract (DCM) showed moderate cytotoxicity against the HEPG2 cell lines with IC₅₀ value of 70 µg/mL, so compound **82** was tested for its cytotoxicity against the HEPG2 cell lines but did not show any activity. The activity of the DCM extract may be due to the presence of cytotoxic aloe-emodin (compound **13**), but unfortunately, an accidental loss of the sample meant it could not be tested.

Flavonoids belong to a group of natural substances with variable phenolic structures, which are abundant in various fruits and vegetables, and in all parts of the plants. They have been reported to have a wide spectrum of biological activities such as antiinflammatory, antiallergic, antiviral, and anticarcinogenic activity (Nijveldt *et al.*, 2001). Luteolin is a natural flavonoid found in fruits and vegetables. It usually occurs in its glycosylated form in celery, green pepper, perilla leaf and camomile tea. Luteolin has many biological activities as antioxidant, anti-inflammatory and anti-allergy activity.

Recent studies have been aimed more on its reported potent anticancer activity against various tumor cells e.g. breast, liver, skin, and prostate cancer cell lines (Song *et al.*, 2017). Our study revealed the isolation of luteolin (**22**) from both the SPE fractions 3 and 4 purified from the MeOH extract of *A. aestivus* leaves. Luteolin (**22**) was tested for its cytotoxicity against both the PC3 prostate cancer and A549 lung cancer cell lines. It showed moderate cytotoxicity with IC₅₀ value of 201 μM for the prostate cancer cells after a 24 h treatment and with an IC₅₀ value of 76.9 μM for the lung cancer cells after a 48 h treatment period. The cytotoxic activity of luteolin has also previously reported on both PC3 and A549 cell lines (Han *et al.*, 2016).

Conclusion

The current findings support the traditional use of *A. aestivus* for the treatment of tumours. These results suggest that the cytotoxicity is higher in the tubers than in the leaves. The observed toxicity in the roots was contributed to by various cytotoxic anthraquinones e.g. (C- α -rhamnopyranosyl bianthracene-9,9',10 (10'H)-trione glycoside **81**). While the cytotoxic activity revealed in the leaves was due to the presence of cytotoxic flavonoids e.g. luteolin (**22**).

3.3 *Ruta chalepensis*

3.3.1 Extraction

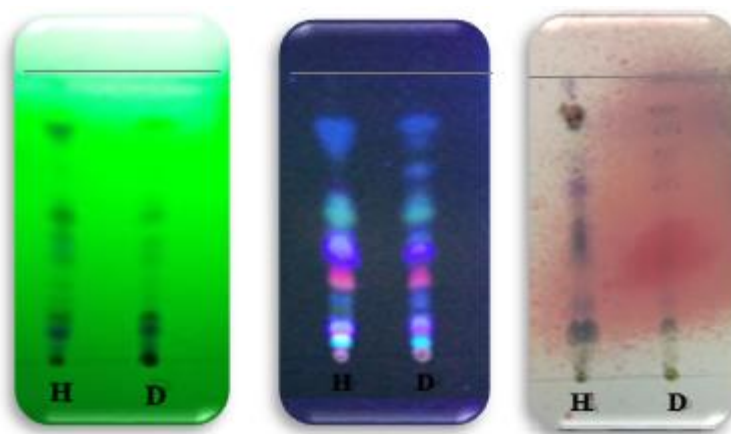
Sequential Soxhlet extraction of the dried and ground aerial parts of *Ruta chalepensis* (RCA) (349.13 g) afforded three extracts: *n*-hexane (RCH), dichloromethane (RCD), and MeOH (RCM). The percentage yields of these extracts are summarized in Table 3.3.1

Table 3.3.1: Percentage yield of the three extracts obtained from *R. chalepensis* aerial parts

Extract	% Yield
<i>n</i> -Hexane (RCH)	2.6
DCM (RCD)	1.15
MeOH (RCM)	19.8

3.3.2 Preliminary analytical TLC screening

The developed TLC plates of three extracts obtained from *R. chalepensis* were viewed under short (254 nm) and long (366 nm) UV light. The TLC plates showed blue fluorescent spots, which may indicate the presence of coumarins (Lee 1965). The TLC plates then sprayed with anisaldehyde reagent followed by heating at 100°C for 5 min to reveal many violet coloured spots with R_f values ranging from 0.16 to 0.94 (Table 3.3.2). The violet colour suggested the presence of alkanes and terpenes in the *n*-hexane extract (Figure: 3.3.1) (Kristanti & Tunjung 2015).



Short UV (254 nm) Long UV (366 nm) Sprayed with anisaldehyde
 Mobile phase: *n*-Hexane: EtOAc = 80:20

Figure 3.3.1: TLC for the three extracts of *R. chalepensis* aerial parts

Table 3.3.2: R_f values of different extracts of *R. chalepensis* aerial parts

<i>n</i> -Hexane R_f values	DCM R_f values
0.01, 0.11, 0.29, 0.43, 0.56, 0.74, 0.84	0.01, 0.11, 0.29, 0.43, 0.56, 0.70, 0.74, 0.84

3.3.3 Analytical HPLC screening of the MeOH extract of *R. chalepensis* aerial parts

The MeOH extract of *R. chalepensis* aerial parts (10 mg/mL) was analysed by Dionex Ultimate 3000 analytical HPLC coupled with a photodiode detector using a gradient mobile phase, 30-100% MeOH/H₂O for 30 min with a volume of injection of 20 μ L and a flow rate of 1 mL/min. (Figure 3.3.2; Table 3.3.3).

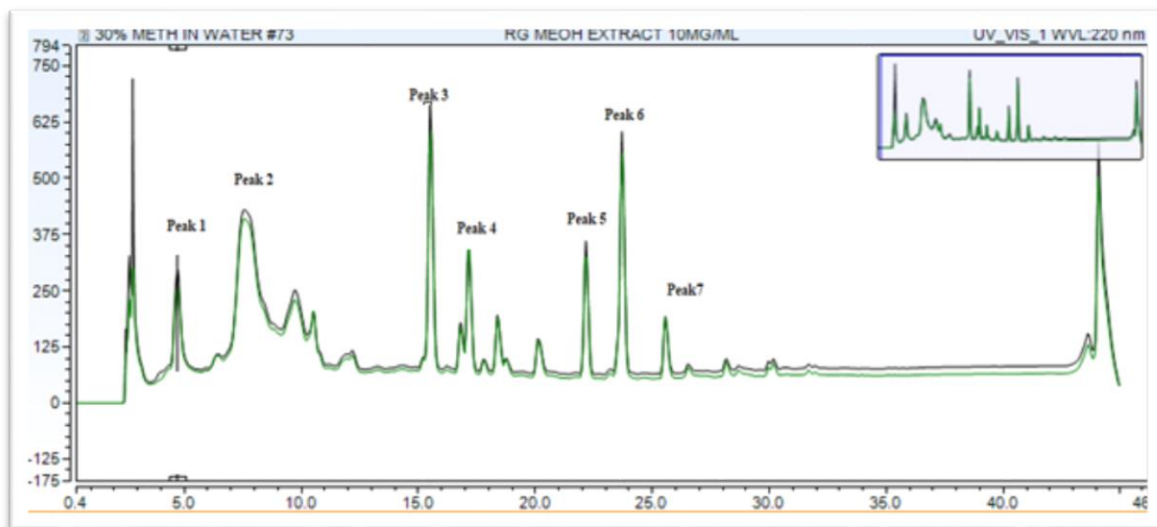


Figure 3.3.2: Analytical HPLC chromatogram of the MeOH extract of *R. chalepensis* aerial parts (observed at 220 nm)

Table 3.3.3: UV-Vis data for all major peaks obtained from diode array detector

Peak No.	Retention Time (min)	UV-Vis absorbances (λ_{max}) (nm)
1	4.8	218, 281, and 326
2	7.7	219, 246, 300, and 340
3	15.8	243 and 325
4	17.2	249 and 321
5	22.1	335
6	23.9	242 and 291
7	25.6	234 and 315

3.3.4 Screening of *R. chalepensis* extracts for cytotoxic activity

The cytotoxic activity, according to the MTT assay, of the *n*-hexane, DCM, and MeOH extracts of *R. chalepensis* aerial parts was assessed against five cancer cell lines; EJ138 (human bladder carcinoma), Hep G2 (human liver hepatocellular carcinoma), A549 (human lung carcinoma), MCF7 (human breast adenocarcinoma), and prostate cancer cell lines (PC3). The RCD extract showed the highest activity throughout all the extracts against the different cancer cell lines with IC_{50} = 25, 15, 55, 60, and 50 $\mu\text{g/mL}$, respectively while, the *n*-hexane, and the MeOH extracts did not show any activity (Table 3.3.4a).

Table 3.3.4a: The IC_{50} ($\mu\text{g/mL}$) of *n*-hexane, DCM and MeOH extracts of *R. chalepensis* aerial parts on the selection of five human cancer cell lines

Cell type	IC_{50} values ($\mu\text{g/mL}$)		
	RCH	RCD	RCM
EJ138	> 100	25 ± 0.98	> 100
Hep G2	> 100	15 ± 0.77	> 100
A549	> 100	55 ± 0.66	> 100
MCF7	> 100	60 ± 1.40	> 100
PC3	> 100	50 ± 1.29	> 100

Values greater than 100 $\mu\text{g/mL}$ were considered as non-cytotoxic (Sahranavard *et al.* 2012).

The results were mean values \pm standard error of the mean derived from $n \geq 12$ from three separate occasions.

The selectivity index (SI) of the active DCM extract of *R. chalepensis* aerial parts was assessed comparing the cytotoxicity results of the human normal prostate cell line (PNT2) with those of human prostate cancer cell line (PC3). The extract revealed low degree of cytotoxic selectivity towards the prostate cancer cells (SI= 0.84), which indicated the low safety of the extract on the normal human cells. The IC₅₀ values of *R. chalepensis* aerial parts extracts in both cell lines and the selectivity index are summarized in Table 3.3.4b.

Table 3.3.4b: The IC₅₀ (µg/mL) values for RC DCM extract on PC3 and PNT2 cells and the selectivity index (SI) using the normal human prostate cells (PNT2).

Cell type	IC ₅₀ values (µg/mL) (RCD)
PC3	50 ± 1.29
PNT2	42 ± 0.57
Selectivity index	0.84

Selectivity index (SI) = The IC₅₀ (µg/mL) of extracts against the normal cells divided by the IC₅₀ (µg/mL) of extracts against the cancer cells, where IC₅₀ is the concentration required to reduce viability by 50% of the cell population (Badisa, *et al.*, 2009).

3.3.5 Chromatographic fractionation of the extracts

Following the systematic, bioassay-guided phytochemical and cytotoxic/anticancer study on *R. chalepensis* aerial parts, further fractionation of the active DCM extract was performed. However, both the inactive MeOH and *n*-hexane extracts of *R. chalepensis* aerial parts were fractionated with the aim of isolating major metabolites to have complete understanding of the phytochemistry of *R. chalepensis*.

3.3.5.1 Vacuum liquid chromatography (VLC)

The DCM (2.05 g) and *n*-hexane (3.26 g) extracts of *R. chalepensis* aerial parts were further fractionated by VLC over silica to collect seven fractions from the *n*-hexane extract (Figure 3.3.3) and six fractions from the DCM extract (Figures 3.3.4), the weights of fractions are listed in Table 3.3.5

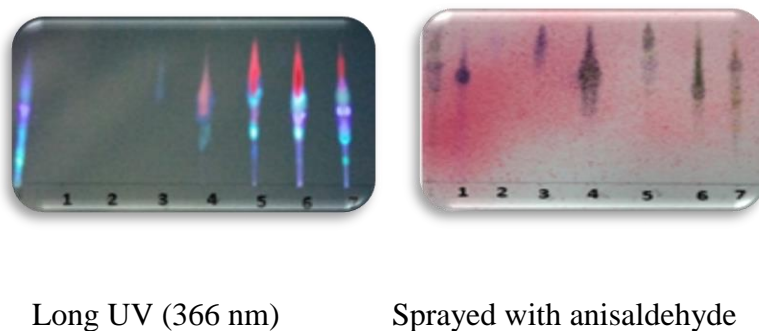


Figure 3.3.3: TLC analysis (mobile phase: Toluene: EtOAc /Acetic acid = 25:24:1) of the VLC fractions of the *n*-hexane extract of *R. chalepensis* aerial parts

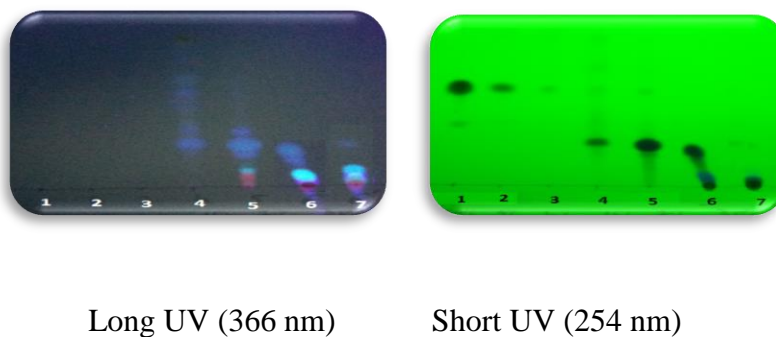


Figure 3.3.4: TLC analysis (mobile phase: 20% EtOAc in *n*-hexane) of the VLC fractions of the DCM extract of *R. chalepensis* aerial parts

Table 3.3.5: Weights of the VLC fractions of the extracts RCH and RCD

Fraction	Mobile phase gradient	Wt of fraction (mg)	Fraction	Mobile phase gradient	Wt of fraction (mg)
RCHF1	100% <i>n</i> -hexane	121	RCDF1	100% <i>n</i> -hexane	9
RCHF2	10% EtOAc / <i>n</i> -hexane	140	RCDF2	5% EtOAc / <i>n</i> -hexane	3
RCHF3	30% EtOAc / <i>n</i> -hexane	65	RCDF3	10% EtOAc / <i>n</i> -hexane	1.4
RCHF4	50% EtOAc / <i>n</i> -hexane	517.8	RCDF4	15% EtOAc / <i>n</i> -hexane	72.7
RCHF5	80% EtOAc / <i>n</i> -hexane	527.3	RCDF5	20% EtOAc / <i>n</i> -hexane	56.4
RCHF6	100% EtOAc	469.9	RCDF6	30% EtOAc / <i>n</i> -hexane	80
RCHF7	50% MeOH/ EtOAc	355	RCDF7	50% EtOAc / <i>n</i> -hexane	217.9

3.3.5.2 Solid phase extraction (SPE)

The MeOH extract of *R. chalepensis* aerial parts (RCM) was fractionated by SPE to collect four fractions (Figures 3.3.5-3.3.8; Table 3.3.6).

Table 3.3.6: Weights of the SPE fractions of the MeOH extract of *R. chalepensis* aerial parts.

Fraction	Mobile phase gradient	Weight of fraction (mg)
RCMF1	20% MeOH/H ₂ O	2440
RCMF2	50% MeOH/H ₂ O	298.6
RCMF3	80% MeOH/H ₂ O	80.9
RCMF4	100% MeOH/H ₂ O	14.9

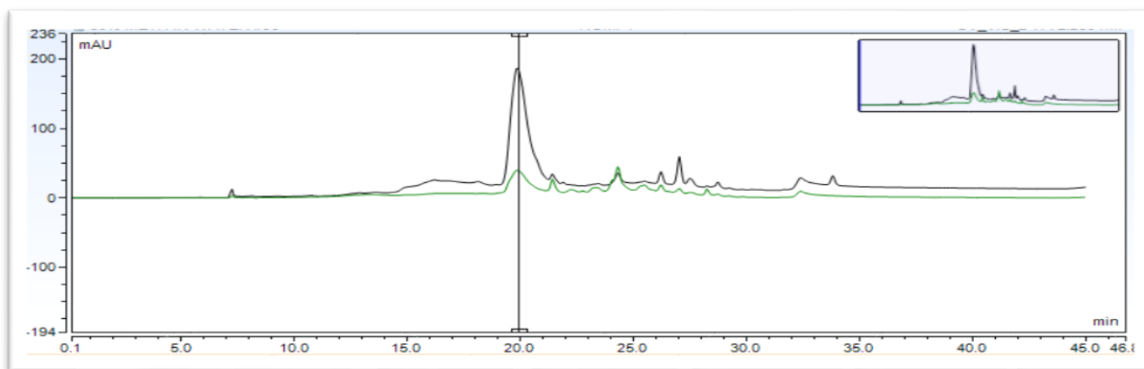


Figure 3.3.5: Analytical HPLC chromatograms of SPE fraction 1 of RCM (observed at 250 nm)

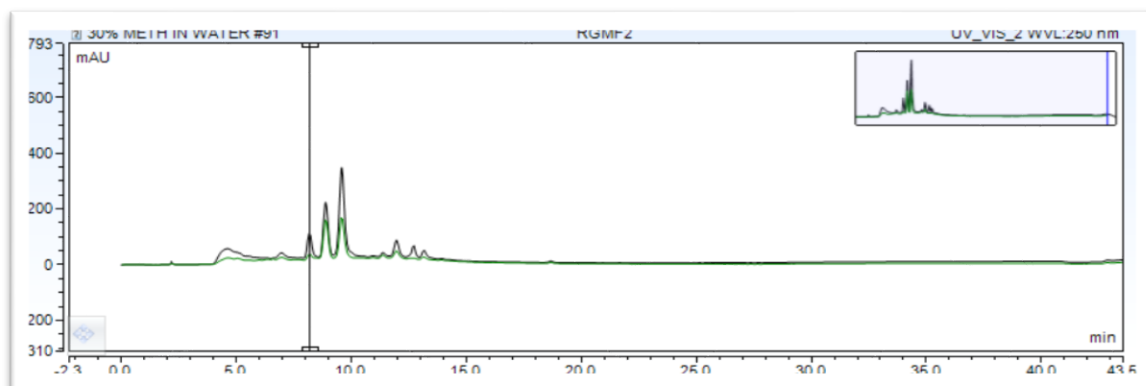


Figure 3.3.6: Analytical HPLC chromatograms of SPE fraction 2 of RCM (observed at 250 nm)

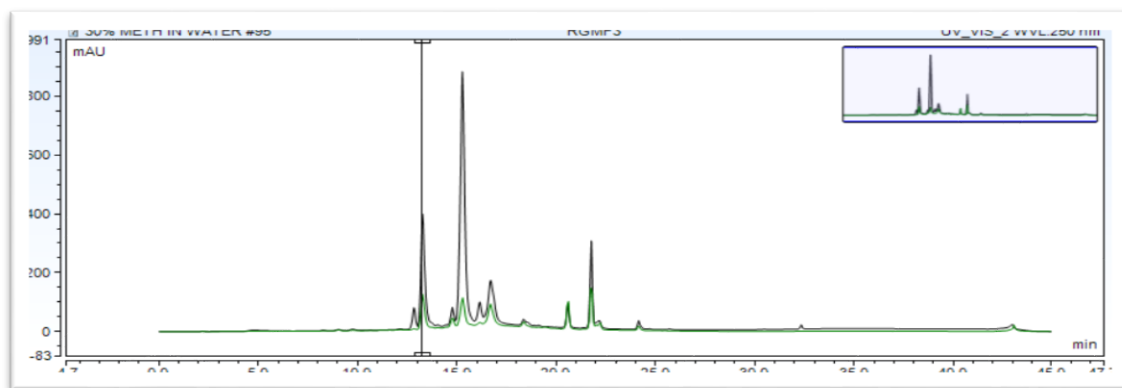


Figure 3.3.7: Analytical HPLC chromatograms of SPE fraction 3 of RCM (observed at 250 nm)

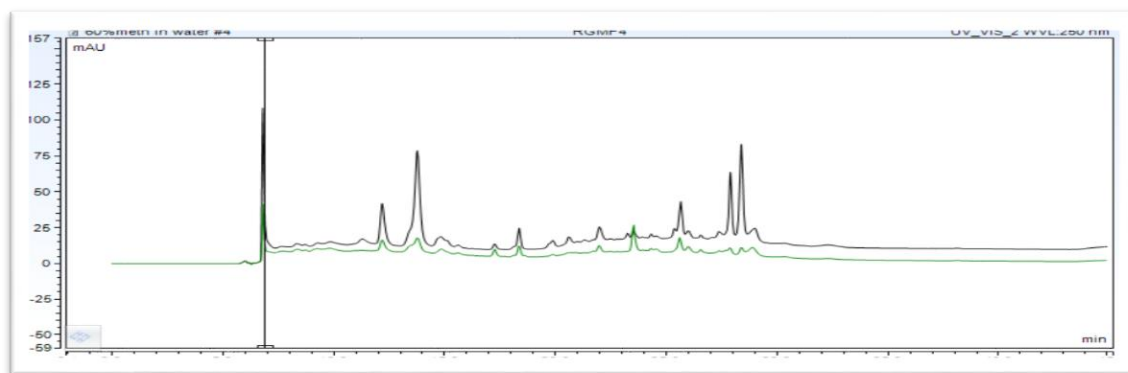


Figure 3.3.8: Analytical HPLC chromatograms of SPE fraction 4 of RCM (observed at 250 nm)

3.3.6 Screening of *R. chalepensis* DCM fractions for cytotoxic activity

The cytotoxic activity of the DCM fractions of *R. chalepensis* aerial parts was assessed against the most sensitive cancer cell line (hepatocellular carcinoma cell line HEPG2). Unfortunately, all the fractions gave IC_{50} values $>100 \mu\text{g/mL}$. For this reason, the fractions were tested again on another sensitive cancer cell line (human bladder carcinoma cells EJ138). The highest activity was revealed in in the VLC DCM F7 with IC_{50} value of

85 $\mu\text{g/mL}$. The IC_{50} values for the DCM fractions of *R. chalepensis* aerial parts on EJ138 are summarised in Table 3.3.7

Table 3.3.7: The IC_{50} ($\mu\text{g/mL}$) of the VLC DCM fractions of *R. chalepensis* aerial parts fractions against EJ138 (human bladder carcinoma cells).

Fraction	F1	F2	F3	F4	F5	F6	F7
IC_{50} ($\mu\text{g/mL}$)	>100	>100	>100	91.44 \pm 1.96	98 \pm 1.98	95.3 \pm 3.31	85.24 \pm 1.93

Data were expressed as means \pm standard error of the mean derived from $n \geq 12$ from three separate occasions

3.3.7 Isolation of compounds from *R. chalepensis*

3.3.7.1 The MeOH extract (RCM)

Isolation of compounds from the SPE fractions 2, 3 and 4 of RCM utilised semi-preparative and preparative reversed-phase HPLC technique (Agilent) employing a 30-100% gradient of MeOH in water for 30 min with a volume of injection of 200 μL and a flow rate of 2 mL/min

The following compounds were isolated from RCMF2: RCMF2-1 (37 mg, $t_R = 15.9$ min), RCMF2-2 (43 mg, $t_R = 16$ min), RCMF2-3 (27 mg, $t_R = 18.6$ min) and RCMF2-4 (13.4 mg, $t_R = 20.3$ min) (Figure 3.3.9) from SPE fraction 2. RCMF2-2 and RCMF2-4 were further purified using 20-50% MeOH/ H_2O gradient to get the two pure compounds RCMF2-2-2 (6 mg, $t_R = 21.2$ min) and RCMF2-4-1 (6.9 mg, $t_R = 21.2$) (Figures 3.3.10-3.3.13).

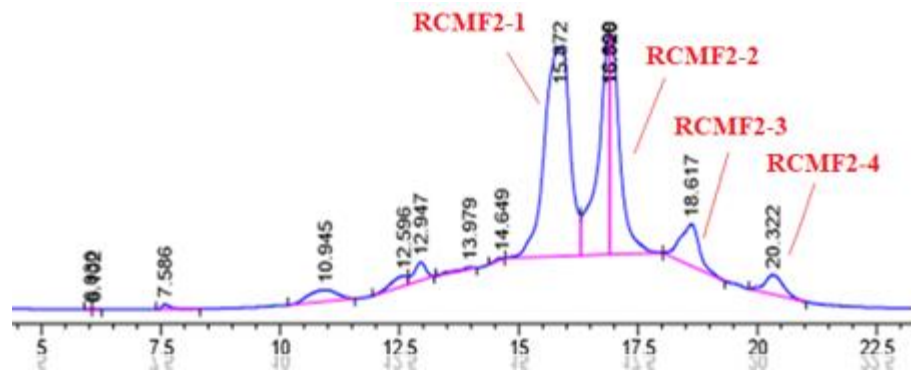


Figure 3.3.9: HPLC chromatogram of isolated compounds from SPE fraction 2 RCM (observed at 310 nm)

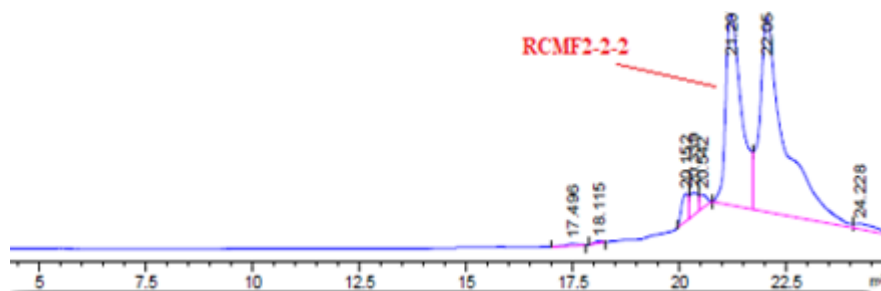


Figure 3.3.10: Purification of the compound RCMF2-2 (observed at 310 nm)

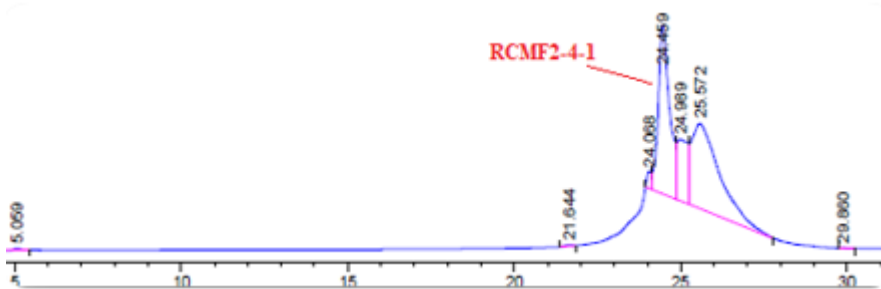


Figure 3.3.11: Purification of the compound RCMF2-4 (observed at 310 nm)

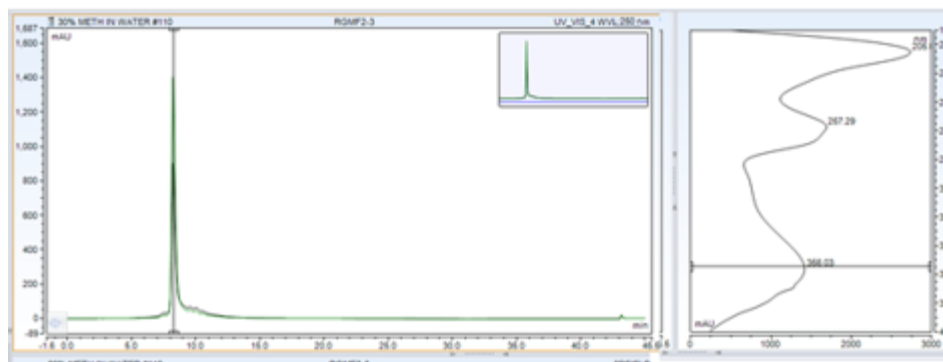


Figure 3.3.12: Analytical HPLC chromatogram of RCMF2-3 (observed at 250 nm)

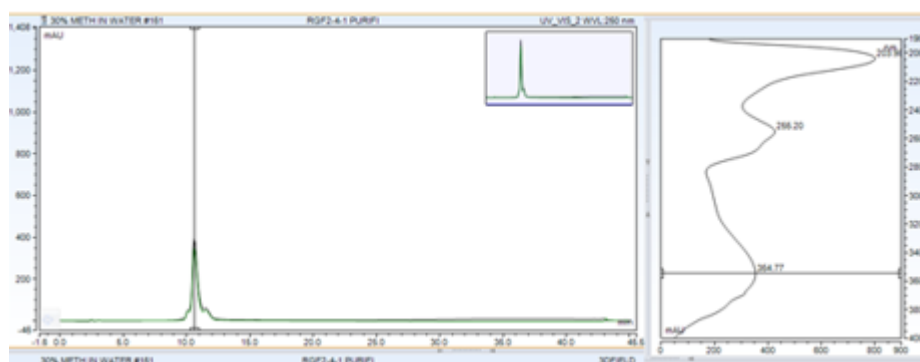


Figure 3.3.13: Analytical HPLC chromatogram of RCMF2-4-1 (observed at 250 nm)

The following compounds were obtained from RCMF3: RCMF3-1 (10.8 mg, $t_R = 15.6$), RCMF3-2 (16.8 mg, $t_R = 17.5$), RCMF3-3 (27 mg, $t_R = 19.2$), RCMF3-4 (5.7 mg, $t_R = 22.4$), RCMF3-5 (4.6 mg, $t_R = 23.7$) and RCMF3-6 (1.8 mg, $t_R = 25.5$) (Figure 3.3.14). The compound RCMF3-2 was further purified using 20-70 % MeOH/H₂O gradient to get the pure compounds RCMF3-2-2 (5 mg, $t_R = 23.4$) (Figure 3.3.15).

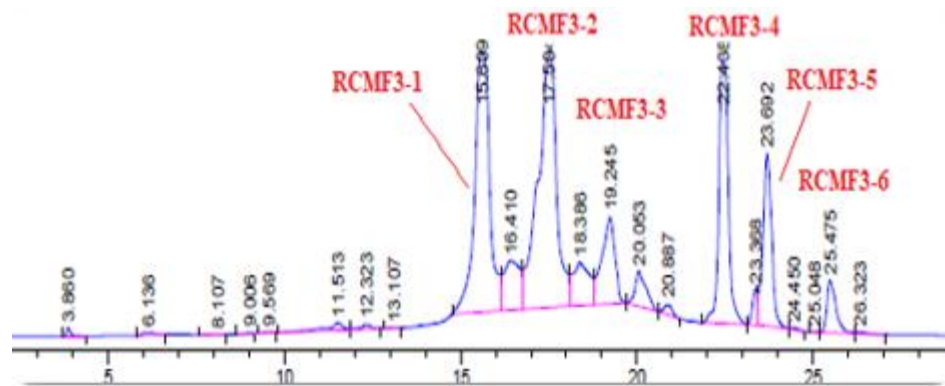


Figure 3.3.14: HPLC chromatogram of isolated compounds from RCM SPE fraction 3 (observed at 310 nm)

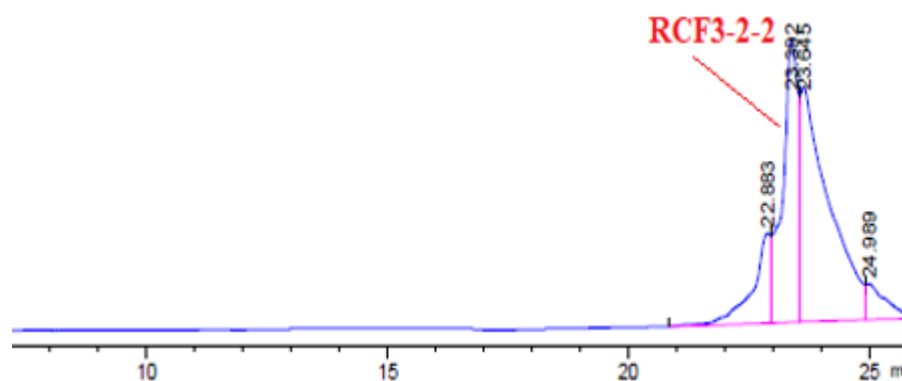


Figure 3.3.15: Purification of the compound RCF3-2 (observed at 310 nm)

3.3.7.2 The DCM extract (RCD)

Separation of the DCM Fraction 5

The DCM Fraction 5 (56.4 mg) of *R. chalepensis* aerial parts was analyzed by prep-HPLC using a gradient solvent system 30-100% MeOH in water. This led to the isolation of the major compound: RCDF5 (14 mg, $t_R = 25.2$) (Figure 3.3.16).

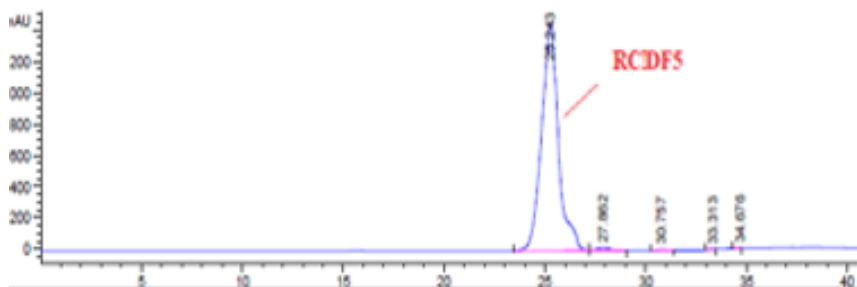


Figure 3.3.16: HPLC chromatogram of isolated compounds from the RCD fraction 5 (observed at 366 nm)

Separation of the DCM Fraction 6

The DCM fraction 6 (80 mg) of *R. chalepensis* aerial parts was analyzed by prep-HPLC using a gradient solvent system 30-100% MeOH in water. This led to the separation of many impure peaks (Figure 3.3.17). Peak 2 was further purified and led to the isolation of the two compounds: RCDF6-1 (12.0 mg, $t_R = 24.2$) and RCDF6-2 (10.2 mg, $t_R = 25.2$) (Figure 3.3.18).

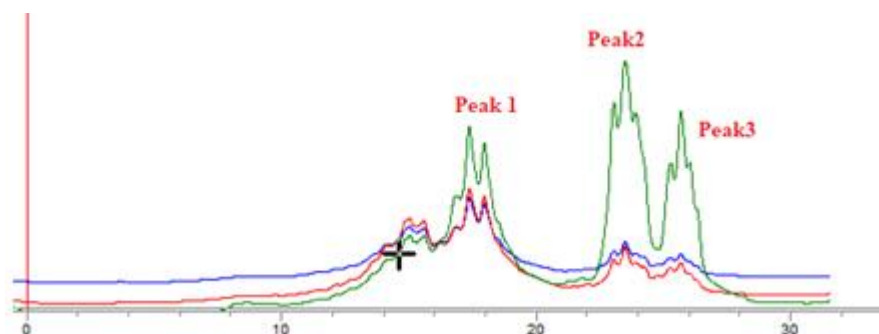


Figure 3.3.17: HPLC chromatograms of isolated compounds from the RCD F6 [observed at 220 nm (green), 254 nm (blue), and 366 nm (red)]

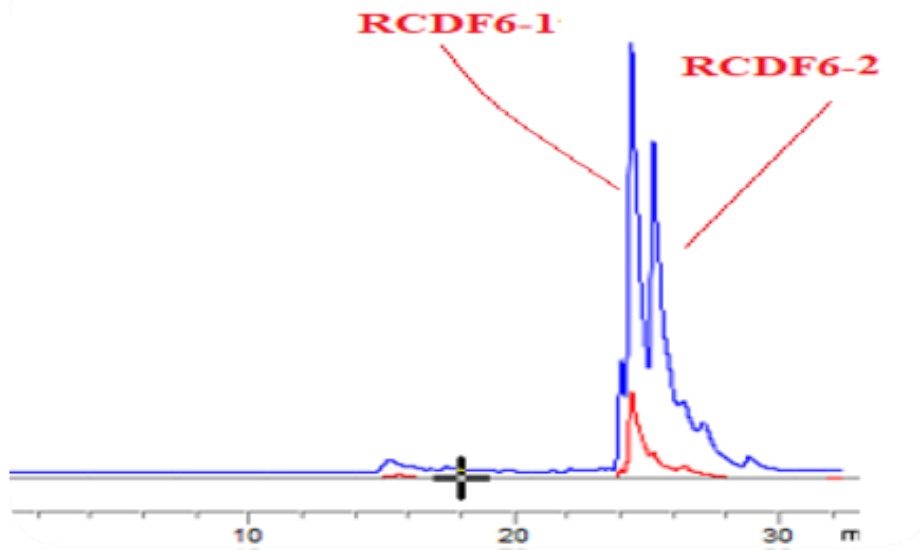


Figure 3.3.18: Purification of peak 2 isolated from RCD F6 (observed at 310 nm)

Separation of the active DCM Fraction 7

The active DCM fraction 7 (217.9 mg) of *R. chalepensis* aerial parts was analyzed by prep-HPLC using a gradient solvent system 50-100% MeOH in water. This led to the isolation of the compounds: RCDF7-9 (5 mg, $t_R = 17.9$) and RCDF7-12 (8 mg, $t_R = 23.8$) (Figure 3.3.19). The compound RCDF7-9 was further purified using a gradient of 50-80% MeOH/water to get the pure compound RCDF7-9-2 (1.3 mg, $t_R = 11.4$) (Figure 3.3.20).

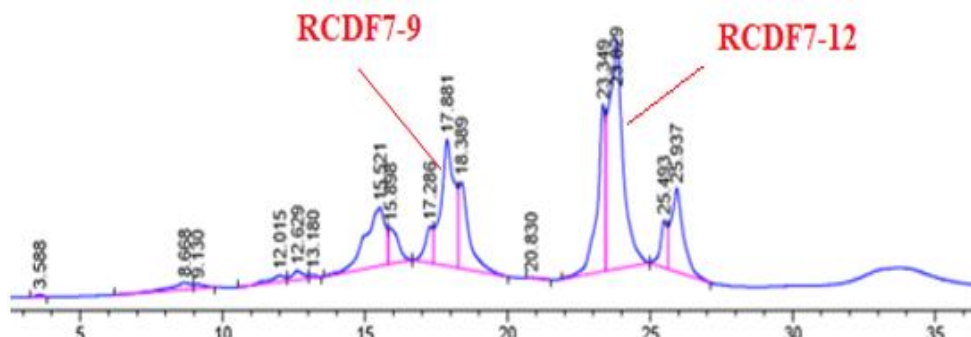


Figure 3.3.19: HPLC chromatogram for the RCD F7 (observed at 310 nm)

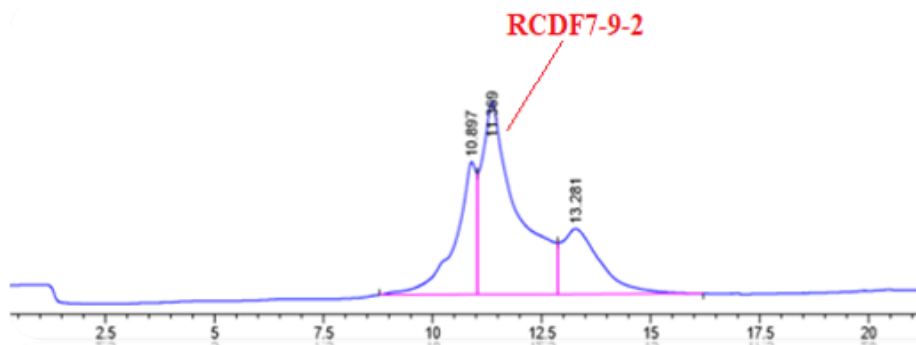


Figure 3.3.20: Purification of the compound RCDF7-9 (observed at 310 nm)

3.3.7.3 The *n*-hexane extract (RCH)

Crystals from n-hexane layer

A pure compound was completely crystallized from the VLC fractions 2 as a white crystal: RCHF2 (140 mg) (Figure 3.3.21).



Figure 3.3.21: Crystals of the compound RCHF2 from *R. chalepensis*

Separation of the n-hexane VLC Fraction 4

The *n*-hexane VLC fraction 4 was chromatographed over silica gel plates 20x20 using 20% EtOAc in *n*-hexane as mobile phase (Figure 3.3.22), the plates showed three separated bands under the long (366 nm) and the short UV light (254 nm). The three bands yielded the compounds: RCHF4-1 (3 mg, $R_f = 0.13$), RCHF4-2 (5.6 mg, $R_f = 0.3$), and RCHF4-3 mixture (18.4

mg, $R_f = 0.62$). The RCHF4-3 mixture was further purified by PTLC (mobile phase: 20% EtOAc in *n*-hexane) into two compounds: RCHF4-3-1 (2.5 mg, $R_f = 0.88$) and RCHF4-3-2 (3.0 mg, $R_f = 0.97$) (Figure 3.3.23).

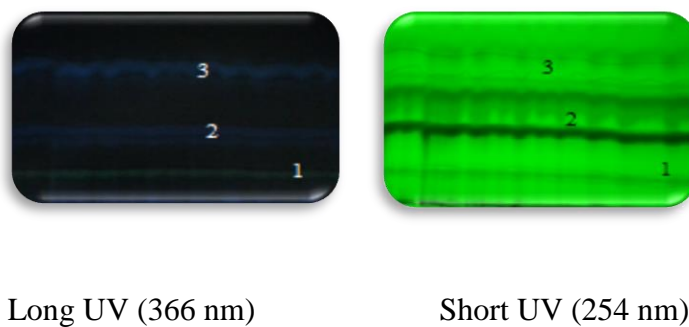
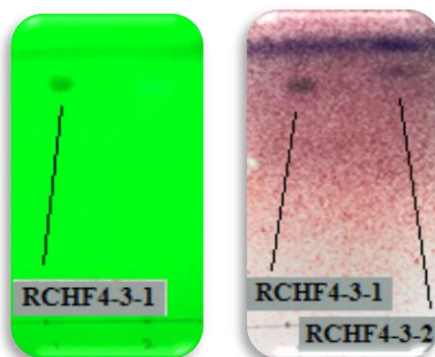


Figure 3.3.22: PTLC separation (mobile phase: 20% EtOAc in *n*-hexane) of the RCH VLC F4



n-Hexane: EtOAc = 80:20

Figure 3.3.23: Purified compounds from RCHF4-3 mixture

Separation of the n-hexane VLC Fraction 7

The *n*-hexane VLC Fraction 7 was chromatographed over TLC silica gel plates 20x20 using 50% MeOH/ EtOAc as a mobile phase. This yielded the pure compounds; RCHF7-2 (0.7 mg, $R_f = 0.3$) and RCHF7-7 (1.7 mg, $R_f = 0.9$) (figure 3.3.24).



Figure 3.3.24: Isolation of the compounds RCHF7-2 and RCHF7-7 from RCH F7

Separation of the n-hexane VLC Fraction 5+ 6+ 7

Portions from the *n*-hexane fractions 5, 6, and 7 (Figure 3.3.25) were mixed together (300 mg) and fractionated with VLC using a small Büchner funnel with a gradient of 0% - 100% EtOAc in *n*-hexane , then 2% and 5% MeOH/ EtOAc) to yield 13 fractions (Table 3.3.8).

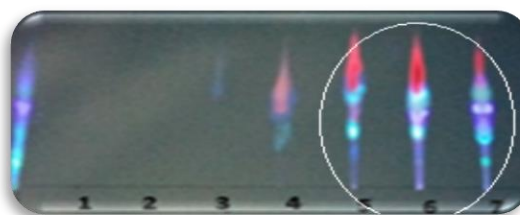


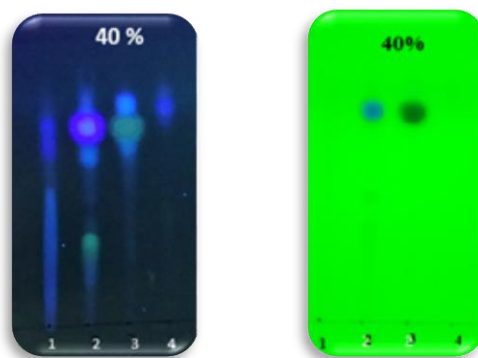
Figure 3.3.25: Fraction 5+6+7 from *R. chalepensis n*-hexane

Table 3.3.8: Different weights of Fraction 5+6+7 from *n*-hexane layer of *R. chalepensis*

Fraction	Mobile phase gradient	The weight of fraction (mg)
RCHF 100 %-H	100% <i>n</i> -hexane	0.9
RCHF 10%	10% EtOAc / <i>n</i> -hexane	0.8
RCHF 20%	20% EtOAc / <i>n</i> -hexane	13.5
RCHF 30%	30% EtOAc / <i>n</i> -hexane	10
RCHF 40%	40% EtOAc / <i>n</i> -hexane	34.7
RCHF 50%	50% EtOAc / <i>n</i> -hexane	63.4
RCHF 60%	60% EtOAc / <i>n</i> -hexane	48.5
RCHF 70%	70% EtOAc / <i>n</i> -hexane	41.4
RCHF 80%	80% EtOAc / <i>n</i> -hexane	18.7
RCHF 90%	90% EtOAc / <i>n</i> -hexane	16.6
RCHF 100% -E	100% EtOAc	8.0
RCHF 2%	2% MeOH/ EtOAc	22.7
RCHF 5%	5% MeOH/ EtOAc	16

RCHF-40%

The fraction RCHF-40 % (34.7 mg) was chromatographed over TLC silica gel plates 20x20, using 50% MeOH/EtOAc as a mobile phase. This lead to the isolation of the pure compound: RCHF 40%-3-3 (2.2 mg, $R_f = 0.74$) (Figure 3.3.26).



Mobile phase: EtOAc: MeOH = 50:50

Figure 3.3.26: Isolation of compounds from RCH fraction 40%

RCHF-50%

The fraction RCHF-50% (63.4 mg) was isolated by prep-HPLC using a gradient solvent system 30-100% MeOH in water. This led to the isolation of the pure compound RCHF 50%-10 (3.2 mg, $t_R = 25.6$) and a mixture RCHF50% (9 mg, $t_R = 12.5$) (Figure 3.3.27). The mixture was purified with PTLC using T:E:A/25:24:1 as a mobile phase, which led to the isolation of the compound: RCHF50%-3 (2.3 mg, $R_f = 0.73$) (Figure 3.3.28).

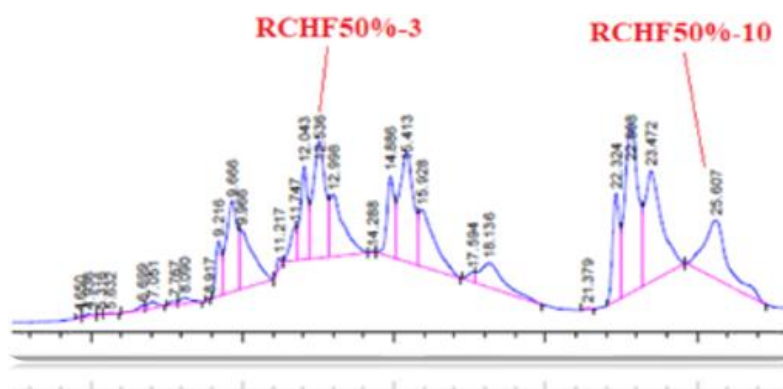
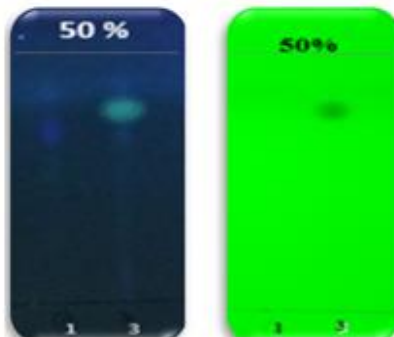


Figure 3.3.27: HPLC chromatogram of isolated compounds from the RCH fraction 50% (wavelength = 310 nm).



Mobile phase: EtOAc: MeOH = 50:50

Figure 3.3.28: Isolation of compounds from RCH fraction 50%

RCHF-60%

The fraction RCHF-60% (48.5 mg) was isolated by prep-HPLC using a gradient solvent system 50-100% MeOH in water. This led to the isolation of the pure compound: RCHF 60%- 4 (5.2 mg, $t_R = 17.9$), RCHF 60%-5 (3.1 mg, $t_R = 22.3$) (Figure 3.3.29).

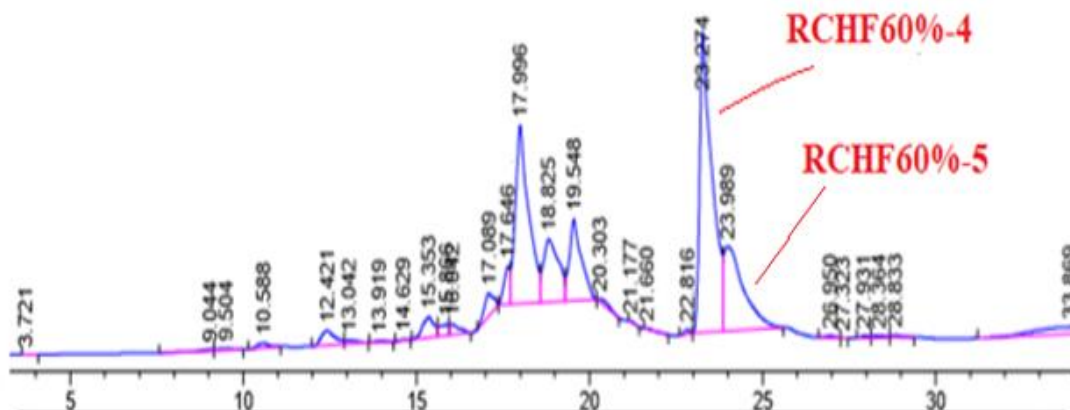


Figure 3.3.29: HPLC chromatogram of isolated compounds from the RCH fraction 60%
(wavelength = 310 nm)

RCHF 80%

The fraction RCHF 80% (18.7 mg) was isolated by prep-HPLC using a gradient solvent system 30-100% MeOH in water. This led to the isolation of the pure compound: RCHF-80%-3 (3 mg, $t_R = 19.3$) (Figure 3.3.30).

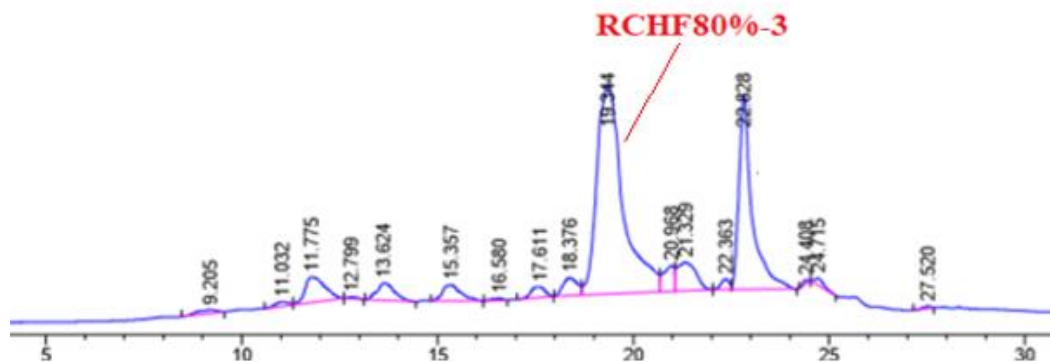
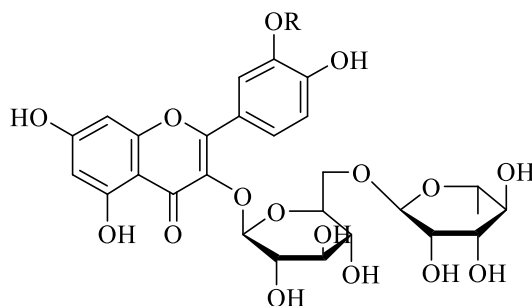


Figure 3.3.30: HPLC chromatogram of isolated compounds from RCH fraction 80% (wavelength = 310 nm)

3.3.8 Characterization of isolated compounds from *R. chalepensis* aerial parts

3.3.8.1 Characterization of flavonoids

Two flavonoids **52** and **83** were isolated from the SPE fractions F2 of RCM (Figure 3.3.31). The UV-Vis spectrum of these two compounds exhibited two major absorption peaks in the ranges 270-275 (Band –II) and 330-360 nm (Band –I) indicating these compounds to be flavonoids (Mabry *et al.*, 1970).



Compounds	R
Rutin (52)	H
Methoxy rutin (83)	CH ₃

Figure 3.3.31: Structure of flavonoids isolated from *R. chalepensis* aerial parts

Characterization of RCMF2-3 as rutin (52)

Yellow powder; The UV-Vis spectrum (MeOH) of this compound exhibited two major absorption peaks at λ_{max} : 257 and 355 nm indicating this compound to be a flavonoid (Mabry *et al.*, 1970). The ESIMS m/z showed a peak at: 611 $[M+H]^+$, indicating that the molecular formula could be C₂₇H₃₀O₁₆. ¹H NMR (600 MHz, CD₃OD) Tables 3.3.7 and Figure 3.3.32 exhibit the common features for flavonoid protons, which include the presence of two aromatic *meta*-coupling protons assigning to; H-6 at δ_{H} 6.23 (d, $J = 2.1$ Hz, 1H) and H-8 at δ_{H} 6.42 (d, $J = 2.0$ Hz, 1H) and at δ_{H} 7.69 (d, $J = 1.9$ Hz, 1H), 7.65 (d, 2.2, 1H) assigned for H-2' and H-6', one aromatic *ortho*-coupled proton assigning to H-5' at δ_{H} (d, $J = 8.5$ Hz, 1H) and one *ortho*-*meta* coupling at δ_{H} 7.65 (dd, $J = 2.2$, $J = 8.3$, 1H) assigned for H-6'. The ¹H NMR spectrum also showed a doublet at δ_{H} 1.14 (d, $J = 6.2$ Hz, 3H) and a signal for the anomeric proton appeared at δ_{H} 4.54 (br s) indicated the presence of a rhamnose, a doublet at δ_{H} 5.12 (d, $J = 7.7$ Hz, 1H) assigned for the β -anomeric glucose

proton H-1''. The signals for the carbon atoms of both rhamnose and glucose moieties were also observable in the ^{13}C NMR spectrum, the signal at δ_{C} 18.0 confirmed rhamnose (Table 3.3.10). All these data confirmed that compound **52** is rutin glycoside and were comparable to the published data (Markham, *et al.*, 1987; Terashima, *et al.*, 1999; Shaoguang Li *et al.*, 2014; Souravh Bais & Naveena Abrol. 2016).

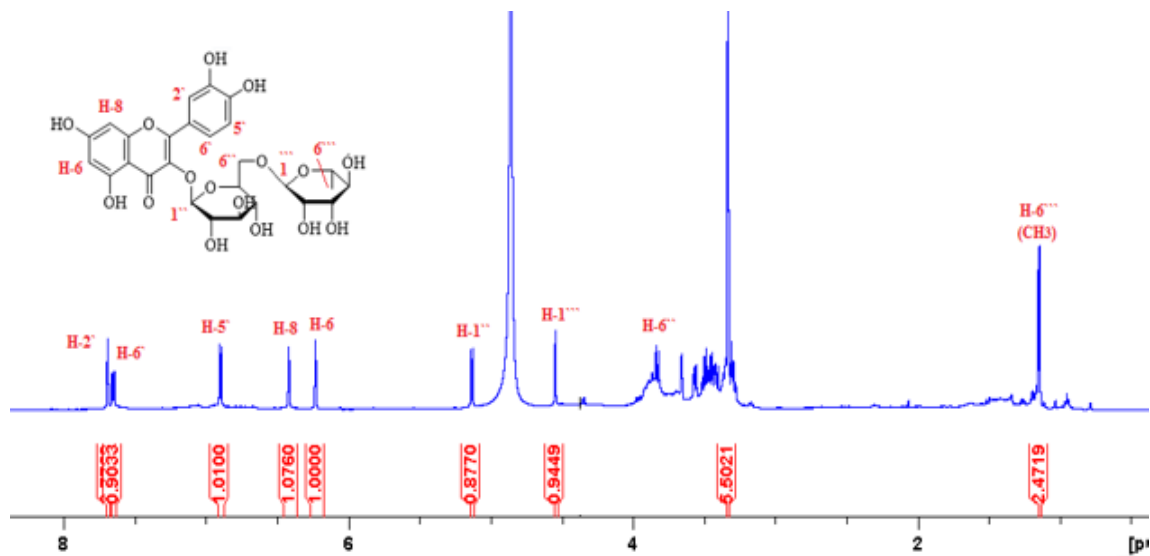


Figure 3.3.32: ^1H NMR spectrum (600 MHz, CD_3OD) of rutin (**52**)

Characterization of RCMF2-4-1 as methoxy rutin (83)

Yellow amorphous powder. The UV-Vis spectrum (MeOH) of this compound showed two major absorption peaks at λ_{max} : 255 and 354 nm, which indicate that this compound might be flavonoid (Mabry *et al.*, 1970), The ESIMS m/z exhibited a peak at: 625 $[\text{M}+\text{H}]^+$, indicating that the molecular formula could be $\text{C}_{28}\text{H}_{32}\text{O}_{16}$. ^1H NMR (600 MHz, CD_3OD) and ^{13}C NMR (150 MHz, CD_3OD); Tables (3.3.9 and 3.3.10) and Figure (3.4.33) showed similar data to rutin (**52**) with an extra singlet peak at δ_{H} 3.92 (3H) compared with rutin (Figure 3.3.34) indicating that this compound is methoxy rutin. The NOESY experiment was performed on compound **83** (Figure 3.3.35) to confirm the position of the methoxy

group on C-3', which was indicated by the close correlation between the unbonded protons H-2' ↔ CH₃ in space (Figure 3.3. 35). The HMBC (Figure 3.3.36) also confirmed the position of -OCH₃ by the correlation from -OCH₃ protons → δ_C C-3' (147.5). All data were comparable to the published data (Markham, *et al.*, 1987; Shaoguang Li *et al.*, 2014; Souravh Bais & Naveena Abrol. 2016).

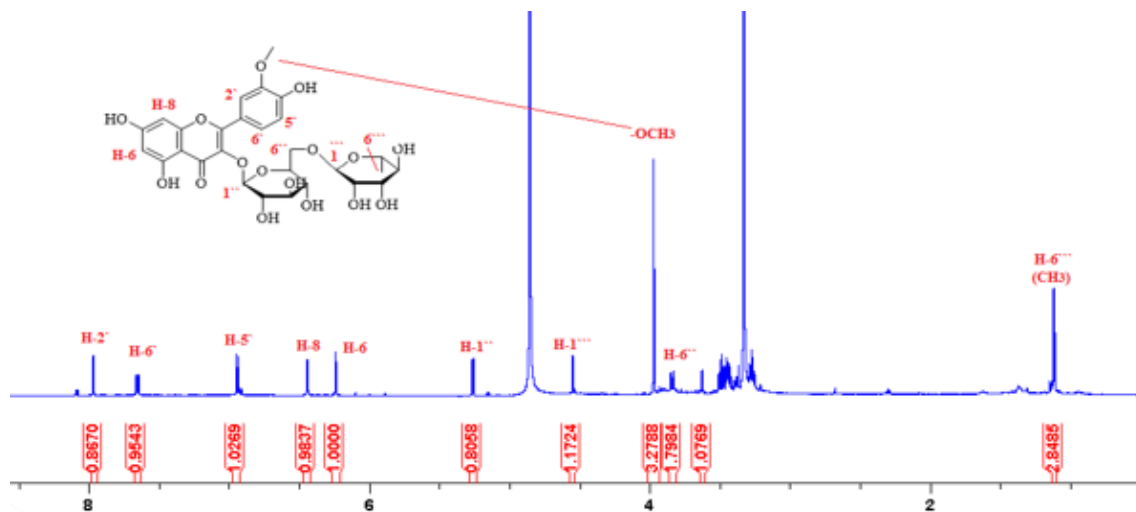


Figure 3.3.33: ¹H NMR spectrum (600 MHz, CD₃OD) of methoxy rutin (**83**)

Table 3.3.9: ¹H NMR (600 MHz, CD₃OD) for flavonoid glycosides: Rutin (**52**) and methoxy rutin (**83**)

Position	Chemical Shift δ (ppm), multiplicity and J in Hz	
	52	83
6	6.23 (d, 2.1,1H)	6.24 (d, 2.1,1H)
8	6.42 (d, 2.0,1H)	6.44 (d, 2.2,1H)
2 ^ˆ	7.69 (d, 1.9,1H)	7.97 (d, 2.2,1H)
5 ^ˆ	6.89 (d, 8.5,1H)	6.94 (d, 8.5,1H)
6 ^ˆ	7.65 (dd; 8.3, 2.2,1H)	7.66 (dd; 8.4, 1.98,1H)
1 ^{ˆˆ}	5.12 (d, 7.7, ,1H)	5.27 (d, 7.6,1H)
6 ^{ˆˆ}	3.82 (d, 10.2, 2H)	3.92 (s, 3H)
H ₃ -6 ^{ˆˆˆ}	1.14 (d, 6.2, 3H)	1.12 (d, 6.3,3H)

Table 3.3.10: ¹³C NMR (150 MHz, CD₃OD) for the flavonoid glycosides rutin (**52**) and methoxy rutin (**83**)

Position	Chemical Shift δ (ppm)				
	52	83		52	83
2	159.5	156.9	6 ^ˆ	123.7	120.3
3	135.7	132.0	1 ^{ˆˆ}	104.8	103.1
4	179.5	178.8	2 ^{ˆˆ}	75.9	75.9
5	163.2	160.6	3 ^{ˆˆ}	71.5	72.3
6	100.0	98.7	4 ^{ˆˆ}	77.4	76.7
7	166.2	166.3	5 ^{ˆˆ}	78.3	76.0
8	95.0	93.6	6 ^{ˆˆ}	68.7	67.1
9	158.5	157.8	1 ^{ˆˆˆ}	102.5	100.9
10	105.7	104.6	2 ^{ˆˆˆ}	72.2	72.2
1 ^ˆ	123.2	124.3	3 ^{ˆˆˆ}	72.4	72.3
2 ^ˆ	117.8	114.9	4 ^{ˆˆˆ}	74.1	74.2
3 ^ˆ	146.0	147.5	5 ^{ˆˆˆ}	69.8	68.4
4 ^ˆ	150.4	150.4	6 ^{ˆˆˆ}	18.0	16.8
5 ^ˆ	116.2	116.3			

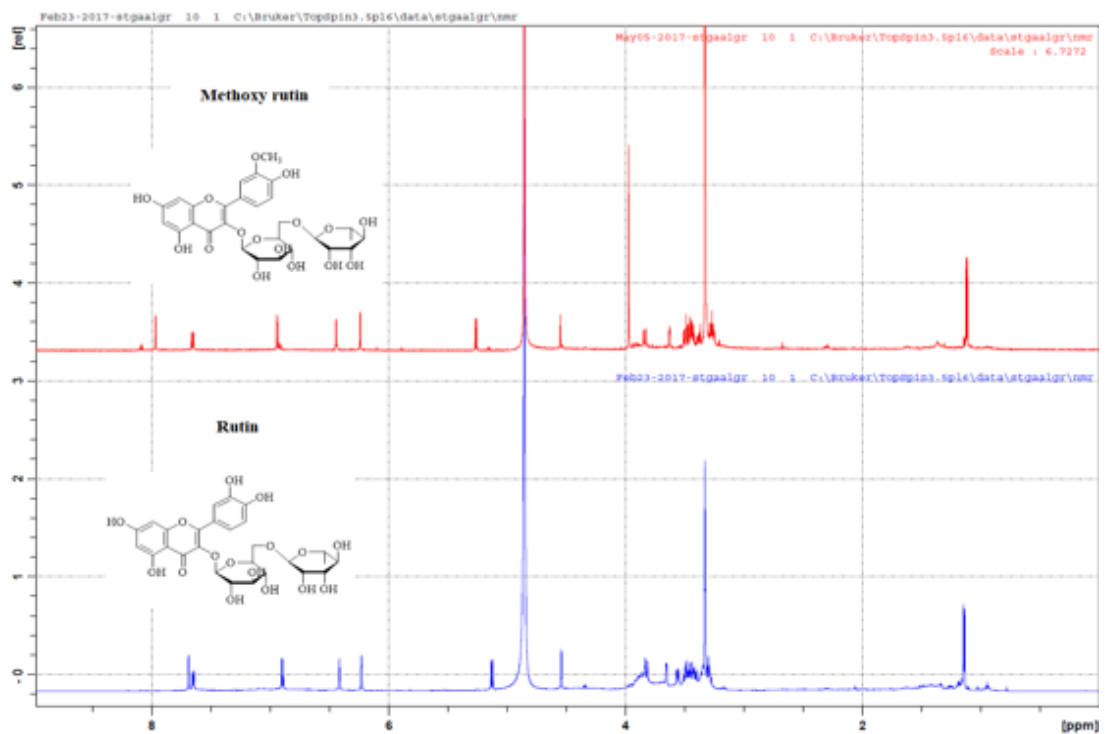


Figure 3.3.34: ^1H NMR spectrum (600 MHz, CD_3OD) of methoxy rutin (83) compared with rutin (52)

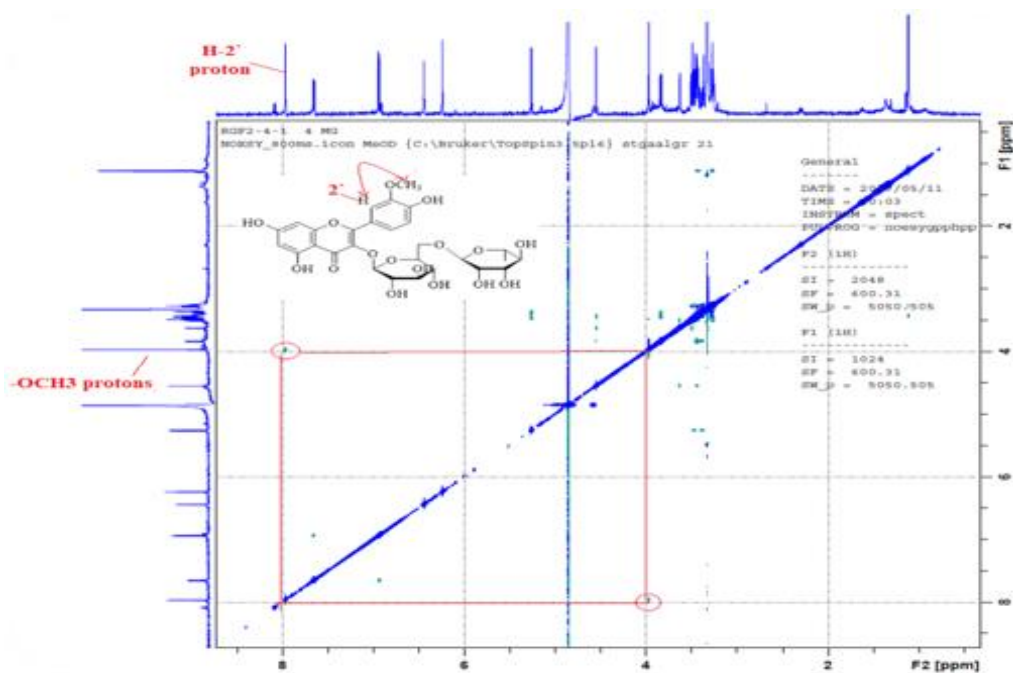


Figure 3.3.35: NOESY spectrum (600 MHz, CD_3OD) of methoxy rutin (83)

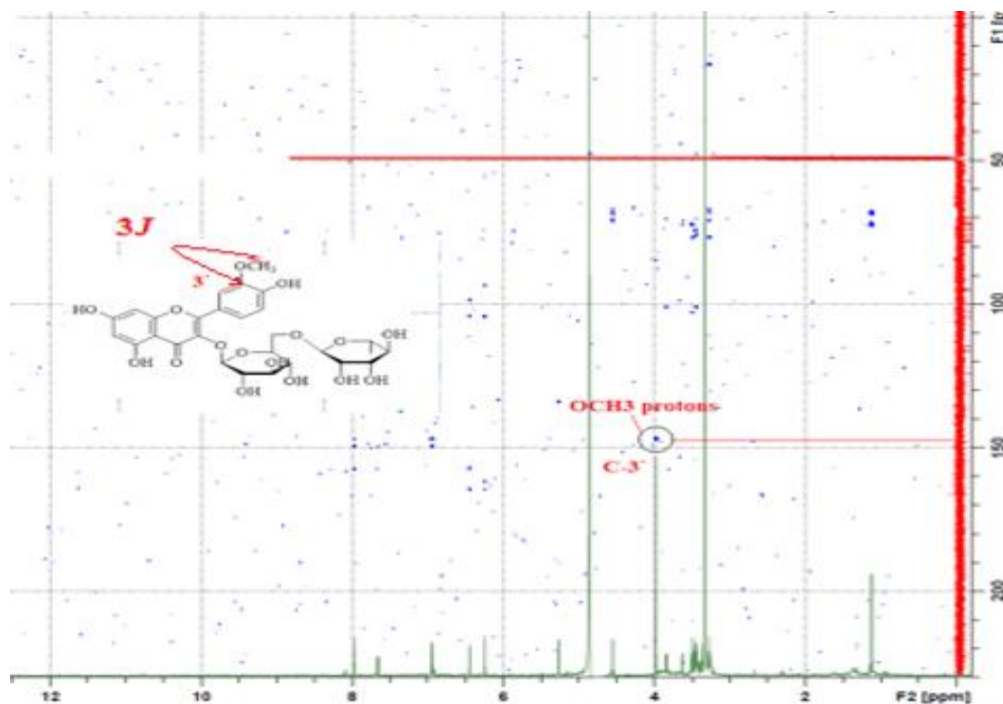


Figure 3.3.36: HMBC correlation of methoxy rutin (**83**)

3.3.8.2 Characterization of disinapoylsucrose

Characterization of RCMF2-2-2 as 3'', 6''-disinapoylsucrose (84)

White amorphous powder. The ESIMS m/z showed a peak at: 753 $[M-H]^-$, indicating that the molecular formula could be $C_{34}H_{42}O_{19}$; 1H NMR (600 MHz, CD_3OD); (Figure 3.4.38) showed two singlet peaks at δ_H 3.90 (3H x2, s, $-OCH_3$) assigning to four methoxy groups, doublets at δ_H 7.69 (1H, d, $J = 15.7$ Hz), δ_H 7.61 (1H, d, $J = 16.3$ Hz), δ_H 6.49 (1H, d, $J = 16$ Hz) and δ_H 6.47 (1H, d, $J = 16.6$ Hz), assigning to four trans protons $-CH=CH-$, two aromatic singlet peaks at δ_H 6.95 (s, 1H) and δ_H 6.91 (s, 1H). The 1H NMR spectrum also showed an anomeric proton of d-glucose at δ_H 5.52 (1 H, d, $J = 4.8$ Hz, H-1'') and 5.54 (1 H, dd, $J = 8.0$ Hz, H-4'') assigning for sucrose. All these data indicated that this compound is sinapoyl glycosides. The ^{13}C NMR (150 MHz, CD_3OD) (Figure 3.3.39) confirmed the

structure where it showed 34 carbon signals including two carbonyl carbons at δ_C 169.2 and δ_C 168.4 assigned for C-9 in both I and II moieties. The HMBC correlations (Figure 3.3.40) performed for the first time on compound **3**. It showed indirect correlations from H6' \rightarrow C-9 (3J) and H5' \rightarrow C-9 (4J) confirmed the skeleton structure of compound **84** (Figure 3.3.37). All data were comparable to the published data (Chen *et al.*, 2001; Wu *et al.*, 2014, Jin *et al.*, 2016).

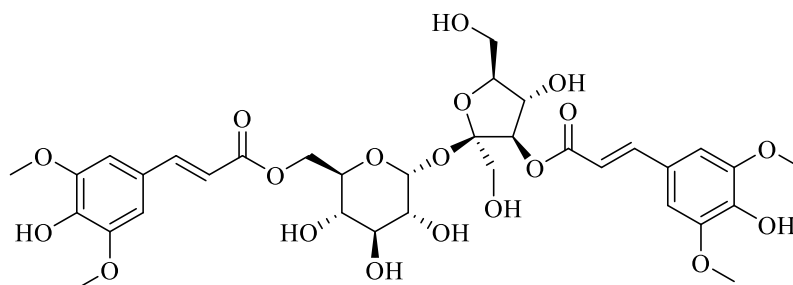


Figure 3.3.37: Structure of 3'', 6''-disinapoylsucrose (**84**)

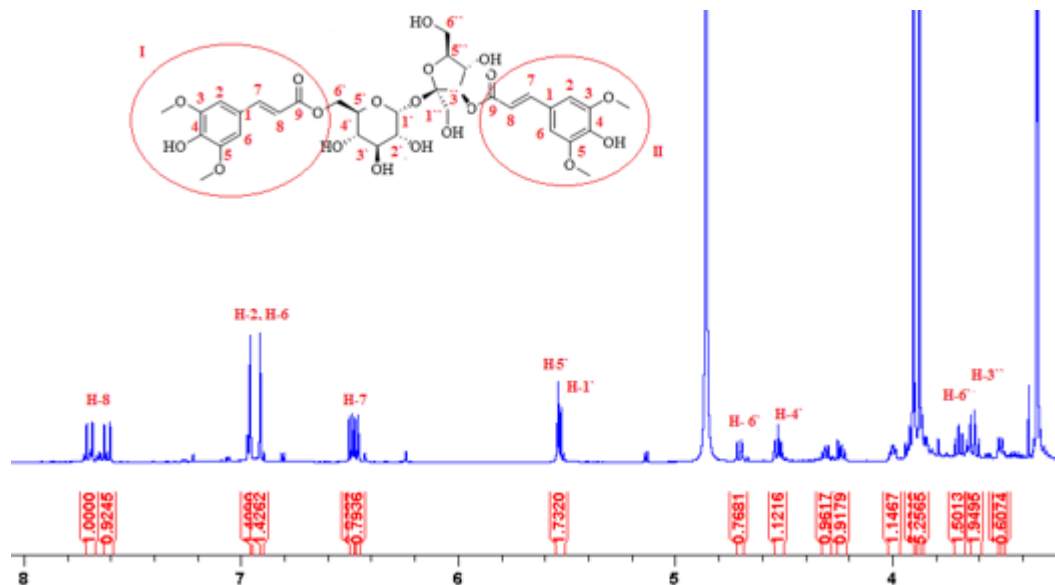


Figure 3.3.38: ^1H NMR spectrum (600 MHz, CD_3OD) of 3'', 6''-disinapoylsucrose (**84**)

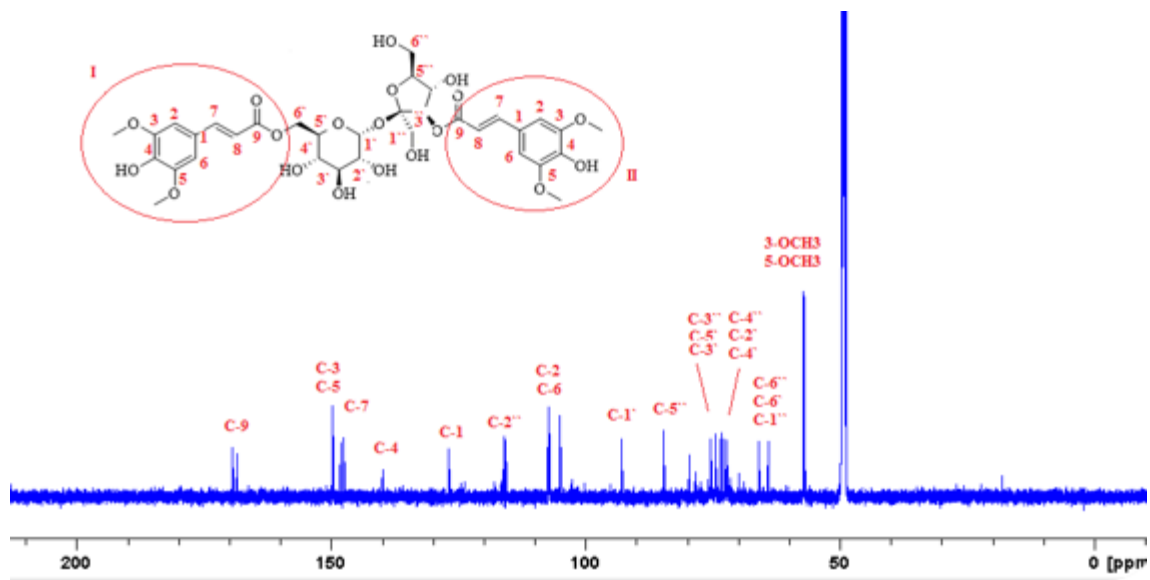


Figure 3.3.39: ^{13}C NMR spectrum (150 MHz, CD_3OD) of 3'', 6''-disinapoylsucrose (84)

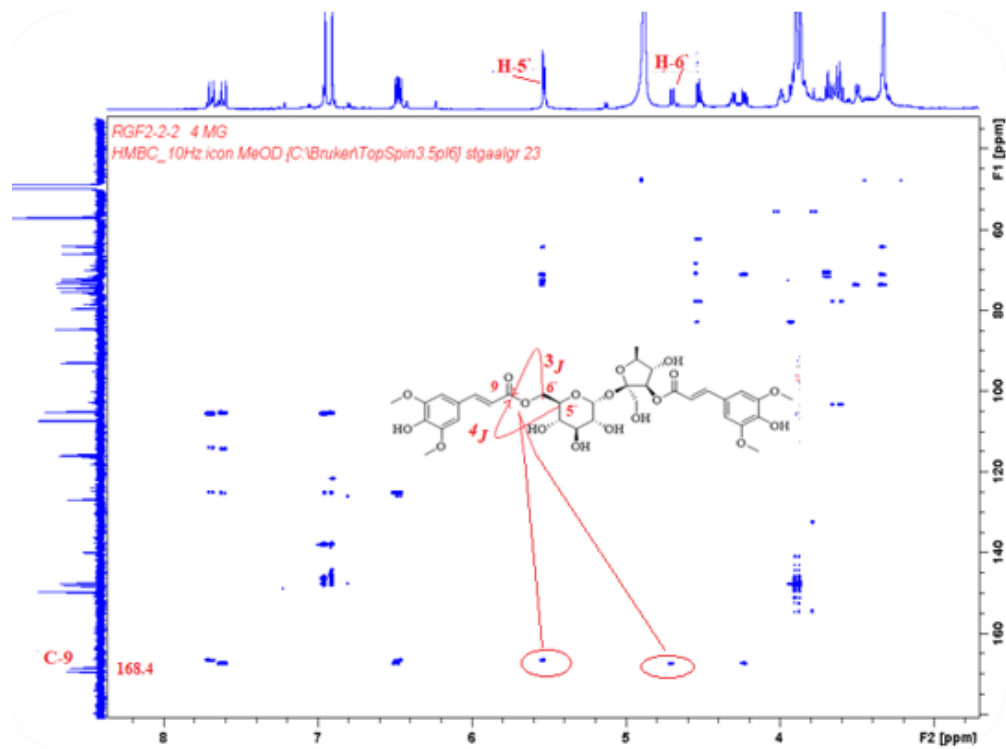


Figure 3.3.40: HMBC correlation of 3'', 6''-disinapoylsucrose (84)

3.3.8.3 Characterization of coumarins

Characterization of RCHF7-7, RCHF7-C, RCH 50%-3, RCH 40% 3-3, and RCDF7-9-2 as bergapten (**63**)

Yellow powder; The ESIMS m/z of this compound showed a molecular ion peak at 215 $[M+H]^+$ indicating the molecular formula $C_{12}H_8O_4$, which was supported by 12 carbon signals in the ^{13}C NMR (600 MHz, $CDCl_3$) Table (3.3.11). Also the appearance of six signal peaks corresponding to six aromatic carbon atoms (between δ_C 93.9 to 159.6 ppm), four olefinic carbon atoms at δ_C 112.0 (C-3) and δ_C 139.2 (C-4), carbonyl group at δ_C 161.5 (C-2) may indicate that this compound is coumarin. 1H NMR spectrum (600 MHz, $CDCl_3$) Table (3.4.12) and Figure (3.3.41) showed coumarin proton signals at δ_H 7.59 (d, $J = 2.4$, 1H, H-2'), δ_H 7.01 (d, $J = 2.4$, 1H, H-3'), δ_H 6.28 (d, $J = 9.8$, 1H, H-3) and δ_H 8.16 (d, $J = 9.8$, 1H, H-4), one aromatic proton signal at δ_H 7.13 (1H, s, H-8), one proton signals at δ_H 4.27 (3H, s, $-OCH_3$). All data confirmed this compound as bergapten **63** (Figure 1.9) and were comparable to the published data (Wu *et al.*, 2003; Chunyan *et al.*, 2008).

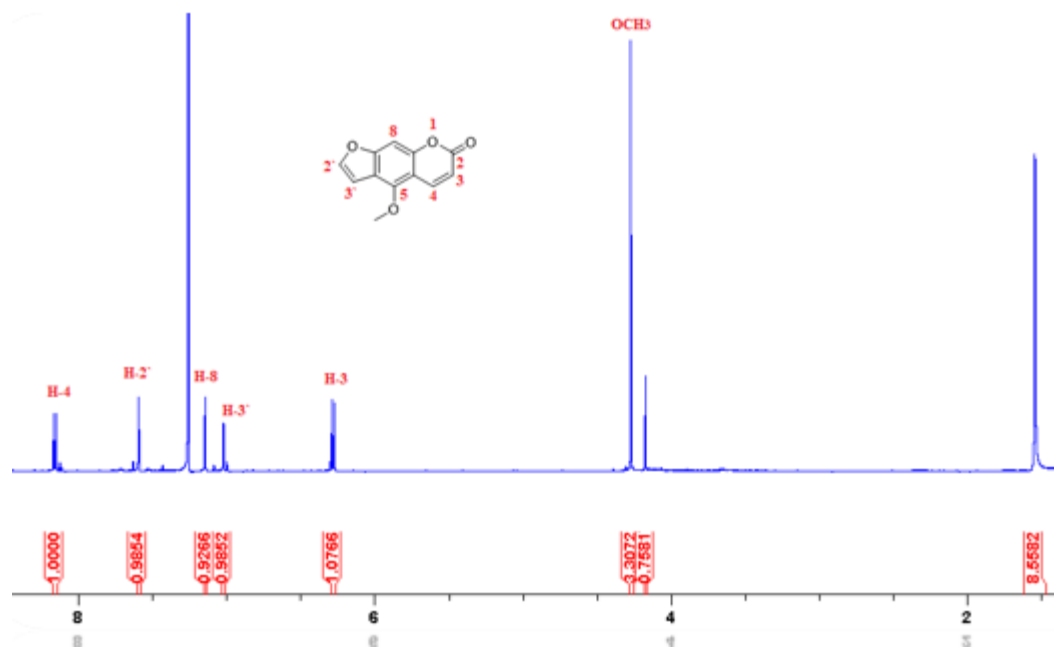


Figure 3.3.41: ¹H NMR spectrum (600 MHz, CDCl₃) of bergapten (**63**)

Characterization of RCMF3-4, RCDF7-12, RCDF6-2, RCHF4-2, RCHF50%-10, RCHF 60%-5 as chalepin (**64**)

White crystals; UV (MeOH) λ_{\max} : 207, and 332 nm, the ESIMS m/z of this compound showed a molecular ion peak at 315 [M+H]⁺ indicating the molecular formula C₁₉H₂₂O₄. ¹H NMR (600 MHz, CDCl₃); Table (3.4.10) and (Figure 3.3.42) showed characteristic peaks for chalepin, which include two aromatic singlets at δ_H 7.19 and 7.48 assigning for H-4 and H-9, respectively, a singlet at δ_H 6.71 assigned for H-5, one multiplet at δ_H 3.20 for H-3, a triplet assigned for H-2 at δ_H 4.71 ($J = 9.0$ Hz) and two doublet of doublets at δ_H 6.17 (dd; $J = 11.0$ Hz, $J = 17.4$ Hz) and δ_H 5.08 (dd, $J = 3.5$ Hz, $J = 10.6$ Hz) assigning for H-4' and H-5', respectively. ¹³C NMR (600 MHz, CDCl₃) Table 3.3.12 confirmed the structure, which showed 19 carbon signals including four methyls at δ_C 24.2, 26.1 and 25.4, a carbonyl carbon at δ_C 159.5 (C-7), two peaks at δ_C 145.8 and δ_C 112.1 assigned

for H-4' and H-5', respectively. All data confirmed this compound as chalepin (**64**) (Figure 1.9) and were comparable to the published data (Richardson *et al.*, 2016).

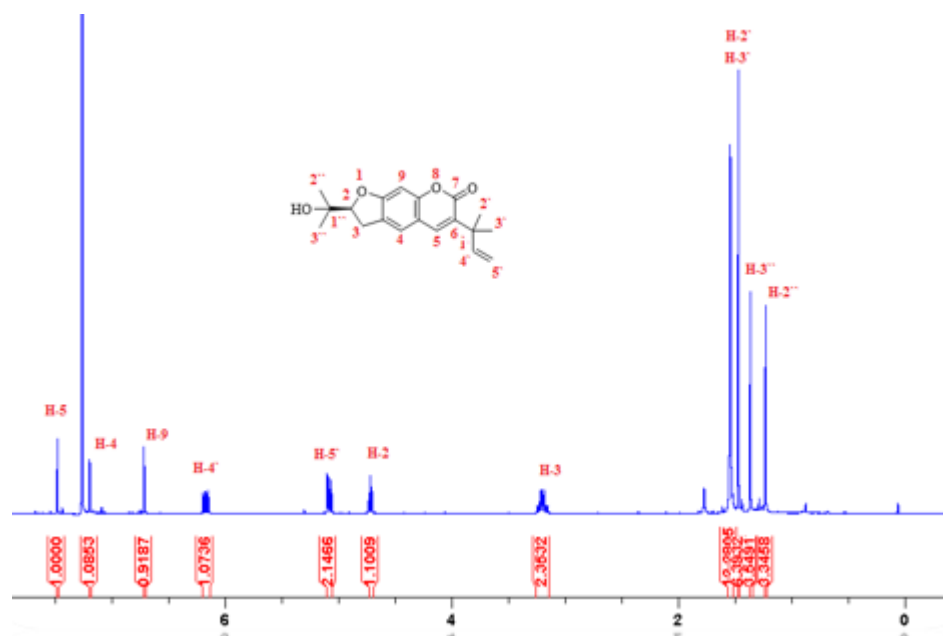


Figure 3.3.42: ^1H NMR spectrum (600 MHz, CDCl_3) of chalepin (**64**)

Characterization of RCDF5, RCDF6-1, and RCHF60%-4 as chalepnsin (**65**)

White crystals; UV (MeOH) λ_{max} : 268, and 320 nm, ESIMS m/z showed a molecular ion peak at 255 $[\text{M}+\text{H}]^+$, indicating the molecular formula $\text{C}_{16}\text{H}_{14}\text{O}_3$. ^1H NMR (600 MHz, CD_3OD); (Tables 3.4.11) and (Figure 3.3.43) showed two aromatic single protons at δ_{H} 6.94 (H-5) and δ_{H} 7.46 (H-8) and one olefinic singlet at δ_{H} 7.92 (H-4), two multiplets at δ_{H} 6.22 (H-12) and δ_{H} 5.10 (H-13), two broad singlets at δ_{H} 7.86 and δ_{H} 4.89 assigned for H-2' and H-3' and one large singlet at δ_{H} 1.51 (6H) assigning for two methyl groups. All these protons data indicated that this compound might be the coumarin chalepnsin **65** (Figure 1.9). The 16 carbon atoms shown in ^{13}C NMR (150 MHz, CD_3OD) Table (3.3.12)

confirmed the structure, which includes two methyls at δ_C 27.0 (C-14 and C-15), a carbonyl carbon at δ_C 162.0 (C-2), two peaks at δ_C 146.9 and δ_C 112.8 assigned for C-12 and C-13, respectively. NOESY experiment (Figure 3.3.44) performed for the first time on chalepnin confirmed also the close correlation between the unbonded protons H-12 and H-13 \leftrightarrow CH₃ protons in space. All data were comparable to the published data (Wu *et al.*, 2003).

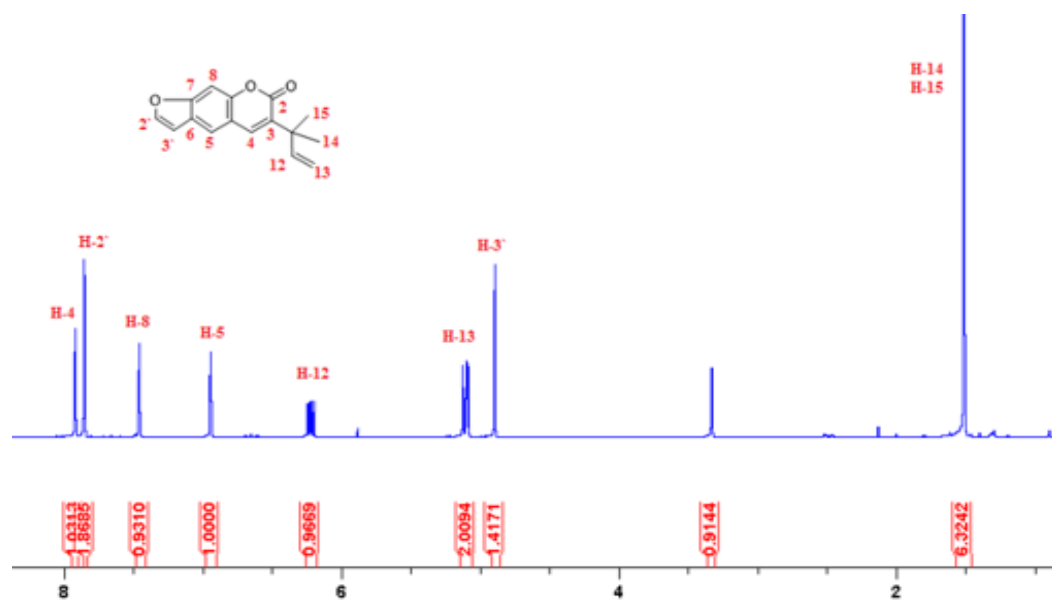


Figure 3.3.43: ¹H NMR spectrum (600 MHz, CD₃OD) of chalepnin (**65**)

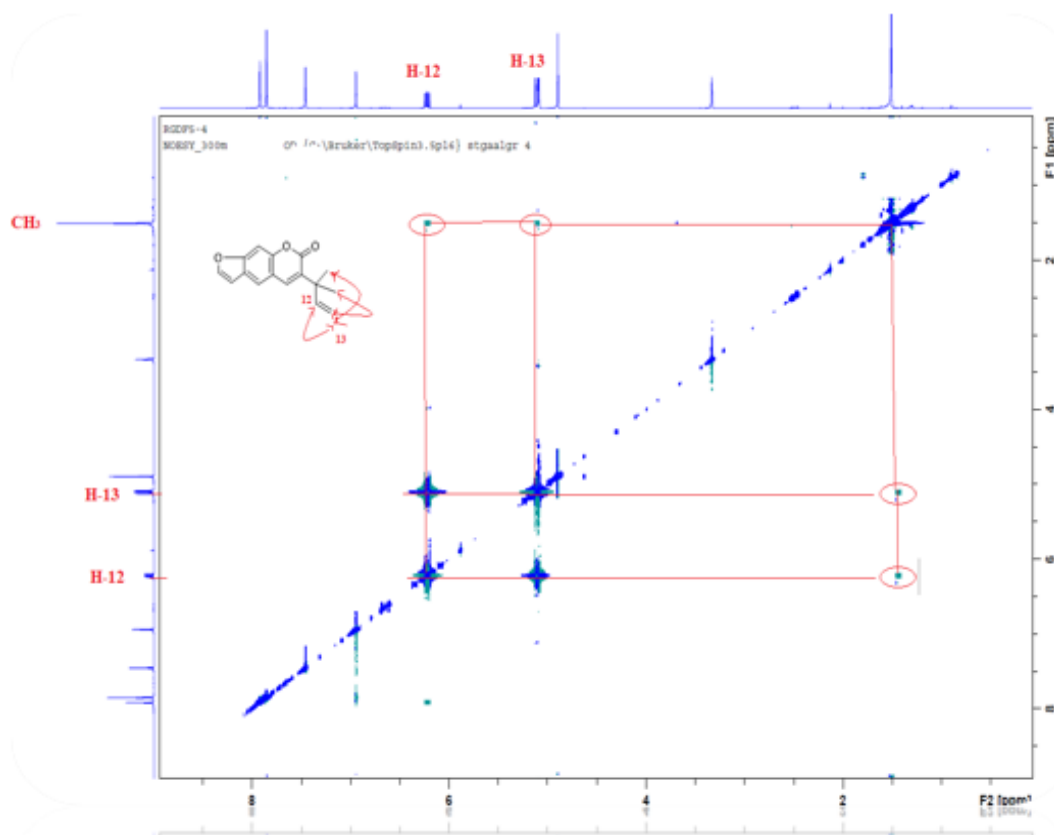


Figure 3.3.44: NOESY spectrum (600 MHz, CD₃OD) of chalepinsin (**65**)

Table 3.3.11: ¹H NMR (600 MHz) of the coumarins: bergapten (**63**), chalepin (**64**) and chalepinsin (**65**)

Position	Chemical Shift δ (ppm), multiplicity and J in Hz		
	63*	64*	65**
2		4.71, t, 9	
3	6.28, d, 9.8, 1H	3.20, m	
4	8.16, d, 9.8, 1H	7.19, s	7.92, s
5	----	7.48, s	6.94, s
5 -OCH ₃	4.27, s, 3H	----	
8	7.13, s, 1H	-----	7.46, s
9	-----	6.71, s	
12			6.22, m

13			5.10, m
14-CH ₃ , 15-CH ₃			1.51, s, 6H
2 [^]	7.59, d, 2.4, 1H	-----	7.86, br s
3 [^]	7.01, d, 2.4, 1H	-----	4.89, br s
4 [^]		6.17, dd; 11.0, 17.4	
5 [^]		5.08, dd; 3.54, 10.56	

*= (CDCl₃), **= (CD₃OD)

Table 3.3.12: ¹³CNMR (150 MHz) of the coumarins: bergapten (**63**), chalepin (**64**) and chalepensis (**65**)

Position	Chemical Shift δ (ppm)			Position	Chemical Shift δ (ppm)		
	63*	64*	65**		63*	64*	65**
2	161.5	90.9	162.0	13			112.8
3	112.0	29.6	133.9	14			27.0
4	139.2	123.2	140.7	15			27.0
5	149.5	138.0	121.5	2 [^]	144.8	25.1	146.9
6	119.1	132.2	126.5	3 [^]	105.0	25.1	107.7
7	159.6	159.5	157.5	4 [^]		145.8	
8	93.9		107.7	5 [^]		112.1	
8 a		154.8		1 ^{^^}		71.8	
9	151.5	97.2	152.6	2 ^{^^}		24.2	
10	105.7	162.4	117.5	3 ^{^^}		26.1	
11		154.8	41.5	5 (O-CH3)	60.1		
12			146.9				

*= (CDCl₃), **= (CD₃OD)

3.3.8.4 Characterization of alkaloids

Characterization of RCMF3-2-2 and RCH 80%-3 as kokusaginine (61)

Yellow powder; ESIMS m/z showed a molecular ion peak at 260 $[M+H]^+$ indicated the molecular formula $C_{14}H_{13}NO_4$. Signals of the 1H NMR (600 MHz, $CDCl_3$); Table (3.4.13) and (Figure 3.3.45) at δ_H 4.0 (6H, s) and at δ_H 4.40 (3H, s) can be assigned clearly to -OCH₃-6, OCH₃-7 and OCH₃-4, respectively. The 1H NMR spectrum also showed signals of two aromatic protons at δ_H 7.49 and δ_H 7.34 assigning for H-5 and H-8, two methine protons at δ_H 7.57 (d, $J = 2.7$ Hz, 1H) assigned for H-1' and δ_H 7.19 (d, $J = 2.7$ Hz, 1H) assigned for H-2'. The ^{13}C NMR (150 MHz, CD_3OD) (Figure 3.3.46 and Table 3.4.14) confirmed the methoxy peaks at δ_C 58.9, 56.0 and 56.1 assigning for 4-OCH₃, 6-OCH₃ and 7-OCH₃, respectively, the two olefinic methine carbons at δ_C 104.6, and 142.6, which assigned for C-1' and C-2', respectively. All these data confirmed the identity of compound **61** as kokusaginine (Figure 1.9). All data were comparable to the published data for kokusaginine (Wu *et al.*, 2003).

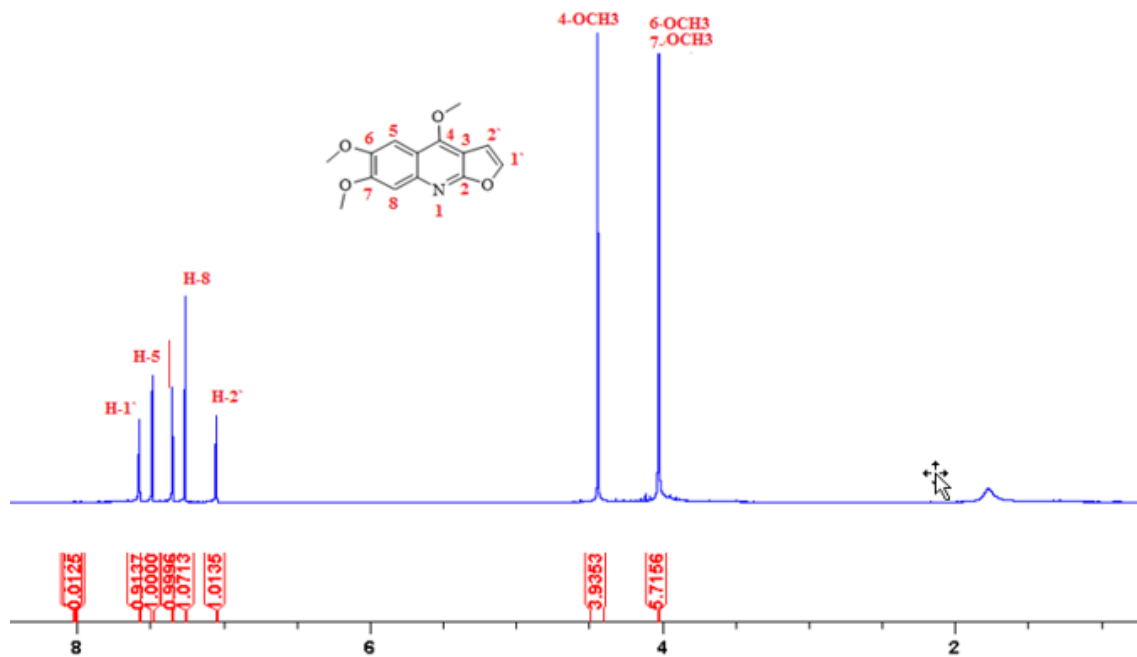


Figure 3.3.45: ¹H NMR spectrum (600 MHz, CDCl₃) of kokusagine (**61**)

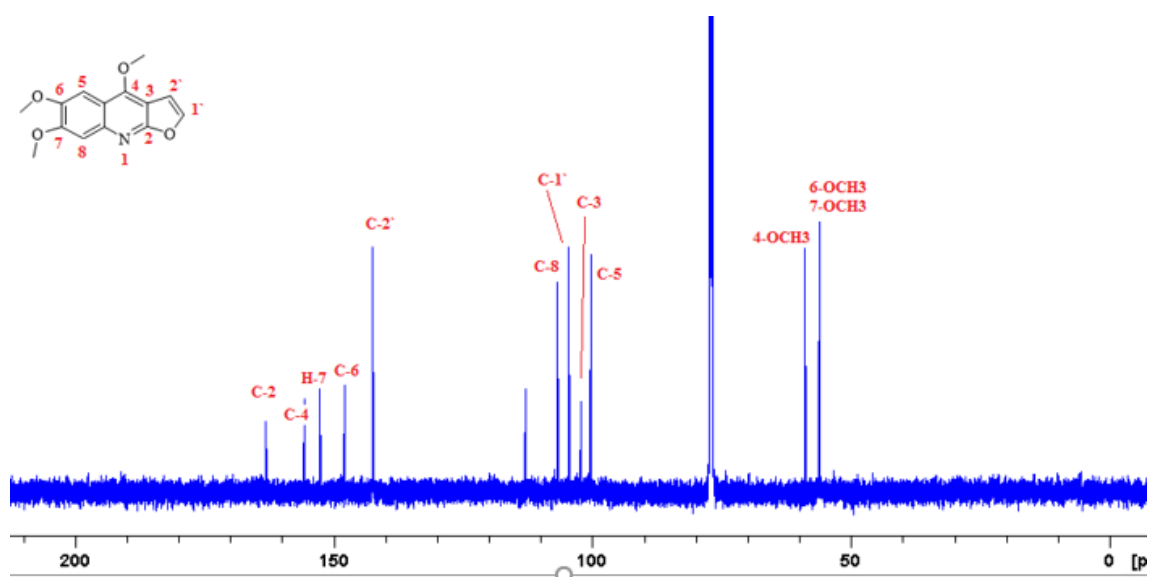


Figure 3.3.46: ¹³C NMR spectrum (150 MHz, CDCl₃) of kokusagine (**61**)

Characterization of RCMF3-1 as graveoline (60)

Yellow powder; ESIMS m/z showed a molecular ion peak at 280 $[M+H]^+$ indicating the molecular formula $C_{17}H_{13}NO_3$. 1H NMR (600 MHz, CD_3COCD_3): (Table 3.4.13 and Figure 3.3.47) showed two *ortho*-*meta* coupling at δ_H 7.10 (ddd, $J = 2.8, J = 1.6, J = 10.5$, 1H) and δ_H 7.84, dd, $J = 5.8, J = 1.3$, 1H, two *ortho*-couplings at δ_H 7.48 (t, $J = 6.8$, 1H) and at δ_H 8.39 (d, $J = 8.6$, 1H), one aromatic singlet at 6.21 assigned for H-3 and N- CH_3 protons at 3.77, a singlet at 6.19 assigning for O- CH_2 -O protons. The ^{13}C NMR (150 MHz, CD_3COCD_3) (Table 3.4.14 and Figure 3.3.48) showed 17 carbon signals including carbonyl carbon at δ_C 182.0 (C-4) and δ_C 101.9 assigned for O- CH_2 -O carbon. All data were compared to the published data and confirmed that this compound is graveoline (60) (Figure 1.9) (Wu *et al.*, 2003).

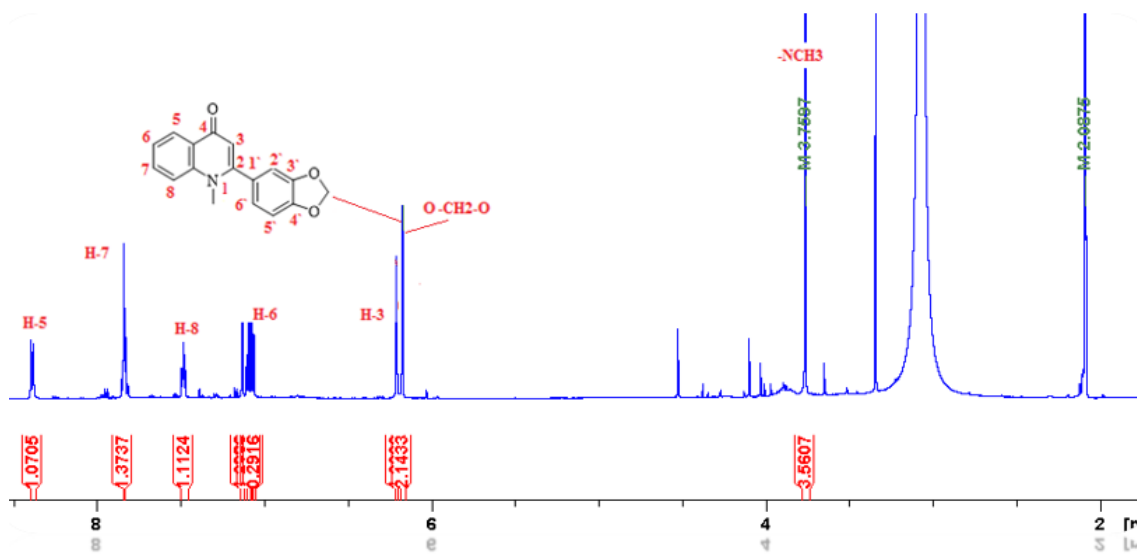


Figure 3.3.47: 1H NMR spectrum 1H NMR (600 MHz, CD_3COCD_3) of graveoline (60)

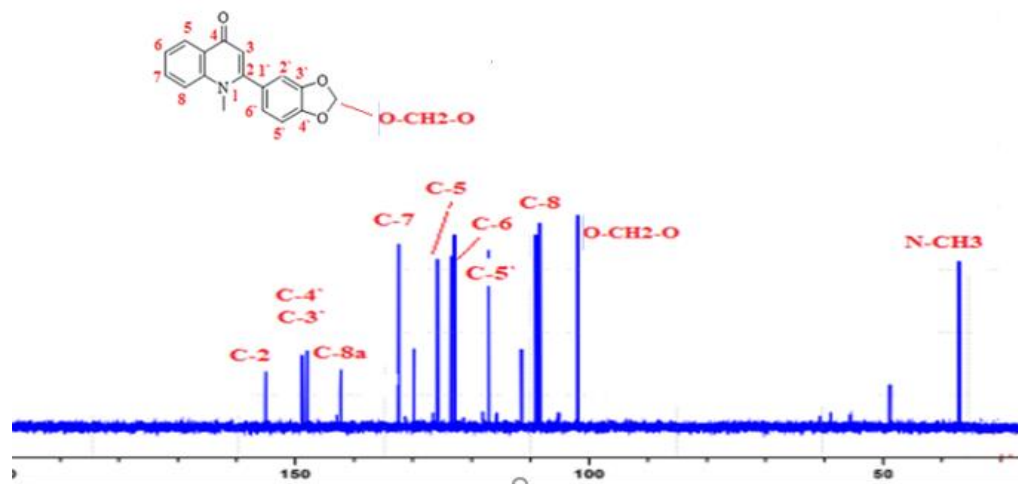


Figure 3.3.48: ^{13}C NMR spectrum (150 MHz, CD_3COCD_3) of graveoline (**60**)

Characterization of RCMF3-6 as 4-hydroxy-2-nonyl-quinoline (85)

Yellow powder; ESIMS m/z showed a molecular ion peak at 272 $[\text{M}+\text{H}]^+$ indicating compound with formula $\text{C}_{18}\text{H}_{25}\text{NO}$. ^1H NMR (600 MHz, MeOD) (Table 3.4.13 and Figure 3.3.50) showed four *ortho* coupled protons at δ_{H} 8.23 (d, $J = 8.4$ Hz, 1H), δ_{H} 7.70 (t, $J = 8.6$ Hz, 1H), δ_{H} 7.41 (t, $J = 7.7$ Hz, 1H) and δ_{H} 7.60 (d, $J = 8.3$ Hz, 1H), one singlet at 6.30 assigned for H-3, two triplets at δ_{H} 2.74 (t, $J = 8.5$ Hz, 2H, H-1') and at δ_{H} 0.91 (t, $J = 6.1$ Hz, 3H, H-9') and multiplet at δ_{H} 1.79, 2H, H-2'). The ^{13}C NMR (150 MHz, CD_3COCD_3) (Figure 3.3.51 and Table 3.4.14) showed 18 carbon signals including six aromatic carbons. All data were compared to the published data and confirmed that this compound is 4-hydroxy-2-nonyl-quinoline (Figure 3.3.49) (Royt *et al.*, 2001).

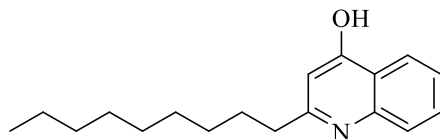


Figure 3.3.49: Structure of 4-hydroxy-2-nonyl-quinoline (**85**)

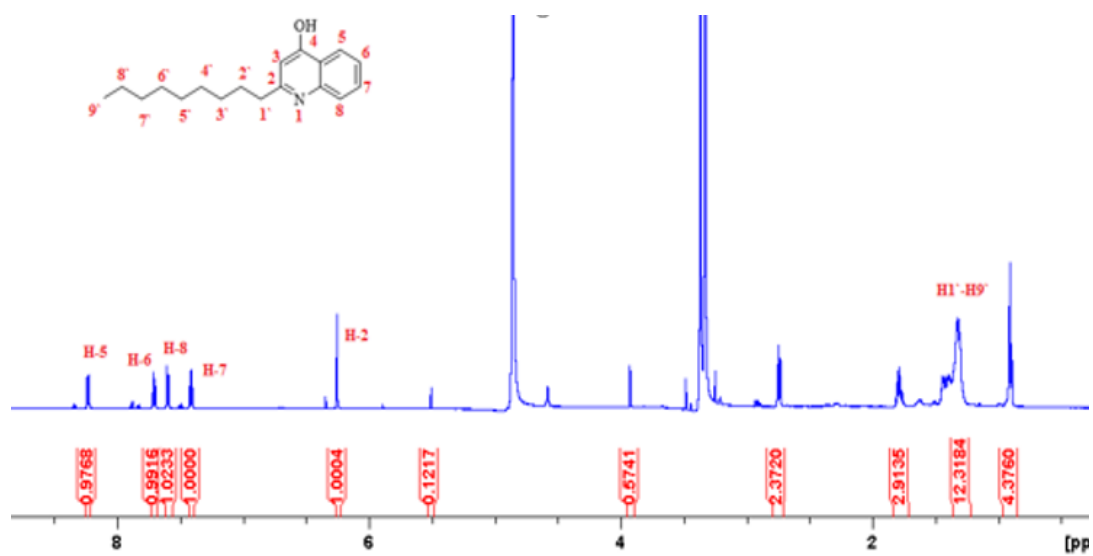


Figure 3.3.50: ^1H NMR spectrum of 4-hydroxy-2-nonyl-quinoline (85)

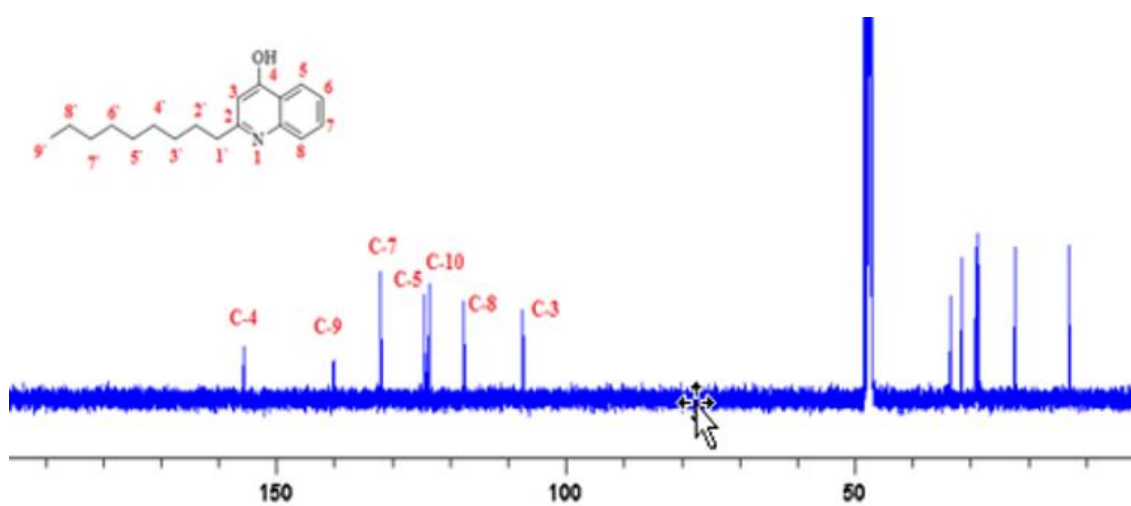


Figure 3.3.51: ^{13}C NMR spectrum of 4-hydroxy-2-nonyl-quinoline (85)

Table 3.3.13: ^1H NMR spectrum (600 MHz, CDCl_3) for alkaloids: kokusaginine (**61**), Graveoline (**60**), 4-hydroxy-2-nonyl-quinoline (**85**)

Position	Chemical Shift δ (ppm), multiplicity and J in Hz		
	61**	60 *	85**
^1H			
3		6.21, s, 1H	6.3, s, 1H
4-OCH ₃	4.40, s, 3H		
5	7.49, s	8.39, d, $J= 8.6$, 1H	8.23, d, 8.4, 1H
6	4.0, s, 6H, -OCH ₃	7.10, ddd; 2.8, 1.6, 10.5, 1H	7.70, t, 8.6, 1H
7	4.0, s, 6H, -OCH ₃	7.84, dd; 5.8, 1.3, 1H	7.41, t, 7.7, 1H
8	7.34, s	7.48, t, $J= 6.8$, 1H	7.60, d, 8.3, 1H
1`	7.57, d, 2.7, 1H		2.74, t, 8.5, 2H
2`	7.19, d, 2.7, 1H	7.11, s, 1H	1.79, m, 2H
9`			0.91, t, 6.1, 3H
N-CH ₃		3.77, s, 3H	
O-CH ₂ -O		6.19, s, 2H	

*= (CD_3COCD_3), **= (CD_3OD)

Table 3.3.14: ^{13}C NMR (chemical shift) for alkaloids: kokusaginine (**61**), graveoline (**60**), 4-hydroxy-2-nonyl-quinoline (**85**) (CD_3OD)

^{13}C	Chemical Shift δ (ppm),			^{13}C	Chemical Shift δ (ppm),		
	61 **	60 *	85 **		61 **	60 *	85 **
1-N-CH3		29.6		2'	142.6	101.9	28.7
2	163.1	155.0	155.8	3'			29.2
3	102.3		107.4	4'		111.5	29.2
4	155.6	182.0	155.8	5'		126.5	29.2
5	100.3	125.8	125.1	6'		122.9	29.0
6	147.9	123.5	123.7	7'		111.5	31.2
7	152.7	132.4	132.0	8'			22.3
8	106.8	108.4	117.7	9'			13.0
9			140.2	4-OCH3	58.9		
10			124.6	6-OCH3	56.0		
1'	104.6		33.6	7-OCH3	56.1		

*= (CD_3COCD_3), **= (CD_3OD)

3.3.8.5 Characterization of alkane

Characterization of RCHF2 crystals as tetradecane (86)

Transparent crystals; ^1H NMR (600 MHz, MeOD); (Figure 3.3.53). MS showed the highest significant peak at m/z : 197 $[\text{M}-\text{H}]^-$. Consequently, the expected molecular weight was 198 attributed to the tetradecane $\text{C}_{14}\text{H}_{30}$ (Figure 3.3.52).



Figure 3.3.52: Structure of tetradecane crystals (**86**)

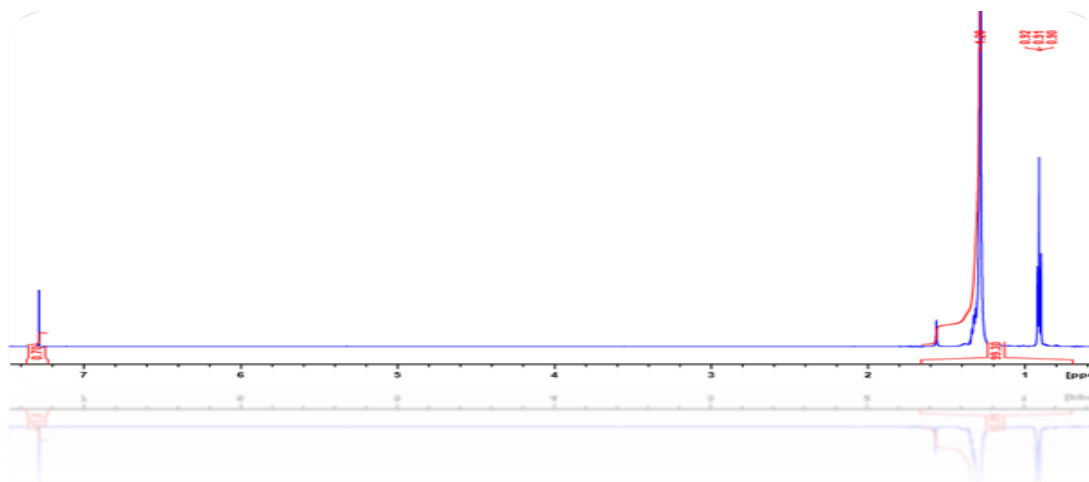


Figure 3.3.53: ^1H NMR spectrum (400 MHz, CDCl_3) of tetradecane crystals (**86**)

3.3.8.6 Characterization of dehydromoskashan derivative

Characterization of RCHF4-3-2 as dehydromoskashan derivative (87)

White powder; ESIMS m/z showed a molecular ion peak at 419 $[\text{M}+\text{H}]^+$ (Figure 3.3.55a) indicating compound with formula $\text{C}_{25}\text{H}_{38}\text{O}_5$ and a peak at 135 (Figure 3.3.55b) indicating the fragment of dehydromoskashan moiety (Ulubelen 1988). ^1H NMR (600 MHz, CDCl_3) (Figure 3.3.56) showed aromatic protons as following: one *ortho* coupling at δ_{H} 6.71 (d, $J = 7.7$ Hz, 1H), one broad singlet δ_{H} 6.68 (s, 1H) and one *ortho-meta* coupling at δ_{H} 6.61 (dd, $J = 1.4$ Hz, $J = 7.8$ Hz, 1H) assigning for H-5, H-3 and H-6, respectively. The ^1H NMR also showed one singlet at δ_{H} 5.90 assigned for O- CH_2 -O (s, 2H), two multiplets at δ_{H} 5.80 (m, 1H) and δ_{H} 5.34 (m, 3H) assigned for H-17' and H-18', respectively. A triplet at δ_{H} 4.05 (t, $J = 6.7$, 4H) assigned for H-13'. The ^{13}C NMR (150 MHz, CDCl_3) (Figure 3.3.57) showed 25 carbon signals including six carbons in the aromatic region (100-150 ppm). The HSQC (Figures 3.3.58) confirmed the attached protons to their carbon atoms; H-3, H-5, H-6 \rightarrow C-3, C-5, C-6 in the aromatic regions. The HMBC (Figures 3.3.59) confirmed the correlation from H-13' \rightarrow C-174.3 (C=O).

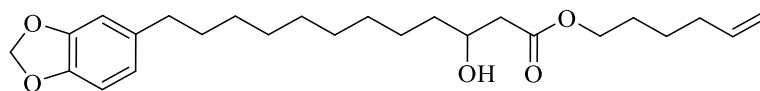


Figure 3.3.54: Structure of dehydromoskashan derivative (**87**)

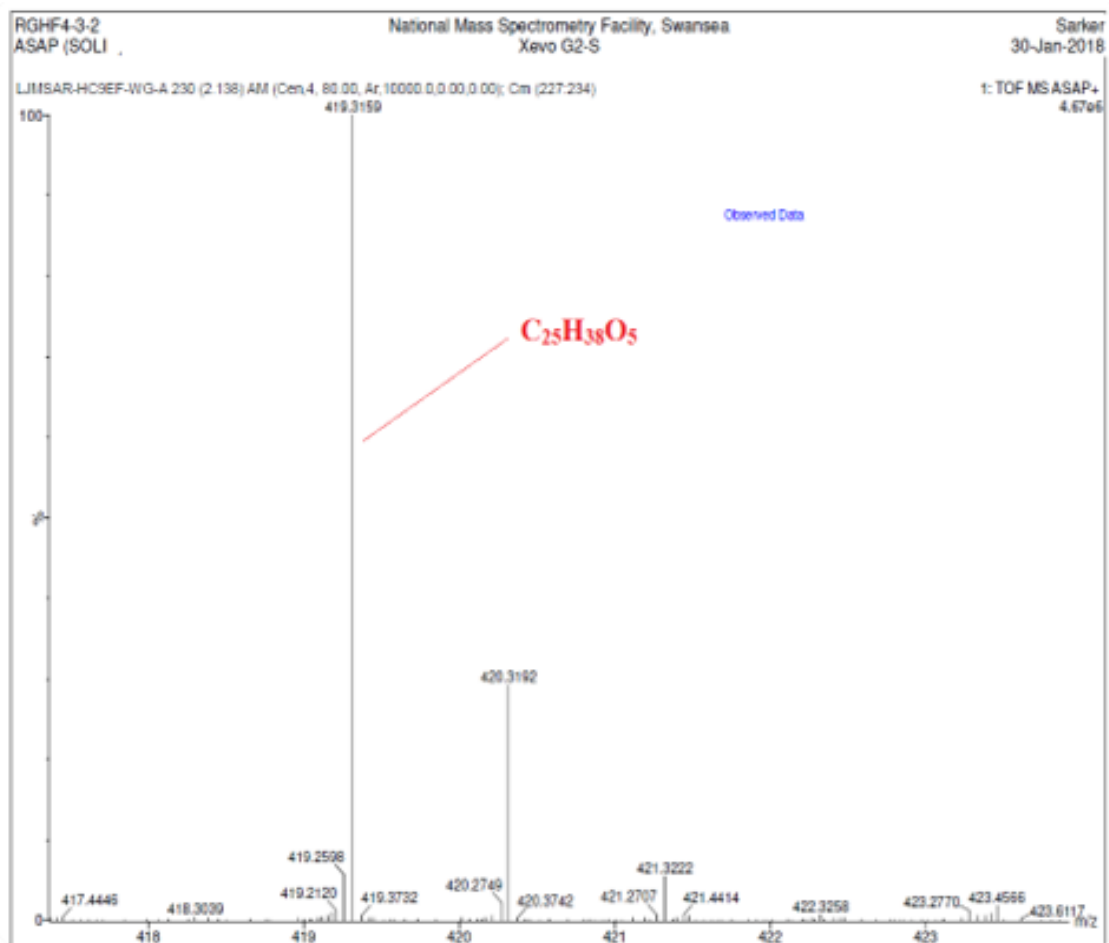


Figure 3.3.55a: MS spectrum (atmospheric solid analysis probe) of dehydromoskashan derivative (**87**)

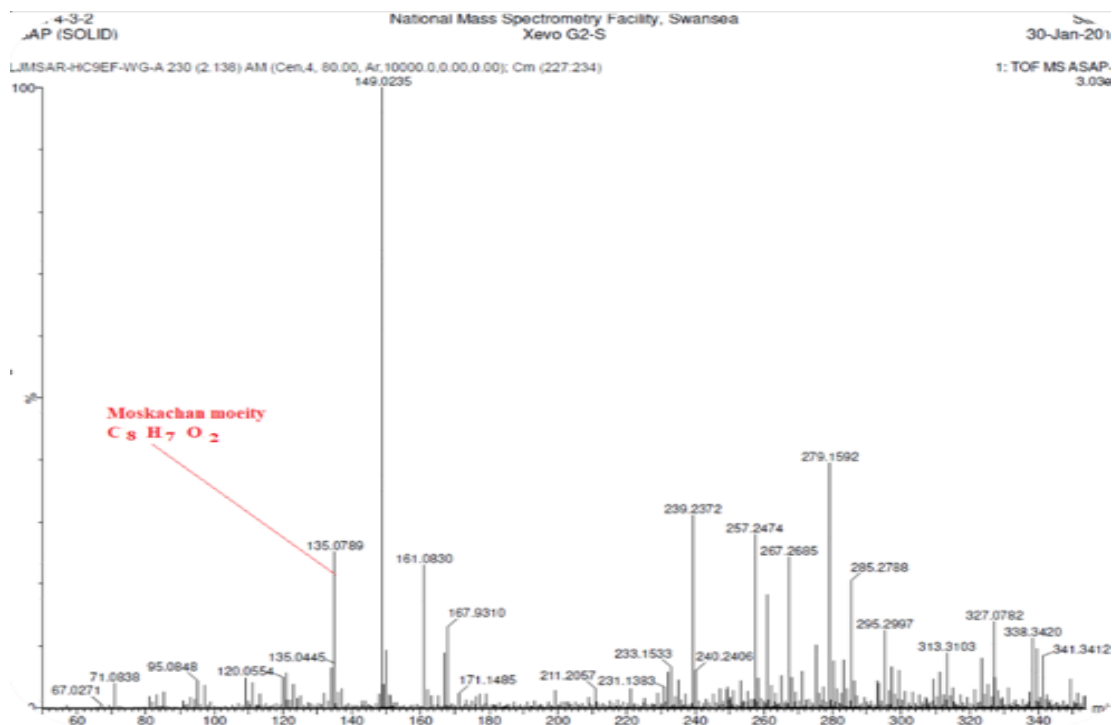


Figure 3.3.55b: MS spectrum (atmospheric solid analysis probe) of dehydromoskachan moiety

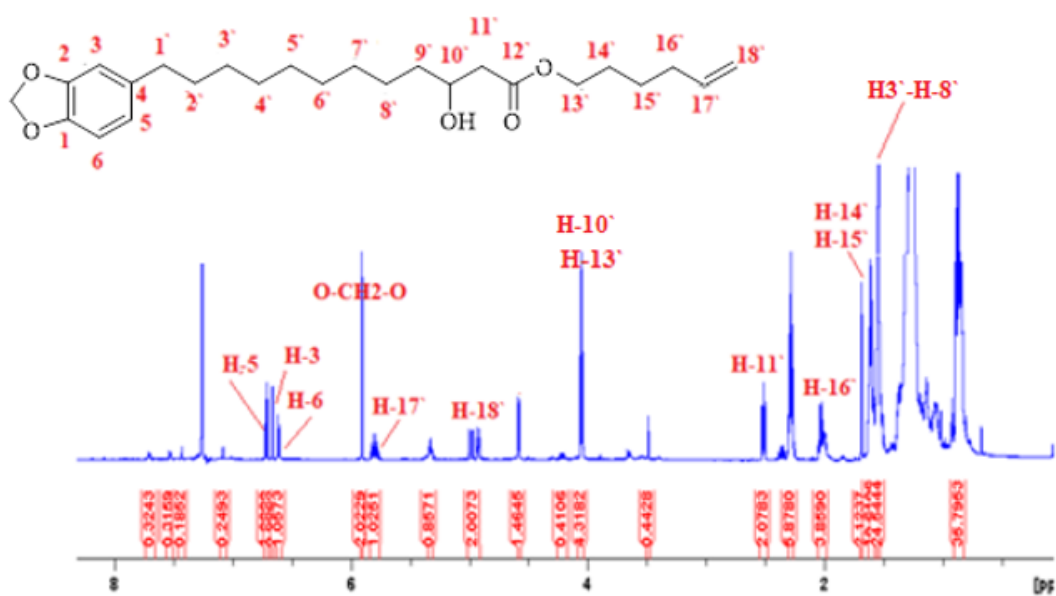


Figure 3.3.56: ^1H NMR spectrum (600 MHz, CDCl_3) of dehydromoskachan derivative (87)

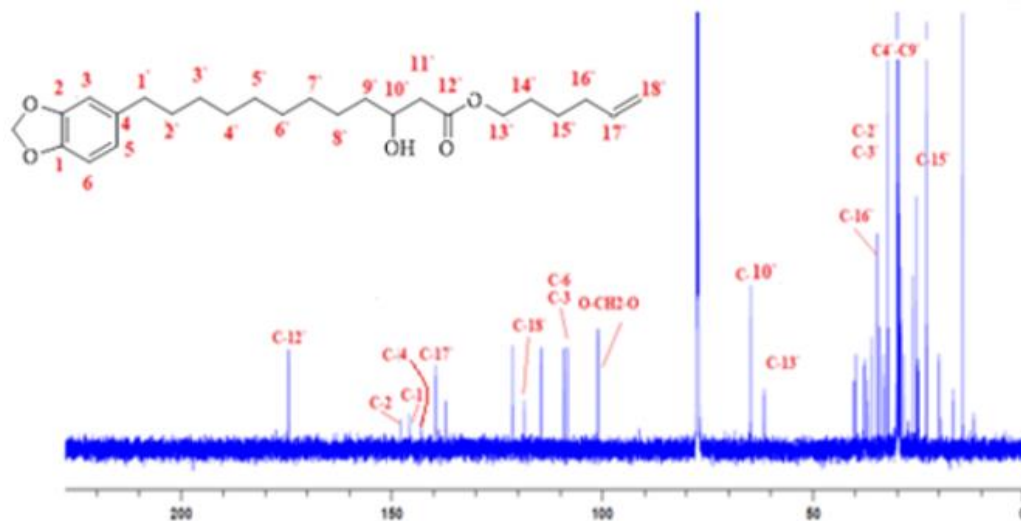


Figure 3.3.57: ^{13}C NMR spectrum (150 MHz, CDCl_3) of dehydromoskachan derivative (87)

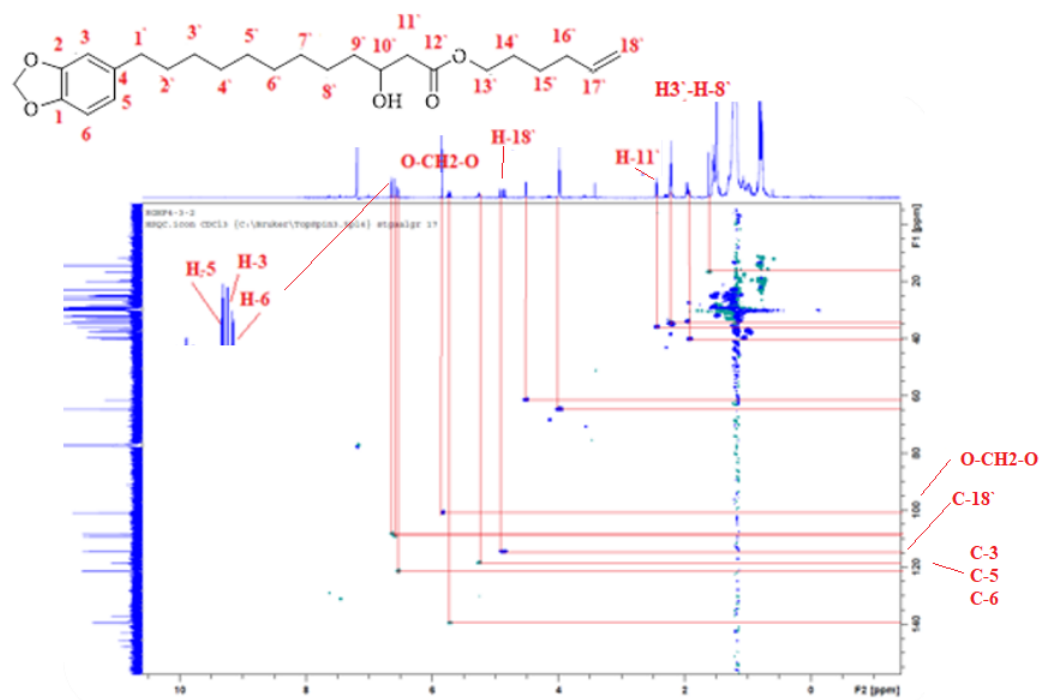


Figure 3.3.58: HSQC spectrum of dehydromoskachan derivatives (87)

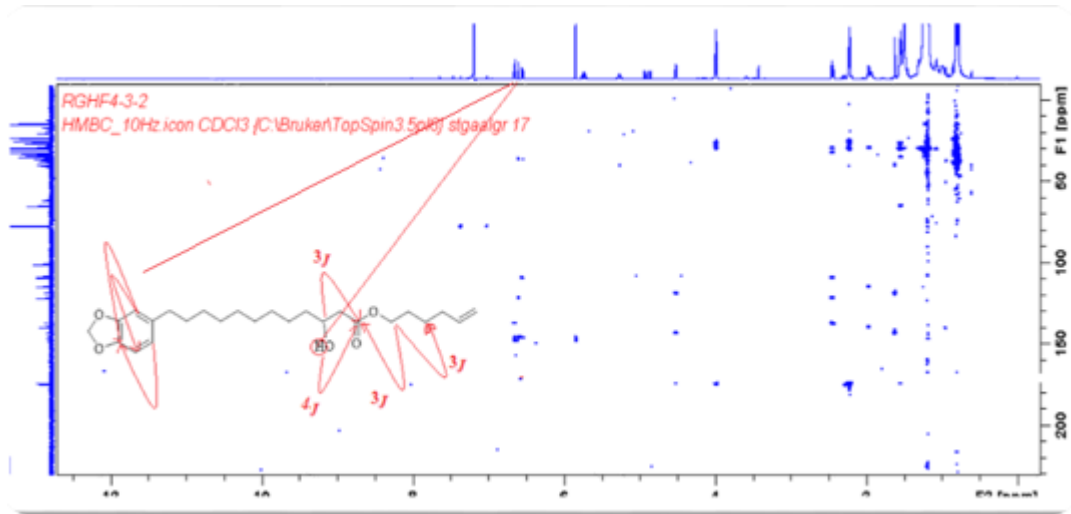


Figure 3.3.59: HMBC spectrum of dehydromoskachan derivative (**87**)

3.3.9 Cytotoxic effect of the isolated compounds from *R. chalepensis* aerial parts

Results presented in Table 3.3.15 and Figures 3.23 -3.24 showed the IC₅₀ values of the isolated compounds from *R. chalepensis* aerial parts compared with the etoposoid standard. The cytotoxicity was observed only in chalepin (**64**) and 4-hydroxy-2-nonyl-quinoline (**85**) against the human lung carcinoma cell lines (A549) with IC₅₀ values of 92 and 97.6 μM, respectively. However, chalepin (**64**) revealed also moderate cytotoxicity against the human urinary bladder cancer cell lines (EJ138) with IC₅₀ value of 117 μM. The structure activity relationship between the furanocoumarins is illustrated in Figure 3.3.63.

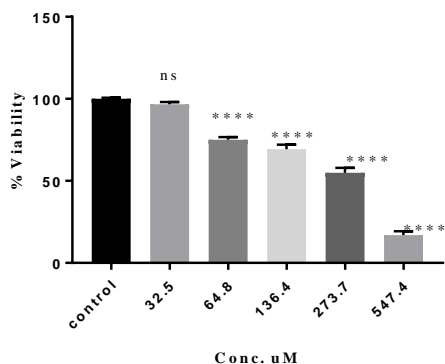
Table 3.3.15: The IC₅₀ (μM) of different isolated compounds from *R. chalepensis* aerial parts on A549 lung cancer cells.

Pure compound	IC ₅₀ μM (HEPG2)	IC ₅₀ μM (A549)	IC ₅₀ μM (E-138)
Rutin (52)	No activity *	No activity *	No activity *
Methoxy rutin (83)	No activity *	No activity *	No activity *
Sinapoyl glycoside (84)	No activity *	NA	NA
Bergapten (63)	No activity *	No activity *	No activity *
Chalepin (64)	No activity *	92 ± 1.47	117±1.58
Chalepensin (65)	No activity *	200±1.61 (48 h)	No activity *
Kokusaginine (61)	No activity *	No activity *	No activity *
Graveoline (60)	No activity *	No activity *	No activity *
4-Hydroxy-2-nonyl-quinoline (85)	No activity *	97.6 ± 1.22	NA
Dehydromoskashan derivatives (87)	Not applied	No activity *	Not applied
Etoposide (78)	NA	61 ± 1.56	NA

*No activity at the highest concentration of 500 μM

NA--- Non-applicable

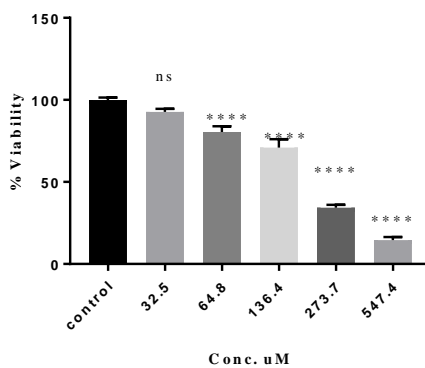
Cytotoxicity of chalepin in EJ138 cells according to the MTT assay



All experiments were carried out in triplicate on separate occasions. Data were expressed as means \pm standard error of the mean derived from $n \geq 12$ from three separate occasions.

Figure 3.3.60: The cytotoxic activity of chalepin (**64**) against EJ138 cells according to the MTT assay

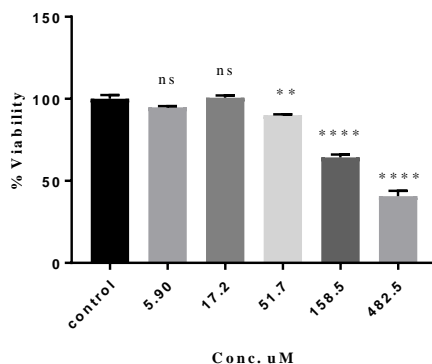
Cytotoxicity of chalepin in A549 cells according to the MTT assay



All experiments were carried out in triplicate on separate occasions. Data were expressed as means \pm standard error of the mean derived from $n \geq 12$ from three separate occasions.

Figure 3.3.61: The cytotoxic activity of chalepin (**64**) against A549 cells according to the MTT assay

Cytotoxicity of 4-hydroxy-2-nonyl quinolinol in A549 cells according to the MTT assay

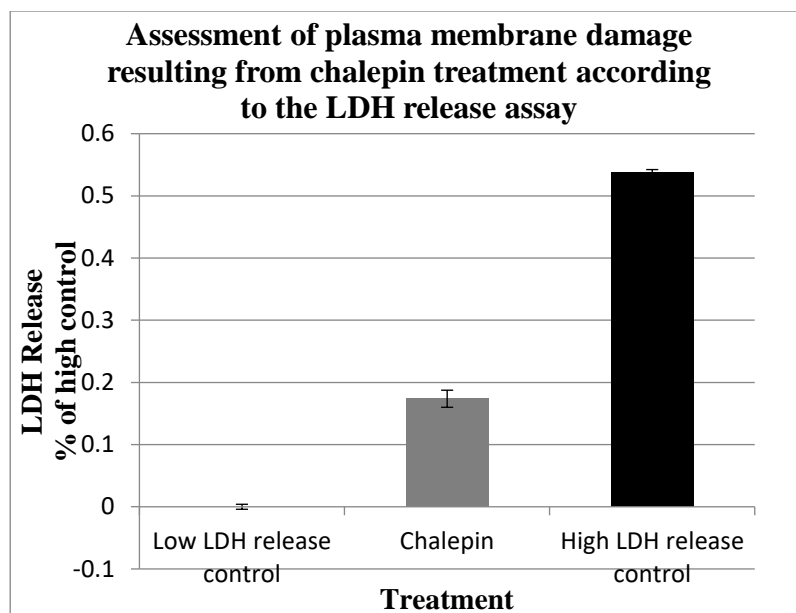


All experiments were carried out in triplicate on separate occasions. Data were expressed as means \pm standard error of the mean derived from $n \geq 12$ from three separate occasions.

Figure 3.3.62: The cytotoxic activity of 4-hydroxy-2-nonyl quinolinol (**85**) against A549 cells according to the MTT assay

3.3.10 The LDH results

Results of the LDH assay presented in Figure 3.3.63 suggest that chalepin (**64**) isolated from the three extracts of RC causes cytotoxicity at IC_{50} values of 92 μ M to the lung cancer cell lines (A549), through at least in part cell membranes damage by measuring the LDH activity at two absorbances: 490 and 690 nm. The LDH activity was performed using a commercial cytotoxicity assay kit produced by Roche (REF 11644793001). The necrotic percentage was 20.4 %, which was expressed using the formula: (sample value/maximal release) \times 100% (Chan *et al.*, 2013).



Data were expressed as means \pm standard error of the mean derived from $n=24$.

Figure 3.3.63: LDH Release result for chalepin (**64**) against the lung cancer cell lines (A549)

Discussion

The family Rutaceae is a family of flowering plants, herbs, shrubs or trees, which is widely distributed throughout the tropical regions, especially in Australia and the Mediterranean region (Roy & Rahman, 2016). It has been reported for its biological activities such as anti-rheumatic, scorpion repellent as contraceptive, abortifacient, emmenagogue for women and in the treatment of some dermatological diseases (De Natale and Pollio, 2012). Previous phytochemical studies on the family Rutaceae and rita species have detected many alkaloids, coumarins, flavonoids, glycosides and tannins (Martinez-Perez *et al.*, 2017).

In the present study, the cytotoxic effect of *R. chalepensis* (RC) aerial parts from the family Rutaceae was tested against five human cancer cell lines, MCF7 (human breast

adenocarcinoma), HepG2 (human liver hepatocellular carcinoma), EJ138 (human bladder carcinoma), A549 (human lung carcinoma), and PC3 (human prostate carcinoma) using the MTT assay. The DCM extract of (RC) aerial parts was the most potent cytotoxic extract against all the tested cell lines with IC₅₀ values of 25, 15, 55, 60 and 50 µg/mL, respectively, whilst the *n*-hexane and MeOH extracts showed little or no cytotoxicity. Selectivity index (SI) for *R. chalepensis* aerial parts was also determined using the human normal prostate cell line (PNT2). The aerial parts revealed low degree of cytotoxic selectivity on prostate cancer cells (SI=0.84). Eleventh known compounds were isolated from the different fractions of *R. chalepensis* including three alkaloids (graveoline **60**, 4-hydroxy-2-nonyl-quinoline **85** and kokusaginine **61**), three coumarins (bergapten **63**, chalepin **64** and chalepensisin **65**), two flavonoid glycosides (rutin **52** and methoxy rutin **83**), one sinapoyl glycoside **84**, one alkane [tetradecane (**86**)] and a new dehydromoskachan derivative (**87**). All the isolated compounds were tested for cytotoxicity against the human liver HepG2 hepatocellular carcinoma, the lung A549 and bladder EJ138 cell lines for 24 h. Both the furanocoumarin chalepin (**64**) and the alkaloid 4-hydroxy-2-nonyl-quinoline (**85**) showed a good cytotoxicity against the A549 with IC₅₀ value of 92 and 97.6 µM, respectively whilst, **64** showed toxicity also against EJ138 with IC₅₀ = 117 µM. Chalepin (**64**) has also been reported as an excellent cytotoxic agent against lung cancer cells A549 (Richardson *et al.*, 2016). The furanocoumarin chalepensisin (**65**) reported a variety of pharmacological activities, including antifertility, antiplatelet aggregation, cytotoxic effects on breast (MCF-7), colon (HT-29), kidney (A-498), lung (A549), pancreatic (PACA-2) and prostate (PC-3), gastric adenocarcinoma (MK-1),

human uterus carcinoma (HeLa), human adult T-cell leukemia/lymphoma (V) and murine melanoma (B16F10) cells (Quintanilla-Licea, *et al.*, 2014; Nakano *et al.*, 2017).

However, in our study the cytotoxic effect of chalepensisin (**65**) against the lung A549 cancer cell lines after 48 h was mild ($IC_{50} = 200 \mu M$). The three furanocoumarins **6365** are characterized by the psoralen nucleus with a furan ring attached with coumarin nucleus (Figures 3.3.64). The major differences between the three furanocoumarins are: the presence of dimethyl allyl group at position 3 in both **64** and **65**; the presence of the isopropyl alcohol group as a substituent on the furan ring at position 5' in chalepin (**64**); the lack of unsaturation at positions 4' and 5' in **64**. It has been suggested that the substitution in the pyrone ring may increase the chemical reactivity of coumarin molecule (Emerole *et al.*, 1981). The lack of unsaturation and the presence of dimethyl allyl group might also modify the cytotoxicity of **64**. It is, therefore, significant to note that compound **64** showed high cytotoxic activity while coumarin **65** showed little cytotoxicity and **63** did not.

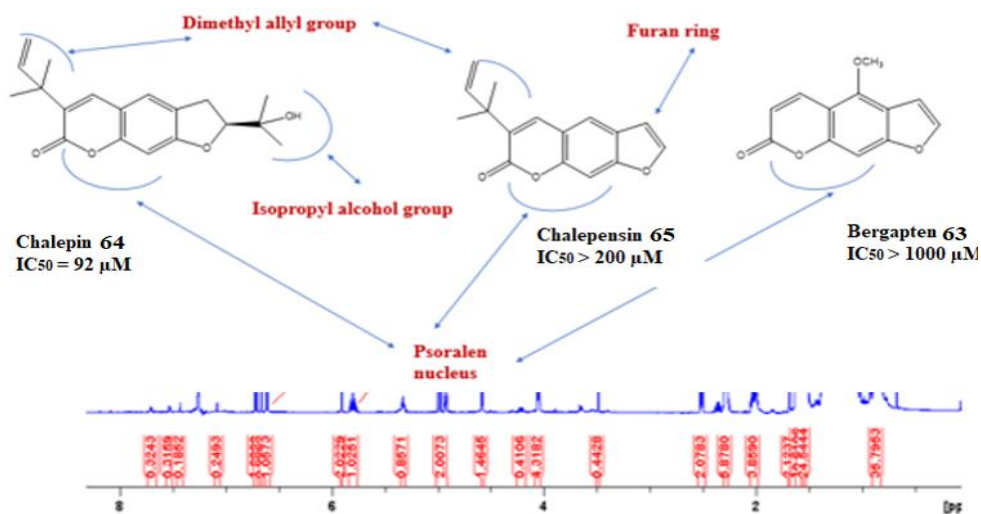


Figure 3.3.64 Structure activity relationship of the three furanocoumarins isolated from *R. chalepensis*

Preliminary findings derived from using the lactate dehydrogenase (LDH) release assay indicated that chalepin-induced cell death might at least in part, involve plasma membrane damage and necrosis (Figures 3.3.63).

Graveoline (**60**) is an alkaloid, which has been extracted previously from *Ruta* species and been conducted on its possible anti-cancer effect. However, it reported antiproliferative activity on HeLa cancer cells with IC₅₀ values of 3.35 µg/mL (Wu *et al.*, 2003). It has been reported by An *et al.* in 2010 that the synthetic graveoline derivatives have anti-angiogenesis potential. In addition, a study applied by Ghosh *et al.*, 2014 revealed that graveoline-induced both apoptotic and autophagic cell death in skin melanoma cells (A375) with IC₅₀ values of 22.23 µg/mL. The alkaloid kokusaginine (**61**) also reported proliferative activity on HeLa cells and KB cancer cells with IC₅₀ values of 3.9 µg/mL and 7.5 µg/mL, respectively (Wu *et al.*, 2003; Molnar *et al.*, 2013) and there is no report on its activity against the lung cancer cells. However, in this study graveoline (**60**) and kokusaginine (**61**) did not show any activity against three types of cancer cell lines, the lung (A549), bladder (EJ138) and the hepatocarcinoma (HEPG2) cell lines.

Flavonoids are ubiquitous in nature. They have been reported in prevention of cancer. Their anticancer activity depends on their chemical structure, concentration, and the type of cancer. Rutin (**52**) and methoxy rutin (**83**) were isolated from the MeOH extract of RC. Both flavonoids were tested for their cytotoxicity against lung cancer cell lines (A549) but did not exhibit any cytotoxicity. It has also been reported that **52** did not show any cytotoxic activity against lung and liver cancer cell lines while it showed activity against the bladder cancer cells IC₅₀ value of 80 M (Sak, 2014).

Sinapic acid is widespread in the plant kingdom (fruits, vegetables, cereal grains, oilseed crops, and some spices and medicinal plants) and as such is common in the human diet. Derivatives of sinapic acid are characteristic compounds in the Brassicaceae family. Sinapic acid shows antioxidant, antimicrobial, anti-inflammatory, anticancer, and anti-anxiety activity (Nićiforović & Abramovi 2014). However, the 3'', 6'-disinapoylsucrose (**84**) isolated from the RCM fraction 2 did not reveal any cytotoxicity against the hepatocellular cancer (HEPG2) at the concentration of 247 uM.

In addition to the above-mentioned compounds, compound **87** has been isolated in this study from the *n*-hexane layer of *R. chalepensis* aerial parts. 1D and 2D NMR spectra clearly indicated the structure of compound **87** as dehydromoskachan C derivative. We searched this compound in various databases, but we could not find any match so, it is likely to be a new compound. Similar moskachans A, B, C, and D have been isolated previously from *R. chalepensis* (Ulubelen 1988). Compound **87** tested for its activity against the lung cancer cell lines (A549) and did not show any activity. However, moskachan D reported promising cytotoxic property against A549 cell line with IC₅₀ values of 18.5 ± 0.65 µg/mL (Richardson *et al.*, 2016).

Conclusion

In conclusion, *R. chalepensis* aerial parts showed a high cytotoxicity against different cancer cell lines with low selectivity index of 0.84 on prostate cancer cells.

Our findings suggest that among furanocoumarins under investigation, compound **64** was the most cytotoxic coumarin, **65** exerted mild cytotoxic effect and **63** was not cytotoxic. Similarly, the alkaloid 4-hydroxy-2-nonyl-quinoline (**85**) was the only cytotoxic alkaloid

among the other alkaloids **60** and **61**. The alkaloid **85** was isolated for the first time from *R. chalepensis*. Therefore, the cytotoxicity of *R. chalepensis* aerial parts may be due to the presence of both the furanocoumarin **64** and the alkaloid **85**. Thus, chalepin (**64**) and 4-hydroxy-2-nonyl-quinoline (**85**) could be promising candidates for the development of anticancer agents. The mechanism of action of chalepin (**64**) might involve with little extent the plasma membrane damage resulting in the release of LDH enzyme. The study revealed a novel compound of moskachan type **87** but did not show any cytotoxic activity against the lung cancer cell lines. Further work should be applied on this compound on other cancer cell lines to check if it has any cytotoxic activity.

3.4 *Arbutus pavarii*

3.4.1 Extraction

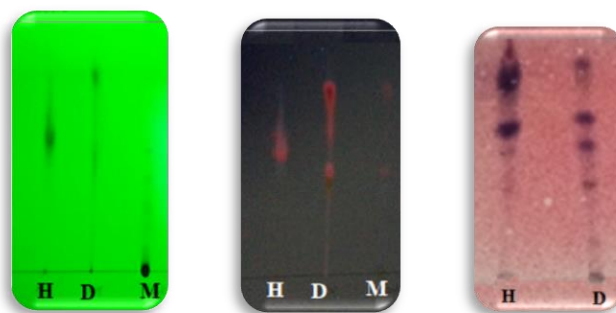
Sequential Soxhlet extraction of the dried and ground aerial parts of *Arbutus pavarii* (APL) leaves (150 g) afforded three extracts: *n*-hexane (APH), dichloromethane (APD), and MeOH (APM). The percentage yields of these extracts are summarized in Table 3.4.1

Table 3.4.1: Percentage yield of the three extracts obtained from *A. pavarii* (APL) leaves

Extract	% Yield
<i>n</i> -Hexane (RCH)	4.42
DCM (RCD)	1.8
MeOH (RCM)	35.98

3.4.2 Preliminary analytical TLC screening

The developed TLC plates of three extracts obtained from *A. pavarii* leaves were viewed under short (254 nm) and long (366 nm) UV light. After spraying with anisaldehyde reagent followed by heating at 100°C for 5 min, some violet coloured spots have appeared mainly in both the *n*-hexane and the DCM layer, which may indicate the presence of phenols, terpenes or sugars. (Figure: 3.4.1). Different R_f values ranging from (0.5-0.9) were recorded (Table 3.4.2) (Kristanti & Tunjung 2015).



Short UV (254 nm) Long UV (366 nm) Sprayed with anisaldehyde

Mobile phase: Toluene: EtOAc /Acetic acid = 25:24:1

Figure 3.4.1: TLC for the three extracts of *A. pavarrii* leaves

Table 3.4.2: R_f values of different extracts of *A. pavarrii* leaves

<i>n</i> -Hexane R _f values	DCM R _f values
0.54, 0.62, 0.84	0.58, 0.69, 0.8, 0.92

3.4.3 Analytical HPLC screening for MeOH extract of *A. pavarrii* leaves

The MeOH extract of *A. pavarrii* leaves (10 mg/mL) was analysed by Dionex Ultimate 3000 analytical HPLC coupled with a photodiode detector using a gradient mobile phase, 30-100% MeOH/H₂O for 30 min with a volume of injection of 20 µL and a flow rate of 1 mL/min. (Figure 3.4.2; Table 3.4.3).

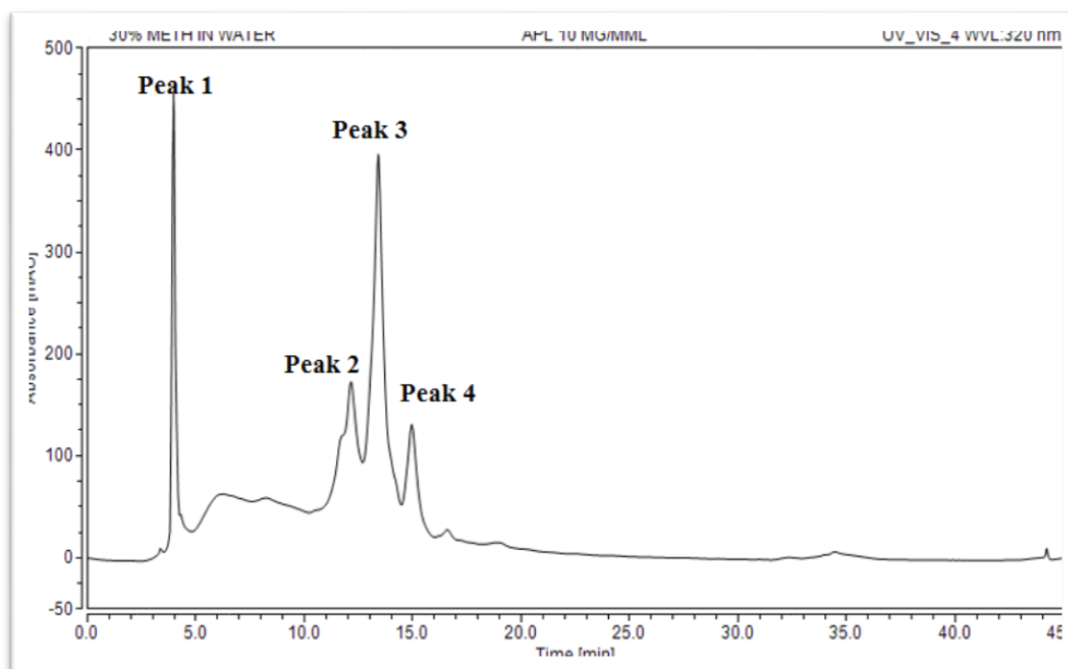


Figure 3.4.2: Analytical HPLC chromatogram the MeOH extract of *A. pavarrii* leaves (observed at 320 nm)

Table 3.4.3: UV-Vis data for all major peaks obtained from diode array detector

Peak No.	Retention Time (min)	UV-Vis absorbances (λ_{max}) (nm)
1	3.9	223, 241 and 275
2	12.0	265 and 355
3	13.0	257 and 356
4	15.0	263 and 351

3.4.4 Screening of *A. pavarii* extracts for cytotoxic activity

The cytotoxic activity, according to the MTT assay, of both the DCM, and MeOH extracts of *A. pavarii* leaves was assessed against five cancer cell lines; EJ138 (human bladder carcinoma), Hep G2 (human liver hepatocellular carcinoma), A549 (human lung carcinoma), MCF7 (human breast adenocarcinoma), and prostate cancer cell lines (PC3). The *n*-hexane extract was not tested for cytotoxicity due to its insolubility in DMSO. The DCM extract showed the highest activity against the prostate cancer cell lines with $IC_{50} = 26 \mu\text{g/mL}$ while, the MeOH extract showed activity against the breast cancer cell lines (MCF7) and prostate cancer cell lines (PC3) with IC_{50} value of 60 and 98 $\mu\text{g/mL}$ respectively (Table 3.4.4a). The selectivity index (SI) of the active DCM extract of *A. pavarii* leaves was assessed comparing the cytotoxicity results of the human normal prostate cell line (PNT2) with those of human prostate cancer cell line (PC3). The extract revealed cytotoxic selectivity towards the prostate cancer cells (SI= 3.5), which indicated the safety of the extract on the normal human cells. The IC_{50} values of *A. pavarii* leaves extracts in both cell lines and the selectivity index are summarized in Table 3.4.4b.

Table 3.4.4a: The IC_{50} ($\mu\text{g/mL}$) of DCM and MeOH extracts of *A. pavarii* leaves on the selection of five human cancer cell lines

Cell type	IC ₅₀ values ($\mu\text{g/mL}$)	
	APD	APM
EJ138	90 ± 0.60	> 100
Hep G2	> 100	> 100
A549	> 100	> 100
MCF7	> 100	60 ± 0.36
PC3	26 ± 0.52	98 ± 0.20

Values greater than 100 $\mu\text{g/mL}$ were considered as non-cytotoxic

Table 3.4.4b: The IC₅₀ (μg/mL) values for AP DCM extract on PC3 and PNT2 cells and the selectivity index (SI) using the normal human prostate cells (PNT2).

Cell type	IC ₅₀ values (μg/mL) (APD)
PC3	26 ± 0.52
PNT2	90 ± 0.26
Selectivity index	3.5

Selectivity index (SI) = The IC₅₀ (μg/mL) of extracts against the normal cells divided by the IC₅₀ (μg/mL) of extracts against the cancer cells, where IC₅₀ is the concentration required to reduce viability by 1 50% of the cell population (Badisa, *et al.*, 2009).

3.4.5 Chromatographic fractionation of the extracts

Following the systematic, bioassay-guided phytochemical and cytotoxic/anticancer study on *A. pavarii* leaves, further fractionation of both the active DCM and MeOH extracts was performed.

3.4.5.1 Vacuum liquid chromatography (VLC)

The DCM (2.4 g) extract of *A. pavarii* leaves was further fractionated over silica using VLC to collect seven fractions (Figure 3.4.3), the weights of fractions are listed in Table 3.4.5

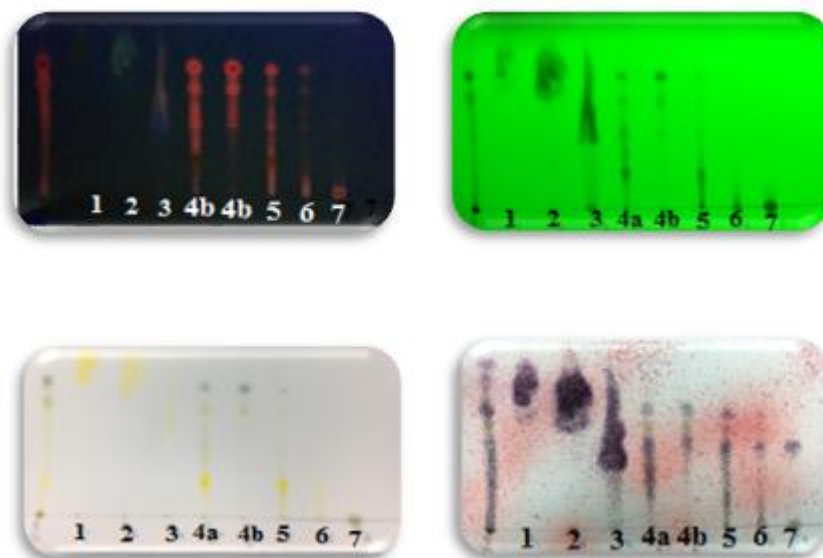


Figure 3.4.3: TLC analysis (mobile phase: 20% EtOAc in *n*-hexane) of the VLC fractions of the DCM extract of *A. pavarii* leaves

Table 3.4.5: Weights of the VLC fractions of the extract APD

Fraction	Mobile phase gradient	Weight of fraction (mg)
APDF1	100% <i>n</i> -hexane	150
APDF2	10% EtOAc / <i>n</i> -hexane	64.2
APDF3	30% EtOAc / <i>n</i> -hexane	41.7
APDF4	50% EtOAc / <i>n</i> -hexane	165.7 (a)+477 (b)
APDF5	80% EtOAc / <i>n</i> -hexane	117.0
APDF6	100% EtOAc	130.8
APDF7	50% MeOH/ EtOAc	97.1

3.4.5.2 Solid phase extraction (SPE)

The MeOH extract of *A. pavarii* leaves (APM) was fractionated by SPE to collect four fractions (Table 3.4.6).

Table 3.4.6: Weights of the SPE fractions of the MeOH extract of *R. chalepensis* aerial parts.

Fraction	Mobile phase gradient	Weight of fraction (mg)
APMF1	20% MeOH/H ₂ O	1627.2
APMF2	50% MeOH/H ₂ O	230.7
APMF3	80% MeOH/H ₂ O	19.0
APMF4	100% MeOH/H ₂ O	45.6

3.4.6 Screening of *A. pavarii* leaves DCM fractions for cytotoxic activity

The cytotoxic activity of the DCM fractions of *A. pavarii* leaves was assessed against the most sensitive cancer cell line (prostate cancer cell line PC3). The highest activity was revealed in in the VLC DCM F4b with IC₅₀ value of 30 µg/mL. The IC₅₀ values for the DCM fractions of *A. pavarii* leaves on PC3 are summarised in Table 3.4.7

Table 3.4.7: The IC₅₀ (µg/mL) of DCM fractions of *A. pavarii* leaves fractions on PC3 (human prostate cancer cell line).

Fraction	F1	F2	F3	F4 a	F4 b	F5	F6	F7
IC ₅₀ µg/mL	>100	>100	>100	40 ± 0.18	30 ± 0.25	98 ± 0.40	>100	>100

3.4.7 Isolation of compounds from *A. pavarii* leaves

3.4.7.1 The MeOH extract

The MeOH extract of *A. pavarii* leaves was analyzed by preparative reversed-phase HPLC employing a 30-100% gradient of MeOH in water for 30 min with a volume of injection of 900 µL and a flow rate of 10 mL/min. This yielded the compound APM-1 (0.5 mg, *t_R* = 16 min) (Figures 3.4.4).

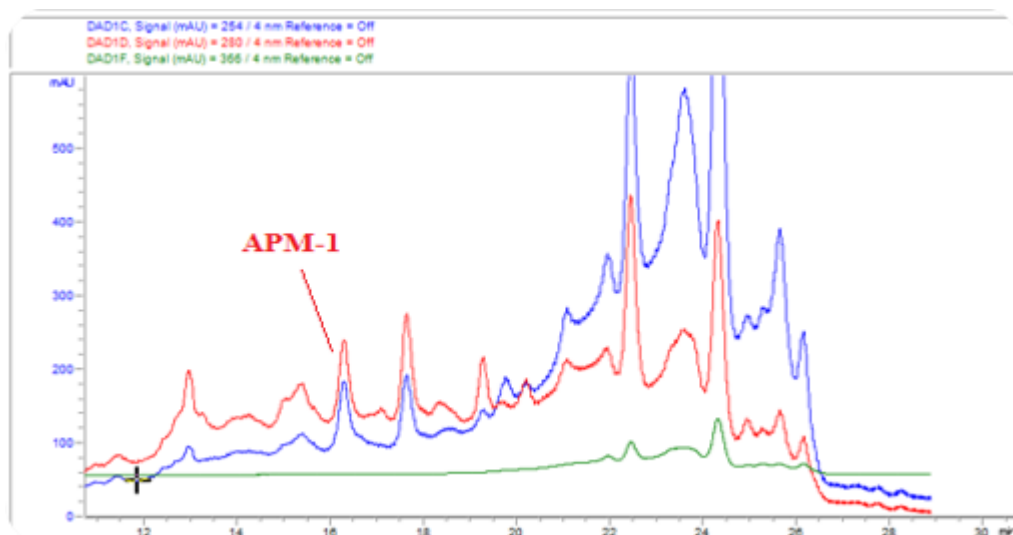


Figure 3.4.4: HPLC chromatograms of separated compounds from the APM extract (observed at 254, 280 and 366 nm)

The active MeOH F4 of *A. pavarii* leaves was analyzed by preparative reversed-phase HPLC (Agilent) employing a 50-100% gradient of MeOH in water for 30 min. This yielded the compound APLMF4-5 (3 mg, $t_R = 33.02$ min) (Figures 3.4.5).

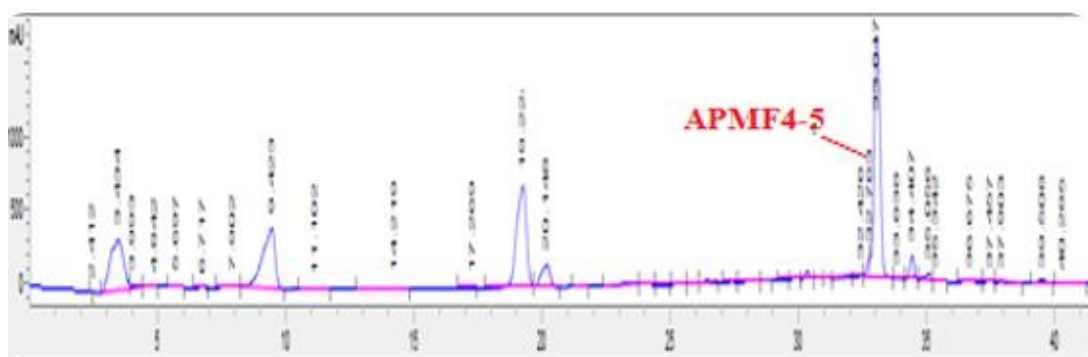


Figure 3.4.5: HPLC chromatogram of separated compounds from SPE fraction 4 of APM (observed at 215 nm)

3.4.7.2 The DCM extract (APD)

Separation of the active DCM Fraction 4

The active DCM Fraction 4b (477 mg) of *A. pavarii* leaves was analyzed by prep-HPLC using a gradient solvent system 50-100% ACN in water. This led to the

isolation of the compounds : APDF4-1 (0.6 mg, $t_R = 17.2$), APDF4-4 (0.2 mg, $t_R = 32.1$) (Figure 3.4.6)

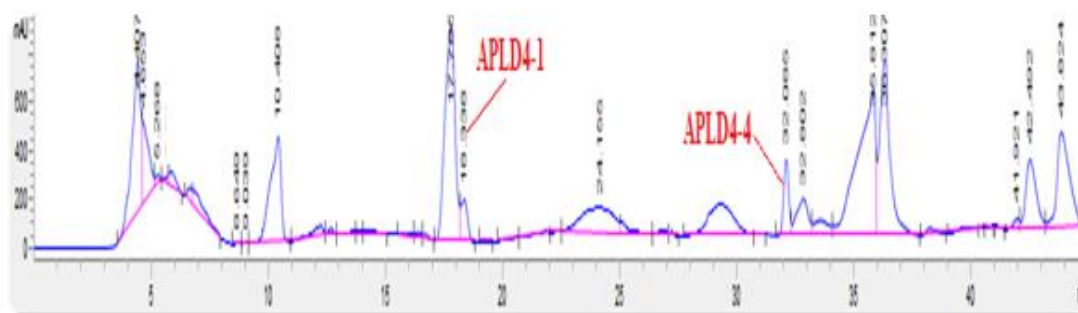


Figure 3.4.6: HPLC chromatogram of separated compounds from the active VLC F4 of APD (observed at 215 nm)

3.4.8 Characterization of isolated compounds from *A. pavarii* leaves

3.8.4.1 Characterization of hydroquinone glycoside

Characterization of APLM-1 as hydroquinone-D-glucopyranoside (arbutin 53)

White powder; UV (MeOH) λ_{\max} : 212 and 282 nm; ESIMS m/z showed a pseudomolecular ion peak at 273 $[M+H]^+$ indicating compound with formula $C_{12}H_{16}O_7$. 1H NMR (600 MHz, CD_3COCD_3) (Figure 3.4.7) and ^{13}C NMR (150 MHz, CD_3COCD_3) Table (3.4.8) spectra showed two aromatic *ortho*-coupled protons at δ_H 6.97(d, $J = 8.9$ Hz, 2H) and δ_C 118.1, δ_H 6.77 (d, $J = 9.0$ Hz, 2H) and δ_C 121.3 and a sugar (glucose) moiety. The 1H - ^{13}C HSQC experiment of **53** (Figure 3.4.8) showed the direct attachment between the anomeric proton at δ_H 4.81 (H-6 \prime) and the carbon (δ_C 103.2), protons at δ_H 6.97 (H-3 and H-5) and the carbon (δ_C 116.3) and the protons at δ_H 6.77 (H-2 and H-6) with the carbon (δ_C 118.8). All comparable data confirmed that compound **53** might be arbutin (Figure 1.7) (Avelino-Flores *et al.*, 2015; Das *et al.*, 2015).

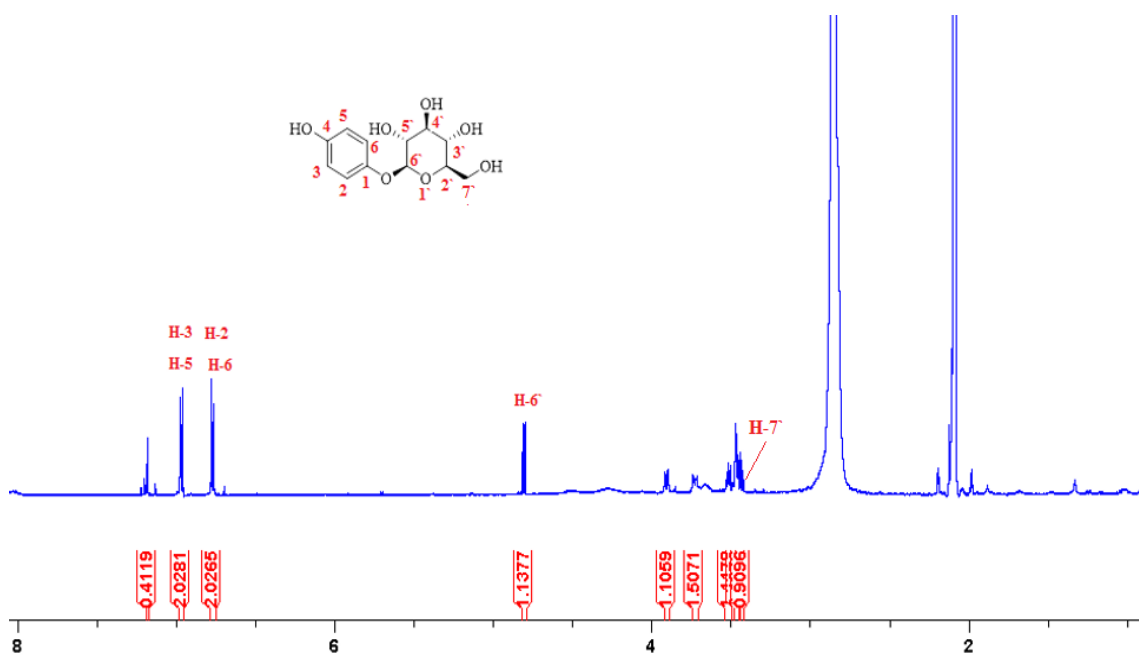


Figure 3.4.7: ^1H NMR spectrum of (600 MHz, CD_3COCD_3) of arbutin (**53**)

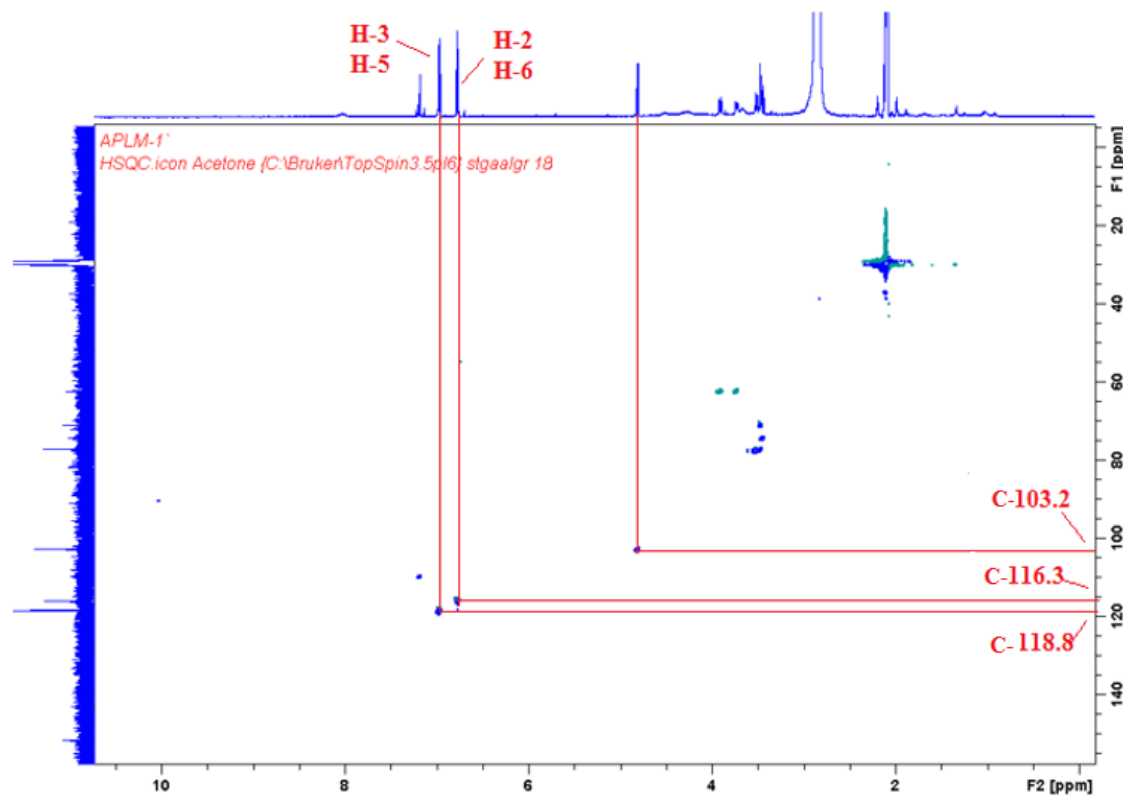


Figure 3.4.8: The ^1H - ^{13}C HSQC experiment (CD_3COCD_3) of arbutin (**53**)

Table 3.4.8: ^1H NMR (600 MHz, CD_3COCD_3) and ^{13}C NMR (150 MHz, CD_3COCD_3) of arbutin (**53**)

Position	Chemical Shift δ (ppm), J in Hz	
	^1H	^{13}C
1		151.8
2	6.77, d, $J=9.0$	118.8
3	6.97, d, $J=8.9$	116.3
4		151.8
5	6.97, d, $J=8.9$	116.3
6	6.77, d, $J=9.0$	118.8
2'	3.5, d,	77.5
3'	3.5, m	
4'	3.7, dd, $J=3.6$, $J=11.2$	
5'	3.91, dd, $J=1.8$, $J=11.4$	71.5
6'	4.81, d, $J=7.6$	103.2
7'	3.45, d, $J=3.9$	62.7

3.4.8.2 Characterization of pentacyclic triterpenes

Characterization of APLM4-5 as ursolic acid (88)

White amorphous powder; UV (MeOH) λ_{max} : 204 nm. ESIMS m/z exhibited sodiated molecular ion peak at 479 $[\text{M}+\text{Na}]^+$ (Figure 3.4.12) indicating compound with formula $\text{C}_{30}\text{H}_{48}\text{O}_3$. ^1H NMR (600 MHz, CD_3OD) Table (3.4.7) and Figure (3.4.13) showed methyl protons at δ_{H} 0.80, 0.86, 0.90, 0.97, 0.98, 0.99 and 1.14. The characteristic signal of ^{13}C NMR spectra Figure (3.4.14) was seen at δ 180.3 due to carboxylic acid at C-28 and the two olefinic carbons at δ_{C} 125.6 (C-12) and 138.3 (C-13) indicating ursolic acid -12-ene triterpenoid. The most obvious two-bond correlations, which can

be deduced from the COSY spectrum was between the H-11 \leftrightarrow H-12 and the H-2 \leftrightarrow H-3 (Figure 3.4.15). The ^1H - ^{13}C HSQC experiment (Figure 3.4.16) showed the attachment of protons to carbon atoms. All comparable data confirmed that compound **88** is the pentacyclic triterpene ursolic acid Figure (3.4.10) (Mishra *et al.*, 2016).

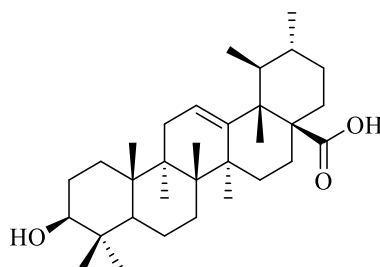


Figure 3.4.10: Structure of ursolic acid (**88**)

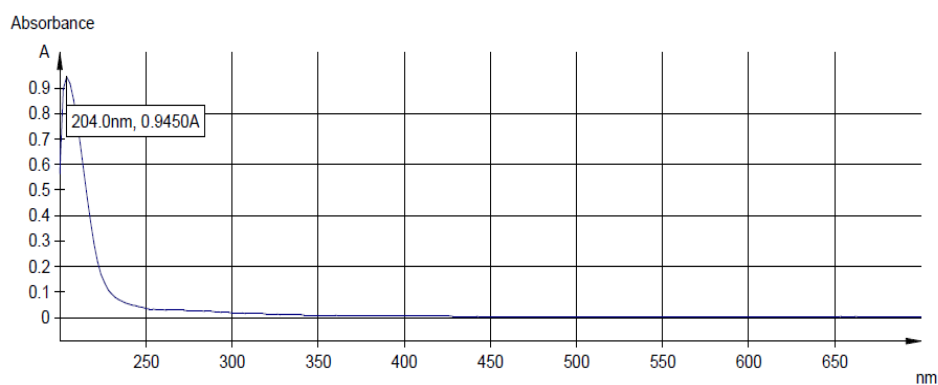


Figure 3.4.11: U.V. spectrum of ursolic acid (**88**) in MeOH

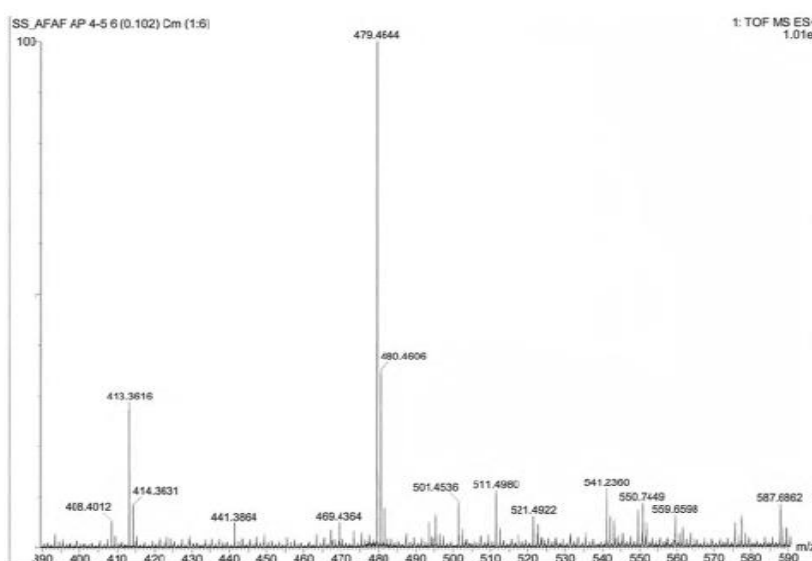


Figure 3.4.12: MS spectrum (TOF MS ES+) of ursolic acid (**88**)

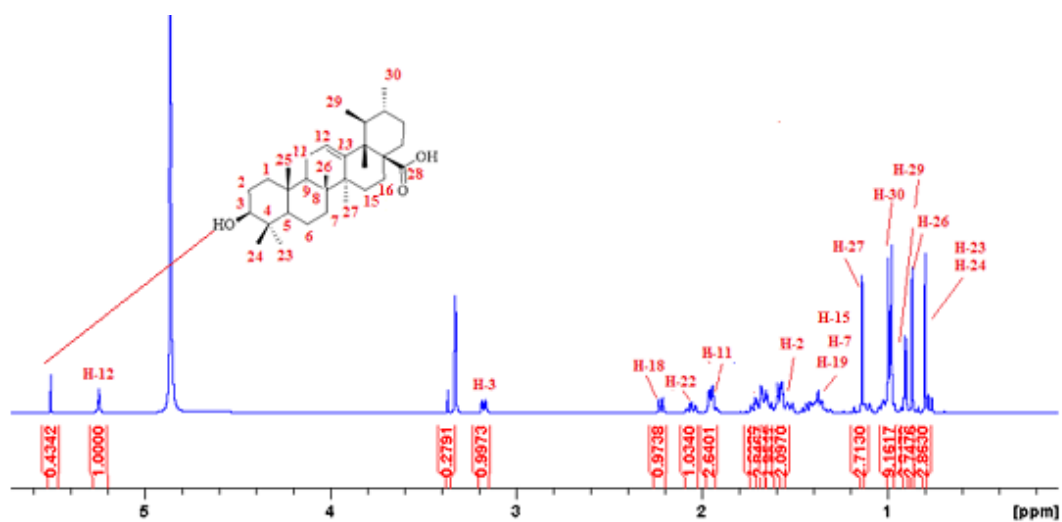


Figure 3.4.13: ^{13}C NMR spectrum (150 MHz, CD_3OD) of ursolic acid (**88**)

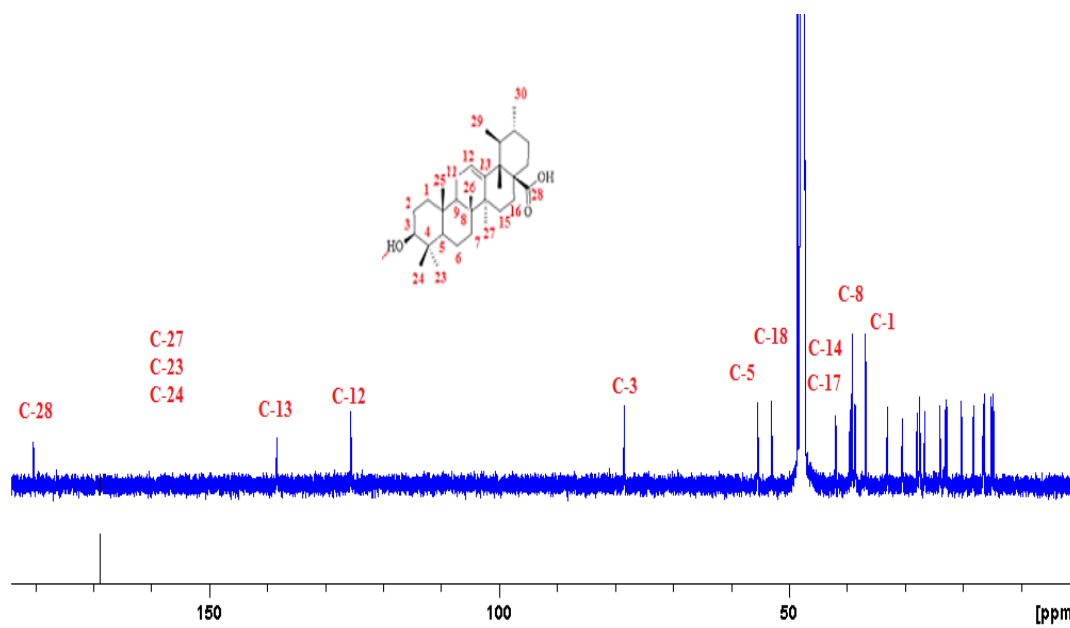


Figure 3.4.14: ^{13}C NMR spectrum (150 MHz, CD_3OD) of ursolic acid (**88**)

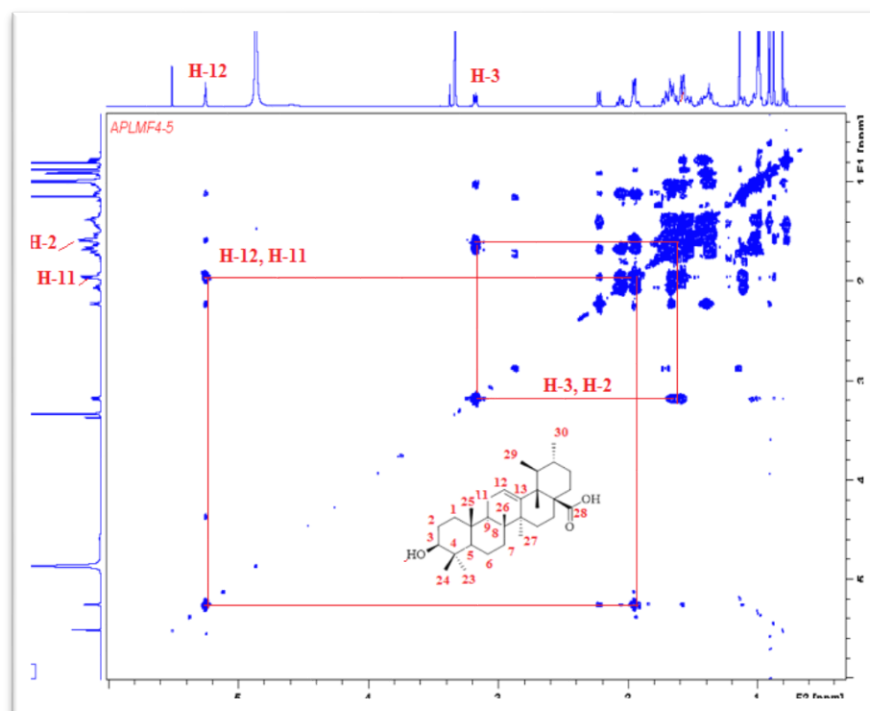


Figure 3.3.15: COSY experiment of ursolic acid (**88**)

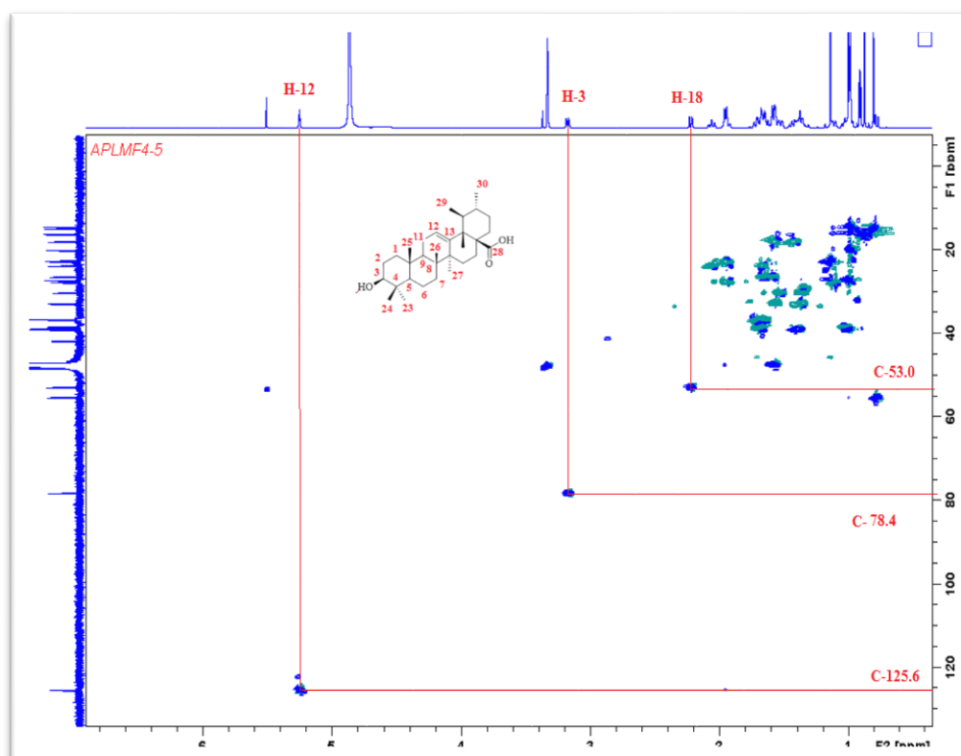


Figure 3.3.16: The ^1H - ^{13}C HSQC experiment of ursolic acid (**88**)

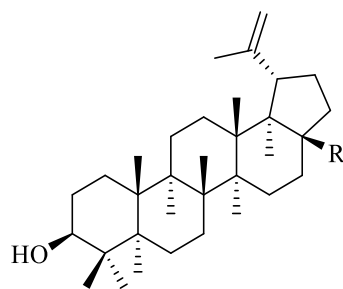
Table 3.4.9: ^1H NMR (600 MHz, CD_3OD) and ^{13}C NMR (150 MHz, CD_3OD) of ursolic acid (**88**)

Chemical Shift δ (ppm), J in Hz			Chemical Shift δ (ppm), J in Hz		
Position	^1H	^{13}C	Position	^1H	^{13}C
1	1.56, t, $J= 3.6$, 2H	38.5	16	1.74, m, 2H	24.0
2	1.73, m, 2H	27.4	17		48.0
3	3.17, dd, $J= 4.8$, $J= 11.5$, 1H	78.4	18	2.23, d, $J= 11.0$, 1H	53.0
4		38.6	19	1.51, t, $J= 3.2$, 1H	39.1
5	0.77, d, $J= 10.5$, 1H	55.4	20	1.44, m, 1H	38.6
6	1.63, m, 2H	18.1	21	1.63, m, 2H	30.4
7	1.35, m, 2H	33.0	22	2.21, dt, $J= 3.7$, $J= 8.82$, 2H	36.7
8		39.4	23	0.91, s, 3H	23.0
9	1.09, t, $J= 3.2$, 1H	47.4	24	0.89, s, 3H	23.9
10		36.7	25	0.86, s, 3H	16.3
11	1.95, dd, $J= 3.7$, $J= 8.8$, 2H	23.9	26	0.89, s, 3H	18.1
12	5.24, t, $J= 3.5$, 1H	125.5	27	1.02, s, 3H	26.5
13		138.3	28		180.3
14		41.9	29	0.90, d, $J= 6.5$, 3H	16.4
15	2.06, t, $J= 4.6$, $J= 13.3$, 2H	30.4	30	0.79, d, $J= 5.2$, 3H	20.2

Characterization of APLD4-4 as betulinic acid methyl ester (89)

White amorphous powder; UV (MeOH) λ_{max} : 208 nm (Figure 3.4.18). ESIMS exhibited the sodiated molecular ion peak at m/z at 493 $[\text{M}+\text{Na}]^+$ indicating a compound with a molecular formula $\text{C}_{31}\text{H}_{50}\text{O}_3$. ^1H NMR (600 MHz, CDCl_3) Table (3.4.7) and Figure (3.4.35) showed methyl protons at δ_{H} 0.78, 0.85, 0.97, 0.99 and

1.00, a doublet coupled protons a δ_{H} 3.21 (dd, $J = 4.4, J = 11.1$, 1H) assigned for H-3, a signal at 3.52 assigning for $-\text{OCH}_3$, two singlet protons at δ_{H} 4.77 and 4.64 assigning for (H-29) and a multiplet at 3.02 (m, 1H, H-19). All data were comparable to the published data for betulinic acid methyl ester and confirmed that the compound **89** is betulinic acid methyl ester (Figure 3.4.17) (Mishra *et al.*, 2016).



Compound No.	R
89	$-\text{COOCH}_3$
90	$-\text{CH}_2\text{OH}$

Figure 3.4.17: Structure of betulinic acid methyl ester (**89**) and betulin (**90**)

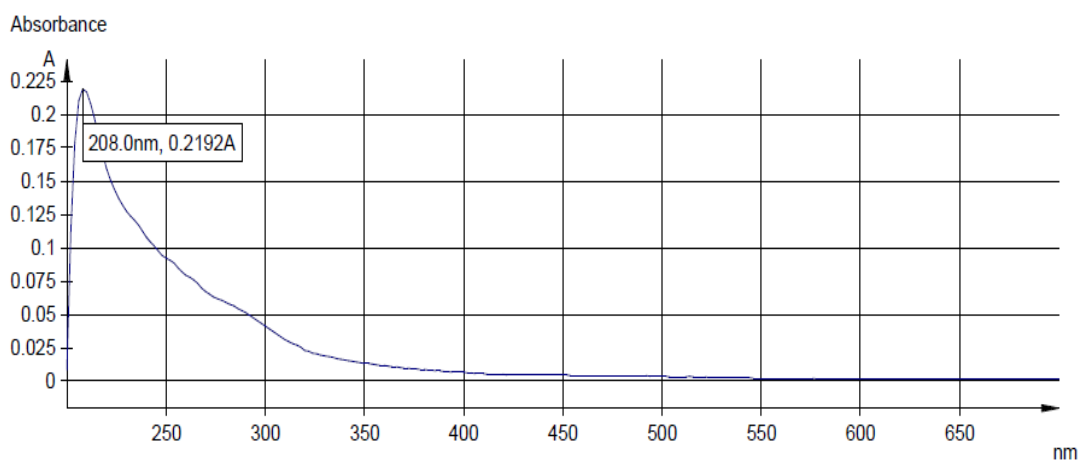


Figure 3.4.18: U.V. spectrum of betulinic acid methyl ester (**89**) in MeOH

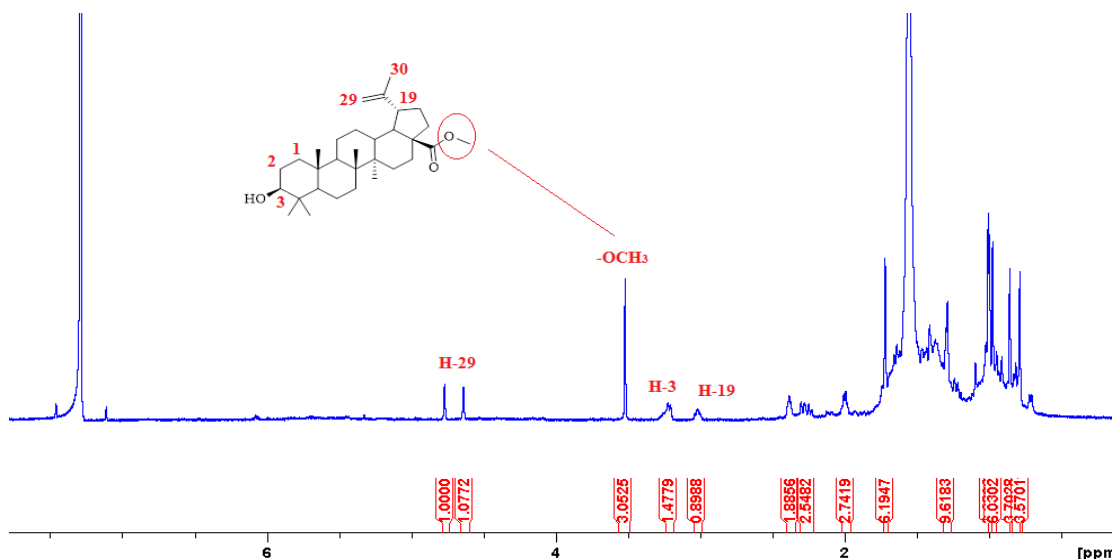
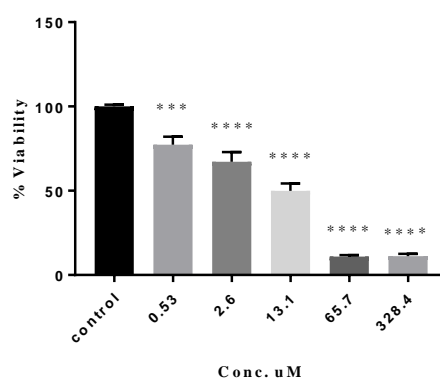


Figure 3.4.19: ^1H NMR spectrum (600 MHz, CDCl_3) of betulinic acid methyl ester (**89**)

3.4.9 Cytotoxic effect of ursolic acid (**88**) from *A. pavarii* leaves

Ursolic acid (**88**) isolated from the MeOH fraction 4 of *A. pavarii* leaves revealed high cytotoxicity against the human prostate cancer cell lines (PC3) with IC_{50} value of $8.22 \mu\text{M} \pm 0.16$ (Figure 3.4.20)

Cytotoxicity of ursolic acid in PC3 cancer cells according to the MTT assay

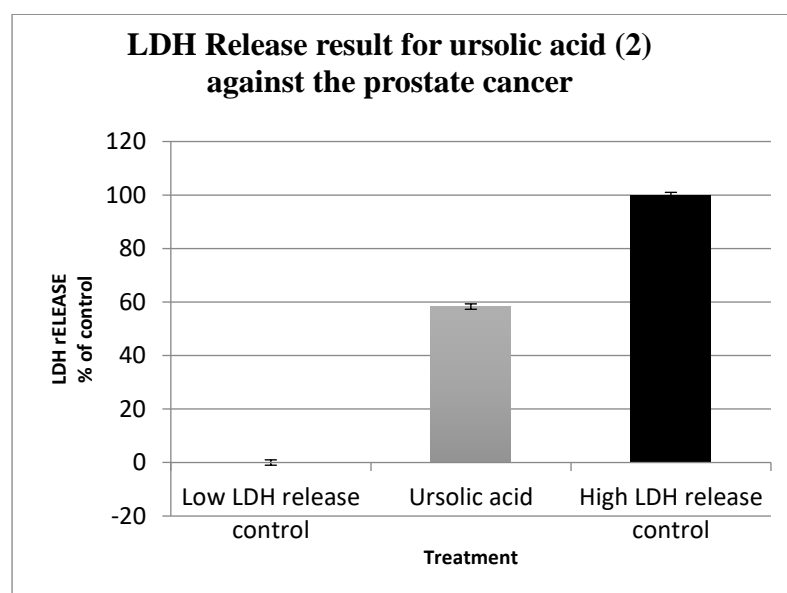


All experiments were carried out in triplicate on separate occasions. Data were expressed as means \pm standard error of the mean derived from $n \geq 12$ from three separate occasions.

Figure 3.4.20: The cytotoxic activity of ursolic acid (**88**) against PC3 cells according to the MTT assay

3.4.10 The LDH results

Results of the LDH assay presented in Figure 3.3.68 suggest that ursolic acid (**88**) isolated from the MeOH extract of APL at IC_{50} value of $8.22 \mu M$ causes cytotoxicity to the prostate cancer cell lines (PC3), through at least in part cell membranes damage by measuring the LDH activity at two absorbances: 490 and 690 nm. The LDH activity was performed using a commercial cytotoxicity assay kit produced by Roche (REF 11644793001). The necrotic percentage was 53.4 %, which was expressed using the formula: $(\text{sample value}/\text{maximal release}) \times 100\%$ (Chan *et al.*, 2013).



Data were expressed as means \pm standard error of the mean derived from $n=24$.

Figure 3.4.21: LDH Release result for ursolic acid (**88**) against the prostate cancer cell lines (PC3)

Discussion

The Ericaceae family or heather family is found most commonly in acid and infertile growing conditions. Many genera from the family Ericaceae are used traditionally as antiseptics, diuretics, laxatives and in the treatment of arthritis, headache, hypertension and urinary infections (Migue *et al.*, 2014; Pavlović *et al.*, 2014). The genus *Arbutus*,

which belongs to the family Ericaceae, is distributed in the Mediterranean region and Europe and revealed the presence of many constituents such as flavonoids, glycosides, phenolic compounds, sterols and triterpenes (Hasan *et al.*, 2011). *A. pavarii* is a species endemic to Al-Jabal El-Akhdar on the eastern coast of Libya (González–Elizondo. *et al.*, 2012; Alsabri *et al.*, 2013; Miguel *et al.*, 2014). The plant revealed many compounds that have been documented to reduce the risk of cancer such as: flavonoids (apigenin_epicatechin, hesperidin, quercetin, naringin and rutin), simple phenolics (arbutin, gallic acid, pyrogallol) (El Hawary *et al.*, 2016).

There are only limited studies performed on *A. pavarii* to study its effect as cytotoxic plant (Hasan *et al.*, 2011; Alsabri *et al.*, 2013; El Hawary *et al.*, 2016). The anti-proliferative activity of *A. pavarii* aerial parts on breast (MCF7 and T47D), hepatocarcinoma HEPG2, and lung (A549) cancer cells was evaluated by the MTT assay and the results were less than 30 µg/ml (Alsabri *et al.*, 2013; El Hawary *et al.*, 2016).

In the present study, the cytotoxic effect of *A. pavarii* leaves (APL) was tested against five human cancer cell lines, MCF7 (human breast adenocarcinoma), HepG2 (human liver hepatocellular carcinoma), EJ138 (human bladder carcinoma), A549 (human lung carcinoma), and PC3 (human prostate carcinoma) using the MTT assay. The *n*-hexane extract was not tested for cytotoxicity due to its insolubility in DMSO. The DCM extract showed the highest activity against the prostate cancer cell lines with $IC_{50} = 26$ µg/mL while, the MeOH extract showed activity against the breast cancer cell lines (MCF7) with $IC_{50} = 60$ µg/mL. Selectivity index (SI) for APL was also determined using the human normal prostate cell line (PNT2). The leaves revealed cytotoxic selectivity on prostate cancer cells (SI= 3.5), which indicated the safety of the extract on the normal human cells.

Three pure compounds were isolated from both the DCM and MeOH fractions of APL including one phenolic glycoside: arbutin (**53**) and two-pentacyclic triterpenes ursolic acid (**88**) and betulinic acid methyl ester (methyl betulate) (**89**). The two triterpenes **88** and **89** were isolated for the first time from *A. pavarii* leaves. However, pentacyclic triterpenes were isolated from the fruits of *A. unedo*; α - and β -amyrin, lupeol and a new natural triterpene (olean-12-en-3 β , 23-diol) (Miguel *et al.*, 2014).

Pentacyclic triterpenes reported many biological activities such as antibacterial, antitumor and antimalarial. Ursolic acid has been reported to possess a wide range of biological activities and it was widely used in Chinese herbal medicines (Wu *et al.*, 2014). Ursolic acid (**88**) reported cytotoxicity against PC3, LNCaP and DU145 prostate cancer cells with IC₅₀ of 35 μ M, 47 μ M and 80 μ M, respectively (Park *et al.*, 2013). The cytotoxic activity of betulin (**90**) and its derivatives has also been reported. They showed selective cytotoxicity against many different tumour cell lines and are promising chemotherapeutic agents for the treatment and prevention of different types of diseases (Csuk 2012).

Ursolic acid (**88**) was tested in this study for cytotoxicity against the human prostate cancer cell lines (PC3) and revealed higher cytotoxicity (IC₅₀= 8.22 μ M) compared with that reported in literature. Our findings also indicated that ursolic acid induced cell death might involve the plasma membrane damage resulting in the release of LDH enzyme from the necrotic prostate cancer cell lines (PC3) cells (Figure 3.1.54). The necrotic percentage was calculated as 53.4 %, by using the formula (sample value/maximal release) \times 100% (Chan *et al.*, 2013). Methyl betulinate (**89**) was isolated from the active VLC DCM F4b of *A. pavarii* leaves, which revealed activity against the prostate cancer cell line (PC3) with IC₅₀ value of 30 μ g/mL. Its presence in fraction APLDF4b might indicates the potency of this fraction.

Arbutin (**53**) is a hydroquinone-D-glucopyranoside that leads to the expression of genes inducing apoptosis in human melanoma cancer cells (Avelino-Flores *et al.*, 2015) and also exhibited high cytotoxicity against MCF-7/Adr (human breast cancer cell lines: Adriamycin-resistant) (Berdowska *et al.*, 2013), therefore is also probably involved in the observed activity of the APLM extract against the breast cancer cell lines (MCF7) ($IC_{50} = 60 \mu\text{g/mL}$).

Conclusion

In conclusion, *A. pavarii* leaves showed a high cytotoxicity against two types of cancer cell lines; the prostate (PC3) cancer cell lines (DCM extract) and the breast (MCF7) cancer cell lines (MeOH extract). The cytotoxicity observed with *A. pavarii* leaves might be due to the presence of the cytotoxic pentacyclic triterpenes ursolic acid (**88**) and betulinic acid methyl ester (**89**) and the hydroquinone- β -D-glucopyranoside arbutin (**53**).

The leaves revealed cytotoxic selectivity on prostate cancer cells (SI= 3.5), which indicated the safety of the extract on the normal human cells.

CHAPTER 4

CONCLUSION

4.0 Conclusion

In conclusion, the phytochemical and cytotoxic/anticancer study on the four medicinal plants from the Libyan flora; *A. aestivus*, *A. pavarii*, *J. phoenicea* and *R. chalepensis*, has provided evidence in support for their traditional uses as antitumour agents. They seem to be promising candidates as anticancer plants and accumulate naturally occurring compounds with interesting cytotoxic/anticancer activities and different selectivity indexes on prostate cancer cells. *A. aestivus* showed the highest selectivity on prostate cancer cells among the four plants while *R. chalepensis* lacks this selectivity.

The importance of clinically anticancer drug is its ability to be selective on cancer cells. Therefore, the high selectivity of *A. aestivus* species (SI=26) towards prostate cancer cells deserves more additional studies which might aid to develop an anticancer drug from it. *A. pavarii* and *J. phoenicea* also revealed moderate selectivity on prostate cancer cells with SI= 3 and 5, respectively.

Bioassay-guided fractionation of these plants led to the isolation of 29 compounds including a new dehydromoskachan C derivative and six compounds isolated for the first time from these plant species. The plants contained a diversity of secondary metabolites, which have proved their importance in the treatment of many ailments including cancer. The four plants under study revealed alkaloids, anthraquinones, flavonoids and coumarins as well as different glycosidic compounds. The secondary

metabolites isolated for the first time in our study are: The biflavonoid, sumaflavone (**76**) from *J. phoenicea* leaves, the alkaloid, 4-hydroxy-2-nonyl-quinoline (**85**) and the glycoside, 3'',6''-disinapoylsucrose (**84**) from *R. chalepensis* aerial parts, the anthraquinone glycoside, C- α -rhamnopyranosyl bianthracene-9, 9', 10 (10'H)-trione (**81**) from *A. aestivus* tubers and the ferulic acid derivative, *p*-hydroxy-phenethyl *trans*-ferulate (**82**) from *A. aestivus* leaves and the pentacyclic triterpenes, methyl betulinate (**89**) and ursolic acid (**88**) from *A. pavarii* leaves. Three compounds revealed good cytotoxicity against the most sensitive cancer cell lines in each plant using the MTT assay. Sumaflavone (**76**) and 4-hydroxy-2-nonyl-quinoline (**85**) exhibited good cytotoxicity against the lung cancer cell lines with IC₅₀ values of 77 and 97.6 μ M, respectively. C- α -rhamnopyranosyl bianthracene-9, 9', 10 (10'H)-trione (**81**) and ursolic acid (**88**) revealed high cytotoxicity against the prostate cancer cell lines with IC₅₀ values of 62 μ M and 8.22 μ M, respectively.

However, this study revealed also highly cytotoxic compounds, which had been reported in the literature, the biflavonoid cupressoflavone (**24**) from *J. phoenicea* leaves and the coumarin chalepin (**64**) from *R. chalepensis* aerial parts against the lung cancer cell lines with IC₅₀ value of 65 and 92 μ M, respectively. Cupressoflavone (**24**) is tested for the first time in this study for its cytotoxicity. Findings also indicated that chalepin (**64**), cupressoflavone (**24**) and ursolic acid (**88**)-induced cell death might involve the plasma membrane damage resulting in the release of LDH enzyme from the necrotic cells with necrotic percentages of 20.4%, 54.0% and 53.4%.

REFERENCES

- Abdel-Sattar, E., Zaitoon, A., El Sayed, A. M. & Bakhashwain, A. A. (2014). Evaluation of some medicinal plants in controlling *Culex pipiens*. *J Egypt Soc Parasitol* **44**: 771-778.
- Achak, N., Romane, A., Abbad, A., Ennajar, M., Romdhane, M. & Abderrabba, A. (2008). The essential oil composition of *Juniperus phoenicea* from Morocco and Tunisia. *J Essent Oil Bear Pl* **11**: 137-142.
- Adamska-Szewczyk, A., Glowniak, K. & Baj, T. (2016). Furoquinoline alkaloids in plants from Rutaceae family. *Curr Issues Pharmacy Med Sci* **29**: 33-38.
- Adinolfi, M. rosa lanzelta, carmela elsa marciano, michelangelo parrilli. (1991). A new class of anthraquinone-anthrone-c-glycosides from *asphodelus ramosus* tubers. *Terrahedron* **41** (25): 4435-4440.
- Ait-Ouazzou, A., Loran, S., Arakrak, A., Laglaoui, A., Rota, C., Herrera, A., Pagan, R. & Conchello, P. (2012). Evaluation of the chemical composition and antimicrobial activity of *Mentha pulegium*, *Juniperus phoenicea*, and *Cyperus longus* essential oils from Morocco. *Food Res Int* **45**: 313-319.
- Akkaria, H., Ezzine, O., Dhahri, S., B'chirc, F., Rekik, M., Hajaji, S., Darghouth, M. A., Ben Jamâa, M.L. & Gharbia, M. (2015). Chemical composition, insecticidal and in vitro anthelmintic activities of *Ruta chalepensis* (Rutaceae) essential oil. *Ind Crops Prod* **74**: 745-751.
- Alghazeer, R., Abourghiba, T., Ibrahim, A. and Zreba, E. (2016). Bioactive properties of some selected Libyan plants. *J Med Plant Res* **10** (6): 67-76.
- Ali, M.S., Fatima, S. & Pervez, M. K. (2008). Haplotin: A new furoquinoline from

Haplophyllum acutifolium (Rutaceae). *J Chem Soc Pak* **30**: 775-779.

Aljaiyash, A.A., Gonaïd, M.A., Islam, M. & Chaouch, A. (2014). Antibacterial and cytotoxic activities of some Libyan medicinal plants. *J Nat Prod Plant Resour* **4**: 43-51.

Alqasoumi, S. I., Farraj, A. I., Abdel-Kader M. S. (2013). Study of the hepatoprotective effect of *J. phoenicea* constituents *Pak J Pharm Sci* **26**: 999-1008.

Alsabri, S. G., El-Basir, H. M., Rmeli, N. B., Mohamed, S. B., Allafi, A. A., Zetrini, A. A., Salem, A. A., Mohamed, S.S., Gbaj, A. & El-Baseir M. M. (2013). Phytochemical screening, antioxidant, antimicrobial and antiproliferative activities study of *Arbutus pavarii* plant. *J Chem Pharm Res* **5**: 32-36.

Al-Said, M. S., Tariq, M., al-Yahya, M. A., Rafatulla, S., Ginnawi, O. T. & Ageel, A. M. (1990). Studies on *Ruta chalepensis*, an ancient medicinal herb still used in traditional medicine. *J Ethnopharmacol* **28**: 305-12.

Alwahsh, M. A. A., Khairuddean, M., Chong, W. K. (2015). Chemical Constituents and Antioxidant Activity of *Teucrium barbeyanum* Aschers. *Rec Nat Prod* **9** (1): 159-163.

Alzand, K.I., Aziz, D. M., Tailang, M. (2014). Isolation, structural elucidation and biological activity of the flavonoid from the leaves of *Juniperus Phoenicia*. *World J Pharm Res* **10**: 951-965.

An, Z. Y., Yan, Y. Y., Peng, D. Ou, T. M., Tan, J. H., Huang, S. L., An, L. K., Gu, L. Q., Huang, Z. S. (2010). Synthesis and evaluation of graveoline and graveoline derivatives with potent antiangiogenic activities. *Eur J Med Chem* **45**: 3895–3903.

Androutsos, G. (2004). History of oncology. Rudolf Virchow (1821-1902): Founder

- of cellular pathology and pioneer of oncology. *J BUON* **9**: 331-336.
- Angioni, A., Barra, A., Russo, M. T., Coroneo, V., Dessi, S., Cabras, P. (2003). The chemical composition of the essential oils of *Juniperus* from ripe and unripe berries and leaves and their antimicrobial activity. *J Agri F Chem* **51**: 3073-3078.
- Anouar, E. H., Osman CP, Weber, J. F. F., Ismail, N. H. (2014). UV/Visible spectra of a series of natural and synthesised anthraquinones: experimental and quantum chemical approaches. *SpringerPlus*. 3:233. doi:10.1186/2193-1801-3-233.
- Antoni, S., Soerjomataram, I., Møller, B., Bray, F. & Ferlay, J. (2016). An assessment of GLOBOCAN methods for deriving national estimates of cancer incidence. *Bull. World Health Organ.* **94**: 174-184.
- Arroo, R. R. J, Alfermann, A. W., Medarde, M., Petersen, M., Pras, N. & Woolley, J. G. (2002). Plant cell factories as a source for anti-cancer lignans. *Phytochem Rev* **1**: 27-35.
- Asheg, A. A., EL-Nyhom, S. E., Ben Naser, K. M., Kanoun, A. H., bouzeed, Y. M. (2014). Effect of *Arbutus pavarii*, *Salvia officinalis* and *Zizyphus Vulgaris* on growth performance and intestinal bacterial count of broiler chickens. *Int J Veter Sci Med* **2**: 151-155.
- Aslantürk, O. S. & Celik, T. A. (2013). Investigation of antioxidant, cytotoxic and apoptotic activities of the extracts from tubers of *Asphodelus aestivus* Brot. *Afr J Pharm Pharmacol* **11**: 610-621.
- Aslantürk, O. S. & Celik, T. A. (2013). Investigation of antioxidant, cytotoxic and apoptotic activities of the extracts from tubers of *Asphodelus aestivus* Brot. *Afr J Pharm Pharmacol* **11**: 610-621.

- Avelino-Flores M del C, Cruz-López M del C, Jiménez-Montejo FE, Reyes-Leyva J. (2015). Cytotoxic Activity of the Methanolic Extract of *Turnera diffusa* Willd on Breast Cancer Cells. *J Med Food* **18** (3): 299-305.
- Aziz, S. S. S. A., Sukari, M. A., Kitajima, M., Aimi, N. & Ahpandi, N. J. (2010). Coumarins from *Murraya paniculata* (Rutaceae). *Malaysian J Anal Sci* **14**: 1-5.
- Babu-Kasimala, M., Tukue, M. & Ermias, R. (2014). Phytochemical screening and antibacterial activity on two common terrestrial medicinal *Ruta chalepensis* & *Rumex nervosus* *Carib J Sci Tech* **2**: 634-641.
- Badisa, R. B., Darling-reed, S. F., Joseph, P., Cooperwood, J. S., Latinwo L. M., Goodman. C. (2009). Selective cytotoxic activities of two novel synthetic drugs on human breast carcinoma MCF-7 cells. *Anticancer Res* **29**: 2993–2996.
- Bais, S., Abrol, N. (2016). Review on chemistry and pharmacological potential of amentoflavone. *Neuroscience* **6**: 16-22.
- Bakhach, J. (2009). The cryopreservation of composite tissues: Principles and recent advancement on cryopreservation of different type of tissues. *Organogenesis* **5**: 119-126. Protocol for the cryopreservation of cell lines. <https://www.sigmaaldrich.com/technical/biology/cryopreservation-of-cell-lines.html>. Available at 24.03.2018.
- Balci, M. (2005). Basic ¹H- and ¹³C-NMR Spectroscopy. Elsevier, pp. 4-406.
- Barrero, A. F., del Moral, J. F., Herrador, M. M., Akssira, M., Bennamara, A., Akkad, S., Aitigri, M. (2004). Oxygenated diterpenes and other constituents from Moroccan *Juniperus phoenicea* and *Juniperus thurifera* var. *africana* *Phytochemistry* **65**: 2507-2515.

- Barrero, A. F., Herrador, M. M., Arteaga, R., del Moral, J. F. Q., Sanchez-Fernandez, E., Akssira, M., Aitigri, M., Mellouki, F., Akkad, S. (2006). The chemical composition of the essential oil from the leaves of *Juniperus phoenicea* L. from North Africa. *J Ess Oil Res* **18**: 168-169.
- Bekhechi, C., Bekkara, F. A., Consiglio, D., Bighelli, A. & Tomi, F. (2012). Chemical Variability of the Essential Oil of *Juniperus phoenicea* var. *turbinata* from Algeria. *Chem Biodivers* **9**: 2742-2753.
- Bell, P. R. & Hemsley, A. R. (2001). *Green Plants: Their Origin and Diversity*. 2nd ed. New York (NY): Cambridge University Press. P. 349.
- Ben Sghaier, M., Louhichi, T., Hakem, A. & Ammari, Y. (2018). Chemical investigation of polar extracts from *Ruta chalpensis* L. growing in Tunisia: Correlation with their antioxidant activities. *J new sci Agri & Bio* **49**: 2971-2978.
- Benazir, J. F., Suganthi, R., Renjini, Devi M. R, Suganya, K., Monisha, K., Nizar, Ahamed K.P, Santhi R. Benazir J. F., *et al.* (2011). Phytochemical profiling, antimicrobial and cytotoxicity studies of methanolic extracts from *Ruta graveolens*. *J Pharmacy Res* **4**: 1407-1409.
- Bennaoum, Z., Benhassaini, H., Falconieri, D., Piras, A., Porcedda, S. (2017). Chemical variability in essential oils from *Ruta* species among seasons, and its taxonomic and ecological significance. *Nat Prod Res* **31**: 2329-2334.
- Berdowska I., Zieliński B., Fecka I., Kulbacka J., Saczko J., Gamian A. (2013). Cytotoxic impact of phenolics from Lamiaceae species on human breast cancer cells. *Food Chem* **141** (2): 1313-21.
- Bertino, J.R., (1997). Irinotecan for colorectal cancer. *Oncology* **24**: S18-S23.

- Birincioglu, S. S., Avci, H., Birincioglu, B., Epikmene, T., Aksit, H., Aydogana, A. & Chmahl, W. (2015). Experimental neuronal lipofuscinosis in sheep fed with *Asphodelus aestivus* seeds; pathological and ultrastructural investigations. *Revue Méd Vét* **166**: 208-214.
- Boik J. (2001) Natural Compounds in Cancer Therapy. Oregon Medical Press, Minnesota, USA.
- Bozyel, M. E., Akkan, F. R., Merdamert, E. & Demir, N. (2016). Antimicrobial Activity of *Asphodelus aestivus* Brot. Tuber Extracts, 9th Conference on Medicinal and Aromatic Plants of Southeast European Countries, Plovdiv, Bulgaristan, pp 140-140.
- Breitmaier, E. (2002). Structure elucidation by NMR in organic chemistry: A Practical Guide. 3^d edn. John Wiley & Sons, Ltd. PP.1-67.
- Brunton, L. L., Knollmann, B. C. & Chabne, B. A. (2011). Goodman & Gilman's The Pharmacological Basis of Therapeutics. Chemotherapy of Neoplastic Diseases, Cytotoxic Agents; chapter 60, 61. McGraw-Hill Companies. 12th ed, pp. 1671, 1705-1730.
- But, P. P. H., Kimura, T., Gue, J. X. & Sung, C. K. (1997). International collation of traditional and folk medicine. Vol 2. World Scientific Publishing Co. Pte.Ltd., Singapore. pp. 16.
- Cairnes, D.A., Ekundayo, O. & Kingston, D.G. (1980). Plant anticancer agents. X. Lignans from *Juniperus phoenicea*. *J Nat Prod* **43**: 493–497.
- Calis, I., Birincioglu, S., Kirmizibekmez, H. & Pfeifferan, B. J. (2006). Secondary Metabolites from *A. aestivus*. *Z Naturforsch* **61**: 1304-1310.

- Campelo, P., Fonseca S. F. (1975). Diterpenes from *Araucaria angustifolia*. *Phytochemistry* **14**: 2299–2300.
- Canel, C., Moraes, R. M., Dayan, F. E. & Ferreira, D. (2000). "Podophyllotoxin". *Phytochemistry* **54**: 115-120.
- Carbonezi C. A., Hamerski, L., Gunatilaka, A. A. L., Cavalheiro, A., Gamboa, I. C., Silva, S. D. H., Furlan, M., Young, M. C. M., Lopes, M. N., Bolzani, V. S. (2007). Bioactive flavone dimers from *Ouratea multiflora* (Ochnaceae) Carlos Alberto. *Brazilian J pharmacog* **17** (3): 319-324.
- Cardoso-Lopes, E. M., Maier, J. A., Da Silva, M. R., Regasini, L. O., Simote, S. Y., Lopes, N. P., Pirani, J. R., Bolzni, V. S., Young, M. C. M. (2010). Alkaloids from stems of *Esenbeckia leiocarpa* Engl. (Rutaceae) as a potential treatment for Alzheimer disease. *Molecules* **15**: 9205-9213.
- Carlos Andres, C. A., Coy Barrera, E. D., Granados Falla, D. S., Delgado Murcia, G. & Cuca Suarez, L. E. (2011). Seco-Limonoids and quinoline alkaloids from *Raputia heptaphylla* and their antileishmanial activity. *Chem Pharm Bull* **59**: 855-859.
- Champavier, Y., Comte, G., Vercauteren, J., Allais, D. P., Chulia, A. J. (1999). Nortriterpenoid and sesquiterpenoid glucosides from *Juniperus phoenicea* and *Galega officinalis*. *Phytochemistry* **50**: 1219-1223.
- Chan, F.K. M, Moriwaki K., and De Rosa M. J. (2013). Detection of necrosis by the release of lactate dehydrogenase (LDH) Activity, *Methods Mol Biol* **979**: 65–70.
- Chaturvedula, V. S. P. & Prakash, I. (2013). Flavonoids from *Astragalus propinquus*. *J Chem Pharm Res* **5** (1): 261-265.

- Chen, C. C., Yu-Lin Huang, Fei-In Huang, Chun-Wen Wang, and Jun-Chih Ou. (2001). Water-Soluble Glycosides from *Ruta graveolens*. *J Nat Prod* **64**: 990-992.
- Chima, N. K., Nahar, L., Majinda, R. R. T., Celik, S. and Sarker, S. D. (2014) Assessment of free-radical scavenging activity of the extracts and fractions of *Gypsophila pilulifera*: Assay-guided isolation of the active component, *Brazilian J Pharmacognosy* **24**: 38-43.
- Christenhusz, M. J. M. & Byng, J. W. (2016). "The number of known plants species in the world and its annual increase". *Phytotaxa*. Magnolia Press. **26**: 201–217.
- Chunyan, C., Bo, S., Ping, L. (2009). Isolation and purification of psoralen and bergapten from *ficus carica* leaves by high-speed countercurrent chromatography. *J Liq Chromatogr Relat Technol* **1**: 136–143.
- Comte G, Chulia AJ, Vercauteren J, Allais DP. (1996). Phenylpropane glycosides from *J. phoenicea*. *Planta Med.* **62**: 88-9.
- Comte, G., Allais, D. P., Simon, A., Essaady, D., Chulia, A. J., Delage, C., Saux, M. (1995). Crystal-structure of sandaracopimaric acid, a lipoxygenase inhibitor from *Juniperus Phoenicea*. *J Nat Pro L* **58**: 239-243.
- Comte, G., Vercauteren, J., Chulia, A. J., Allais, D. P. & Delage, C. (1997). Phenylpropanoids from leaves of *Juniperus phoenicea*. *Phytochemistry.* **45**: 1679-82.
- Cooper, G.M. (2000). *The Cell: A molecular approach*. 2nd ed. Sunderland, M.A.: Sinauer Associates; The development and causes of cancer. Available from: <https://www.ncbi.nlm.nih.gov/books/NBK9963>.
- Cooposamy, R. M. & Magwa, M. L. (2006). Antibacterial activity of chrysophanol

- isolated from *Aloe excelsa* (Berger). *Afri J Biotech* **5** (16): 1508-1510.
- Cosentino, S., Barra, A., Pisano, B., Cabizza, M., Pirisi, F. M., Palmas, F. (2003). Composition and antimicrobial properties of Sardinian *Juniperus* essential oils against foodborne pathogens and spoilage microorganisms. *J Food Prot* **66**: 1288-1291.
- Cragg, G. M. & Newman, D. J. (2005). Plants as a source of anti-cancer agents. *J Ethnopharmacol* **100**: 72–79.
- Creemers, G.J., G. Bolis, M. Gore, G. Scarfone & A.J. Lacave et al., (1996). Topotecan, an active drug in the second-line treatment of epithelial ovarian cancer: Results of a large European phase II study. *J Clin Onc* **14**: 3056-3061.
- Csuk, R. (2012). Targeting Cancer by betulin and betulinic acid (Chapter 11), Novel apoptotic regulators in carcinogenesis. P. 267-287.
- Dagne E & Abiy Yenesew. (1994). IUPAC Anthraquinones and chemotaxonomy of the Asphodelaceae *Pure & Appl. Chem* **66**: 2395-2398. Printed in Great Britain.
- Danielsen, K., Aksnes, D. W., Francis, G. W. (1992). NMR study of some anthraquinones from rhubarb. *Magnetic Resonance in Chem* **30** (4): 359-60.
- Darwish F.M. & Reinecke M. G. (2003). Ecdysteroids and other constituents from *Sida spinosa* L. *Phytochemistry* **62** (8): 1179-1184.
- Das, N. M., Mohan, V. R., Parthipan, B. P. (2015). Isolation, purification and characterization of arbutin from *Cleidion nitidum* (Muell. Arg.) Thw. ex Kurz. (Euphorbiaceae), *IJSR* **5** (11). www.ijsr.net.
- Davin, L. B., Lewis, N. G. (2000) Dirigent proteins and dirigent sites explain the mystery of specificity of radical precursor coupling in lignan and lignin

- biosynthesis. *Plant Physiol* **123**: 453–461.
- Dawidar, A.M., Ezmirly, S. T., Abdel-Mogib, M. (1991). Sesquiterpenes and diterpenes from *Juniperus phoenicea* L., *Pharmazie* **46**: 472-473.
- Demirgan, R., Karagöz, A., Pekmez, M., Önay-Uçar, E., Fulya T. Gürer, A., C. and Mat, A. (2015). In Vitro Anticancer Activity and Cytotoxicity of Some Papaver Alkaloids on Cancer and Normal Cell Lines. *Mitteilungen Klosterneuburg* **65** (4): 275-284.
- De Natale, A. & Pollio A. (2012). A forgotten collection: the Libyan ethnobotanical exhibits (1912-14) by A. Trotter at the Museum O. comes at the University Federico II in Naples, Italy. *J Ethno bio Ethnomed* **8**: 4.
- Derwich, E., Benziane, Z. & Boukir, A. (2010). The chemical composition of leaf essential oil of *Juniperus phoenicea* and evaluation of its antibacterial activity. *Int J Agric Biol* **12**: 199–204.
- Dos Santos R. N. & de Vasconcelos Silva M. G. (2008). Constituintes químicos do caule de *Senna reticulata* Willd. (Leguminosae). *Quim Nova* **31** (8): 1979-1981.
- Edhun K. & Qian H.E. (2010). Aloe Vera: A Valuable Ingredient for the Food, Pharmaceutical and Cosmetic Industries—A Review, *Crit Rev Food Sci Nutr* **44**: 91-96.
- El Darier, S. M. & El-Mogaspi, F. M. (2009). Ethnobotany and Relative Importance of Some Endemic Plant Species at El-Jabal El-Akhdar Region Libya). *World J Agri Sci* **5**: 353-360.
- El Hawary, S. S., El Shabrawy, A., Ezzat, S. M., El-Shibani, F. A. (2016). Evaluation of the Phenolic and Flavonoid Contents, Antimicrobial and Cytotoxic Activities of Some Plants Growing in Al Jabal Al-Akhdar in Libya. *Int J Pharmacol &*

Phytol Res **8**: 1083-1087.

El Mistiri, M., Salati, M., Marcheselli, L., Attia, A., Habil, S., Alhomri, F., Spika, D., Allemani, C. & Federico, M. (2015). Cancer incidence, mortality, and survival in Eastern Libya: an updated report from the Benghazi Cancer Registry. *Ann Epidemiol* **25**: 564-8.

El Sayed, K., Al-Said, M. S., El-Feraly F. S., & Ross, S. A. (2000). New Quinoline Alkaloids from *Ruta chalepensis*. *J Nat Prod* **63**: 995-997.

El Shibani, F. A. (2017). A Pharmacognostical Study of *Arbutus pavarii* Pampan Family Ericaceae and *Sarcopoterium spinosum* L. Family Rosaceae Growing in Libya. Ph.D. Thesis in Pharmaceutical Sciences (Pharmacognosy), Cairo University, chapter 3.

El-Fattah, H. A., El-Halim, O. B. A., Nagaya, H., Takeya & K. Itokawa, H. (1997). Cytotoxic bianthrone C-glycosides from *Asphodelus aestivus* tubers. *Alex J Pharm Sci* **11**: 77-81.

Elmezogi, J., Ben Hussein, G., Cadmour, M., Abdolgader, A. & Erhuma, M. (2013). Cytotoxic activity of selected Libyan medicinal plants on human breast adenocarcinoma cell Line [MCF-7]. *Indo J Pharm* **24**: 127-130.

Elmhdwi, M. F., Attitalla, I. H. & Khan, B. A. (2015). Evaluation of antibacterial activity and antioxidant potential of different extracts from the leaves of *Juniperus phoenicea*. *J Plant Patho Microb* **9**: 2157-7471.

El-Mokasabi, F. M (2014). The state of the art of traditional herbal medicine in the Eastern Mediterranean Coastal Region of Libya. *Middle East J Sci Res* **21**: 575-582.

- Elmore, S. (2007). Apoptosis: A review of programmed cell death. *Toxicol Pathol* **35**: 495–516.
- El-Sawi, S. A. & Motawae H. M. (2008). Labdane, Pimarane and Abietane diterpenes from the fruits of *Juniperus phoenicea* L. grown in Egypt and their activities against human liver carcinoma. *Can.J Pure and Appl Sci* **2**:115-122.
- El-Sawi, S. A., Motawae, H. M. & Ali, A. M. (2007). Chemical composition, cytotoxic activity and antimicrobial activity of essential oils of leaves and berries of *Juniperus phoenicea* grown in Egypt. *Afr J Tradit Compl. Altern Med* **4**: 417-26
- El-Sawi, S. A., Motawae, H. M., Sleem, M. A., El-Shabrawy, A. R., Sleem, A. & Ismail, M. A. (2013). Phytochemical screening, investigation of carbohydrate contents, and antiviral activity of *Juniperus phoenicea* L. growing in Egypt. *J Her Spi Med Pl* **20**: 83-91.
- Emam, A. M., Swelam, S., Megally, N. Y. (2009). Furocoumarin and quinolone alkaloid with larvicidal and antifeedant activities isolated from *Ruta chalepensis* leaves. *J Nat Prod* **2**: 10-22.
- Emam, A., Eweis, M. & Elbadry, M. (2010). A new furoquinoline alkaloid with antifungal activity from the leaves of *Ruta chalepensis* L., *Drug Disc Ther* **4**: 399-404.
- Emerole G, Thabrew MI, Anosa V, Okorie DA. (1981). Structure-activity relationship in the toxicity of some naturally occurring coumarins-chalepin, imperatorin and oxypeucedanine. *Toxicol* **20**:71–80.
- Encyclopedia Britannica Online Academic Edition. Encyclopedia Britannica Inc., (2012). <http://www.britannica.com/EBchecked/topic/250316/gymnosperm>

- Ennajar, M, Bouajila J, Lebrihi, A., Mathieu, F., Savagnac, A., Abderraba, M., Raies, A. & Romdhane, M. (2010). The influence of organ, season and drying method on chemical composition and antioxidant and antimicrobial activities of *Juniperus phoenicea* L. essential oils. *J Sci Food Agric* **90**: 462-70.
- Ennajar, M., Bouajila, J., Lebrihi, A., Mathieu, F., Abderraba, M., Raies, A. & Romdhane, M. (2009). Chemical composition and antimicrobial and antioxidant activities of essential oils and various extracts of *Juniperus phoenicea* L. (Cupressaceae). *J Food Sci.*, **74**: 364-71.
- Espinosa, E., Zamora, P., Feliu, J., Barón, M. G. (2003). Classification of anticancer drugs—a new system based on therapeutic targets. *Cancer Treat Rev* **29**: 515-523.
- Evans, A. (2003). *In vitro* and *ex vivo* studies on the toxicity and efficacy of a selection of non-viral transfection reagents. Thesis (PhD) Liverpool John Moores University, P. 32-34.
- Fafal, T., Yilmaz, F. F., Birincioğlu, S. S., Hoşgör-Limoncu, M. & Kivçak, B. (2016). Fatty acid composition and antimicrobial activity of *Asphodelus aestivus* seeds. *H V M Bioflux* **8**, 103-107.
- Faguet, G. B. (2015). A brief history of cancer: age-old milestones underlying our current knowledge database. *Int J Cancer* **136**: 2022-36.
- Fatma, W., H.M. Taufeeq, W.A. Shaida and W. Rahman. (1979). Biflavanoids from *Juniperus macropoda* Boiss. and *Juniperus phoenicea* Linn. (Cupressaceae). *Indian J Chem* **17**: 193-194.

- Fonseca, S. F., Rúveda, E. A., Chesney, J. D. (1980). ^{13}C NMR analysis of podophyllotoxin and some of its derivatives. *Phytochem.*, 19, (7): 1527-1530.
- Fujita, T., Kadoya, Y., Aota, H., Nakayama, M. (1995). A New Phenylpropanoid Glucoside and other constituents of *Oenanthe javanica*. *Biosci Biotechnol Biochem*, **59** (3): 526-528.
- Gencsoylu, L. (2009). An extract from *Asphodelus aestivus* brot. showing toxicity against tetranychus cinnabarinus boisd., the carmine spider mite. *Fresenius Environmental Bulletin* **18**: 519-523.
- Ghosh, S., Bishayee, K., Khuda-Bukhsh, A. R. (2014). Graveoline isolated from ethanolic extract of *Ruta graveolens* triggers apoptosis and autophagy in skin melanoma cells: a novel apoptosis-independent autophagic signaling pathway. *Phytother Res* **28** (8):1153-62.
- González, M. A., Guaita D. P., Royero, J. C., Zapata, B., Agudelo, L., Arango, A. M., Galvis, L. B. (2010). Synthesis and biological evaluation of dehydroabietic acid derivatives. *Euro J Med Chem* **45**: 811-816.
- González-elizondo, M.S., González-elizondo, M., Sørensen, P. D. (2012). *Arbutus bicolor* (Ericaceae, Arbutae), A new species from Mexico. *Acta Botanica Mexicana* **99**: 55-72.
- Gordaliza, M., Garcia, P. A., del Corral, J. M., Castro, M. A. & Gomez-Zurita, M. A. (2004). Podophyllotoxin: Distribution, sources, applications and new cytotoxic derivatives. *Toxicon* **44**: 441–459.
- Gray, A. I., Igoli, J. O., Edrada-Ebel, R. (2012). Natural products isolation in modern drug discovery programs. *Meth. Mol Biol* **864**:515-534.
- Gunaydin, K. & Savci, S., (2005). Phytochemical studies on *Ruta chalepensis* (LAM.)

- Lamarck. *Nat Prod Res* **19**: 203–210.
- Han, K., Meng, W., Zhang, J. J., Zhou, Y., Wang, Y. L., Su, Y., Lin, S., Gan, Z., Sun, Y., Min, D. (2016). Luteolin inhibited proliferation and induced apoptosis of prostate cancer cells through miR-301. *Onco Targets Ther* **9**: 3085–3094.
- Hasan, H. H. Habib, I. H., Gonaid, M. H. & Islam, M. (2011). Comparative phytochemical and antimicrobial investigation of some plants growing in Al Jabal Al-Akhdar. *J Nat Prod Plant Resour* **1**: 15-23.
- Hegazy, A. K, Al-Rowaily, S. L., Faisal, M., Alatar, A. A, El-Bana, M. I. & Assaeed, A. M. (2013). Nutritive value and antioxidant activity of some edible wild fruits in the Middle East. *J Med Plants Res* **7**: 938-946.
- Heinrich, M., Barnes, J., Garcia, J. P., Gibbons, S. & Williamson, E. M. Fundamentals of Pharmacognosy and Phytotherapy E-Book (2018). 3rd ed., Churchill Livingstone P. 39.
- Himes, R. H. (1991). Interactions of the Catharanthus (Vinca) alkaloids with tubulin and microtubules. *Pharmacol Ther* **51**: 257–67.
- Hirschmann, G. S., Aranda, C., Kurina, M., Rodríguez, J. A., Theoduloz, C. (2007). Biotransformations of imbricatolic acid by *Aspergillus niger* and *Rhizopus nigricans* cultures *Molecules* **12** (5):1092-1100.
- Hortasa, L., L., Larrána, P. P., González-Muñoz, M. J. , Falqué, E., Domínguez, H. (2018). Recent developments on the extraction and application of ursolic acid. A review. *Food Res Int* **103**: 130–149.
- Houssen, W. E. & Jaspars A. M. (1998). Isolation of Marine Natural Products. Natural Products Isolation. 2nd ed., P. 365-408.

<http://www.botanicus.org/item/31753000802832>

<http://www.botanicus.org/title/b12069590>, (both accessed 2011.01.16).

- Huang, Q., Lu, G., Shen, H. M., Chung M. C. & Ong, C. N. (2007). Anti-Cancer Properties of Anthraquinones from Rhubarb. *Medicinal Research Reviews* **27**: 609: 630.
- Hussein, S.A.M., Merfort, L. & Nawwar, M.A.M. (2003). Lignans and other phenylpropanoids from leaves of *Juniperus phoenicea*. *J Saudi Chem Soci* **7**: 105-110.
- Ibrahim T. A., El-Hela, A. A. El-Hefnawy H. M., Areej, M. Al-Taweel, A. M. & Perveen, S. (2017). Chemical composition and antimicrobial activities of essential oils of some coniferous plants cultivated in Egypt. *Iran J Pharm Res* **16**: 328–337.
- Jin, H. G., Ko, H. J., Chowdhury, M. A., Lee, D. S., Woo, E. R. (2016). A new indole glycoside from the seeds of *Raphanus sativus*. *Arch Pharm Res* **39**:755–761.
- Kangshan, M., Gang, H., Jianquan, L., Adams, R. P., Milne, R. I. (2010). Diversification and biogeography of *Juniperus* (Cupressaceae): variable diversification rates and multiple intercontinental dispersals. *New Phytologist* **188**: 254-272.
- Kartesz, J., Brouillet, L., Egan, R., Anderso, L., McMullen, M., Stotler, R. & Crandall, B. (2018). USDA, NRCS. The PLANTS Database (<http://plants.usda.gov>), National Plant Data Team, Greensboro, NC 27401-4901 USA, 25 January.
- Kaushal, C.K. & Srivastava, B., (2010). A process of method development: A chromatographic approach. *J Chem Pharm Res* **2** (2):519-545.

- Kessler, H., Gehrke, M., Griesinger, C. (1988). Two-dimensional NMR spectroscopy, principles and survey of the experiments, *Ang. Chem* **100** (4): 507- 54.
- Khelifi, D., Sghaier, R. M., Amouri, S., Laouini, D., Hamdi, M. & Bouajila, J. (2013). Composition and antioxidant, anti-cancer and anti-inflammatory activities of *Artemisia herba-alba*, *Ruta chalapensis* L. and *Peganum harmala* L. *Food Chem Toxicol* **55**: 202–208.
- Kingston, D. G. I., (2005). Taxol and its analogs. In: Cragg, G.M., Kingston, D.G.I., Newman, D.J. (Eds.). *Anticancer agents from natural products*. Chapter 6.
- Kipling, M. D. Waldron., H. A. (1975). Percivall Pott and cancer scroti. *Br J Ind Med* **32**: 244-6.
- Kong, Y. C., Lau, C. P., Wat, K. H., Ng, K.H., But, P. P., Cheng, K. F. (1989). Antifertility principle of *Ruta graveolens*. *Planta Med* **55**: 176–8.
- Korulkin, D. U. & Muzychkina, R. A. (2014). Biosynthesis and Metabolism of Anthraquinone Derivatives. *Int J Chem and Mol Engin* **8**: 454-457.
- Kostova, I. A., Ivanova, B., Mikhova, B. & Klaiber, I. (1999). Alkaloids and coumarins from *Ruta graveolens*. *Monatsh Chem* **130**: 703-707.
- Kristanti H., Tunjung, W. A. S. (2015). Detection of alkaloid, flavonoid, and terpenoid compounds in bread (*Artocarpus communis* Forst.) leaves and pulps. ISSN 2413-0877. **2**: 129-133.
- Kuete, V., Karaosmanoğlu O., Sivas H. (2017). Chapter 10 – Anticancer Activities of African Medicinal Spices and Vegetables. *Medicinal Spices and Vegetables from Africa. Therapeutic Potential Against Metabolic, Inflammatory, Infectious and Systemic Diseases*. P. 271–297.

- Kuetea V., Viertel, K., Efferth T. (2013). Antiproliferative potential of African medicinal plants chapter 18, pharmacology and chemistry, *Med Plant Res in Africa*. P. 711–724.
- Kuhlmann, S, K. Kranz, B. Lücking, A.W. Alfermann & Petersen, M. (2002). Aspects of cytotoxic lignan biosynthesis in suspension cultures of *Linum nodiflorum*. *Phytochemistry Reviews* **1**: 37–43.
- Latif, A., Amer, H. M., Hamad, M. E., Alarifi, S. A. R., & Almajhdi, F. N. (2014). Medicinal plants from Saudi Arabia and Indonesia: *In-vitro* cytotoxicity evaluation on Vero and HEp-2 cells, *Journal of Medicinal Plants Research*, **8** (34): 1065-1073.
- Lee, E. C. (1965). A pharmacognostic study of the root of *heracleum mantegazzij*. num somier et levier. M. S. in Pharmacognosy, P. 50
- Lee, K. H. & Xiao, Z., (2005). Podophyllotoxins and analogs. In: Cragg, G. M., Kingston, D.G.I., Newman, D.J. (Eds.), *Anticancer agents from natural products*. Chapter 5. Brunner-Routledge Psychology Press, Taylor & Francis Group, Boca Raton, FL, pp. 71–88.
- Lee, M. S., Cha, E. U., Sul, J. Y., Song I. S., Kim, J. Y. (2011). Chrysophanic acid blocks proliferation of colon cancer cells by inhibiting EGFR/mTOR Pathway. *Phytother Res* **25**: 833–837.
- Lewis, J. R. (1983). The biological activity of some Rutaceous compounds. In: Waterman P.G., Grundon M.F., editors. *Chemistry and Chemical Taxonomy of Rurales*. London: Academic Press; pp. 301-318.
- Linnaeus. (1753). The Gymnosperm Database, *Juniperus*: 1038.

- List, P. & Horhammer, L. (1979). *Handbuch der Pharmazeutischen Praxis*. Berlin: Springer-Verlage.
- Liu, L. F. (1989). DNA topoisomerase poisons as antitumor drugs. *Annu Rev Biochem* **58**: 351–75.
- Louhaichi, M., Salkini, A. K., Estita, H. E. & Belkhir, S. (2011). Initial Assessment of Medicinal Plants Across the Libyan Mediterranean Coast *Advan Environm Biol* **5**: 359-370.
- Lovelock, J. E. & Bishop, M. W. H. (1959). Prevention of freezing damage to living cells by dimethyl sulphoxide. *Nature*, **183**: 1394–1395.
- Lu, L. Zhang, M.S. Wai, D.T. Yew, J. Xu. (2012). Exocytosis of MTT formazan could exacerbate cell injury. *Toxicol In Vitro* **26** (4): 636–644.
- Mabry, T. J., Markham, K. R., Thomas, M. B. (1970). The systematic identification of flavonoids. Springer-Verlag, New York. Heidelberg. Berlin. P. 41-57.
- Mahavorasirikul W, Viyanant V, Chaijaroenkul W, Itharat A, Na-Bangchang K. (2010). Cytotoxic activity of Thai medicinal plants against human cholangiocarcinoma, laryngeal and hepatocarcinoma cells *in vitro*. *BMC Complement Altern Med* **10**:55.
- Majdoub, O., Dhen, N., Souguir, S., Haouas, D., Baouandi, M., Laarif, A. & Chaieb, I. (2014). Chemical composition of *Ruta chalepensis* essential oils and their insecticidal activity against *Tribolium castaneum*. *Tunis J Plant Prot* **9**: 83-90.
- Mahavorasirikul, W., Viyanant, V., Chaijaroenkul, W., Itharat, A., Na-Bangchang, K. (2010). Cytotoxic activity of Thai medicinal plants against human cholangiocarcinoma, laryngeal and hepatocarcinoma cells *in vitro*. *BMC Complement Altern Med* **10**:55.

- Malmir, M., Serrano, R., Caniça, M., Silva-Lima, B., Silva, O. (2018). A Comprehensive review on the medicinal plants from the genus *Asphodelus*. *Plants* **7** (20): doi:10.3390/7010020.
- Mandal, S., Nayak, A., Kar, M., Banerjee, S. K., Das, A., Upadhyay, S. N., Singh, R. K., Banerji, A., Banerji, J. (2010). Antidiarrhoeal activity of carbazole alkaloids from *Murraya koenigii* Spreng (Rutaceae) seeds. *Fitoterapia* **81**: 72-74.
- Manju, K., Jat, R. K. & Anju, G. (2012). Review of medicinal plants used as a source of anticancer agents. *Int J Drug Res Tech* **2**: 177-183.
- markers in extant conifers- A review. *The Botanical Review*. 67:141- 238.
- Markham KR, Sheppard C, Geiger H (1987). ¹³C NMR studies of some naturally occurring amentoflavone and hinokiflavone biflavonoids. *Phytochemistry* **26**: 3335-3337.
- Martínez-Pérez, E. F., Hernández-Terán, F. & Benjamín, L. (2017). In vivo effect of *Ruta chalepensis* extract on hepatic cytochrome 3 A1 in rats. *Afr. J. Tradit. Complement Altern Med*. **14**: 62-68.
- Matsuura, K., Canfield, K., Canfield, W. M. & Kurokawa M. (2016). Metabolic regulation of apoptosis in cancer. International review of cell and molecular biology, **327**: 43-87.
- Mazari, K., Bendimerad, N., Bekhechi, C. & Fernandez, X. (2010). Chemical composition and antimicrobial activity of essential oils isolated from Algerian *Juniperus phoenicea* L. and *Cupressus sempervirens* L. *J. of Medici Pl Res* **4**: 959-964.
- Mejrib, J. A. & Mejria, M. M. (2010). The chemical composition of the essential oil of *Ruta chalepensis* L. Influence of drying, hydrodistillation duration, and plant

- parts. *Indus Crops & Prod* **32**: 671-673.
- Miguel, M. G., Faleiro, M. L., Guerreiro, A. C. & Antunes, M. D. (2014). *Arbutus unedo* L, Chemical and Biological Properties. *Molecules* **19**: 15799-15823.
- Mishra, T., Arya, R. K., Meena, S., Joshi, P., Pal, M., Meena, B., Upreti D. K., Rana T.S., Datta, D. (2016). Isolation, characterization and anticancer potential of cytotoxic triterpenes from *Betula utilis* bark. *PLoS One* **11** (7): e0159430. doi:10.1371/journal.pone.0159430.
- Molnar, J., Ocsosvzki, I., Puskas, L., Ghane, T., Hohmann, J., Zupko, I. (2013). Investigation of the antiproliferative action of the quinoline alkaloids kokusaginine and skimmianine on human cell lines. *Current Signal Transduction Therapy*. **8** (2): 148 – 155.
- Morte, M. & Honrubia, M. (1996). *Tetraclinis articulata* (Cartagena Cypress) In Bajaj Y. P. S. (editors). *Biotechnology in Agriculture and forestry*. Vol. 35., Springer-Heidelberg: Berlin, pp. 407–23.
- Moser, B. R. (2008). Review of cytotoxic cephalostatins and ritterazines: isolation and synthesis. *J Nat Prod* **71**: 487-91.
- Mosmann, T. (1983). Rapid colorimetric assay for cellular growth and survival: application to proliferation and cytotoxicity assays. *J Immunol Meth*, **65**: 55-63.
- Moudi, M., Rusea, G., Yien CYS & Nazre. M. (2013). Vinca alkaloids. *Int J Prev Med* **4**: 1231–1235.
- Muranaka, T., M. Miyata, K. Ito, K., Tachibana, S. (1998). Production of podophyllotoxin in *Juniperus chinensis* callus cultures treated with oligosaccharides and biogenetic precursor. *Phytochemistry* **49**: 491-496.

- Musiliyu, M., Badisa V. D., latinwo, L. M., Waryob. C., Ugochukwu, N. (2010). *In vitro* cytotoxicity of benzopyranone derivatives with basic side chain against human lung cell lines. *Anticancer Res* **30**: 4613-4618.
- Myanmar Medicinal Plant Database. Updated (2006). <http://keyserver.lucidcentral.org/keyserver/data/04030b0401024b0c8e070e0105010a0f/media/Html/Asphodelaceae.htm>
- Nahar, L., & Sarker, S. (2012). Steroid dimers: Chemistry and applications in drug design and delivery. Chichester: Wiley. P. 242-286.
- Nakano, D., Ishitsuka, K., Matsuda, N. Ai Kouguchi, A., Tsuchihashi R., Okawa, M., Okabe, H., Tamura, K., Kinjo, J. (2017) Screening of promising chemotherapeutic candidates from plants against human adult T-cell leukemia/lymphoma (V): coumarins and alkaloids from *Boenninghausenia japonica* and *Ruta graveolens*, *J Nat Med* **71** (1) : 170–180.
- Nakata, H., Sashida, Y., Shimomura, H. (1982). A new phenolic compound from *Heracleum lanatum* Michx. var. *nippinicum* Hara. *Chem Pharm Bull* **30** (12):4554-4556.
- Nautiyal, O. H. (2013). Natural products from the plant. Microbial and marine species. *The Experiment* **10**: 611-646.
- Nemati, F, Dehpouri A, Eslami B, Mahdavi V, Mirzanejad S. (2013). Cytotoxic properties of some medicinal plant extracts from Mazandaran, Iran *Iran Red Crescent Med J* **15**: e8871.
- Newman D. J. and Cragg, G. M. (2017). Current Status of Marine-Derived Compounds as Warheads in Anti-Tumor Drug Candidates. *Mar. Drugs* **15**(4): 99

- Ni'ciforovi'c, N. and Abramovi, H. (2014). Sinapic Acid and Its Derivatives: Natural Sources and Bioactivity. *Compr Rev Food Sci Food Saf* **13**: 34-51.
- Nijveldt, R. J., Nood, E. V., Hoorn, D. V., Boelens, P. G., Norren, K. V., Leeuwen, P. V. (2001). Flavonoids: a review of probable mechanisms of action and potential applications. *Am J Clin Nutr* **74**: 418–425.
- Ntalli, N. G., Manconi, F., Leonti, M., Maxia, A. & Caboni, P. (2011). Aliphatic ketones from *Ruta chalepensis* (Rutaceae) induce paralysis in root-knot nematodes. *J Agric Food Chem* **59**: 7098-103.
- Otto, A., Wilde V. (2001). Sesqui-, di-, and triterpenoids as chemosystematic markers in extant conifers—a Botanical review, **67** (2): 141-238.
- Öztürk, M., Tümen, I., Uğur, A., Aydoğmuş-Öztürk, F., Topçu, G., (2011). Evaluation of fruit extracts of six Turkish Juniperus species for their antioxidant, anticholinesterase, and antimicrobial activities. *J Sci Food Agric* **91**: 867–876.
- Park, J. H., Kwon, H. Y., Sohn, E. J., Kim, K. A., Kim, B., Jeong, S. J., Song, J. H., Koo, J. S., Kim, S. H. (2013). Inhibition of Wnt/ β -catenin signaling mediates ursolic acid-induced apoptosis in PC-3 prostate cancer cells. *Pharmacol Rep* **65** (5): 1366-74.
- Patel, S., Geewala, N., Suthar, A., Shah, A. (2009). In-vitro cytotoxicity activity of Solanum nigrum extract against HELA cell line and VERO cell line. *Int J Pharm & Pharm Sci* **1**: 38-46.
- Pavlović, D., Lakušić, B., Kitić, D., Milutinović, M. & Kostić, M. (2014). Antimicrobial activity of selected plant species of Genera *Arbutus* L., *Bruckent halia* Rechb. *Calluna* Salisb. and *Erica* L. (Ericaceae). *Sci J Fac Med Niš* **31**: 81-85.

- Payne, S., Miles, D. (2008). Chapter 4. Mechanisms of anticancer drugs. CRC Press, p. 34-46.
- Peksel, A , Imamoglu, S., Kiymaz, N. A. & Orhan, N. (2013). Antioxidant and radical scavenging activities of *Asphodelus aestivus* Brot. Extracts. *Int J Food Prop* **16**: 1339-1350.
- Peksel, A., Altas-Kiymaz & N., Imamoglu, S. (2012). Evaluation of antioxidant and antifungal potential of *Asphodelus aestivus* Brot. growing in Turkey. *J Med Plants Res* **6**: 253-265.
- Petrillo, A. D., González-Paramás, A. N., Era, B., Medda, R., Pintus, F., Santos-Buelga, C. & Fais, A. (2016). Tyrosinase inhibition and antioxidant properties of *Asphodelus microcarpus* extracts. *BMC. Complemen Altern Med* **16**: 453.
- Phonde, R.Y. & Magdum, C.S. (2015). Hyphenated Techniques: an overview. *Inter J Univ Pharm Bio Sci* **4** (3): 2319-8141.
- Polatoğlu, K., Demirci, B., Can Başer KH. (2016). High amounts of *n*-alkanes in the composition of *A. aestivus* Brot. flower essential oil from Cyprus. *J Oleo Sci* **65**: 867-870.
- Pollio, A., A. De Natale, E. Appetiti, G., Aliotta & Touwaide. A. (2008). Continuity and change in the Mediterranean medical tradition: *Ruta* spp. (Rutaceae) in Hippocratic medicine and present practices. *J Ethnopharmacol* **116**: 469–482.
- Prakash, A. O. (1986). Potentialities of some indigenous plants for antifertility activity, *Int J Crude & Drug Res* **24**: 19-24.
- Pretsch, E. and Clerc, J.T. (1997). Spectra Interpretation of Organic Compounds, Weinheim, VCH.

- Priyadarshini, K. & Aparajitha k. U. (2012). Paclitaxel against cancer: A short review. *Med Chem* **2**: 139-141.
- Qnais, E. Y., bdulla F. A. & Abu Ghalyun, Y. Y. (2005). Antidiarrheal effects of *Juniperus phoenicia* L. leave extract in rats. *Pak J Bio Sci* **8**: 867-871.
- Quintanilla-Licea, R., Mata-Cárdenas, B. D., Vargas-Villarreal, J., Bazaldúa-Rodríguez, A. F., Ángeles-Hernández, I. K., Garza-González, J. N., Hernández-García M. E. (2014). Antiprotozoal activity against *Entamoeba histolytica* of plants used in Northeast Mexican traditional medicine. Bioactive compounds from *Lippia graveolens* and *Ruta chalepensis*. *Molecules* **19** (12): 21044-21065.
- Radha M.H. & Laxmipriya N.P. (2015). Evaluation of biological properties and clinical effectiveness of Aloe vera: A systematic review. *J Tradit Complement Med* **5**: 21–26.
- Rahier, N. J., Thomas, C. J. & Hecht, S. M. (2005). Camptothecin and its analogs. In *Anticancer Agents from Natural Products*, Cragg, G. M., Kingston, D. G. I., Newman, D. J. 2nd edn. Taylor & Francis: Boca Raton, Fl, 5–22.
- Rahman, A. and Choudhary, M. I. (1996). *Solving Problems with NMR Spectroscopy*, Academic Press. PP. 213-343.
- Rajkumar, S. & Jebanesan, A. (2008). Bioactivity of flavonoid compounds from *Poncirus trifoliata* L. (Family: Rutaceae) against the dengue vector, *Aedes aegypti* L. (Diptera: Culicidae). *Parasitol Res* **104**: 19- 25.
- Ramdani, M., Lograda, T., Silini, H., Zeraib, A., Chalard, P. *et al.*, (2013). Antibacterial activity of Essential oils of *Juniperus phoenicea* from Eastern Algeria. *J Applied Pharmaceu Sci* **3**: 022-028.

- Rauter, A.P., Palma, F. B., Justino, J., Araújo, M. E. & Santos, S. P. (2013). Natural products in the new millennium: Prospects and industrial application. pringer Science & Business Media, Science. P. 287.
- Rich. ex Bartling. (1830). Cupressaceae. The Gymnosperm Database. assessed on 12/2017.
- Richards, S.A. & Hollerton, J.C. (2011). Essential Practical NMR for Organic Chemistry. 1st edn. <http://eu.wiley.com/> P. 6-10, 42-43.
- Richardson, J.S., Sethi, G., Lee, G.S., Malek, S. N. (2016). Chalepin: isolated from *Ruta angustifolia* L. Pers induces mitochondrial mediated apoptosis in lung carcinoma cells. *BMC Complement Altern Med* **16** (1): 389.
- Riss, T.L., Moravec, R.A., Niles, A.L., Duellman, S., Benink, H.A. Worzella, T.J., Minor, L. (2013). Cell Viability Assays. Assay Guidance Manual [Internet]. Bethesda (MD): Eli Lilly & Company and the National Center for Advancing Translational Sciences; 2004-. Available from: <https://www.ncbi.nlm.nih.gov/books/NBK144065/>
- Rojas-Sepúlveda, A. M., Mendieta-Serrano M., Antúnez Mojica M. Y., Salas-Vidal, E., Marquina S., Luisa Villarreal, M., María Puebla, A., Delgado, J. I. & Alvarez L. (2012). Cytotoxic Podophyllotoxin Type-Lignans from the Steam Bark of *Bursera fagaroides* var. *fagaroides*. *Molecules* **17**: 9506-9519.
- Roy, D. & Rahman, A. H. M. M. (2016). Systematic study and medicinal uses of Rutaceae family of Rajshahi district, Bangladesh. *Plant Environm. Dev* **5**: 26-32.
- Royt, P. W., Honeychuck, R. V., Ravich, V., Ponnaluri, P., Pannell, L. K. Buyer, J. S.,

- Chandhoke, V., Stalick, W. M., DeSesso, L. C., Donohue, S., Ghei, R., Relyea, J. D. and Ruiz, R. (2001) 4-Hydroxy-2-nonylquinoline: A Novel Iron Chelator Isolated from a Bacterial Cell Membrane. *Bio organic Chem* **29**: 387–397.
- Sahranavard, S., Naghibi, F., Ghaffari, S. (2012). Cytotoxic activity of extracts and pure compounds of *Bryonia aspera*. *Int J Pharm Pharm Sci* **4**(3): 541-3.
- Sak, K. (2014). Cytotoxicity of dietary flavonoids on different human cancer types. *Pharmacogn Rev* **8** (16): 122–146.
- San Feliciano, A., M. Gordaliza, J.M.M. del Corral, M.A. Castro, M.D. GarcíaGrávalos P. Ruiz-Lázaro. (1993c). Antineoplastic and antiviral activities of some cyclo lignans. *Planta Medica* **59**: 246-249.
- Sánchez de Medina, F., Gámez, M. J., Jiménez, I., Osuna, J. I., Zarzuelo, A. (1994). Hypoglycemic activity of juniper "berries", *Planta Med* **60**: 197-200.
- Sarker, S.D., Latif Z., Gray A. I. (2005). Natural products isolation; Methods in biotechnology. 2nd ed., Humana Press Inc. P. 133- 377
- Sarker, S.D., Nahar L. (2012). Natural products isolation; Methods in molecular biology. 3rd ed., Humana Press - Springer-Verlag, USA.
- Schmelzer, G. H. & Gurib-Fakim A. (2013). Plant resources of tropical Africa. *Medici Pl* **2**, 417.
- Seca, A. M. L. & Silva, A. M. S. (2007). The Chemical Composition of the Juniperus Genus (1970-2004). Recent Progress in Medicinal Plants, *Phytomedicines* **16**: 401–522.
- Seidel, V., Windhövel, J., Eaton, G., Alfermann, A. W., Arroo, R. R. J., Medarde, M., Petersen, M., Woolley, J. G. (2002). Biosynthesis of podophyllotoxin in *Linum*

- album cell cultures. *Planta* **215**: 1031-1039.
- Severino, V. G., Cazal, C. M., Forim, M. R., da Silva, M. F., Rodrigues-Filho, E., Fernandes, J. B. & Vieira, P. C. (2009). Isolation of secondary metabolites from *Hortia oreadica* (Rutaceae) leaves through high-speed counter-current chromatography. *J Chromatogr A*, **1216**: 4275-4281.
- Shaoguang, L., Meifeng Z., Yuxiang L., Yuxia S., Hong Y., Liying H., Xinhua L. (2014). Preparative isolation of six anti-tumour biflavonoids from *Selaginella doederleinii* Hieron by high-speed counter-current chromatography. *Phytochem Anal* **25**: 127–133.
- Smith, D.L., Liu YM., Wood K.V. (1991) Structure elucidation of natural products by mass spectrometry. In: Fischer N.H., Isman M.B., Stafford H.A. (eds). Modern phytochemical methods. Recent advances in phytochemistry (Proceedings of the phytochemical society of North America), 25. Springer, Boston, MA.
- Song, S., Su, Z., Xu, H., Niu, M., Chen, X., Min, H., Zhang, B., Sun, G., Xie, S., Wang, H., Gao, Q. (2017). Luteolin selectively kills STAT3 highly activated gastric cancer cells through enhancing the binding of STAT3 to SHP-1. *Cell Death and Disease* 8, e2612; doi: 10.1038/cddis.
- Stassi, V., Verykokidou, E., Loukis, A., Harvala, C. & Philianos, S. (1996), The Antimicrobial activity of the essential oils of four Juniperus species growing wild in Greece. *Flavour Fragr J* **11**: 71–74.
- Stevens, P. F. (2001 onwards). "Ericaceae". Angiosperm Phylogeny. Website. Available at <http://www.mobot.org/MOBOT/research/APweb/>. Latest Retrieved 29 December 2014.
- Su, W. C., Fang, J. M., Cheng, Y. S. (1994). Labdanes from *Cryptomeria japonica*.

- Phytochemistry* **37**: 1109- 1114.
- Sudhakar, A. (2009). History of Cancer, Ancient and Modern Treatment Methods. *J Cancer Sci Ther*, **1**, 1-4.
- Supabphol, R. & Tangjitjareonkun, J. (2014). Chemical Constituents and Biological Activities of *Zanthoxylum limonella* (Rutaceae): A Review, *Tropical J Pharm Res* **13**: 2119-2130.
- Swanston-Flatt, S. K., Day C., Bailey, C. J. & Flatt, P. R. (1990). Traditional plants treatments for diabetes. Studies in normal and streptozotocin diabetic mice. *Diabetologia* **33**: 462-464.
- Tabacik, C. and Y. Laporthe. (1971). Diterpenes de *Juniperus phoenica* Constituants majeurs. *Phytochemistry* **10**: 2147-2153.
- Taniguchi, M., Yanai, M., Xiao, YQ. Kido, T., Baba, K. (1996). Three isocoumarins from *Coriandrum sativum*. *Phytochemistry* **42**(3): 843- 846.
- Terkmane, S., Gali, L., Bourrebaba, L., Shoji, K., Legembre, P., Konstantia, G., Ioanna, C. & Bedjou, F. (2017). Chemical composition, antioxidant, and anticancer effect of *Ruta chalepensis*'s extracts against human leukemic cells. *Phytothérapie* 1-12.
- Tesso, H. (2005). Isolation and structure elucidation of natural products from plants, PhD. Thesis at the Institute of Organic Chemistry, University of Hamburg. PP. 19- 24.
- Torre, L. A., Bray, F., Siegel, R. L., Ferlay, J., Tieuvent, J. L. & Jemal, A. (2015). Global cancer statistics. 2012, *Ca Cancer J Clin* **65**: 87–108.
- Treutlein, J. Smith, G. F., Wyk B. V. & Wink, M. (2003). Phylogenetic relationships

in Asphodelaceae (subfamily Alooideae) inferred from chloroplast DNA sequences (rbcL, matK) and from genomic fingerprinting (ISSR). *Taxon* **52**: 193-207.

Tsopmo, A., Awah, F. M., Kuete, V. (2013). Medicinal plant research in Africa. Chapter: 12-lignans and stilbenes from African medicinal plants. Elsevier, P: 435–478

Ulubelen, A. & Güner, H. (1988). Isolation of dehydromoskachen C from *Ruta chalepensis* var. *latifolia*. *J Nat P* **51**: 1012-1013.

Ulubelen, A. & Terem, B. L. (1988). Alkaloids and coumarins from roots of *Ruta chalepensis*, *Phytochemistry* **27**: 650-651.

Ulubelen, A., Ertugrul, L., Birman, H., Yigit, R., Erseven, G., Olgac, V. (1994). Antifertility effects of some coumarins isolated from *Ruta chalepensis* and *R. chalepensis* var. *latifolia* in rodents. *Phytother Res* **8**: 233–236.

USDA, NRCS. (2017). The PLANTS Database, [Online] <http://plants.usda.gov> [Accessed 12th March 2017, 18th April 2017 and 29th October 2017].

Wang, W. S., Li, E. W. & Jia, Z. J. (2002). Terpenes from *Juniperus przewalskii* and their antitumor activities. *Pharmazie* **57**: 343-345.

Wansi, J. D., Wandji, J., Mbaze Meva'a, L., Kamdem Waffo, A. F., Ranjit, R., Khan, S. N., Asma, A., Iqbal, C. M., Lallemand, M. C., Tillequin, F., Fomum, T. Z. (2006). Alpha-glucosidase inhibitory and antioxidant acridone alkaloids from the stem bark of *Oriciopsis glaberrima* ENGL (Rutaceae). *Chem Pharm Bull* (Tokyo), **54**: 292-296.

Wenkert, E., Buckwalter, B. L. (1972). Carbon-13 nuclear magnetic resonance spectroscopy of naturally occurring substances. X. Pimaradienes. *J Am Chem*

Soc **94**: 4367-4369.

Wichtl, M. (1994). *Herbal Drugs and Phytopharmaceuticals*. Medpharm, Scientific Publishers, Stuttgart, pp. 283.

Wickramaratne, D. B. M., Mar, W., Chai, H., Castillo, J. J., Farnsworth, N. R., Soejarto, D. D., Cordell, G. A., Pezzuto, I. M. & Kinghorn, A. D. (1995). Cytotoxic constituents of *Bursera permollis*. *Planta Med* **61**: 80–81.

Williams, D.H. and Fleming, I. (1989). “Spectroscopic methods in organic chemistry”, 4th edn. Mc Grow Hill Co. (UK) Ltd.

Wu, P. P., Zhang, K., Lu, Y. J., He, P., Zhao, S. Q. (2014). In vitro and in vivo evaluation of the antidiabetic activity of ursolic acid derivatives. *Eur J Med Chem* **80**: 502-508.

Wu, T. S., Shi L. S., Wang, J. J., Iou, S. C., Chang, H. C., Chen, Y. P., Kuo, W. H., Chang, Y. L. Ming, C. (2003). Cytotoxic and Antiplatelet Aggregation Principles of *Ruta graveolens*. *J Chinese Chem Soci* **50**: 171-178.

Wu, Y. J. , Shi, Q. Y., Lei, H. L., Jin, Y., Liu, X. S., Luan, L. J. (2014). Simple and efficient preparation of 3,6'-disinapoylsucrose from *Polygalae Radix* via column chromatographic extraction and reversed-phase flash chromatography. *Sep Purif Technol.* **135**: 7-13.

Xia, Z. Q., Costa, M. A., Proctor, J., Davin, L.B. & Lewis, N. G. (2000) Dirigent-mediated podophyllotoxin biosynthesis in *Linum flavum* and *Podophyllum peltatum*. *Phytochemistry* **55**: 537–549.

Yan-Qiu Meng, Y. O. Dan Liu a, Ling-Li Cai a, Hong Chen b, Bo Cao b, Yi-Zheng Wang (2009). The synthesis of ursolic acid derivatives with cytotoxic activity

and the investigation of their preliminary mechanism of action. *Bioorg Med Chem* **17**: 848–854.

Young, R. E. (2013). The history of breast cancer surgery: Halsted's radical mastectomy and beyond. *J Austr Med st* **4**: 53.

Zanoni, T. A. & Adams, R. P. (1975). The genus *Juniperus* (Cupressaceae) in Mexico and Guatemala: numerical and morphological analysis. *Boletín de la Sociedad Botánica de México* **35**: 69-92.

Zeichen, S. R., Rey, A., Argañaraz, E. & Bindstein, E. (2000). Perinatal toxicology of *Ruta chalepensis* (Rutaceae) in mice. *J Ethnopharmacol* **69**: 93-8.

Zellagui, A., Belkassam, A., Belaidi, A. & Gherraf, N. (2012). Environmental impact on the chemical composition and yield of essential oils of Algerian *Ruta Montana* (Clus.) L and their antioxidant and antibacterial activities. *Adv Environ Biol* **6**: 2684-2688.

Zhao, W., Pu, J. X., Du, X., Su, J., Li, X. N., Yang, J. H., Xue, Y. B., Li, Y., Xiao, W. L., Sun, H., D. (2011). Structure and cytotoxicity of diterpenoids from *isodon adenolomus*. *J Nat Prod* **74**: 1213–1220.

Meetings, Conferences and Publications

Meetings

Poster Presentation

Afaf Al-Groshi, Andrew R. Evans, Fyaz M. D. Ismail, Hiba A. Jasim, Nicola Dempster, Lutfun Nahar, and Satyajit D. Sarker. (25-27 June 2018). Bioassay-guided isolation of cytotoxic compounds from the Libyan plant *Juniperus phoenicea*. Phytopharm 22nd International Congress, Horgen and ZHAW Wädenswil, Switzerland

Oral presentation

Afaf Al-Groshi, Andrew R. Evans, Fyaz M. D. Ismail, Nicola Dempster, Lutfun Nahar, and Satyajit D. Sarker. (2-5th July 2018). In vitro cytotoxicity of *Ruta chalepensis* against human cancer cell lines. Phytochemical Society of Europe's Young Scientist's Meeting on Advances in Phytochemical Analysis (Trends in Natural Products Research).

Conferences

Poster Presentation

Al Groshi A, Evans AR, Ismail F, Nahar L, Sarker S. (Monday 22nd June 2015) Phytochemical and cytotoxicity studies on *Juniperus phoenicea* grown in Libya, Faculty of Science Postgraduate Research Seminar & Poster Day, James Parsons lower lecture theatre and exhibition area, Byrom Street.

Al Groshi A, Evans AR, Ismail F, Nahar L, Sarker S. (Tuesday 8th September 2015). Phytochemical and cytotoxicity studies on *Juniperus phoenicea* grown in Libya,

APS conference, PharmSci, Nottingham University, East Midlands Conference Centre Nottingham /UK).

Afaf Al Groshi, Lutfun Nahar, Andrew Evans, Abdurazag Auzi, Fyaz M. D. Ismail, and Satyajit D. Sarker (15th-17th June 2017). Cytotoxicity of *Asphodelus aestivus* against two human cancer cell lines. Poster presentation, 2nd International Conference and Exhibition on Marine Drugs and Natural Products, London.

Afaf Al-Groshi, Andrew R. Evans, Fyaz M. D. Ismail, Lutfun Nahar and Satyajit D. Sarker. (Tuesday 28th November 2017). Cytotoxicity of *Ruta chalepensis* Against Human Cancer Cell Lines. The pharmaceutical analysis postgraduate research awards and careers symposium - 2017. Royal Society of Chemistry, London

Publications

Al Groshi A, Evans AR, Ismail F, Nahar L, Sarker S. 2018. Cytotoxicity of Libyan *Juniperus phoenicea* against Human Cancer Cell Lines A549, EJ138, Hepg2 and MCF7 *Pharmaceutical Sciences*, :3-7

Tasmia Tahsin, Jean Duplex Wansi, Afaf Al Groshi, Andrew Evans, Lutfun Nahar, Claire Martin, Satyajit D. Sarker (2017). Cytotoxic properties of the stem bark of *Citrus reticulata* Blanco (Rutaceae). *Phytotherapy Research*, DOI: 10.1002/ptr.5842.

Khan KM, Nahar L, Mannan A, Arfan M, Khan G, Al Groshi A, Evans A, Dempster NM, Ismail F, Sarker SD. 2018. Liquid chromatography mass spectrometry analysis and cytotoxicity of *Asparagus adscendens* roots against human cancer cell lines. *Pharmacognosy Magazine*, 13 :890-894

Khan KM, Nahar L, Al-Groshi A, Zavoianu AG, Evans A, Dempster NM, Wansi JD, Ismail FMD, Mannan A, Sarker SD. 2016. Cytotoxicity of the Roots of *Trillium*

govanianum Against Breast (MCF7), Liver (HepG2), Lung (A549) and Urinary Bladder (EJ138) Carcinoma Cells *Phytotherapy Research*, 30 :1716-1720

In Preparation

Afaf Al-Groshi, Andrew R. Evans, Fyaz M. D. Ismail, Hiba A. Jasim, Nicola Dempster, Lutfun Nahar, and Satyajit D. Sarker. Isolation of Cytotoxic Compounds from the Libyan Plant *Juniperus phoenicea*. *Phytotherapy Research*.

Appendix

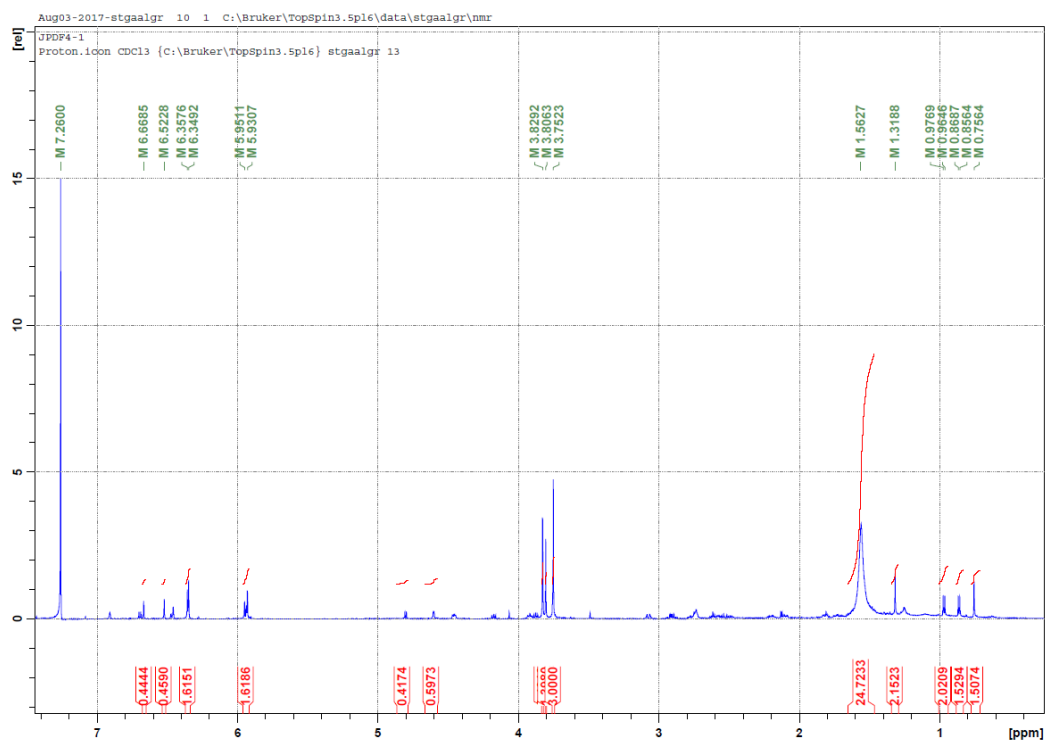
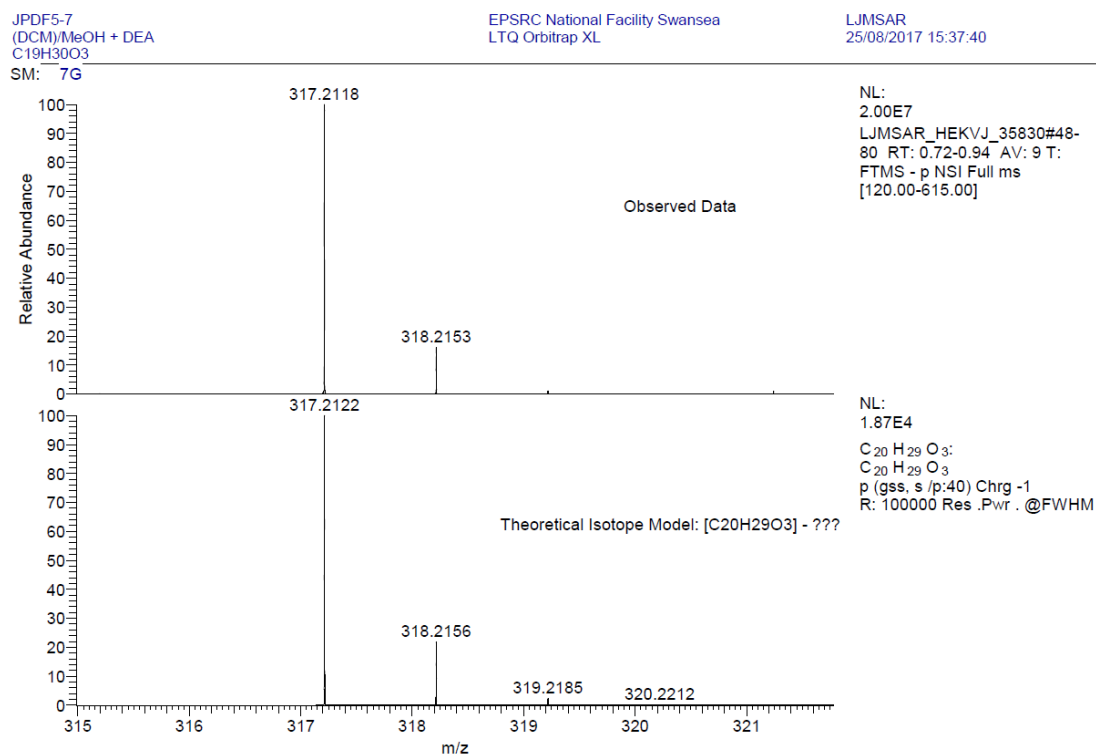
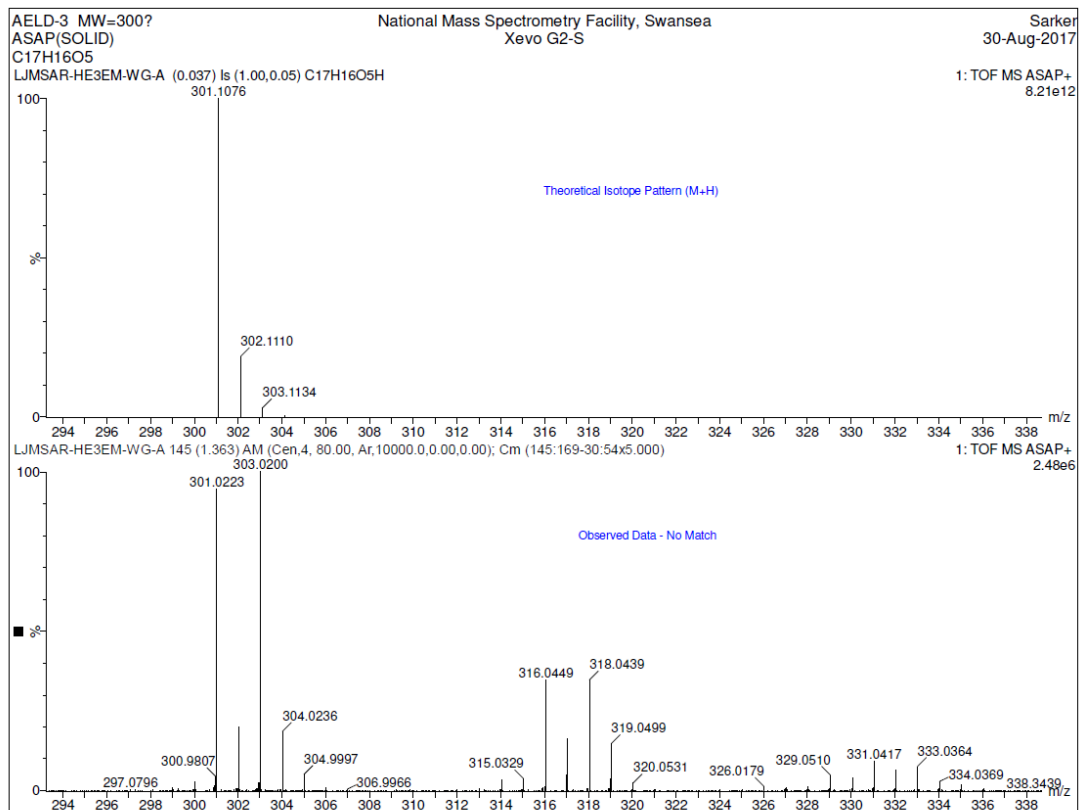
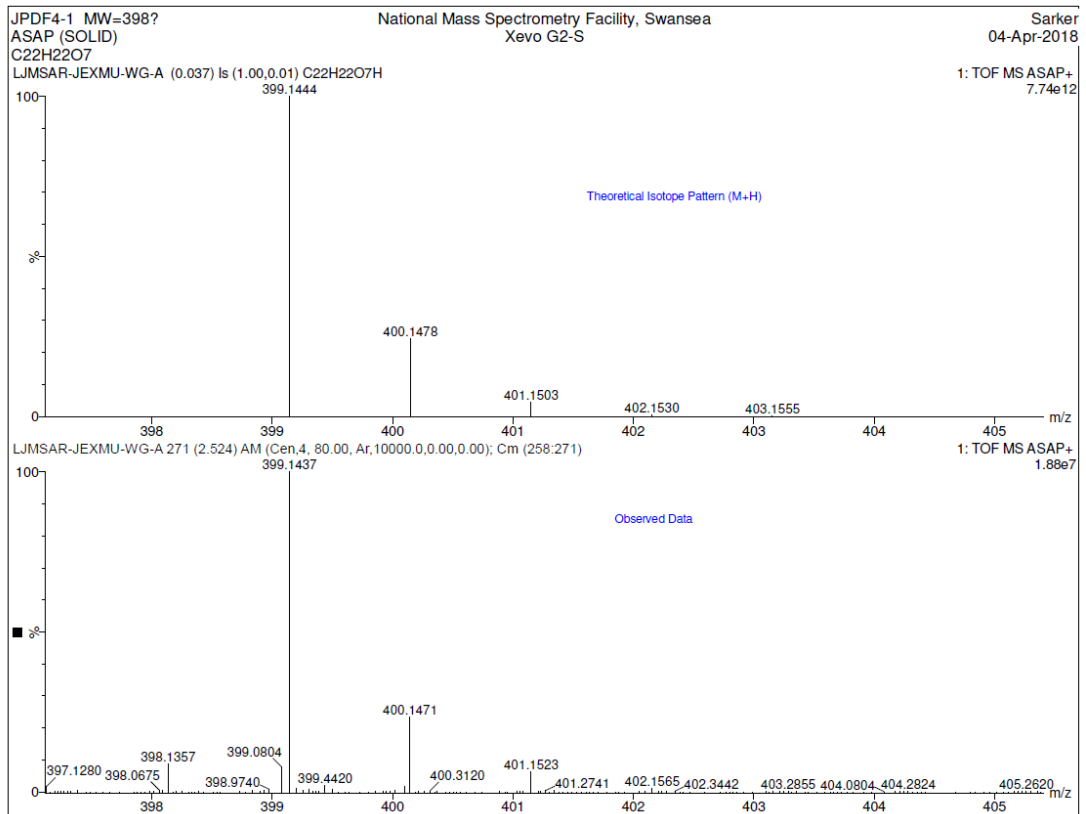
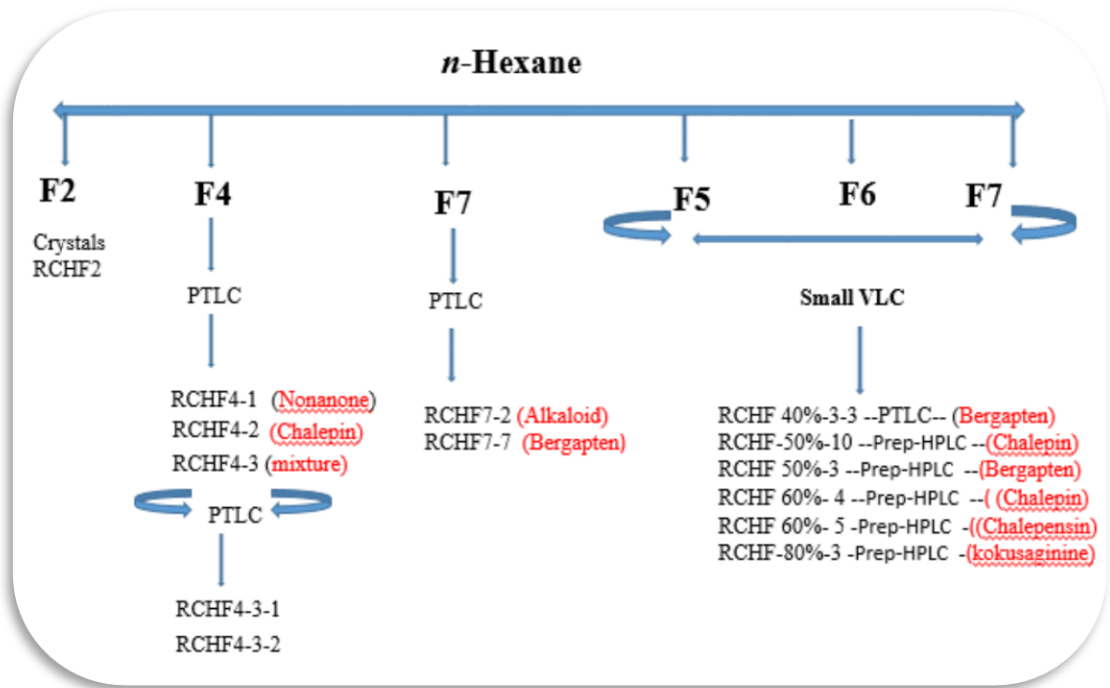


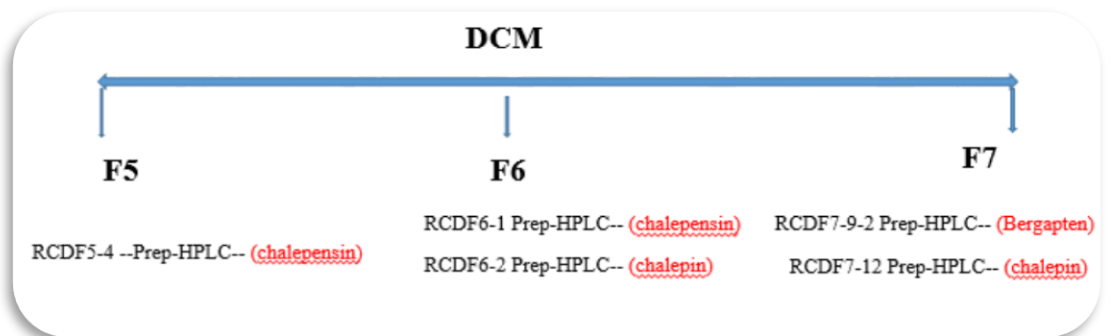
Figure 1: ^1H NMR spectrum (600 MHz, CDCl_3) of deoxydophyllotoxin A methyl ether (**8**)







Ruta chalepensis scheme summary (RCH)



Ruta chalepensis scheme summary (RCD)



Research Article

Cytotoxicity of Libyan *Juniperus phoenicea* against Human Cancer Cell Lines A549, EJ138, Hepg2 and MCF7

Afaf Al Groshi^{1,2}, Andrew R. Evans¹, Fyaz M. D. Ismail¹, Lutfun Nahar¹, Satyajit D. Sarker^{1*}

¹Medicinal Chemistry and Natural Products Research Group, School of Pharmacy and Biomolecular Sciences, Liverpool John Moores University, James Parsons Building, Byrom Street, Liverpool L3 3AF, UK.

²Pharmacognosy Department, Faculty of Pharmacy, Tripoli University, Tripoli, Libya.

Article Info

Article History:

Received: 15 October 2017

Revised: 7 December 2017

Accepted: 8 December 2017

ePublished: 15 March 2018

Keywords:

-*Juniperus phoenicea*
-Cupressaceae
-Cytotoxicity
-Cancer cell lines
-Solid phase extraction
-Vacuum liquid chromatography
-MTT assay

ABSTRACT

Background: The current study was undertaken to assess the cytotoxicity of the leaves of Libyan *Juniperus phoenicea* (Cupressaceae) against human cancer cell lines.

Methods: The cytotoxicity of the *n*-hexane, dichloromethane (DCM) and methanol (MeOH) extracts of the leaves of *J. phoenicea* (JP), obtained from sequential Soxhlet extractions, was assessed against four human cancer cell lines: EJ138 (human bladder carcinoma), HepG2 (human liver hepatocellular carcinoma), A549 (human lung carcinoma) and MCF7 (human breast adenocarcinoma) using the MTT assay.

Results: The cell line A549 was the most sensitive to the JP extracts, with the highest level of cytotoxicity with the IC₅₀ values of 16, 13 and 100 µg/mL for the DCM, *n*-hexane and MeOH extracts, respectively. However, generally the most potent cytotoxic extract across the other cells tested was the *n*-hexane extract, followed by the DCM extract, whilst the MeOH extracts showed little or no cytotoxicity. The percentage of viability of cells decreased as the concentration of test compounds increased. The cytotoxicity of various chromatographic fractions from the extracts was also studied against the A459 cells. For the *n*-hexane fractions, the IC₅₀ values were 160, 62, 90, 30, 9.5 and 40 µg/mL for fractions 1 to 5 and 7, respectively. Fractions 4 and 5 showed the greatest effect. DCM fractions 2, 3 and 4 had the IC₅₀ values of 60, 92 and 19 µg/mL, respectively, and DCM fractions 5 to 8 were non-cytotoxic. Fractions 1 and 2 of the MeOH extract were non-cytotoxic, whereas cytotoxicity was observed for fractions 3 and 4 with IC₅₀ values of 50 and 85 µg/mL, respectively.

Conclusion: The outcome of the present study suggested that the JP leaves possess cytotoxic activities. The high level of cytotoxicity of the *n*-hexane and DCM extracts suggested that lipophilicity might affect the cytotoxicity of JP, where the less polar compounds had the strongest cytotoxicity.

Introduction

Juniperus phoenicea L. (Family: Cupressaceae) is a well-known Libyan medicinal plant, which has been used in Libyan traditional medicine for centuries for the treatment of various human ailments including tumours and cancers. In fact, in Egypt around 1500 BC was the first recorded use of using the *Juniperus phoenicea* medicinally, which was to relieve joint and muscle pain. This plant is used in folk medicine to treat rheumatism, gout, oedema, diarrhoea, poor appetite and urinary tract diseases. It is also reported to eliminate gastrointestinal bacteria and parasites.^{1,2} There are some reports on its use as a female contraceptive by some tribes.¹ The juniper berry was studied as a possible treatment for diet controlled diabetes mellitus.³

Several compounds, *i.e.*, terpenoids (monoterpenes: predominantly α -pinene, α -phyllandrene and δ -3-carene; sesquiterpenes: mainly δ -cadinene; diterpenes), phenolics

(*e.g.*, flavonoids and biflavones, phenylpropanoids and lignans), furanone glycosides, hydrocarbons, and sterols, have been isolated from the leaves and berries of *J. phoenicea* grown in different countries.⁴⁻⁸ Podophyllotoxin and deoxypodophyllotoxin were also found in the aerial parts of many *Juniperus* species including *J. phoenicea*.⁹

Various biological activities for *J. phoenicea* have been reported to date. The essential oils from this plant exhibited moderate antibacterial and antifungal activities.^{5-8,10-13} Elmhdwi *et al.*¹⁴ demonstrated that the extracts from *J. phoenicea* had antibacterial activity against both Gram-positive and Gram-negative bacteria including multiple-drug-resistant (MDR) strains. This activity was attributed to the abundance of α -pinene and the overall chemical constituents of these extracts. Antioxidant activity of this plant was detected using the ABTS radical-scavenging assay with the strongest

*Corresponding Author: Satyajit D. Sarker, E-mail: S.Sarker@ljmu.ac.uk

©2018 The Authors. This is an open access article and applies the Creative Commons Attribution (CC BY), which permits unrestricted use, distribution, and reproduction in any medium, as long as the original authors and source are cited. No permission is required from the authors or the publishers.

antioxidant effect being found with the MeOH extract.⁶ The aqueous extract of *J. phoenicia* showed anti-diarrhoeal effect *in vivo* on experimental rat models of diarrhoea by reducing intestinal fluid accumulation and inhibiting intestinal motility.² Akkol *et al.*¹⁵ revealed remarkable anti-inflammatory and antinociceptive activities of five *Juniperus* species. Cairnes & Ekundayo⁹ showed that the ethanolic extract of *J. phoenicea* twigs and leaves and two isolated compounds, desoxypodophyllotoxin and *p*-peltatin-methyl ether, were cytotoxic in the KB cell cultures (human cervix carcinoma). A MeOH extract of *J. phoenicea* from Saudi Arabia and Indonesia displayed high cytotoxicity in Vero (normal monkey kidney) and HEP-2 (human laryngeal carcinoma) cell lines.¹⁶ In addition, this plant also displayed significant cytotoxicity against both MCF7 (human breast adenocarcinoma) and HCT-116 (human colon carcinoma) cell lines.¹

As a part of our continuing phytochemical and bioactivity studies on Libyan medicinal plants,¹⁷⁻²² we now report on the cytotoxicity of the extracts and fractions of the leaves of *J. phoenicea* growing in Libya against four human cancer cell lines: human bladder carcinoma cell line (EJ138), human hepatocellular carcinoma cell line (HepG2), human lung carcinoma cell line (A549) and human breast adenocarcinoma cell line (MCF7).

Materials and Methods

Plant material

The leaves of *Juniperus phoenicea* L. were collected from Al-Jabal Al Akhdar, Libya, in 2013. The plant material was identified at the Faculty of Science Herbarium, Tripoli-Libya, and a voucher specimen (no. D68122) has been retained there. Leaves of this plant were air-dried, powdered and kept in a tightly closed amber coloured container for subsequent studies.

Extraction

Ground leaves of *J. phoenicea* (86.5 g) were Soxhlet-extracted, sequentially, with *n*-hexane, DCM and MeOH, 800 mL each. Ten cycles were allowed for each extraction, and the temperature of the heating mantle for all extractions was kept constant at 60°C. The extracts were filtered and evaporated to dryness using a rotary evaporator at a temperature not exceeding 45°C under reduced pressure. All extracts were stored at 4°C.

Fractionation techniques

The crude extracts of *J. phoenicea* leaves were separated into various fractions using vacuum liquid chromatography (VLC) on silica gel for the *n*-hexane and DCM extracts, and solid-phase extraction (SPE) on reversed-phase C₁₈ silica for the MeOH extract.^{23,24} The *n*-hexane extract (4.6 g) was fractionated by VLC eluting with *n*-hexane-ethyl acetate mixtures of increasing polarity to yield seven fractions: F1: 82.5 mg, F2: 555 mg, F3: 998.7 mg, F4: 655.5 mg, F5: 118.8 mg F6: 22.1 mg, F7: 103.7 mg. Similarly, the DCM extract (1.289 g) was fractionated by VLC, starting elution with *n*-hexane-

DCM mixtures, then increasing polarity with MeOH to yield eight fractions: F1: 15 mg, F2: 20 mg, F3: 41 mg, F4: 134 mg, F5: 128.5 mg F6: 9.3 mg, F7: 2.7 mg and F8: 2.4 mg. The dried MeOH extract (1.4 g) was re-suspended in 10% MeOH in water, and subjected to solid phase extraction (SPE) using a cartridge (20 g) pre-packed with reversed-phase silica C₁₈ (ODS). A step gradient was applied starting with 20% MeOH in water, then 50%, 80% and 100% MeOH in water (200 mL each). Four fractions were collected: F1: 895 mg, F2: 135 mg, F3: 54 mg, F4: 25 mg, and these fractions were dried using a rotary evaporator and a freeze dryer.

MTT assay

The cytotoxic activity of the *n*-hexane, DCM and MeOH extracts of *J. phoenicea* were assessed against EJ138 (human bladder carcinoma), HepG2 (human liver hepatocellular carcinoma), A549 (human lung carcinoma) and MCF7 (human breast adenocarcinoma) cell lines. In addition, fractions obtained from *n*-hexane, DCM and MeOH extracts of *J. phoenicea* were also assessed for cytotoxicity against the cell line A549, as the extracts showed the highest level of activities against this cell line. The cells were seeded into 24-well plates (5 x 10⁴ cells/well) and incubated under 5% CO₂, 95% humidity at 37°C for 24 h. The different extracts or isolated fractions were diluted in medium containing DMSO (0.01% (v/v) (including the negative control), to achieve extract concentrations of (0, 0.8, 4, 20, 100 and 500 µg/mL) or isolated fraction concentrations of (0, 0.4, 2, 10, 50 and 250 µg/mL). These doses were then used to treat the cells for 24 h before assessment using the MTT assay²⁵ following the standard protocol. Briefly, each treatment was removed from the 24-well plates of cells and replaced with MTT solution (0.5 mg/mL MTT in medium (1 mL/well)). The cells were then incubated under 5% CO₂, 95% humidity at 37°C for 2 h. The MTT solution was then removed from each well of cells and replaced with isopropanol (0.5 mL/well) to lyse the cells, and to release and solubilise the blue formazan product. The absorbance reading (540 nm) of lysates from treated cells in each well on each occasion was recorded and was expressed as a percentage of the mean value of the control absorbance on each occasion. The results for each treatment and dose derived from at least 12 wells (n≥12) from three or more separate occasions. To determine IC₅₀ values, data were presented in EXCEL graphs with the dose value (µg/mL) on the X-axis on a log¹⁰ scale and the % viability compared to control on the Y-axis. The IC₅₀ values are determined from the trend line of the data points.

Statistical analysis

All experiments were carried out in triplicate on separate occasions. Data were expressed as means ± standard error of the mean. The graphs were plotted using nonlinear regression with the use of Microsoft Excel version 2013.

Results and Discussion

In the present study, the cytotoxic effect of *J. phoenicea*

leaf extracts against four human cancer cell lines, MCF7, HepG2, EJ138 and A549, was determined using the MTT assay. Although cytotoxicity of *J. phoenicea* against MCF7 was reported previously,⁴ to the best of our knowledge, this is the first report on the assessment of cytotoxicity of *J. phoenicea* leaf extracts and fractions against HepG2, EJ138 and A549 cell lines. The extracts of *J. phoenicea* showed the highest level of cytotoxic activity against the human lung adenocarcinoma cell line A549 with the IC₅₀ values of 16, 13 and 100 µg/mL, respectively, for the *n*-hexane, DCM and MeOH extracts (Table 1). Whilst the DCM extract appeared to be the most cytotoxic extract against the A549 cells, the *n*-hexane extract was the most cytotoxic across the board against HepG2, EJ138 and MCF7 having respective IC₅₀ values of 10, 40 and 14 µg/mL. The DCM extract also resulted in cytotoxicity in all cell lines tested with IC₅₀ values of 50 µg/mL for EJ138 cells, 42 µg/mL for HepG2 cells, 16 µg/mL for MCF7 cells and 13 µg/mL for A549 cells. The MeOH extract showed low-level of cytotoxicity in EJ138 (IC₅₀ 130 µg/mL), HepG2 (IC₅₀ 900 µg/mL), A549 (IC₅₀ 100 µg/mL) and MCF7 (IC₅₀ >1000 µg/mL) (Table 1). According to Sahranavard *et al.*,²⁶ plant extracts are only considered to be cytotoxic to cells if the IC₅₀ value is <100 µg/mL, therefore these MeOH extract results were regarded as non-cytotoxic to each of the cell lines tested. The higher level of cytotoxic activity of the *n*-hexane and DCM extracts suggested that lipophilicity might have an impact on the cytotoxic activity of *J. phoenicea*, where the less polar (high lipophilic) compounds showed the strongest cytotoxic effect. However, it is known that lipophilicity is one of the major factors that influences the transport, absorption, and distribution of chemicals in biological systems. Bioassay-guided phytochemical and biological fractionation is an approach whereby a crude extract of plant is fractionated and re-fractionated, continually monitored fractions by appropriate bioassay(s), until a pure biologically active fraction/compound is found.²⁴ To adopt this approach, *n*-hexane, DCM and MeOH extracts were further fractionated by two different techniques: solid-phase extraction for MeOH extract and VLC for the *n*-hexane and DCM extracts to get different fractions

(four fractions from MeOH extract, seven fractions from *n*-hexane extract and eight fractions from DCM extract). All fractions were tested for cytotoxicity against the A549 cell line, as these cells appeared to be the most sensitive to the all three extracts. Taken that IC₅₀ values >100 µg/mL are considered as non-cytotoxic, *n*-hexane fractions 1 (F1) and 6 (F6), DCM fractions 1, and 5 to 8 (F1, F5, F6, F7 and F8) and MeOH fractions 1 and 2 (F1 and F2) were all regarded as non-cytotoxic in the A549 cells. However, *n*-hexane fractions 2 to 5 and 7 (F2, F3, F4, F5 and F7) were cytotoxic. In addition, DCM fractions 2 to 4 (F2, F3 and F4) and MeOH fractions 3 and 4 (F3 and F4) were also considered cytotoxic (Table 2). The most potent fractions appear to be *n*-hexane fraction 5 (F5) with an IC₅₀ value of 10 µg/mL and DCM fraction 4 (F4) with an IC₅₀ value of 19 µg/mL.

Whilst the MeOH fraction 1 (F1), which was the most polar fraction of all, was found to be non-cytotoxic, an interesting observation was that doses 2, 10 and 50 µg/mL did appear to trigger proliferation in the A549 cells with approximately a 20% increase in viability compared to the control (0 µg/mL) (Figure 1). However, further interrogation of these data indicated that only the 50 µg/mL dose resulted in a statistically significant difference compared to the control (P<0.05). There was high variability in the data resulting from fraction 1 (F1), and this might have contributed to this anomaly.

Several phytochemicals, *e.g.*, alkaloids, flavonoids, lignans, phenols, steroids and terpenes have been demonstrated to possess prominent cytotoxic properties against cancer cells.²⁷

Notably, all these groups of phytochemicals have previously been isolated from the leaves and berries of *J. phoenicea* and other *Juniperus* species grown in different countries.^{9,28-30} Podophyllotoxin, which is also present in *J. phoenicea* at a low level,³¹ is a well-known cytotoxic compound against cancer cell lines. Its cytotoxicity is mediated by inhibition of microtubule formation and this compound serves as a unique starting compound for the semisynthesis of anticancer drugs that are known to inhibit topoisomerase II such as etoposide, teniposide, or etopophos.³¹

Table 1. The IC₅₀ (µg/mL) of *n*-hexane, DCM and MeOH extracts of *J. phoenicea* on a selection of four cancer cell lines.

Cell type	IC ₅₀ values (µg/mL)		
	<i>n</i> -Hexane	DCM	MeOH
Human bladder carcinoma cells (EJ138)	40	50	130
Human hepatocellular carcinoma cells (HepG2)	10	42	900
Human lung carcinoma cells (A549)	16	13	100
Human breast adenocarcinoma cells (MCF7)	14	16	> 1000

The IC₅₀ values for the *n*-hexane, DCM and MeOH extracts of *J. phoenicea* different on the cell lines of four different cancer types. Values greater than 100 µg/mL were considered as non-cytotoxic.

Table 2. The IC₅₀ (µg/mL) of *n*-hexane, DCM and MeOH fractions of *J. phoenicea* fractions on A549 (human lung carcinoma) cells.

Extracts	IC ₅₀ values (mg/mL) of the fractions							
	F1	F2	F3	F4	F5	F6	F7	F8
<i>n</i> -Hexane	160	62	90	30	9.5	>1000	40	NA
DCM	>1000	60	92	19	>1000	>1000	>1000	>1000
MeOH	>1000	244	50	85	NA	NA	NA	NA

The IC₅₀ values for the *n*-hexane, DCM and MeOH fractions of *J. phoenicea* on A549 human lung carcinoma cells. Values greater than 100 µg/mL were considered as non-cytotoxic. NA = Not applicable.

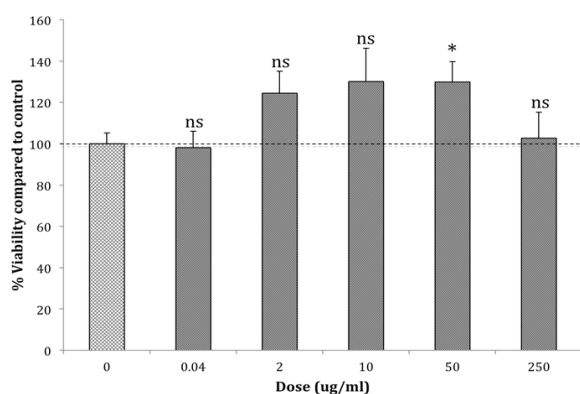


Figure 1. The cytotoxic activity of *J. phoenicea* MeOH fraction 1 (F1) against A549 human lung carcinoma cell line. The asterisk * indicates a significant difference when compared to control ($P < 0.05$) and ns indicates no significant difference to control. The results are mean values \pm SEM derived from $n \geq 12$ from three separate occasions.

Ren *et al.*³² detailed the anticancer effects of the flavonoids, which were shown to inactivate carcinogen, inhibit proliferation, arrest the cell cycle, induce apoptosis and differentiate, inhibit angiogenesis, prevent oxidation and reverse multidrug resistance. Previous studies had shown that many flavonoids and polyphenolic compounds were present in some *Juniperus* species.³³⁻³⁵

Conclusion

The outcome of the present study suggested that the *J. phoenicea* leaves possess cytotoxic activities. The high level of cytotoxic activities of the *n*-hexane and DCM extracts suggested that lipophilicity might affect the cytotoxic activity of *J. phoenicea*, where the less polar (high lipophilic) compounds might have the strongest cytotoxic effect. As terpenes are the main lipophilic compounds previously reported from less polar extracts and essential oils of *J. phoenicea*, it is reasonable to assume that the cytotoxicity observed with the less polar extracts was contributed by various cytotoxic terpenes as well as the lignans, podophyllotoxin and deoxy-podophyllotoxin.

Acknowledgments

One of us (Afaf Al Groschi) thanks the Libyan Government for a PhD scholarship to conduct this study and also special thanks from Afaf to Mrs. Elham Omran El-Agori for the samples of *J. phoenicea* grown in Libya and Dr. Mohamed Abu Hadra for botanical identification of the plant.

Conflict of interests

The authors claim that there is no conflict of interest.

References

- Aljaiyash AA, Gonaid M, Islam M, Chaouch A. Antibacterial and cytotoxic activities of some Libyan medicinal plants. *Journal of Natural Product and Plant Resources*. 2014;4(2):43-51.
- Qnais EY, Abdulla FA, Abu Ghalyun YY. Antidiarrheal effects of *J. phoenicea* L. leaf extract in

- rats. *Pak J Bio Sci*. 2005;8(6):867-71. doi:10.3923/pjbs.2005.867.871
- Sánchez de Medina F, Gámez MJ, Jiménez I, Osuna JI, Zarzuelo A. Hypoglycemic activity of juniper "berries". *Planta Med*. 1994;60(3):197-200. doi:10.1055/s-2006-959457
- El-Sawi SA, Motawae HM, Ali AM. Chemical composition, cytotoxic activity and antimicrobial activity of essential oils of leaves and berries of *J. phoenicea* L. grown in Egypt. *Afr J Tradit Complement Altern Med*. 2008;4(4):417-26. doi:10.4314/ajtcam.v4i4.31236
- El-Sawi SA, Motawae HM. Labdane, pimarane and abietane diterpenes from the fruits of *J. phoenicea* L. grown in Egypt and their activities against human liver carcinoma. *Canadian Journal Of Pure & Applied Sciences*. 2008;2:115-22.
- Ennajar M, Bouajila J, Lebrihi A, Mathieu F, Savagnac A, Abderraba M, et al. The influence of organ, season and drying method on chemical composition and antioxidant and antimicrobial activities of *J. phoenicea* L. essential oils. *J Sci Food Agric*. 2009;90(3):462-70. doi:10.1002/jsfa.3840
- Derwich E, Benziane Z, Boukir A. Chemical composition of leaf essential oil of *J. uniperus phoenicea* and evaluation of its antibacterial activity. *Int J Agric Biol*. 2010;12(2):199-204.
- Alzand KI, Aziz DM, Tailang M. Isolation, structural elucidation and biological activity of the flavonoid from the leaves of *Juniperus phoenicea*. *World J Pharm Res*. 2014;3(10):966-80.
- Cairnes DA, Ekundayo O, Kingston DG. Plant anticancer agents. X. Lignans from *J. phoenicea*. *J Nat Prod*. 1980;43:495-7. doi:10.1021/np50010a010
- Stassi V, Verykokidou E, Loukis A, Harvala C, Philianos S. The antimicrobial activity of the essential oils of four *Juniperus* species growing wild in Greece. *Flavour Fragr J*. 1996;11(1):71-4. doi:10.1002/(sici)1099-1026(199601)11:1<71::aid-ffj536>3.3.co;2-0
- Angioni A, Barra A, Russo MT, Coroneo V, Dessi S, Cabras P. Chemical composition of the essential oils of *Juniperus* from ripe and unripe berries and leaves and their antimicrobial activity. *J Agri Food Chem*. 2003;51(10):3073-8. doi:10.1021/jf026203j
- Mazari K, Bendimerad N, Bekhechi C, Fernandez X. Chemical composition and antimicrobial activity of essential oils isolated from Algerian *J. phoenicea* L. and *Cupressus sempervirens* L. *J Med Plant Res*. 2010;4(10):959-64. doi:10.5897/JMPR10.169
- Ait Ouazzou A, Loran S, Arakrak A, Laglaoui A, Rota C, Herrera A, et al. Evaluation of the chemical composition and antimicrobial activity of *Mentha pulegium*, *J. phoenicea*, and *Cyperus longus* essential oils from Morocco. *Food Res Int*. 2012;45(1):313-9. doi:10.1016/j.foodres.2011.09.004
- Elmhdwi MF, Attitalla IH, Khan BA. Evaluation of antibacterial activity and antioxidant potential of different extracts from the leaves of *J. Phoenicea*. *J*

- Plant Pathol Microbiol. 2015;6(9):1-8. doi:10.4172/2157-7471.1000300
15. Akkol EK, Guvenc A, Yesilada E. A comparative study on the antinociceptive and anti-inflammatory activities of five *Juniperus* taxa. *J Ethnopharmacol.* 2009;125(2):330-6. doi:10.1016/j.jep.2009.05.031
 16. Abdul L, Haitham MA, Moawia EM, Alarifi Saud AR, Fahad NA. Medicinal plants from Saudi Arabia and Indonesia: *In vitro* cytotoxicity evaluation on Vero and HEp-2 cells. *J Med Plant Res.* 2014;8(34):1065-73. doi:10.5897/jmpr2014.5481
 17. Al-Tubuly RA, Auzi A, Al-Etri-Endi A, Nahar L, Sarker S. Effects of *Retama raetam* (Forssk.) Webb & Berthel. (Fabaceae) on the central nervous system in experimental animals. *Arch Biol Sci.* 2011;63(4):1015-21. doi:10.2298/abs1104015a
 18. Auzi AA, Gray AI, Salem MM, Badwan AA, Sarker SD. Feruhermonins A-C: three daucane esters, from the seeds of *Ferula hermonis* (Apiaceae). *J Asian Nat Prod Res.* 2008;10:701-7. doi:10.1080/10286020802016040
 19. Auzi ARA, Hawisa NT, Sherif FM, Sarker SD. Neuropharmacological properties of *Launaea resedifolia*. *Rev Bras Farmacogn.* 2007;17(2):160-5. doi:10.1590/s0102-695x2007000200004
 20. Elmezogi J, Zetrini A, Ben Hussain G, Anwair M, Gbaj A, Nahar L, et al. Evaluation of anti-inflammatory activity of some Libyan medicinal plants in experimental animal. *Arch Biol Sci.* 2012;64(3):1059-63. doi:10.2298/abs1203059e
 21. Geroushi A, Auzi AA, Elhwegi AS, Elzawam F, Elsherif A, Nahar L, et al. Anti-inflammatory sesquiterpenes from the root oil of *Ferula hermonis*. *Phytother Res.* 2011;25(5): 774-7. doi:10.1002/ptr.3324
 22. Geroushi A, Auzi AA, Elhwegi AS, Elzawam F, El Sherif A, Nahar L, et al. Antinociceptive and anti-inflammatory activity of *Ferula hermonis* root oil in experimental animals. *Lat Am J Pharm.* 2010;29:1436-9.
 23. Sarker SD, Latif Z, Gray AI. *Natural Products Isolation.* 2nd ed.. USA: Humana Press Inc, Springer-Verlag; 2005.
 24. Sarker SD, Nahar L. *Natural Products Isolation.* 3rd ed. USA: Humana Press, Springer-Verlag; 2012.
 25. Mosmann T. Rapid colorimetric assay for cellular growth and survival: application to proliferation and cytotoxicity assays. *J Immunol Methods.* 1983;65(1-2):55-63. doi:10.1016/0022-1759(83)90303-4
 26. Sahranavard S, Naghibi F, Ghaffari S. Cytotoxic activity of extracts and pure compounds of *Bryonia aspera*. *Int J Pharm Pharm Sci.* 2012;4(3): 541-3.
 27. Fernando W, Rupasinghe HPV. Anticancer properties of phy-tochemicals present in medicinal plants of North America. In: Kulka M editor. *Using Old Solutions to New Problems—Natural Drug Discovery in the 21st Century.* Croatia: InTech; 2013.
 28. Comte G, Vercauteren J, Chulia AJ, Allais DP, Delage C. Phenylpropanoids from leaves of *Juniperus phoenicea*. *Phytochemistry.* 1997;45(8):1679-82. doi:10.1016/s0031-9422(97)00197-0
 29. Barrero AF, del Moral JF, Herrador MM, Akssira M, Bennamara A, Akkad S, et al. Oxygenated diterpenes and other constituents from Moroccan *Juniperus phoenicea* and *Juniperus thurifera* var. *africana*. *Phytochemistry.* 2004;65(17):2507-15. doi:10.1016/j.phytochem.2004.07.021
 30. Aboul-Ela M, El-Shaer N, El-Azim TA. Chemical constituents and hypoglycemic effect of *Juniperus phoenicea*: Part I. *Alex J Pharm Sci.* 2005;19(2):109-16.
 31. Renouard S, Lopez T, Hendrawati O, Dupre P, Doussot J, Falguieres A, et al. Podophyllotoxin and deoxypodophyllotoxin in *Juniperus bermudiana* and 12 other *Juniperus* species: optimization of extraction, method validation, and quantification. *J Agric Food Chem.* 2011;59(15):8101-7. doi:10.1021/jf201410p
 32. Ren W, Qiao Z, Wang H, Zhu L, Zhang L. Flavonoids: Promising anticancer agents. *Med Res Rev.* 2003;23(4):519-34. doi:10.1002/med.10033
 33. Pisarev DI, Novikov OO, Novikova MY, Zhilyakova ET. Flavonoid Composition of *Juniperus oblonga* Bieb. *Bull Exp Biol Med.* 2011;150(6):714-7. doi:10.1007/s10517-011-1231-1
 34. Nasri N, Tlili N, Elfalleh W, Cherif E, Ferchichi A, Khaldi A, et al. Chemical compounds from Phoenician juniper berries *Juniperus phoenicea*. *Nat Prod Res.* 2011;25(18):1733-42. doi:10.1080/14786419.2010.523827
 35. Nemati F, Dehpouri AA, Eslami B, Mahdavi V, Mirzanejad S. Cytotoxic properties of some medicinal plant extracts from Mazandaran, Iran. *Iran Red Crescent Med J.* 2013;15(11):e8871. doi:10.5812/ircmj.8871